A Study of the Green Leaf Volatile Biochemical Pathway as a Source of Important Flavour and Aroma Precursors in Sauvignon Blanc Grape Berries

---

A thesis
submitted in partial fulfilment
of the requirements for the Degree of
Doctor of Philosophy

at
Lincoln University
by
Andriy Podolyan

Lincoln University
2010

Abstract of a thesis submitted in partial fulfilment of the requirements for the Degree of Doctor of Philosophy

A Study of the Green Leaf Volatile Biochemical Pathway as a Source of Precursors of Important Aroma Compounds in Sauvignon Blanc Grape Berries

by

Andriy Podolyan

Green leaf volatiles (GLVs) are short-chain acylic aldehydes, alcohols and esters produced by plants via enzymatic metabolism of polyunsaturated fatty acids (PUFAs). GLVs are known to affect flavour and aroma of fruits and vegetables, including grapes. It has also been suggested that C6 and C5 GLVs are the precursors of volatile thiols, the aroma compounds that are important in Sauvignon blanc wine. GLVs are produced during grape berry development and released in high quantities upon berry crush.

GLV aldehydes are formed from PUFAs by the action of two enzymes, lipoxygenase (LOX) and hydroperoxide lyase (HPL). This biochemical pathway is well characterised in other plant species and is known as the GLV pathway. To date, the GLV pathway has not been characterised in grapes. This thesis focuses on identification and initial characterisation of LOX and HPL genes and enzymes involved in the GLV-pathway.

LOXs are a group of non-haem iron-containing dioxygenases that catalyse oxygenation of PUFAs producing PUFA-hydroperoxides. The most common PUFA substrates in plants are linoleic acid (LA, 18:2) and α-linolenic acid (LnA, 18:3). Depending on the position of oxygenation of the 18-carbon chain PUFAs, all plant LOXs are classified as 13(S) - and 9(S)-LOXs. 13(S)-LOXs are further regarded as type II and type I enzymes, depending on the presence or absence of transit peptides in the amino acid sequences of these enzymes respectively.

HPLs belong to the CYP74 enzyme family, which is represented by atypical members of cytochrome P450 oxidases superfamily. HPLs cleave PUFA-hydroperoxides, producing aldehydes and oxoacids. Depending on the substrate specificity, HPLs are classified as 13-HPLs, 9/13-HPLs or 9-HPLs.

The research reveals the complexity of the genetic makeup of the GLV metabolic pathway in grapes. Eighteen putative LOX genes and six putative HPL genes were identified in the Pinot noir grape genome. Phylogenetic analysis of the identified grape LOXs classified them as members of two groups, type II 13-LOXs and 9-LOXs, whereas all identified grape HPLs were classified as 13-HPLs (CYP-74B) and 9/13-HPLs (CYP-74C).

Several LOX and HPL genes were expressed at different levels in Sauvignon blanc berry. Study of selected LOX and HPL gene expression revealed different levels of expression and differential tissue distribution of individual LOX and HPL genes within the berry. The studied genes also displayed different patterns of expression across different stages of berry development, upon wounding and in berries infected with *Botrytis cinerea*. Amongst the four LOX gene studied, transcripts of *VvLOXA* were the most abundant at all stages during berry development. *VvLOXO* was induced transiently upon berry damage and was a clear candidate involved in berry response to wounding. Expression levels of *VvLOXC* and *VvLOXO* were significantly increased in berries infected with *Botrytis cinerea* compared to the uninfected berries.

In vitro biochemical analysis of the reaction products of recombinant VvLOXA (LOXA-TP) and VvLOXO (LOXO-TP) confirmed that these two enzymes are 13-LOXs. Both enzymes preferred LnA as a substrate. Both enzymes had the same temperature optima of 25°C, but preferred different pH conditions. Recombinant LOXA-TP preferred acidic environment and had pH optimum of pH 5.5, while LOXO-TP preferred neutral-to-basic conditions and had pH optimum of pH 7.5.

Preliminary experiments with recombinant VvHPLA showed its ability to metabolise 13(S)-hydroperoxides, releasing C6 volatile aldehydes. Recombinant VvHPLA exhibited maximum activity with 13(S)-hydroperoxides of LnA as substrate at pH 5.0.

Keywords: grapevine, *Vitis vinifera*, Sauvignon blanc, aroma compounds, volatile thiols, green leaf volatiles, lipoxygenase, hydroperoxide lyase, PUFA metabolism, plant defence response, plant wounding, grape berry development

Note in Proof

Some aspects of this thesis have been published in:

Podolyan A, White J, Jordan B, Winefield C. (2010). Identification of the lipoxygenase gene family from Vitis vinifera and biochemical characterisation of two 13-lipoxygenases expressed in grape berries of Sauvignon Blanc. *Functional Plant Biology,* **37**(8), 767-784.

Acknowledgements

First and foremost, I would like to thank my supervisors for giving me an opportunity to work on this project and for all their continuous support during these years. I am particularly thankful to Dr. Chris Winefield, who taught me the basics of molecular biology and later became my principle project supervisor. I would like to thank Prof. Brian Jordan for his support over the years as my associate supervisor. I am grateful to Chris and Brian for being approachable and always ready to discuss any aspects of the project. A special thankyou for their patient proofreading of my writing. Many thanks to Dr Mike Trought, who provided his help and advice on the viticultural aspects of this study.

I thank New Zealand Foundation for Research, Science and Technology (contract number UOAX0404) for funding this project and paying my stipend. I also thank Lincoln University and specifically Agriculture and Life Sciences Division for providing facilities and additional funding during the years of study.

I want to thank Pernod Ricard, New Zealand, for allowing me to collect berry samples from the Booker vineyard on the Brancott Estate. I also thank Marlborough Wine Research Staff for their help in sample collection.

There are numerous people at Lincoln University and outside, whom I have had the privilege to work and interact with during these years. Their contribution has been invaluable, and has enabled me to complete this body of work. A special thankyou goes to Jackie White for managing the lab and helping me with the sample preparations. I thank Jenny Zhao and Rosy Tung for their assistance in HPLC analysis and Jason Breitmeyer for his help with GC-MS analysis. I would also like to thank my friends and colleagues for support and friendship I needed.

My special thanks go to all my family for their invaluable contribution. I am immensely grateful to my wife Anastasija, who always inspired me and helped me to get through all the challenges and emotional struggles during this time. I am eternally indebted to my parents, who raised and educated me. They have made me the person I am today, and this is I am most grateful for.

I also thank everyone who contributed to the completion of this project and who was not mentioned here.

Table of Contents

List of Tables

List of Figures

Acronyms

12(S)-HPETE - 12(S)-hydroperoxy-5Z, 8Z, 10E, 14Z-eicosatetraenoic acid

13(S)-HPODE - 13(S)-hydroperoxy-9Z,11E-octadecadienoic acid

13(S)-HPOTrE - 13(S)-hydroperoxy-9Z,11E,15Z-octadecatrienoic acid

15(S)-HPETE - 15(S)-hydroperoxy-5Z, 8Z, 11Z, 13E-eicosatetraenoic acid

3MH - 3-mercaptohexan-1-ol

3MHA - 3-mercaptohexylacetate

4MMP - 4-mercapto-4-methylpentan-2-one

4MMPOH - 4-mercapto-4-methylpentan-2-ol

5(S)-HPETE - 5(S)-hydroperoxy-6E, 8Z, 11Z, 14Z-eicosatetraenoic acid

9(S)-HPODE - 9(S)-hydroperoxy-10E,12Z-octadecadienoic acid

9(S)-HPOTrE - 9(S)-hydro(pero)xy-10E,12Z,15Z-octadecatrienoic acid

AA - arachidonic acid

ADH - alcohol dehydrogenase

cDNA - complementary DNA

CDS - coding sequence

CMC - critical micelle concentration

Ct value - crossing threshold value

cTP - chloroplast transit peptide

daa - days after harvest

EDTA - ethylenediaminetetraacetic acid

gDNA - genomic DNA

FA – fatty acid

GLV - green leaf volatile

GOI – gene of interest

GSH - glutathione

GST - glutathione S-transferase

HKG - housekeeping gene

HPL - hydroperoxide lyase

IB - inclusion bodies

IPTG - isopropyl β-D-1-thiogalactopyranoside

JA - jasmonic acid

LA - linoleic acid

LB medium - Luria Bertani medium

LnA - α-linolenic acid

LOX - lipoxygenase

MeJA - methyl jasmonate

PCD - programmed cell death

PCR - polymerase chain reaction

PG - plastoglobule

PUFA - polyunsaturated fatty acid

qPCR - quantitative PCR

SNP - single nucleotide polymorphism

TBE buffer - Tris-Borate-EDTA buffer

TP - transit peptide

TSC analysis - two standard curves analysis

Chapter 1
Introduction

The New Zealand wine industry is a rapidly growing primary sector and important contributor to the New Zealand economy. According to the New Zealand Institute of Economic Research (NZIER), the value-added contribution of the wine industry to the Gross Domestic Product (GDP) in 2008 reached NZ$1.5 billion and continues to grow. The industry is export-driven with a target goal of NZ$2 billion achieved from wine exports by 2020 (New Zealand Wine Growers Strategic Plan, 2010). Sauvignon blanc remains the best-selling New Zealand wine varietal both domestically and internationally. Specifically, Sauvignon blanc from Marlborough region has internationally been recognized as possessing unique flavour and aroma characteristics that are considered stylistically to be a definitive benchmark for this varietal (Rachman 1999; Rand *et al.* 2007). These unique features contribute to the premium prices paid for Marlborough Sauvignon blanc worldwide.

Despite all the success, New Zealand's share on the world wine market is small compared with other New World producers such as Australia, Chile or the USA. The only way for New Zealand wine industry to remain profitable and retain its position on the World Market is to produce wine of premium quality with characteristics distinct from other wines. With this in mind, New Zealand winegrowers support and promote research programs aimed to understand factors that determine and affect wine quality. In 2008 the research contribution exceeded almost twice the value of all grape and wine levies combined (http://www.nzwine.com/report/).

Arguably, the largest wine-related research programme in New Zealand is the Sauvignon Blanc Programme. The Sauvignon Blanc Programme was established in 2004 as a partnership of the New Zealand winegrowers, government and New Zealand research institutions. The programme aims to provide a better understanding of what determines the uniqueness of New Zealand Sauvignon blanc and to provide winegrowers with tools and methods, which would allow them to create a desirable wine style (http://www.sbprogramme.co.nz). Such methods include improving conventional viticultural and winemaking techniques as well as novel methods for regulating flavour and aroma compounds.

One of the objectives of the Sauvignon Blanc Programme is to identify and characterise physiological and biochemical factors involved in the synthesis of wine flavour and aroma compounds. This involves studying biochemical pathways that have a potential contribution to wine quality and isolation and characterisation of the key genes coding for the enzymes participating in such pathways.

The research described in this thesis contributes to characterisation of the biochemical pathway known as green leaf volatile (GLV)-pathway. The pathway is involved in the formation of short-chain acylic compounds collectively known as green leaf volatiles (GLVs) which have been shown to contribute to flavour and aroma in other plant species. Using a set of molecular and biochemical techniques, the role of the GLV pathway in important physiological processes, including development and stress response has been studied.

Chapter 2
Literature review

2.1 Flavour and aroma compounds in Sauvignon blanc wine

Sauvignon blanc is a white wine made from berries of the green-skinned grape cultivar Sauvignon blanc (*Vitis vinifera* L., cv. Sauvignon blanc). Sensory analysis of Sauvignon blanc wines from different countries describes important aroma characteristics of this varietal as sweet sweaty passion fruit, capsicum, passion fruit skin/stalk, boxwood/cat urine, grassy, mineral/flinty, citrus, bourbon, apple lolly/candy, tropical, mint, fresh asparagus, canned asparagus, stone fruit, apple and snow pea (Lund *et al.* 2009). New Zealand Sauvignon blanc wines predominate in fruity and green characteristics, such as tropical, sweet sweaty passion fruit, apple, stone fruit, capsicum, passion fruit skin/stalk, and fresh asparagus (Lund *et al.* 2009). In recent years, there has been a tendency to sub-divide New Zealand Sauvignon blanc into two styles based on their sub-origin. The wines from the Northern region of New Zealand, which includes Hawkes Bay and all areas North from this, are normally riper and richer and include descriptives such as melon, nectarine and other stone fruits. The Southern regions (South Island and areas of North Island below Hawkes Bay) produce lighter and crisper Sauvignon blanc styles with passion fruit, gooseberry, capsicum and various herbaceous characters (www.sbprogramme.co.nz/About_New_Zealand_Sauvignon_Blanc). Certainly the most important Southern style is world-acclaimed Marlborough Sauvignon blanc, which originates from the Marlborough region in the Northeast of the South Island. To date, Marlborough Sauvignon blanc is being considered as an international benchmark for the varietal (Rachman 1999; Rand *et al.* 2007).

Although united by the concept of Marlborough Sauvignon blanc, different wines produced in the Marlborough regions can be discriminated through sensory analysis (Parr *et al.* 2004). Such variation depends on a number of factors discussed below.

Arguably, the major factor contributing to the Marlborough Sauvignon blanc style variation is the difference in sub-regional distribution of vineyards within the Marlborough region. Furthermore, factors such as seasonal differences in the quality of grapes produced and winemaking techniques employed by different wineries further

add to style variation. In addition, there is some evidence of variation in the quality of wines produced from different parts of the same vineyard (Bramley 2005; Trought 1996).

Wine quality is a complex trait that is difficult to define. To a great extent wine quality is attributed to flavour and aroma. Flavour and aroma composition of the wine is determined by its chemical constituents and their interaction with human taste and olfactory receptors. Therefore, identification of key compounds that define individual sensory attributes and their interaction will help to understand what determines a particular wine style. Arguably, two most important groups of chemical compounds affecting Marlborough Sauvignon blanc aroma are methoxypyrazines and volatile thiols (Lund *et al.* 2009).

Methoxypyrazines are a group of nitrogen-containing heterocyclic compounds that even at trace concentrations contribute to capsicum, vegetative and herbaceous notes in wine (Allen and Lacey 1999). The three most important methoxypyrazines in wine are 2-methoxy-3-isopropylpyrazine (IPMP), 2-methoxy-3-*sec*-butylpyrazine (s-BMP) and 2-methoxy-3-isobutylpyrazine (IBMP) (Allen and Lacey 1999). All three compounds have very low perception detection thresholds (1-2 ng/L in water) and therefore affect significantly the aroma profile of wine (reviewed in Allen and Lacey 1999). Methoxypyrazines are formed in grapes and their final concentration in wine has been shown to be influenced by grape cultivar, growing conditions and viticultural practice (reviewed in Allen and Lacey 1999).

Although of high importance, methoxypyrazines were beyond the scope of this project. The research described in this thesis will be related to the formation of the precursors of the second major group of important aroma compounds in Sauvignon blanc wine, namely volatile thiols.

Volatile thiols are a group of compounds which possess a thiol (-SH) group. Individual volatile thiols have been found to contribute significantly to the varietal aroma of Sauvignon blanc wines. As shown in Figure 2.1, 4-mercapto-4-methylpentan-2-one (4MMP, [i]), 4-mercapto-4-methylpentan-2-ol (4MMPOH, [ii]) and 3-mercaptohexan-1-ol (3MH, [iii]) correspond to broom or box tree, citrus zest and passion fruit odours respectively (Darriet 1993; Darriet *et al.* 1991; Tominaga *et al.* 1998a). Tominaga *et al.* (1996) has also identified the presence in Sauvignon wine of 3-mercaptohexylacetate

(3MHA) exhibiting box tree aroma with grapefruit and passion fruit notes (Figure 2.1, iv).

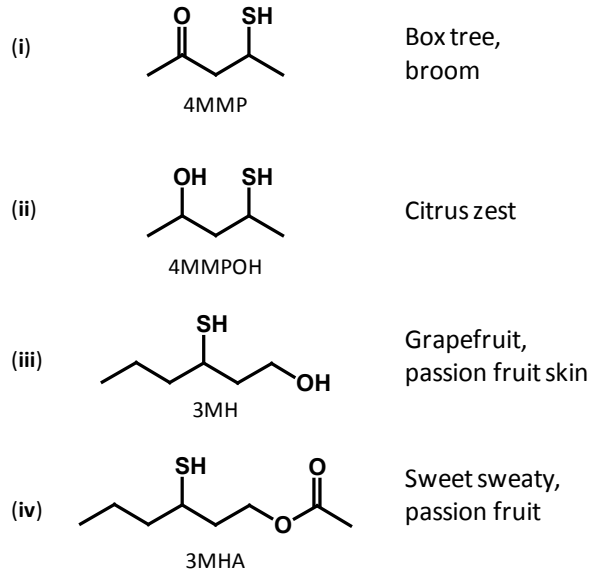

Figure 2.1 Chemical structures and sensory attributes of major volatile thiols affecting Sauvignon blanc wine aroma

4MMP, 4MMPOH and 3MH are thought to be released during alcoholic fermentation from their non-volatile precursors, S-cysteine or S-glutathione conjugates, while 3MHA is likely to be formed by esterification of 3MH in fermenting musts (Darriet *et al.* 1993; Tominaga *et al.* 1996; Tominaga *et al.* 2006; Tominaga *et al.* 1998b).

The importance of volatile thiols in New Zealand Sauvignon blanc has been studied by quantifying their levels in a number of commercial wines and comparing them with the wines from other countries (Nicolau *et al.* 2007). The research has shown increased levels of volatile thiols in most of the New Zealand wines.

Although the importance of volatile thiols in the Sauvignon blanc wine aroma is well documented, little is known about their biosynthesis. The next section will review the proposed biochemical pathways leading to the formation of volatile thiols in wine.

2.2 Precursors of the volatile thiols in Sauvignon blanc berries

Unlike methoxypyrazines, volatile thiols are not identified in grapes. It has been suggested that volatile thiols are liberated from their corresponding non-volatile precursors by wine yeast (*Saccharomyces cerevisiae*) during fermentation of grape must. There are several hypotheses that have been put forward to describe the formation of volatile thiols in wine.

2.2.1 Formation of volatile thiols from cysteinylated precursors

According to the most widely accepted hypothesis, the non-volatile precursors of 4MMP, 4MMPOH and 3MH have been identified as S-4-(4-methylpentan-2-one)-L-cysteine (4MMP-cysteine), S-4-(4-methylpentan-2-ol)-L-cysteine (4MMPOH-cysteine) and S-3-(hexan-1-ol)-L-cysteine (3MH-cysteine) respectively (Tominaga *et al.* 1998b). It has been shown that S-cysteine conjugates found in grapes can be catabolised *in vitro* to their corresponding volatile thiols by a β-lyase enzyme extracted from a bacterium *Eubacterium limosum* (Tominaga *et al.* 1998b). Therefore, it has been proposed that the release of the volatile thiols during alcoholic fermentation of grape must occurs due to the action of a β-lyase-like enzyme produced by wine yeast (*Saccharomyces cerevisiae*) (Tominaga *et al.* 1998b).

A biosynthetic mechanism of the formation of S-cysteine conjugates in grapes has been proposed by Peyrot des Gachons *et al.* (2002a). This mechanism implies the breakdown of corresponding S-glutathione conjugates (Figure 2.2). The theory was supported by identification in Sauvignon blanc must of S-3-(hexan-1-ol)-glutathione, a possible precursor of S-3-(hexan-1-ol)-L-cysteine and subsequently of 3-mercaptohexan-1-ol (3MH) (Peyrot des Gachons *et al.* 2002b). Furthermore, Thibon and colleagues (2010) observed a correlation between an increase in S-cysteine conjugate levels in grapes infected with *Botrytis cinerea* pathogen and levels of volatile thiols in the wine produced from the botrytised grapes.

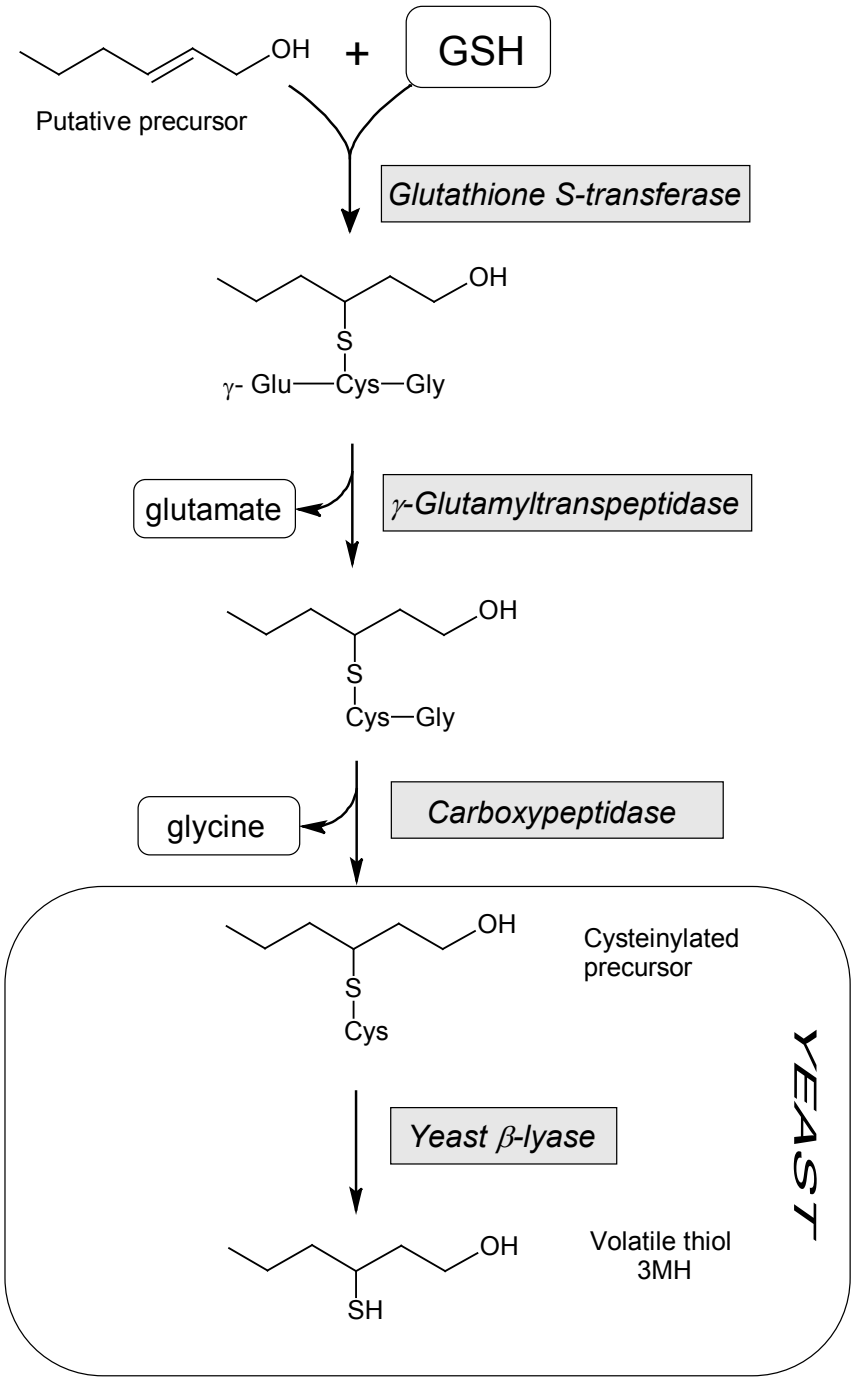

Figure 2.2 Suggested biochemical pathway leading to the formation of volatile thiols

According to this hypothesis, a putative precursor in grape berry becomes conjugated to a molecule of glutathione (GSH) by glutathione S-transferase (GST) enzyme. The conjugate is then transported by the GST or another transporter protein to a storage compartment such as vacuole. In some instances, the glutathionated precursor undergoes a subsequent action of γ-glutamyltranspeptidase producing Cys-Gly-conjugate, which can be further metabolised by carboxypeptidase or dipeptidase, releasing a cysteinylated precursor of the volatile thiol. The further metabolism occurs upon berry crushing and fermentation of the grape must by yeast. Here, a putative yeast β-lyase cleaves the cysteine residue off and converts the cysteinylated precursor to the volatile thiol.

Figure 2.2 illustrates the suggested biochemical pathway from the formation of S-glutathione conjugates through to the release of volatile thiols. The initial step of this pathway involves a formation of S-glutathione conjugate from the tripeptide glutathione (GSH) and an appropriate precursor by glutathione S-transferase (GST, EC 2.5.1.18). Further metabolism of the S-glutathione conjugate by γ-glutamyltranspeptidase and carboxypeptidase or dipeptidase eliminates glutamate- and glycine-groups respectively, leading to the formation of the S-cysteine conjugate (Jakoby *et al.* 1984; Peyrot des Gachons *et al.* 2002b; Wolf *et al.* 1996). These processes are thought to take place in grape berry tissues. Upon crushing of grape berries and during fermentation, the cysteinylated precursors are released and converted by a yeast β-lyase into corresponding volatile thiols (Tominaga *et al.* 1998b).

In vitro biochemical assays which studied the conversion of S-cysteines to volatile thiols, used S-cysteine conjugates chemically synthesised by Michael-type addition of L-cysteine to the corresponding unsaturated precursor (Peyrot des Gachons *et al.* 2000; Tominaga *et al.* 1998b). In an experiment by Tominaga *et al.* (1998b), for example, S-4-(4-methylpentan-2-one)-L-cysteine was obtained by an addition reaction of L-cysteine hydrochloride with mesityl oxide. The reduction of S-4-(4-methylpentan-2-one)-L-cysteine with sodium borohydride yielded another cysteinylated precursor, S-4-(4-methylpentan-2-ol)-L-cysteine. S-3-(hexan-1-ol)-L-cysteine was obtained by reducing S-3-(hexan-1-al)-L-cysteine prepared from (*E*)-2-hexenal and L-cysteine. Mesityl oxide and (*E*)-2-hexenal therefore provide substrates for *in vitro* generation of non-volatile precursors and subsequently of volatile thiols (Figure 2.3).

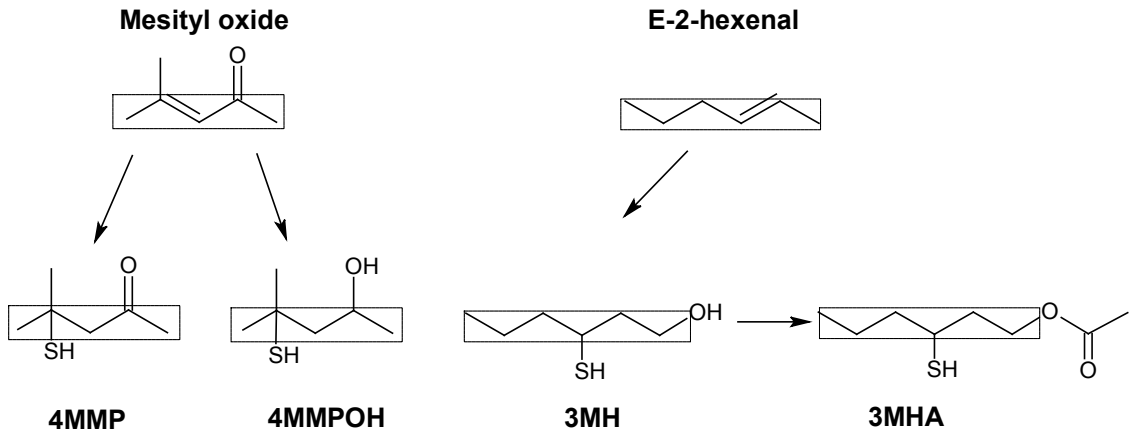

Figure 2.3 Structural similarities between volatile thiols and their *in vitro* precursors

Mesityl oxide is used for synthesis of 4MMP and 4MMPOH, while (*E*)-2-hexenal is used as a precursor for *in vitro* synthesis of 3MH and 3MHA. The carbon backbones are outlined by dashed line.

As can be seen from Figure 2.3 carbon backbones of the synthetic precursors and synthesised compounds (outlined by dashed line) are represented by short aliphatic chains, containing either 5 or 6 carbon atoms covalently bonded one with another. It is reasonable to suggest, therefore, that the same compounds exist in grapes and serve as carbon backbones for the final products, volatile thiols. Interestingly, while the presence of mesityl oxide has not yet been reported in plants, the existence of C6 and C5 unsaturated aldehydes (including (*E*)-2-hexenal), alcohols and esters is well documented (Angerosa *et al.* 2000; Matsui 2006).

2.2.2 Alternative precursors of volatile thiols

An alternative pathway to the one described above has been proposed by Schneider *et al*. (2006). The authors have shown that deuterated (*E*)-2-hexenal and mesityl oxide added to must of the grape cultivar Melon B., were converted into 3MH and 4MMP respectively. However, the identified deuterated 3MH accounted for only 10% of the total 3MH content in wine. Moreover, it has been recently suggested that cysteinylated conjugates and (*E*)-2-hexenal were not the major precursors of 3MH (Subileau *et al.* 2008). Rather it was suggested by the authors that GSH-conjugates could be the direct precursors of the volatile thiols.

Furthermore, a recent study by Roland *et al.* (2010) supports the role of GSH-conjugates as direct precursors of the volatile thiols and proposes two different origins of their formation. According to the authors, a part of the total GSH-conjugate content derives from grapes, whereas the other part can be formed during the initial stages of the winemaking process. The authors have shown that addition of glutathione and (*E*) -2-hexenal to the grape musts significantly increases the production of 3MH and 3MHA. The research also indicates significant differences in the amounts and ratios of GSH-conjugates in juices derived from different grape cultivars (Roland *et al.* 2010). For instance, the initial GSH-conjugates content in Sauvignon blanc juice was four-fold higher compared to juices from another white cultivar, Melon B. Furthermore, the research shows that different grape cultivars respond differently to artificially supplemented precursors. While the addition of (*E*)-2-hexenal and GSH increased the content of GSH-precursors almost by 70 % in Melon B., in Sauvignon blanc juices the increase was only about 2% of the initial content (Roland *et al.* 2010).

Despite the controversy around the mechanism of formation of the precursors and subsequent liberation of thiols, all suggested pathways implicate the existence of short-chain compounds, which serve as carbon backbones for the formation of thiols. Based on the structural similarity, the most likely candidates to be the precursors of volatile thiols are the C6 and C5 products of catalytic degradation of polyunsaturated fatty acids. These compounds will be reviewed in more details in the following section.

2.3 Green leaf volatiles (GLVs)

The presence of short-chain volatiles in grape juice and wine and their contribution to the final flavour and aroma composition of wine has been well documented (reviewed in Clarke and Bakker 2004; Jackson 2008). Amongst the vast range of volatile compounds present in grape must, C6 volatiles represent a large proportion of the total volatile content. For example, C6 compounds have been reported to constitute 93% of total volatile compounds in Chardonnay grapes and musts (Baumes *et al.* 1988). C6 volatiles (represented by C6 aldehydes, alcohols and esters) belong to a group of volatile compounds collectively known in plants as green leaf volatiles (GLVs) because of their aroma characteristics, which are often associated with the scent of freshly cut grass (Matsui 2006). C6 aldehydes such as hexanal, (*E*)-2-hexenal and (*Z*)-3-hexenal are formed rapidly upon berry crushing and during maceration of grape must (Ramey *et al.* 1986). During fermentation a significant proportion of C6 aldehydes are normally converted to the corresponding alcohols and esters (Clarke and Bakker 2004).

The olfactory detection thresholds of C6 aldehydes and their corresponding derivatives, alcohols and esters, vary greatly. For example, the detection thresholds in water for hexanol, (*Z*)-3-hexenol and (*E*)-2-hexenol are 2500, 70 and 400 µg/kg respectively, while the detection thresholds for the corresponding aldehydes are 5, 0.25 and 17 for hexanal, (*Z*)-3-hexenal and (*E*)-2-hexenal respectively (http://www.leffingwell.com/odorthre.htm). Since most of the grape derived C6 aldehydes during fermentation are converted into corresponding alcohols with high detection thresholds, their influence on the overall flavour and aroma of the resulting wines is often relatively insignificant. It has been reported however that New Zealand Sauvignon blanc wines, in addition to high levels of methoxypyrazines and volatile thiols, possess increased concentrations of C6 alcohols and acetates such as (*Z*)-3-hexenol and hexyl acetate that are well above their perception thresholds (Nicolau *et al.* 2007). Moreover, in Marlborough Sauvignon blanc wines, the high concentration of hexanol and (*E*)-2-hexenyl butyrate discriminates these wines together with wines from Victoria State in Australia, from wines originating in other parts of the world (Berna *et al.* 2009). These findings indicate that wine styles, as well as chemical composition of wines can be associated with particular geographical regions.

French wines are often characterised by the term “terroir”, which implies reflection of a combination of factors such as location, climate, soil and viticultural practices on the final wine style. Therefore, the chemical composition, and subsequently the aroma potential of wines, is likely to be different depending on terroir.

In biological systems, most of the chemical processes are catalysed by enzymes and regulated by intricate signal-response systems. The formation of many chemical compounds in living organisms is a result of action not by one, but rather sequential action of a number of enzymes arranged in biochemical pathways. In turn, the formation and regulation of the enzymes in a biochemical pathway is linked directly to the genetic makeup of a particular organism and genes that code for such enzymes. Therefore, the reported variation in the chemical composition and subsequently in wine styles is likely to be determined by a combination of such factors as genetic makeup of the grapes and environmental conditions they are grown.

As has been mentioned before, C6 volatile components are formed as a result of mechanical damage of grape berries during harvest, crushing and maceration. However, these compounds are also produced and released from intact berries during development (Kalua and Boss 2009). The formation of C6 components in both, intact and damaged grape berries, can be attributed to the enzyme directed metabolism of polyunsaturated fatty acids via a biochemical pathway known as lipoxygenase-hydroperoxide lyase (LOX-HPL) or GLV-pathway, which is well characterised in plants (reviewed by Matsui 2006). As will be discussed in detail in later chapters, the primary products of GLV-pathway, the short chain volatile aldehydes, can undergo a further reduction to corresponding alcohols and esters, or can be isomerised to produce a spectrum of compounds known as GLVs. Furthermore, the GLV-pathway gives rise not only to the C6 GLVs, but also to C9 compounds as will be discussed later.

As can be concluded from the discussion above, C6 compounds are abundant in plants and their biosynthesis is well documented. In contrast, relatively little is known about the mechanism of C5 volatile formation. It has been suggested, that C5 compounds can be formed via GLV-pathway in anaerobic conditions as a result of β-oxidation of 13-alkoxyl radicals by LOX itself (Gardner *et al.* 1996). The increased production of C5 volatiles has also been observed in Arabidopsis (Salas *et al.* 2006) and potato plants, where HPL expression was silenced. It is also possible, that some C5 compounds are

formed as a result of co-oxidation of grape carotenoids such as norisoprenoids by LOX activity, as it has been shown that LOXs are involved in degradation of plant carotenoids producing a range of carbonyl fragments (reviewed in Robinson *et al.* 1995).

The current investigation will focus on the functional characterisation of the GLV-pathway. Specifically, the research will be focused on individual members of LOX and HPL families involved in the formation of C6 and potentially C5 volatiles in grape berries. The GLV- pathway will be studied in the context of the direct involvement of C6 and C5 volatiles in the grape lifecycle as well as their potential influence on wine quality. Some aspects of C9 compound formation will also be touched on briefly as alternative products of GLV-pathway.

2.4 Lipoxygenases

Lipoxygenases (LOX, linoleate:oxygen oxidoreductase, EC 1.13.11.-) are a group of enzymes that account for the first step in the LOX - pathway. They belong to a class of non-haem iron-containing dioxygenases and catalyse hydroperoxidation of lipids and fatty acids containing cis, cis-1,4-pentadiene moieties in plants, animals and microorganisms (reviewed by Feussner and Wasternack 2002). Unlike in mammals, where oxygenated fatty acids derive mainly from C20-fatty-acid precursors such as arachidonic acid (AA), LOX-substrates in plants are mostly represented by C18 members of polyunsaturated fatty acids (PUFAs), in particular linoleic (LA, 18:2) and α-linolenic (LnA, 18:3) acids (Blée 1998). The oxidation of C18 PUFAs accomplished by LOXs in plants results almost exclusively in the production of 9- and 13-hydroperoxides (Blée 1998). Further metabolism of PUFA-hydroperoxides leads to the formation of a vast number of compounds in the plant collectively known as oxylipins irrespective of their structure and chain length (Grechkin 1998). A large number of publications accumulated over the past three decades demonstrate the great physiological importance of plant oxylipins and the LOXs responsible for their production (reviewed in Feussner and Wasternack 2002; Liavonchanka and Feussner 2006; Porta and Rocha-Sosa 2002; Siedow 1991; Wasternack 2007).

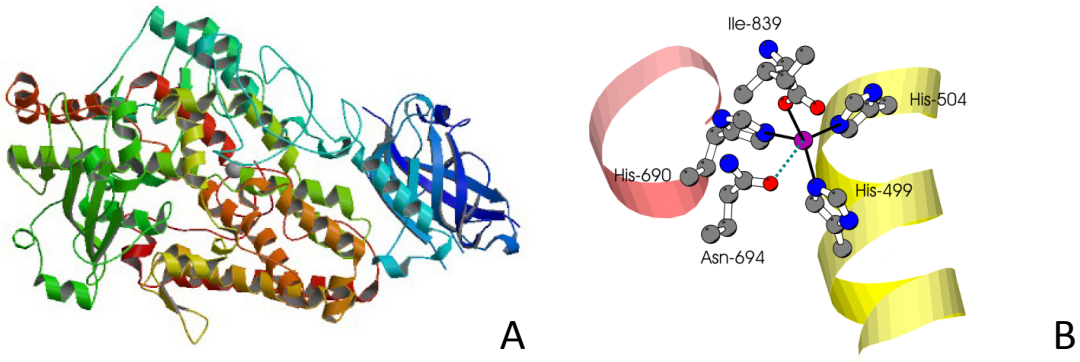

Figure 2.4 Typical plant LOX structure

The figure represents a structural model of the best-studied plant lipoxygenase, soybean LOX-1 (A) (derived from crystal structure at 1.40 Å resolution) and the amino acid residues involved in catalytic iron binding (B). The β-sheet PLAT domain is shown in blue, and the rest of the molecule makes up the catalytic LOX domain, represented mostly by α-helixes (A). The catalytic atom of iron is shown in grey (A) and in purple (B). The figures are acquired from PDB database http://www.rcsb.org/.

2.4.1 LOX protein structure

Plant LOXs have molecular weight of between 94-103 kDa and polypeptide length of between 838-923 amino acids (Shibata and Axelrod 1995). As shown in Figure 2.4.A, functional LOX monomers are represented by two main domains, an N-terminal β-barrel domain (also known as PLAT or LH2 domain, shown in blue) and a mostly α-helical catalytic domain or LOX-domain (Schneider *et al.* 2007). The suggested roles of the N-terminal domain include mediation of LOX-binding to liposomes and lipid bodies, calcium binding and in controlling translocation between subcellular compartments (reviewed by Hughes *et al.* 2001). The C-terminal catalytic domain of LOXs is highly conserved and is characterised by the presence of a motif known as the LOX-motif, His-x4-His-x4-His-x17-His-x8-His. Three of these histidines together with either an His/Asn/Ser at the conserved position, and the C-terminal isoleucine are responsible for binding a molecule of catalytic iron as depicted in Figure 2.4.B (Minor *et al.* 1996).

2.4.2 Proposed catalytic mechanism of plant LOXs

It has been proposed that the mechanism of PUFA-hydroperoxide formation by LOXs consists of three main steps: 1 – enzyme activation, 2 – removal of a proton from the activated methylene group, 3 – incorporation of a hydroperoxy group (Robinson *et al.* 1995). Both, the position of the proton removal and oxygen incorporation determines the regiospecificity and stereospecificity of an individual LOX enzyme (Perez Gilabert and Carmona 2002).

Catalytic iron in the native form of LOX enzymes is in the ferrous (Fe^{2+}) form, which cannot co-ordinate dioxygen molecules (reviewed in Robinson *et al.* 1995). Therefore, to maintain the LOX reaction at the maximum velocity, all LOX protein molecules have to be activated by conversion of inactive (Fe^{2+}) into active (Fe^{3+}) LOX form. Such conversion is initiated by trace amounts of PUFA-hydroperoxides in the presence of molecular oxygen and FA substrate (Schilstra *et al.* 1992).

The mechanism by which the activated LOX incorporates a hydroperoxy-group into an acyl-chain of linoleic acid is schematically illustrated in Figure 2.5. After the stereoselective removal of hydrogen from the methylene carbon on a cis, cis-1, 4-pentadiene unit (Figure 2.5.A), molecular oxygen (O_2) is introduced into the fatty acid

chain at the end of the pentadiene moiety either at the position C9 or C13. This promotes the movement of one double bond towards the second double bond, attaining a trans-configuration and forming an unstable peroxyl radical (Figure 2.5.B). The highly unstable peroxyl is instantaneously reduced to its hydroperoxy form (Figure 2.5.C).

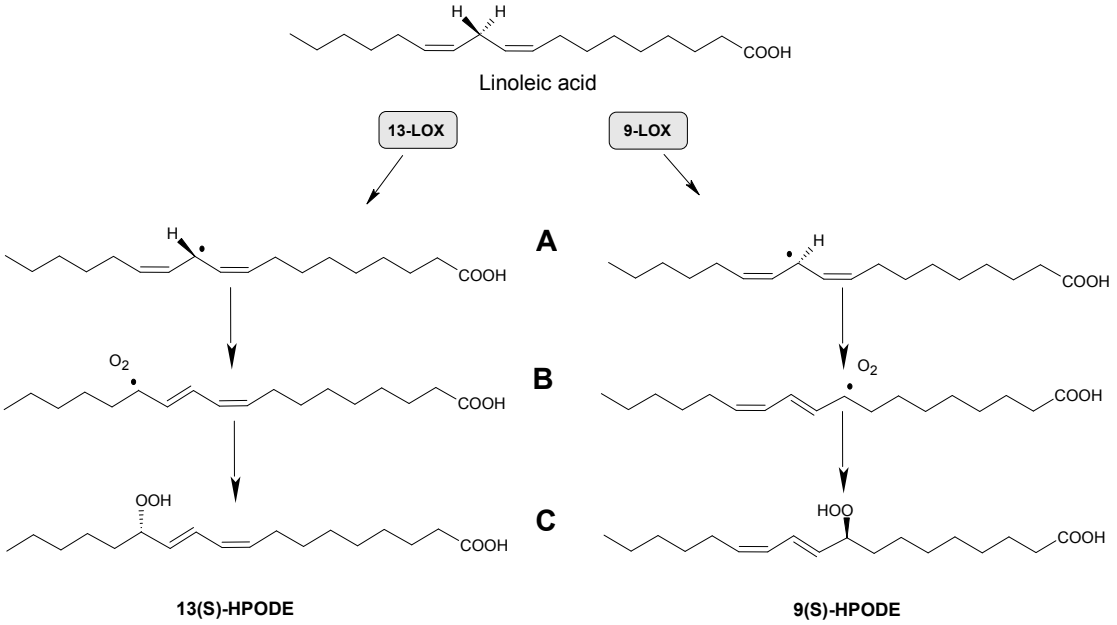

Figure 2.5 The LOX-catalysed oxygenation of linoleic acid into 13(S)-HPODE and 9(S)-HPODE

The metabolism of linoleic acid is catalysed by activated 13-LOX or 9-LOX and consists of A) – stereospecific hydrogen removal from the methylene group between two double bonds; B) – binding of molecular oxygen and formation of intermediate peroxyl radical, C) – reduction of the fatty acid peroxyl radical to fatty acid hydroperoxide.

Most of the functionally characterised LOXs act in a regiospecific manner, transforming LA into either (9Z,11E)-13-hydro(pero)xy-9,11-octadecadienoic (13-HPODE) or (10E,12Z)-9-hydro(pero)xy-10,12-octadecadienoic (9-HPODE) acids; and LnA acid into either (9Z,11E, 15Z)-13-hydro(pero)xy-9,11,15-octadecatrienoic (13-HPOT) or (10E,12Z,15Z)-9-hydro(pero)xy-10,12,15-octadecatrienoic (9-HPOT) acids (Grechkin 1998). Regiospecificity and stereospecificity of mammalian and plant LOXs have been attributed to certain amino acid residues located inside the substrate binding pocket of LOX proteins (Liavonchanka and Feussner 2006; Sloane *et al.* 1991). Specifically, a single amino acid residue (amino acid residue 557 in soybean LOX1) has been suggested to influence 13(S)- or 9(S)-regiospecificity of plant LOXs

(Liavonchanka and Feussner 2006). At this conserved position, all characterised plant 13-LOXs contain either phenylalanine or histidine residues, whereas all 9-LOX members contain a valine (Figure 2.6).

LOX stereospecificity (the ability of LOX enzyme to produce either S- or R-enantiomers) has been attributed to another amino acid within the LOX domain (residue 542 in soybean LOX1) (Coffa and Brash 2004). All plant LOXs identified to date contain alanine at this specific site and all PUFA-hydroperoxides formed by plant LOXs exist as S-stereoforms (Liavonchanka and Feussner 2006).

Two models exist currently that describe the mechanism determining regio- and stereospecificity of LOXs, the space related model and the substrate orientation model (Figure 2.6). The space-related model (Figure 2.6. B) has been proposed based on data from mammalian LOXs (Sloane *et al.* 1995). According to this model, the substrate always penetrates the active site with its methyl end first and the position of oxygenation is determined by the depth of a substrate-binding pocket. In comparison, the substrate orientation model better explains the action mechanism of plant LOXs. According to this model, the position of oxygenation is determined depending on the orientation of the substrate molecule penetrating the LOX binding pocket (Gardner 1991). Penetration of the fatty acid molecule with its methyl end leads to formation of 13-hydroperoxide, whereas penetration with its carboxylic group yields 9-hydroperoxides Figure 2.6.A).

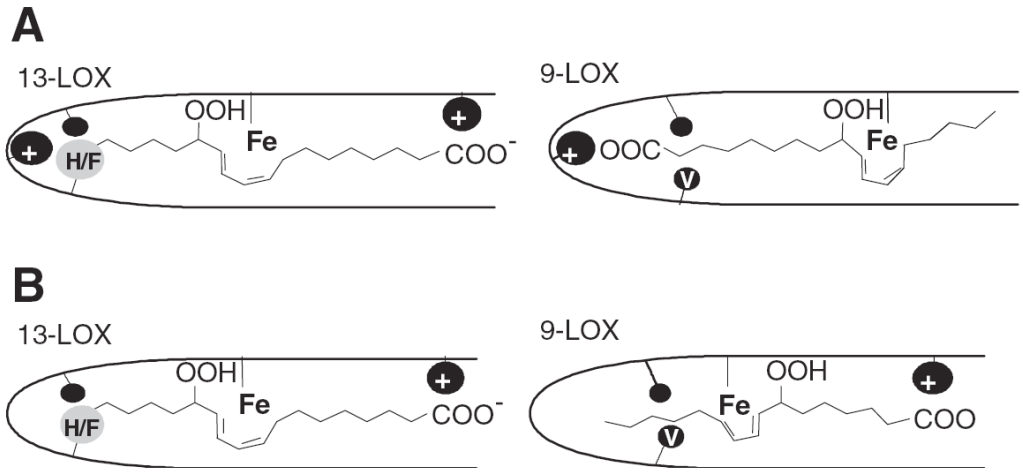

Figure 2.6 Two proposed models explaining the mechanism underlying LOX regiospecificity (reproduced from Figure 3 from Liavonchanka and Feussner 2006).

A – substrate orientation theory; B – space-related theory.

It should be noted however, that the existing models for the structural and mechanistic basis for LOX region and stereospecificity are insufficient to account for all observed activities. For example, several plant LOXs exhibit dual regiospecificity, producing both, 13- and 9-hydroperoxides at various ratios (Porta and Rocha-Sosa 2002).

2.4.3 "Non-standard" behaviour of LOXs

Although PUFAs are considered to be the main substrates for LOXs, the ability of these enzymes to work on other substrates has been demonstrated. Kühn *et al*. (1991) reports oxygenation of 12-keto-(9Z)-octadecanoic acid methyl ester by soybean LOX1, resulting in the production of 9, 12-diketo-(10E)-octadecanoic acid methyl ester and 12-keto-(10E)-dodecenoic methyl ester. Similarly, (10E,15Z)-9-hydroperoxy-12-oxo-13-hydroxy-10,15-octadecadienoic acid (α-ketol hydroperoxide) was identified as the product of *in vitro* 13-HPOTrE metabolism in wheat seedlings (Grechkin *et al.* 1991). The site of LOX action in these substrates is (3Z)-butene-1-one residue rather than classical 1,4-pentadiene moiety of PUFAs (Grechkin 1998).

Another example of deviation from the conventional behaviour is involvement of LOXs in degradation of plant carotenoids. In their review, Robinson *et al.* (1995) describe

cases where LOX activity led to loss of colour in tomato, peas and beans. The authors suggest the observed loss of pigmentation is caused by lipoxygenase-driven degradation of various carotenoids located in chloroplasts and chromoplasts of plants. These findings are important to our research, as products of carotenoid metabolism are another important source of aroma and flavour precursors in grapevine (Oliveira *et al.* 2006).

Another important feature of some LOXs is their ability, under certain conditions, to further metabolise PUFA-hydroperoxides, which was mentioned in section 2.3.

2.4.4 Classification of LOXs

The classification of plant LOXs is complicated due to structural differences, substrate specificity, pH optimum and mechanistic properties (Blée 1998). Historically, LOXs have been classified based on their biochemical properties and pH optima (Siedow 1991). Recently, a new classification of the LOX superfamily has been proposed.

Depending on the position of oxygenation on a fatty acid backbone (either at carbon-9 or carbon-13), LOXs can be divided into 9-LOX or 13-LOX subclasses respectively (Liavonchanka and Feussner 2006). This classification, however, is also relative because a number of LOXs display dual regiospecificity and are able to produce either 13- or 9-hydroperoxides to a greater or lesser extent (Porta and Rocha-Sosa 2002). Another suggested classification separates 13-LOXs into type I and type II enzymes based on their protein structure and overall sequence similarity (Shibata and Axelrod 1995). Type I LOXs lack a plastid transit peptide and have high sequence similarity among them, whereas type II LOXs feature plastid transit peptide and exhibit low-to-moderate sequence similarity with the members of the type I family. Interestingly, members of type I 13-LOXs are found predominantly in legume plants (reviewed in Feussner and Wasternack 2002) . To date, there are no 9-LOXs reported to possess a plastid transit peptide, and all 9-LOXs are regarded as type I 9-LOXs.

2.4.5 Cellular and subcellular localisation of LOXs

LOXs have been found in many plant organs and tissues, including leaves, stems, roots, flowers, fruits and seeds (reviewed in Agrawal *et al.* 2004; Andreou *et al.* 2009; Baysal and Demirdöven 2007; Feussner and Wasternack 2002; Gardner 1991). It has been observed, that 13-LOXs are present mostly in green plant tissues and are more abundant

than 9-LOXs, which are found mostly in non-green organs (Grechkin 1998). The highest concentration of 13-LOXs appears to be in the stroma or within the envelope fraction of chloroplasts (Liavonchanka and Feussner 2006), whereas the members of 9-LOX subfamily have only been found in the cytosol (Feussner and Wasternack 2002). Recently, LOX members that are similar to type I 13-LOXs have been found within a lipid monolayer enclosing lipid bodies (Feussner *et al.* 2001; Hause *et al.* 2000). It has been suggested that these enzymes are involved in the mobilization of neutral lipids contained in lipid bodies during seed germination (Feussner *et al.* 2001) and fruit ripening (Leone *et al.* 2006).

Subcellular localisation is an important factor determining LOX's functionality, which has also a direct impact on the physiological role of the particular LOX protein *in planta*.

2.4.6 Physiological roles of LOXs

The main role of LOXs appears to be their involvement in PUFA metabolism and in the generation of biologically active oxylipins.

Of particular interest to this current study is the role of LOXs in grape berries as it relates to flavour and aroma formation. LOXs involvement in maturation and ripening has been reported in kiwifruit (Zhang *et al.* 2006a), saskatoon (Rogiers *et al.* 1998), strawberry (Leone *et al.* 2006) and tomato (Griffiths *et al.* 1999a). Processes occurring during fruit maturation and ripening have been associated mainly with degradation of cell membranes and senescence (Rogiers *et al.* 1998). Recently, extensive data has been accumulated on the involvement of LOXs in plant defence against pathogens, herbivores and abiotic stress (reviewed by Blee 2002; Matsui *et al.* 2006; Porta and Rocha-Sosa 2002). LOXs are also involved in mobilization of storage lipids as a carbon source for the germinating seedlings of some oilseed plants (Feussner *et al.* 2001; Porta and Rocha-Sosa 2002).

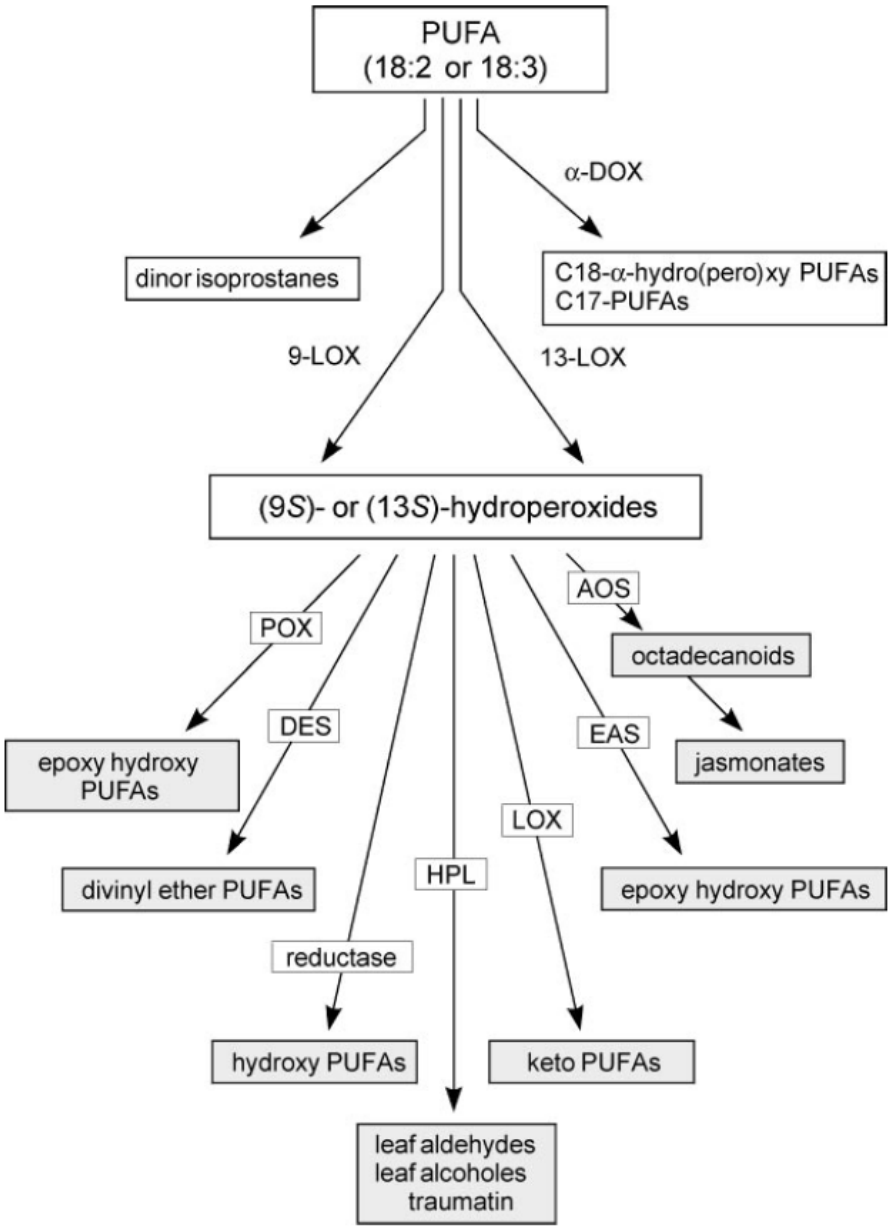

Figure 2.7 Metabolism of PUFAs leading to 9-LOX-derived and 13-LOX-derived oxylipins in plants (reproduced from Figure 3 from Feussner and Wasternack 2002).

AOS, allene oxide synthase; **DES,** divinyl ether synthase; **α-DOX**, α-dioxygenase; **EAS**, epoxy alcohol synthase; **HPL**, hydroperoxide lyase; **LOX**, lipoxygenase; **POX**, peroxygenase; **PUFAs**, polyunsaturated fatty acids.

LOX activity represents the key gateway for the biosynthesis of oxylipins. The range and physiological functions of oxylipins, however, is determined mostly by subsequent enzymatic activity (Figure 2.7). Although a number of enzymes can metabolise PUFA-hydroperoxides in plants, the most prevalent and the best studied to date are members of

CYP74 family: allene oxide synthase (AOS), hydroperoxide lyase (HPL) and divinyl ether synthase (DES), which are reviewed later.

2.4.7 LOX genes

Plant LOXs are typically encoded by members of LOX-gene families of varying sizes. Six members have been reported in Arabidopsis, 14 members in potato (Liavonchanka and Feussner 2006), 16 members in rice (Agrawal *et al.* 2004), 15 members in medicago and at least 19 members in soybean (Shin *et al.* 2008). Genes coding for LOXs in plants share some structural similarities and usually consist of 8-10 exons with highly conserved exon/intron boundaries (Lutteke *et al.* 2003).

As described in section 2.4.4, genes coding for LOXs in plants can be classified as 13- and 9-LOXs based on regiospecificity of the enzymes they encode. The 13-LOXs in turn, can be divided into two families, type I and type II, with respect to their amino acid sequence homology and presence or absence of putative transit peptide sequences. Feussner and Wasternack (2002) have employed the classification of LOXs based on presence or absence of transit peptide and suggested an alternative naming for plant LOXs. According to this nomenclature, *AtLOX1* gene from Arabidopsis, for example, is known as *LOX1_At_1*, showing that *AtLOX1* is a type I LOX. In the discussion below, the original gene names as well as their alternative names (in parenthesis) will be used.

2.4.7.1 Arabidopsis LOX genes

In *Arabidopsis thaliana*, two out of six identified LOX genes are 9-LOXs and the remaining four are 13-LOXs as determined by *in vitro* biochemical assays of the corresponding recombinant proteins (Bannenberg *et al.* 2009). Based on the sequence analysis, all four Arabidopsis 13-LOXs are type II genes (Bannenberg *et al.* 2009). Transcripts of *AtLOX1* (*LOX1_At_1*), a 9-LOX gene, has been found in young seedlings, leaves, roots and inflorescences of Arabidopsis plants with the highest levels reported in roots and young seedlings (Melan *et al.* 1993). Recent studies indicate the importance of *AtLOX1* together with another 9-LOX gene, *AtLOX5*, in regulating lateral root development and defence response via activating specific signalling cascades (Vellosillo *et al.* 2007). In comparison, transcripts of *AtLOX2* (*LOX2_At_1*), a 13-LOX, have been found in leaves and in inflorescences, but not in roots, stems and seeds (Bell

and Mullet 1993). Furthermore, *AtLOX1* and *AtLOX2* transcript levels in different tissues, showed differential response upon treatment with MeJA. While *AtLOX2* accumulated rapidly in MeJA-treated leaves, there was no accumulation observed in MeJA treated roots (Bell and Mullet 1993). In contrast, *AtLOX1* was not induced in MeJA-treated leaves, while had increased levels of its transcripts in MeJA-treated roots (Bell and Mullet 1993; Melan *et al.* 1993). Although non-responsive to MeJA treatment, *AtLOX1* was induced in Arabidopsis leaves inoculated with *Pseudomonas syringea*, indicating its potential role in response to pathogens (Melan *et al.* 1993).Wounding of Arabidopsis leaves resulted in expression of *AtLOX2,* rather than *AtLOX1* (Bell and Mullet 1993). Moreover, *AtLOX2* had been suggested to be required for the production of wound-induced jasmonates in leaves, as the mutant plants with reduced *AtLOX2* expression failed to produce JA upon wounding (Bell *et al.* 1995). *AtLOX3*, *AtLOX4* and *AtLOX6* were identified as type II 13-LOXs, but have not been extensively characterised at this time.

2.4.7.2 Potato LOX genes

In potato three different LOXs have been characterised (Royo *et al.* 1996). Two of the three, *Lox2* (*LOX2_St_1*) and *Lox3* (*LOX2_St_2*) have been described as 13-LOXs, while the third, *Lox1* (*LOX1_St_1*), is reported to encode a 9-LOX. All three genes exhibit differential transcript distribution throughout the plant. *Lox1* was found to be expressed in tubers and roots, *Lox2* is expressed in leaves and *Lox3* is expressed in leaves and roots. Similar to *AtLOX2* from *Arabidopsis*, transcripts of potato type II 13-LOX genes, *Lox2* and *Lox3* were found to accumulate after wounding of leaves, whereas *Lox1* appeared to be involved in the tuber development and did not show any change in transcription patterns associated with plant damage (Royo *et al.* 1996).

2.4.7.3 Tomato LOX genes

The LOX-gene family in tomato seems to be similar to that of potato. At the nucleotide level, tomato genes *TomLoxA* and *TomLoxB* resemble *Lox1* from potato, *TomLoxC* is similar to *Lox2*, and *TomLoxD* shows identity with the potato *Lox3* gene (Heitz *et al.* 1997). Similar to potato *Lox2* and *3*, *TomLoxC* and *TomLoxD* possess N-terminal extensions and are both targeted to the chloroplast (Heitz *et al.* 1997). In contrast, *TomLoxA* and *TomLoxB lack* sequences encoding chloroplast transit peptides and are

thought to be 9-LOXs. This classification was further supported by experiments on transgenic tomato plants, in which levels of *TomLoxA* and *TomLoxB* expression were silenced (Griffiths *et al.* 1999b). The reduction in *TomLoxA* and *TomLoxB* transcript levels did not result in a reduction of C6 volatiles in transgenic tomato fruits (Griffiths *et al.* 1999b).

TomLoxC transcripts were found to accumulate in fruits upon ripening, while *TomLoxD* was not found to be expressed in fruits (Heitz *et al.* 1997). The transcript profile of *TomLoxC* during the fruit development further implicates LOXs involvement in the disintegration of thylakoid membranes and chloroplast-to-chromoplast transition during fruit ripening (Thelander *et al.* 1986). Interestingly, unlike its homologue *Lox2* from potato, *TomLoxC* transcripts were not detected in tomato leaves after wounding (Heitz *et al.* 1997). Instead, *TomLoxD* was expressed transiently in wounded tomato leaves (Heitz *et al.* 1997). These observations suggest that despite the high sequence similarity and close phylogenetic relationship between potato and tomato LOXs, homologous genes from these closely related species are regulated differently, and may well have differing physiological functions in each species.

2.4.7.4 LOX genes from monocot species

Analysis of the monocot rice (*Oriza sativa* L.) genome revealed, that in rice at least 16 members of LOX family (*OsLOX1-16*) are involved in the octadecanoid pathway with sequence similarities among the members ranging from 25% to 99% (Agrawal *et al.* 2004). Moreover, monocot LOXs are predicted to be targeted to a range of compartments in addition to the chloroplast including microbodies, nucleus and the mitochondrial inner membrane (Agrawal *et al.* 2004). Interestingly, seven rice LOXs were suggested to be involved, not only in the octadecanoid pathway, but also in fatty acid biosynthesis (Agrawal *et al.* 2004). Four of the seven LOXs, showed high sequence homology with type II-LOX genes characterised in barley, tomato and potato (Agrawal *et al.* 2004).

Maize (*Zea mays* L.), in addition to several typical LOXs, has been recently reported to contain a LOX gene encoding an enzyme with unusual properties (Gao *et al.* 2008). Based on phylogenetic analysis, *ZmLOX6* (*LOX2_Zm_6*) is distantly related to other plant LOXs and despite its predicted cytoplasmic localisation, has been isolated from

chloroplasts (Gao *et al.* 2008). *ZmLOX6* is expressed predominantly in maize leaves and transcription of the gene is induced strongly by treatment with JA and the fungal pathogen *Cochliobolus carbonum (Gao et al. 2008)*. However, the biochemical characterisation of the recombinant ZmLOX6 protein has revealed that, unlike other plant LOXs, ZmLOX6 fails to produce PUFA-hydroperoxides and instead forms odd-chain fatty acids and C5 compounds (Gao *et al.* 2008).

It is unclear if such atypical LOXs are present only in monocot-species. Further characterisation of dicot genomes with large LOX families will help to determine whether novel LOX action is widely spread among all plants. This pathway is interesting in the context of C5 compound biosynthesis.

2.5 Hydroperoxide lyase (HPL) and green leaf volatile (GLV)-pathway

PUFA-hydroperoxides are relatively unstable compounds, which in a cell-free environment may decompose spontaneously. In plant cells however, the metabolism of 13- and 9-hydroperoxides is accomplished predominantly by enzyme action, producing a vast range of oxylipins (reviewed in Andreou *et al.* 2009). Although several enzymes have been shown to be involved in degradation of LOX products, the major PUFA-hydroperoxide-metabolising enzymes belong to a family of CYP74 oxidases (Feussner and Wasternack 2002).

2.5.1 CYP74 enzyme family

CYP74 enzyme family is represented by atypical members of a large cytochrome P450 oxidase superfamily (Stumpe and Feussner 2006). In contrast to other members of the P450 superfamily, members of CYP74 family do not act as monooxygenases, but rather metabolise PUFA-hydroperoxides producing oxylipins (Lee *et al.* 2008). Furthermore, in contrast to other P450s, CYP74 enzymes do not require either oxygen or a NADPH-reductase for catalytic function, and instead utilises the hydroperoxide moiety in a FA-hydroperoxide substrate to perform the reaction (Noordermeer *et al.* 2001a).

To date, three distinct members of the CYP74 family have been well characterised in plants, namely allene oxide synthase (AOS), hydroperoxide lyase (HPL) and divinyl ether synthase (DES) (Figure 2.8) (Blée 1998; Howe and Schilmiller 2002; Stumpe and Feussner 2006).

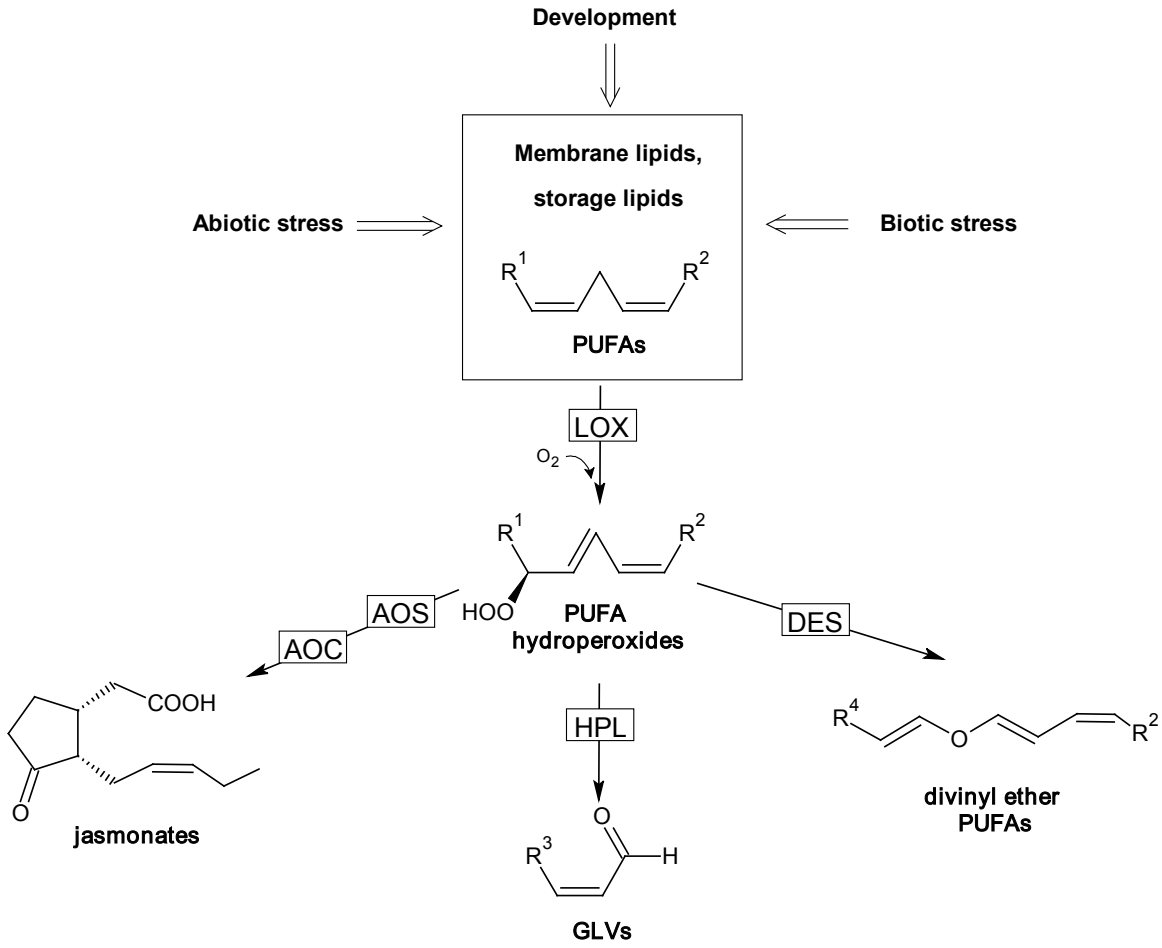

Figure 2.8 The most common branches of the LOX pathway and their products

Metabolism of PUFA-containing lipids is initiated by enzymatic action of LOXs regulated by various developmental and environmental stimuli. The products of LOX action, PUFA-hydroperoxides, are further metabolised by members of the CYP74 family to produce oxylipins. **AOS**: allene oxide synthase, **AOC**: allene oxide cyclase, **HPL**: hydroperoxide lyase, **DES**: divinyl ether synthase, **LOX**: lipoxygenase.

AOS catalyses the first committed enzymatic step in the production of jasmonic acid (JA) and its derivatives (collectively known as jasmonates). This group of compounds play an important role in intra- and intercellular plant signalling (Weber 2002). HPL enzymes produce short-chain volatile aldehydes (GLVs, important signalling and antimicrobial molecules) and oxoacids, the precursors of wound healing hormone traumatin (Blée 1998). Action of DES results in the production of divinyl ethers such as colneleic and colnelenic acids, which are deterrents to pests and pathogens (Vancanneyt *et al.* 2001).

It is generally accepted, that AOS enzymes that are specific to 13(S)-hydroperoxides as substrates are regarded as CYP74A subfamily, while HPLs exhibiting substrate specificity towards 13(S)-hydroperoxides are classified as CYP74B (Stumpe and Feussner 2006). AOS and HPL members that prefer 9(S)-hydroperoxides or exhibit dual regiospecificity (metabolise both 13(S)- and 9(S)-hydroperoxides) are regarded as CYP74C, and DES enzymes form CYP74D subfamily (Stumpe and Feussner 2006).

Although members of CYP74 subfamilies metabolise PUFA-hydroperoxides into a number of different oxylipins, they share many structural and functional similarities amongst themselves, including sequence similarities and mechanism of catalysis (reviewed by Brash 2009). This is supported by recent structural studies of CYP74 enzymes by Toporkova *et al.* (2008) and Lee *et al.* (2008), which showed that even a single amino acid substitution can convert AOS to a protein displaying HPL activities.

Although all CYP74 enzymes produce a range of very important plant oxylipins, the further review will focus mainly on the HPL branch of the LOX pathway (otherwise known as GLV-pathway) as a likely source of important flavour and aroma precursors in wine.

2.5.2 Hydroperoxide lyase, HPL

HPL accounts for the second step in the GLV-pathway leading to the production of short-chain aliphatic volatiles and oxoacids by catalysing the cleavage of PUFA-hydroperoxides formed by LOXs (Vancanneyt *et al.* 2001).

2.5.2.1 Classification of HPLs

Although HPLs have been studied for some time, they still remain unregistered in the EC enzyme classification system. HPLs can be classified dependant on the mechanism of cleavage into two types, “homolytic” and “heterolytic” (Grechkin 1998). The latter type of HPLs can be classified dependant on substrate specificity into 13-, 9/13- and 9-HPLs. Figure 2.9 illustrates possible fates of 13- and 9-hydroperoxides depending on type or class of HPLs involved in the metabolism.

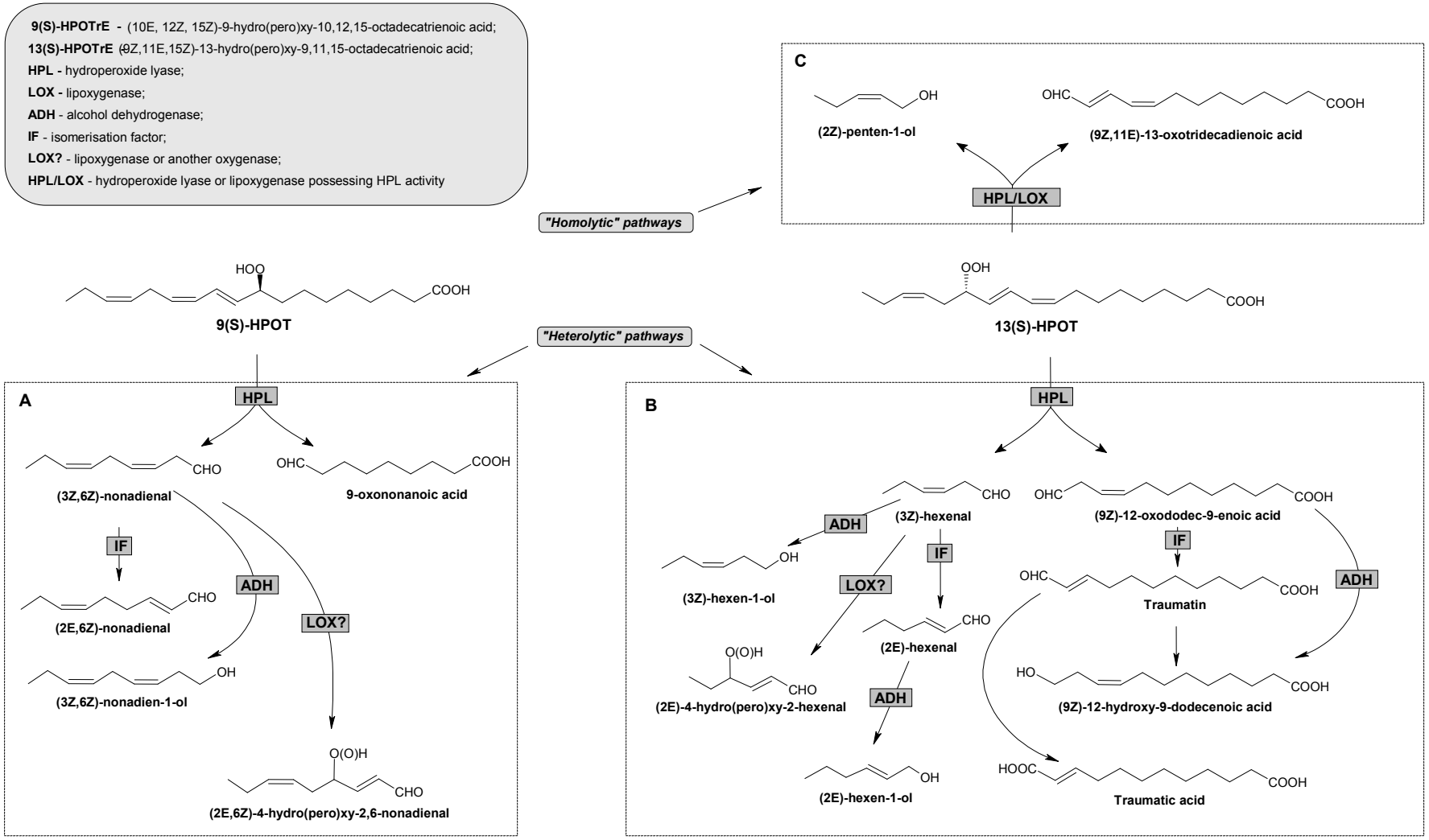

Figure 2.9 Overview of PUFA-hydroperoxide metabolism via different branches of GLV-pathway.

2.5.2.1.1 The "homolytic" branch

As shown in Figure 2.9.C, the "homolytic" mechanism of HPL cleavage is accomplished via β-scission of 13-hydroperoxides, which results in the formation of C5 volatile compounds and C13 oxoacids (Grechkin 1998; Salch *et al.* 1995). The existence of "homolytic" HPLs has been reported predominantly in lower plants and fungi (Gardner 1995). Formation of C5 volatile aldehydes has also been reported in higher plants, but it is not clear whether the C5 compounds are formed by a "homolytic" HPL or as a result of secondary activity of LOX enzymes (Gardner 1989; Salch *et al.* 1995).

Although not well studied, the "homolytic" branch of the GLV-pathway is of high interest for the current investigation as a potential source of C5 precursors of important flavour and aroma compounds in grapes.

2.5.2.1.2 The "heterolytic" branch

In contrast to the "homolytic" branch, the "heterolytic" decomposition of both 13- and 9-hydroperoxides is well studied and is the major source of GLVs in plants (Matsui 2006). "Heterolytic" HPLs perform PUFA-hydroperoxide cleavage by forming intermediate short-lived hemiacetals, which spontaneously decompose producing aldehydes and oxoacids (Grechkin *et al.* 2006). The further review will be dedicated to "heterolytic" HPLs as the best studied to date type of HPLs.

Based on substrate preference, HPLs can be grouped into three classes: 13-HPLs, 9/13-HPLs and 9-HPLs. The 13-HPLs utilise either 13-HPODE or 13-HPOT as a substrate, and form C6 aldehydes and C12 oxoacids by cleaving the carbon-carbon bond adjacent to peroxidised C13 atom, as shown in Figure 2.9. B. Similarly, the 9-HPLs convert 9-HPODE or 9-HPOT into C9 aldehydes and C9 oxoacids (Figure 2.9.A) (Blée 1998; Grechkin 1998; Mita *et al.* 2005). The 9/13-HPLs can work on both 9- and13-hydroperoxides with similar efficiency to produce either C9 or C6 compounds (Feussner and Wasternack 2002).

Notably, members of different HPL classes also group into two distinct phylogenetic clades. Specifically, 13-HPLs form CYP74B clade and 9/13- and 9-HPLs together with 9-AOSs form the CYP74C clade (Stumpe and Feussner 2006).

2.5.2.2 Structure and reaction mechanism

HPLs, like other cytochrome P450 enzymes, are haem-containing proteins. Crystallographic structures of HPLs have not been reported to date. However, the crystal structure of closely related AOS from *Arabidopsis* has been recently solved (Lee *et al.* 2008).

A recent study comparing the crystal structures of prokaryotic and eukaryotic P450s revealed, that members of P450 superfamily share a common structural fold even when they share a low level of sequence similarity (Lee *et al.* 2008). Based on these observations, it can be suggested that HPLs, as per other P450 members, possess a triangular shape with an active-site haem, bound by highly conserved residues, between parallel helices of the protein (Noordermeer *et al.* 2001a). Despite the high structural resemblance with other P450s (as judged from comparison of *Arabidopsis* AOS with other P450s from other organisms), members of CYP74 possess a number of features and properties unique to this family. For instance, all CYP74s include a nine amino acid insertion in the important haem-binding loop, which alters the active site topology and potentially alters the redox interaction, which is typical for P450 enzymes (Lee *et al.* 2008). This, together with some other structural differences of CYP74s, is thought to preclude a conventional monooxygenase activity and determines the ability of CYP74 members to utilise a hydroperoxide moiety of PUFA-hydroperoxides for their structural rearrangements (Lee *et al.* 2008).

As shown in Figure 2.10, the first intermediate product of HPL activity (as well as AOS and DES activity) is an epoxyallylic radical carbocation formed from the acyl hydroperoxide (Feussner and Wasternack 2002). However, unlike AOS and DES enzymes, which deprotonate the carbocation producing stable products, HPLs rearrange positive charges on the carbocation, thereby cleaving the carbon backbone of the hydroperoxide and producing an aldehyde and an oxoacid (Figure 2.10). Study by Lee and colleagues (2008) suggests that specialisation of HPL activity may be governed by a few important amino acid residues within its active site. The authors have shown that

when one of the important residues in *Arabidopsis* AOS protein was substituted with the residue specific for HPL enzymes, the mutated form of the protein exhibited HPL activity. This observation is very important for predicting CYP74 protein activities based on its amino acid sequence information and should be taken into account when characterising plant HPLs.

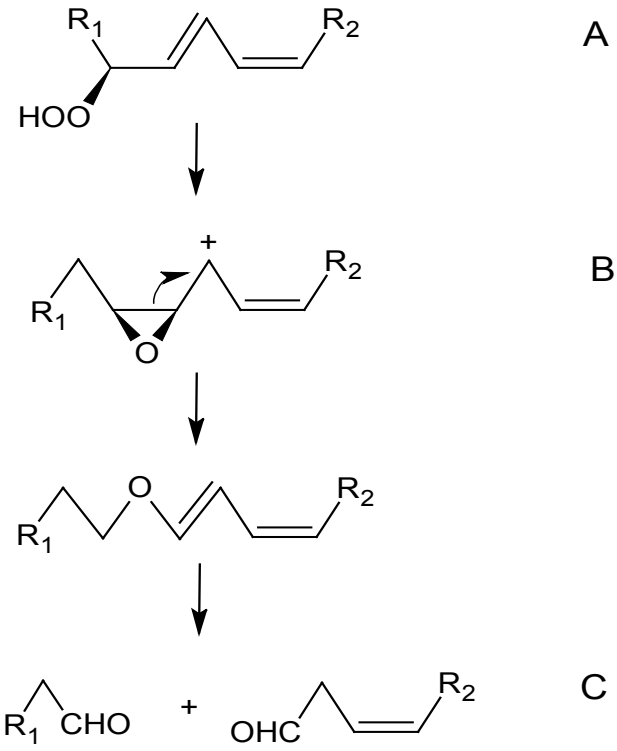

Figure 2.10 Proposed reaction mechanism of HPL enzyme (according to Feussner and Wasternack 2002).

A PUFA-hydroperoxide (**A**) is converted into final products, a volatile aldehyde and an oxoacid (**C**) via intermediate formation of an epoxyallylic radical carbocation (**B**).

2.5.2.3 Subcellular localisation

Plant HPLs have been found to be localised in various organs and tissues, often co-localising with the corresponding LOXs (Froehlich *et al.* 2001; Grechkin 1998). In green tissues 13-HPLs are localised in chloroplast thylakoids and in the outer membrane of the chloroplast envelope (Feussner and Wasternack 2002; Liavonchanka and Feussner 2006).

In contrast to 13-HPLs, localisation of the HPLs involved in metabolism of 9-hydroperoxides is not well documented. Most of 9- and 9/13-HPLs characterised to date, have been found in non-green organs and have an extraplastidal localisation (Froehlich *et al.* 2001; Grechkin 1998). Furthermore, subcellular localisation studies using fluorescently labelled chimeric constructs indicate that 9-HPL and 9/13-HPL are localised to lipid bodies in almond and medicago respectively (De Domenico *et al.* 2007; Mita *et al.* 2005).

2.5.2.4 Isomerisation of C6 and C9 aldehydes, their reduction and oxygenation

The primary unsaturated derivatives of HPL action, cis-unsaturated aldehydes, usually isomerise and form secondary compounds, trans-unsaturated derivatives (Figure 2.9). Most of this isomerisation is thought to be spontaneous. However, the presence in plants of alkenal isomerases suggests a possible enzymatic involvement in the isomerisation reaction (Grechkin 1998; Phillips *et al.* 1979).

The primary and secondary HPL products may also undergo aldehyde reduction by means of alcohol dehydrogenase leading to the formation of corresponding alcohols (Figure 2.9). Alternatively, cis-aldehydes may undergo subsequent oxygenation to produce corresponding oxy- or peroxy-aldehydes (Gardner and Grove 1998; Gardner and Hamberg 1993; Takamura and Gardner 1996). It is unclear, however, whether this conversion is driven by LOX or by another kind of oxygenases (Gardner and Grove 1998; Takamura and Gardner 1996). Oxygenated products are also of interest to the current research as they possess active sites in the form of hydroxy- or peroxy-groups and may represent sites targeted for conjugation with GSSH by GSTs. These compounds are similar to the non-volatile precursors of volatile thiols identified in grapes as described in section 2.2.

2.5.2.5 Physiological significance of GLVs

The GLVs produced via the LOX-HPL pathway play important roles as plant scent sources, volatile phytoalexins, and as signalling and antimicrobial compounds (Blée 1998). Treatment of plant organs with C6 volatiles induces accumulation of anthocyanins, phytoalexins, terpenoids in plants implying a role for such compounds, together with jasmonates, in signalling and activating major defence and stress related pathways in plants (Duan *et al.* 2005).

Plants, infected by pathogens accumulate GLVs. Both, 13- and 9-HPL products possess bacteriocidal and antifungal properties and their accumulation inhibits the pathogen growth during the earlier stages of the infection (reviewed in Blée 1998). Further accumulation of GLV is toxic to plant cells and leads to plant hypersensitive response via programmed cell death (PCD) (Buonaurio and Servili 1999; Croft *et al.* 1993). PCD results in death of plant cells adjacent to the pathogen site, thereby preventing the spread of the pathogen.

HPL-derivatives have also been implicated in indirect plant defence against insects by attracting natural enemies of the pests (reviewed by Matsui 2006).

Apart from aldehydes, another primary product of HPL activity is the wound hormone called traumatin (Figure 2.9. B). This hormone has been found to be responsible for inducing callus growth and wound healing, representing a class of 12-oxo-10(E)-dodecenoic acids (Bonner and English 1938; Zimmerman and Coudron 1979). Recently, a derivative of traumatin, 9-hydroxy-traumatin has been identified in soybean and alfalfa seedlings by Gardner (1998). In contrast to traumatin, which possesses wound-healing properties, 9-hydroxy-traumatin has been suggested to exhibit cytotoxic properties similar to those exhibiting by 4-hydroxy-2-nonenal (Noordermeer *et al.* 2000a).

2.5.3 HPL genes

As described in section 2.5.1, HPL belongs to CYP74 family of PUFA-hydroperoxide-metabolising enzymes. The first cDNA, encoding an HPL was obtained from the bell pepper (Matsui *et al.* 1996). Over 30 full-length HPL sequences from various plant species have since been identified and characterised (Hughes *et al.* 2009).

2.5.3.1 Arabidopsis HPL gene

Only one HPL gene (*AtHPL*), encoding a 492 aa 13-HPL (CYP74B) protein has been found to be present in the Arabidopsis genome (Bate *et al.* 1998; Matsui *et al.* 1999). High levels of *AtHPL* transcripts were detected predominantly in reproductive organs such as inflorescences and siliquas. Relatively low levels of *AtHPL* was detected in leaves and only trace amounts of *AtHPL* were found in Arabidopsis stems (Matsui *et al.* 1999). The presence of the sequence encoding a putative chloroplast transit peptide (cTP) at N-terminus of *AtHPL*, predicts that the mature AtHPL protein is localised to the chloroplast, although no studies confirming the chloroplastic targeting of AtHPL has been reported to date.

Similarly to *AtLOX2*, *AtHPL* expression was transiently expressed after wounding and MeJA treatment, however the response time of *AtHPL* was slower compared to *AtLOX2* (Matsui *et al.* 1999). These observation led to suggestion by the authors that *AtHPL* is a "late response gene", in contrast to *AtAOS*, which is also transiently induced by wounding and jasmonate treatments, and is considered to be an "early response gene" (Bate *et al.* 1998; Matsui *et al.* 1999).

In contrast to wounding, pathogen infection did not appear to have any influence on the level of *AtHPL* gene, and the role of this particular HPL-gene has been associated with anti-herbivore response only (Matsui *et al.* 1999).

Interestingly, an analysis of volatile aldehydes in *AtHPL* T-DNA mutant revealed that the T-DNA disruption of *AtHPL* gene did not change significantly the overall content of C6 volatiles (Salas *et al.* 2006). Instead, an increased LOX activity and almost 4-fold increase in the amount of C5 compounds was observed in *AtHPL* knockout (KO) mutant (Salas *et al.* 2006). Based on the results obtained, the authors suggested the existence of other HPL genes in Arabidopsis, although to date there has been only one HPL gene identified in the Arabidopsis genome.

2.5.3.2 Tomato HPL gene

A cDNA encoding 476 aa HPL gene from tomato, *LeHPL* has been isolated and studied (Matsui *et al.* 2000a). Recombinant *LeHPL* showed high substrate specificity against

13-hydroperoxides and therefore was regarded as a 13-HPL (CYP-74B) member (Matsui *et al.* 2000a).

Similar to *AtHPL*, the highest level of *LeHPL* has been observed in flowers and flower buds, followed by lower levels of expression in tomato leaves (Howe *et al.* 2000). In contrast to *AtHPL*, *LeHPL* lacks a cTP sequence (Howe *et al.* 2000). However, *in vitro* import assays have shown that LeHPL protein is targeted to isolated chloroplasts, specifically, to their outer envelope (Froehlich *et al.* 2001).

Damage, caused to tomato leaves by a chewing insect, induced both, the local and systemic induction of *LeHPL* gene, suggesting its defensive or signalling role in response to herbivores (Howe *et al.* 2000).

2.5.3.3 Potato HPL gene

Potato HPL gene, *StHPL*, structurally and functionally resembles *LeHPL* from tomato (Vancanneyt *et al.* 2001). *StHPL* encodes 13-HPL protein and its highest expression was observed in young potato leaves (Vancanneyt *et al.* 2001). Upon wounding, *StHPL* expression in older leaves increased transiently with the highest levels observed 4 hours after wounding. In contrast, *StHPL* expression in young leaves was high both before and after wounding (Vancanneyt *et al.* 2001).

Antisense-mediated depletion of *StHPL* transcripts in transgenic potato plants was used to investigate how the suppression of this enzyme may affect potato oxylipin metabolism and response to insect feeding (Vancanneyt *et al.* 2001). A dramatic decline in *StHPL* mRNA levels was observed in both young and old leaves of the transgenic lines. As a result, the endogenous levels of HPL-derived volatiles decreased by almost 50% and the level of aphids, feeding on the HPL-depleted plants, increased two-fold in regard to the WT-plants (Vancanneyt *et al.* 2001). These observations also support the suggested role of HPL-derived volatiles in plant defence systems against insects.

Impact of depletion of both LOX and HPL genes on the volatile composition in leaves of potato plants have been recently studied (Salas *et al.* 2005). This experiment showed that antisense *StHPL* transgenic lines increased in the LOX activity and the content of C5 volatiles, whereas silencing of LOX-genes resulted in a severe decrease in both the

amount of volatile produced by the leaves and in the intensity of their aroma (Salas *et al.* 2005).

The experiments with HPL depleted potato plants and HPL KO-mutants of Arabidopsis (section 2.5.3.1) observed an increase in C5 volatiles, which may most likely be attributed to atypical homolytic activities exerted by LOXs in the absence of corresponding HPLs as discussed in section 2.4.3.

2.5.3.4 Cucumber HPL gene

The first representative member of 9/13-HPL was isolated from cucumber (Matsui *et al.* 2000b). Members of 9/13-HPL genes were initially associated with the *Cucurbitaceae* family, but have recently been reported from other plant species (reviewed by Hughes *et al.* 2009). Unlike 13-HPL members, whose transcripts are only found in green tissues, transcripts of 9/13-HPLs have also been detected in underground tissues such as roots and nodules (Chehab *et al.* 2006; Hughes *et al.* 2006).

In cucumber, expression of 9/13-HPL gene, *Cs9HPL* changes throughout developmental stages and is at its highest level in young cotyledons and 30-day old flowers and mature fruits (Matsui *et al.* 2006). Mechanical wounding resulted in a transient increase of *Cs9HPL* expression (Matsui *et al.* 2006). In contrast to *AtHPL*, *Cs9HPL* was induced upon infection with a fungal pathogen (Matsui *et al.* 2006). The observed increase in *Cs9HPL* expression also correlated with the increase in levels of both, C6 and C9 volatiles (Matsui *et al.* 2006).

To check whether overexpression of 9/13-HPL gene would result in an increased level of C9 compounds in other plants, *Cs9HPL* from cucumber was cloned and overexpressed in tomato plants, where high activity of 9-LOX but not 9-HPL was observed (Matsui *et al.* 2001). Surprisingly, although transgenic plants displayed increased levels of *Cs9HPL* transcripts, only small change in the accumulation of C9 volatiles was observed in tomato fruits. Furthermore, the disruption of tomato fruit tissue has resulted in increased levels of C6 volatiles, despite the abundance of 9-LOX in the fruit (Matsui *et al.* 2001). One of the possible explanations for the observed results was that 9-hydroperoxides formed by tomato 9-LOX are spatially separated from and therefore are unavailable to cucumber 9/13-HPL enzyme within tomato fruit cells. Furthermore, Matsui and colleagues (2001) suggested that the failure to produce

increased levels C9 compounds upon fruit disruption can be explained by the much higher catalytic activity of 13-LOX (or several LOXs) compared to the 9-LOX. This, in turn, resulted in insufficient amounts of substrate being available for cucumber 9/13-HPL, which prefers 9-hydroperoxides as substrate.

The number of characterised plant LOX and HPL genes is not limited to the genes described above. This knowledge is a valuable source of information, which helps to predict properties of grapevine LOXs and HPLs and is a stepping-stone for further investigation.

2.6 Grape LOXs and HPLs

Although presence of LOX and HPL proteins in grape berries has been suggested for a long time (Iglesias *et al.* 1991; Ramey *et al.* 1986), there is relatively little known about size and structure of LOX and HPL families and the corresponding biology of individual family members.

A single putative LOX-gene sequence has been used in transcriptome-wide gene expression (da Silva *et al.* 2005) and has also been included in a number of grape defence response studies (Chong *et al.* 2008; da Silva *et al.* 2005; Petit *et al.* 2008). Recent research indicates that water deficit alters expression of a putative LOX and a putative HPL gene in Cabernet sauvignon and Chardonnay cultivars (Deluc *et al.* 2009). However, to date there has been no extensive molecular and biochemical characterisation of grape LOXs and HPLs.

2.7 Grape PUFAs

Lipids and fatty acids (FAs) play essential roles in plants, including grapevine. They are building blocks of all cell membranes, a source of energy and important storage material. Moreover, certain lipids and FAs serve as a source of flavour and aroma compounds in grape juices and wines (Clarke and Bakker 2004).

2.7.1 Lipid and FA distribution within grape berry

Lipids and FAs are differentially distributed across different berry tissues. In mature berries of red grape cultivar Cabernet sauvignon, most of the neutral lipids (96%) are concentrated in berry seeds, while phospholipid fraction is the most abundant in the pericarp and skins (69 and 61% respectively) (Miele *et al.* 1993). According to a number of studies, the most prevalent fatty acid in grape berries of *Vitis vinifera* cultivars is linoleic acid (LA, 18:2), reaching over 40% of the berry total FA content (Gallander and Peng 1980; Iglesias *et al.* 1991; Miele *et al.* 1993). In white Macabeo grapes, LA is the largest component of neutral and phospholipid fractions, while α-linolenic acid (LnA, 18:3) can be found predominantly in the glycolipid fraction of skin (Iglesias *et al.* 1991).

FA acid composition in different Vitis species seems to be species-dependant. For example, saturated acids such as myristic (14:0), palmitic (16:0) and stearic (18:0) acids were reported to be predominant in berries of *Vitis labrusca* var. "Concord" (Bauman *et al.* 1977; Higgins and Peng 1976). In comparison, *Vitis vinifera* unsaturated fatty acids were highest in all lipid fractions, represented by linoleic (18:2) and linolenic (18:3) fatty acids (Miele *et al.* 1993; Roufet *et al.* 1987).

2.7.2 Grape berry FA content and composition during development

Development of grape berries can be divided into three stages (Coombe 1992; Jackson 2000). In stage I, the berry shows rapid cell division, followed by cell enlargement and seed endosperm development. During this stage, the berry remains green and hard. During stage II (also called "lag phase"), berry growth slows, the seed embryo develops and the seed coat hardens. At the end of the lag phase berries of coloured varieties start to lose green colour and this turning point is also known as veraison. Veraison is often associated with the beginning of the third stage, ripening. During ripening tissues

soften, total acidity decreases and sugar content increases (Coombe 1992; Jackson 2000).

Physiological changes over berry development also involve changes in lipids and fatty acid composition. These changes related to changes in the structure of various cell membranes and in the content of storage lipids. Such changes will potentially have a profound effect on the outcome of GLV-pathway due to their importance in determining LOX and HPL substrate availability.

Lipid and fatty acid composition of the berry undergoes significant changes across the development, despite relatively small changes in the overall total lipid content (Roufet *et al.* 1987; Rubio *et al.* 2009).

As mentioned earlier, the two most common plant LOX substrates are LA and LnA. It seems that content of LA and LnA in *V. vinifera* grape berries increases during the development of the berry reaching its maximum around veraison, after which it declines back to the levels observed in pre-veraison berries (Iglesias *et al.* 1991; Roufet *et al.* 1987). Most of these changes can be attributed to developmentally driven transformation in berry cell membranes, plastids and lipid-like globules (Hardie *et al.* 1996a; Hardie *et al.* 1996b).

As has been observed by Hardie *et al.* (1996a), plastids in pericarp cells of grape berries contain relatively large inclusions of lipid matter, which the authors termed as lipid-like globules. The size and number of lipid globules in the pericarp cells changes as berry develops (Hardie *et al.* 1996b). During anthesis, the most of the plastids contain a few small in size lipid-bodies surrounded by stromal grana. During the berry development the lipid-like globules increase in size and reach its maximum size when the berry is almost ripe (19-20°Brix) (Hardie *et al.* 1996a). However, at a late ripe berry stage, the size and number of the lipid-like globules has reduced, most likely as a result of loss of membrane integrity and subsequent disorganisation of the cellular structure (Hardie *et al.* 1996a). The observed changes will most likely involve participation of grape LOX and possibly HPL enzymes, as these enzymes have been reported to participate in senescence and programmed cell death (PCD) (reviewed by Maccarrone *et al.* 2001).

2.7.3 FA composition in grape musts

Another important factor for this research is the lipid and FA content in grape musts obtained after berry crushing, as the musts are a direct substrate source for enzymes involved in the GLV-pathway. Changes in the overall lipid fractions composition has been observed in Cabernet Sauvignon musts compared to the lipid composition of the intact berry (Miele *et al.* 1993). Specifically, neutral, phospholipid and glycolipid fractions represented 35, 25 and 40% of the total must lipid content respectively (Miele *et al.* 1993). Similarly, the individual FA content of musts was different to the FA composition of pre-crushed berries. The most abundant in musts were palmitic (26%), linoleic (21%), stearic (16%), oleic (11%) and linolenic (7%) FA (Miele *et al.* 1993).

As mentioned earlier, the concentration of LA in musts is 3-fold higher than LnA, which potentially should result in the higher content of hexanal compared to the unsaturated product of GLV pathway such as (*E*)-2-hexenal or (*Z*)-3-hexenal. However, the content of (*E*)-2-hexenal in musts is normally higher than other GLVs (Clarke and Bakker 2004).This indicates that the substrate concentration is not the limiting factor in this case and most likely some other factors (such as an enzyme affinity for the substrate) will determine the final GLV content.

Due to time constraints, FA analysis of Sauvignon blanc berry will not be included in the current investigation and is likely to be a part of the following studies.

2.8 Key objectives of the research project

This research project aims to determine the size and structure of the grape LOX and HPL families and characterise individual members expressed in grape berry, with the focus on those members potentially involved in the formation of GLV volatiles. It is suggested that GLV volatiles are grape berry derived precursors of important flavour and aroma compounds found in wine.

The key objectives of this work are:

- To identify LOX and HPL gene members in the grape genome.
- To study gene expression of Sauvignon blanc grape berry expressed LOXs and HPLs.
- To study biochemical properties of selected recombinant LOX and HPL proteins.

The results of this study will help to increase our understanding of LOX and HPL involvement in grape development, stress response and defence mechanisms in grapevine and will lead to establishing links between changes in grapevine physiology and wine quality.

Chapter 3
Materials and Methods

3.1 Chemicals

Unless otherwise specified, the highest purity reagents and MiliQ grade water were used in all experiments.

3.2 Bioinformatic tools

3.2.1 *In silico* grape genome mining

The complete grape genome (*V. vinifera*, cv. Pinot noir, quasi-homozygous genotype PN40024) sequence was analysed using web-based tools provided by the French-Italian Public Consortium (http://www.genoscope.cns.fr/spip/Vitis-vinifera-e.html; accessed 21.05.2010). Nucleotide sequences of known plant LOX and CYP74 genes were used in BLAST alignments (http://www.genoscope.cns.fr/cgi-bin/blast_server/projet_ML/blast.pl; accessed 21.05.2010) and BLAT alignments (http://www.genoscope.cns.fr/blat-server/cgi-bin/vitis/webBlat; accessed 21.05.2010), in order to find sequences similar to query sequences derived from other plant species in the grape genome. The identified genomic contigs and scaffolds, containing putative LOX and HPL sequences, were analysed using the web-based GenScan software (http://genes.mit.edu/GENSCAN.html; accessed 21.05.2010) to predict coding sequences and intron-exon structures. Location of individual sequences on grape chromosomes was determined using Grape Genome Browser (http://www.genoscope.cns.fr/externe/GenomeBrowser/Vitis/; accessed 21.05.2010). The designated names and genomic details for the identified grape LOXs and CYP74 gene family members are presented in Table 4.1 and Table 4.4 respectively.

3.2.2 Sequence alignment and phylogeny

DNA sequences of the predicted grape LOXs and CYP74 members were *in silico* translated into amino acid sequences using the Geneious 4.8 software package (Biomatters Ltd., Auckland, New Zealand). For the majority of grape LOXs and

CYP74s, corresponding accession numbers were retrieved from the GenBank and are presented in Table 4.1 and Table 4.4.

Nucleotide and amino acid sequences of biochemically characterised plant LOXs (other than grape) were retrieved from GenBank (http://www.ncbi.nlm.nih.gov/Genbank; accessed 21.05.2010) and UniProt (http://www.uniprot.org; accessed 21.05.2010) and named according to Feussner and Wasternack (2002) and a proposed nomenclature scheme (Shibata *et al.* 1994) (Table 4.2). The amino acid sequences were then aligned with the predicted grape LOXs amino acid sequences using the ClustalW algorithm (Thompson *et al.* 1994) as part of Geneious 4.8 software package. The same software package was used to generate an unrooted phylogenetic tree based on the ClustalW-generated alignments using the neighbour-joining method (Saitou and Nei 1987) applying 1000 bootstrap replicates. To validate the obtained groupings, another unrooted phylogenetic tree was generated in the same manner based on an alignment constructed using conserved LOX-domain region only.

3.2.3 Protein structure prediction of putative LOXs and HPLs

In order to predict subcellular localisation of mature proteins, amino acid sequences of the predicted proteins were submitted to TargetP 1.1 Server (http://www.cbs.dtu.dk/services/TargetP/; accessed 21.05.2010) and ChloroP 1.1 Server (http://www.cbs.dtu.dk/services/ChloroP/; accessed 21.05.2010) (Dyrlov Bendtsen *et al.* 2004; Emanuelsson *et al.* 2007; Emanuelsson *et al.* 1999). These web-based services allow identification of transit and signal peptides within amino acid sequences, predicts their cleavage sites and potential localisation of mature peptides. Additionally, the amino sequences were also submitted to and analysed using the WoLF PSORT server (http://wolfpsort.org/; accessed 21.05.2010) (Horton *et al.* 2007).

3.3 Plant material and trial conditions

Grapevine (Vitis vinifera L.) cultivar Sauvignon blanc material was sourced from three different locations: Booker vineyard (Brancott Estate, Marlborough, New Zealand); Lincoln University research vineyard (Lincoln, Canterbury, New Zealand) and fruiting cuttings grown in a glasshouse at Lincoln University as describe later.

3.3.1 Experimental sites

The Booker vineyard is a commercial vineyard operated by Pernot Ricard NZ Ltd. and located Brancott Estate in the southern part of Wairau Valley, near Blenheim (41°.56' South, 173°.85' East). Grape vines in the vineyard represent mass selected clone UCD1 of the white grape *Vitis vinifera* L., cv. Sauvignon blanc grafted onto SO4 rootstock. The vines are planted in a North-South orientation.

The Lincoln University research vineyard is situated on the Lincoln University campus, Canterbury, New Zealand (43°.38' South, 172°.27' East). The vineyard has three rows of Sauvignon blanc vines represented by mass selected clones also grafted onto the SO4 rootstock. The rows in the vineyard are planted in a North-South orientation.

3.3.2 Fruiting cuttings

Fruiting cuttings, which were used in MeJA elicitation experiments, were grown essentially according to the method of Mullins and Rajasekaran (1981).

Uniform hardwood cuttings (consisting of four to six nodes) were collected in late winter of 2007, from well-ripened dormant canes. The canes were obtained from the Lincoln University research vineyard, Canterbury, New Zealand. The canes were stored damp at 4°C in plastic bags until use.

To initiate root growth, dormant canes were cut transversally just below the level of the lowest bud and placed in a tray with pumice (1-4 mm grade) so the bottom 8-10 cm of the cutting was buried in the substrate. Trays with 50-60 canes in each were then placed a shade-house on electric heat-pads that maintained the pumice in the trays at between 24-26°C. Ambient air temperature varied between 4 and 10°C (Appendix A.1.1.A). Under such conditions root initiation was promoted while bud burst was retarded. The cuttings were regularly watered and monitored for an approximately four-week period.

Plants with roots of between 10-15 cm were then transferred into pots or PB8 plastic bags (Egmont Commercial, Christchurch, New Zealand) filled with potting mix. Each $1m^3$ of the potting mix contained 800 litres composted bark and 200 litres pumice, supplemented with fertilisers (2 kg osmocote (16 - 3.9 - 10 NPK), 1 kg agricultural lime, 1 kg Hydraflo [Scotts Australia Pty Ltd, NSW, Australia]) .

Potted cuttings were then moved to a glasshouse and grown from November to March without artificial light supplementation. The temperature in the glasshouse was maintained at 24-25 ° C during the day and 16-18 ° C during the night.

After the bud burst, the top two buds containing inflorescences were left to develop and remaining buds were removed. All leaves adjacent inflorescences were removed as soon as they became accessible. Later, the shoot tips were excised leaving inflorescences in terminal positions. In 15-20 days after the bud burst, a weaker of the two inflorescences was removed, and a lateral bud below the stronger inflorescence was allowed to develop into a shoot with leaves to support further growth and development of the bunch (Appendix A.1.1.B). The plants were then grown at standard greenhouse conditions, regularly watered and prevented from overgrowing (Appendix A.1.1.C).

3.3.3 Berries of different developmental stages

Berries for gene expression studies were collected throughout berry development in the 2006, 2007, 2008 and 2009 seasons from the Booker vineyard, Marlborough, New Zealand. Each season, samples were collected at eight berry developmental stages. Berries of the earliest stage, stage 1 (7-8 mm in diameter), were collected 20 days after anthesis (daa). The subsequent samplings were undertaken approximately at the following time points: stage 2 ~ 30 daa (8-9 mm), stage 3 ~ 50 daa (pre-veraison, 10-11 mm) , stage 4 ~ 60 daa (immediately post-veraison, 11-13 mm), stage 5 ~ 80 daa (13-15 mm, 15-17 °Brix), stage 6 ~ 90 daa (13-16 mm, 17-20 °Brix), stage 7 ~ 100 daa (14-16 mm, 19-21 °Brix) and stage 8 ~ 110 daa (14-16 mm, 20-23 °Brix) (Appendix A.1.2). In each season, veraison took place approximately 50-60 days after anthesis. Berries harvested 110 days after anthesis had soluble solids levels of 20-23°Brix and were considered fully ripe.

Variation in berries size and stage of development within a bunch, between bunches on a vine and between bunches on different vines represents a significant issue for sample

collection in grapevine. Lund et al. (2008) have shown that individual berries collected at a certain developmental stage on the basis of size, soluble solids content, texture or colour are remarkably coordinated in their transcriptional activity. Therefore, in order to reduce berry-to-berry variation during the sampling, bunches from the basal position of 20-30 independent vines were harvested, and only those berries typical for a given stage were collected as indicated in Appendix A.1.2. The harvested berries were immediately frozen in liquid nitrogen. A total pool of berries from 20-30 different vines was collected for each stage. The berries were transported on dry ice and stored in a freezer at -80°C until use.

3.3.4 Berry fractions

Sauvignon blanc berries of 80-90 daa were collected in 2009 in Lincoln University research vineyard and used to analyse transcript distribution in different parts of grape berries. The skin fraction was separated by squeezing the pulp out of the berry. The remaining part of the berry was then pressed through a sieve to separate seeds from the pulp fraction. All three fractions were frozen immediately and stored in a freezer at -80°C.

3.3.5 Methyl jasmonate (MeJA) treatment

The MeJA treatment protocol used in this study was adapted from an experiment previously conducted by Cheng et al. (2006).

Fruiting cuttings possessing bunches at around 90 days after veraison stage were used. The plants were grown as described in section 3.3.2. Control plants were grown in a separate glasshouse with the same growing conditions to prevent cross-contamination of the air around control plants with the highly volatile methyl jasmonate.

MeJA (95%; Sigma-Adrich, New Zealand) was diluted 1:10 with 95% ethanol, followed by a further 1:500 dilution with MiliQ water containing 0.1% Triton X-100, resulting in a final concentration of 822.4 µmol/L MeJA. The solution was sprayed onto the leaves and bunches (approximately 10 mL for each plant). Control leaves and bunches were treated with 0.1% Triton X-100 containing 0.2% ethanol. Prior to the treatment, leaves and bunches were harvested as an untreated control. Treated leaves and bunches were harvested from three treated plants and two control plants at 0.5 hr,

1 hr, 3 hr, 6 hr, 12 hr and 24 hr after spraying, frozen quickly using liquid nitrogen, and stored at -80°C.

3.3.6 Wounding

Wounding experiments were performed in 2008 season in the Lincoln University Vineyard, Canterbury, New Zealand on Sauvignon blanc berries at between 80 to 90 days after anthesis. Without separating bunches from vines, individual berries were pierced 1-2 times each with a 12-gauge needle to induce a wound response and left on the vine. The berry samples were then collected at time intervals 0.5 h, 1 h, 3 h, 6 h, 9 h, 12 h and 24 h after wounding (Appendix A.1.3 A). At each time point three individually wounded bunches were collected, immediately snap-frozen in liquid nitrogen and stored in a freezer at -80°C as biological replicates. In the same way three non-wounded bunches were collected prior to wounding as an untreated control.

3.3.7 Pathogen infected berries

Berries infected with grape pathogen *Botrytis cinerea* Pers.: Fr were collected from the Booker vineyard, Marlborough, New Zealand at harvest (100-110 days after anthesis) in the 2007 season. Three groups of samples were collected: berries with visible signs of pathogen infection (indicated by red arrows in Appendix A.1.3.B); berries from the infected bunches, but without visible signs of pathogen (indicated by yellow arrows in Appendix A.1.3.B); and healthy berries harvested from vines distantly separated from the infected vines. The berries were snap-frozen in liquid nitrogen and stored in a freezer at -80°C.

3.4 Total RNA isolation

Extra care was taken for preparation of total RNA to avoid ribonuclease contamination. The work area, pipette sets and glassware were treated with RNase ZAP® (Sigma-Aldrich, Auckland, New Zealand). Water and all buffers were sterilised in autoclave for 20 minutes at 15 psi (1.05 kg/cm^3) on liquid cycle, or filter-sterilised using 0.22 µm filters (Millex™, Millipore) where autoclaving was not appropriate. A separate set of electrophoresis equipment was used to run RNA gels.

Two methods were used for the RNA isolation. The CTAB method (see section 3.4.2) was used when larger amounts (up to 100 µg) of RNA were required. A second RNA extraction using the Spectrum™ Plant Total RNA Kit (Sigma-Aldrich, Auckland, New Zealand), which yields between 3 to10 µg of total RNA was used mainly for qPCR analysis (see section 3.4.3 for a detailed description).

3.4.1 Plant material for RNA extractions

Sauvignon blanc berries or leaves were collected as described in section 3.3, snap-frozen in liquid nitrogen and stored at -80°C until use. Immediately before extraction, the frozen material was ground to a fine powder in liquid nitrogen with mortar and pestle. Unless otherwise specified, a whole berry was used in the extraction, including seeds.

3.4.2 CTAB extraction method

The CTAB RNA extraction protocol was essentially that described by Zeng and Yang (2002) with modification described in Reid *et al*. (2006). Briefly, 2 grams of fine tissue powder were added to 25 mL extraction buffer (2% CTAB, 2% PVPP, 300 mM Tris-HCl (pH 8.0), 25 mM EDTA, 2 M NaCl, 0.05% spermidine) at 65°C in 50 mL falcon tube, shaken vigorously and incubated at 65°C in a water bath for 10 min. The sample was further homogenised using a PT-DA 3012/2T probe on a Polytron PTMA3100 homogeniser (Kinematica, Biolab/Thermofisher Scientific, Auckland, New Zealand). Then an equal volume of chloroform:IAA (24:1) was added and mixed the solution vigorously using a IKA® Genius 3 vortex (IKA® Werke GmbH & Co. KG; Global Science, Auckland, New Zealand). The samples were subsequently centrifuged for 15 min at 3500 ×*g* at 4 °C in a refrigerated Haraeus-Christ Varifuge K centrifuge (Heraeus

Sepatech GmbH, Osterode, Germany) to separate the organic and aqueous phases. An equal volume of chloroform:IAA (24:1) was then added, the solution was mixed and centrifuged as previously for 15 min at 3500 ×*g* at 4 °C. The upper aqueous phase was then transferred to a new 50 mL falcon tube and 0.1 volume of 3 M sodium acetate and 0.6 volume of isopropanol added. The sample was mixed by inversion and subsequently incubated at -80°C for 30 min. The nucleic acids were pelleted by centrifugation for 30 min at 4000 ×*g* at 4°C. The supernatant was discarded and the pellet dissolved in 1 mL 1×TE buffer (pH 7.5). The resuspended nucleic acid solution was then transferred to a 1.5 mL tube, to which 0.3 volume of 8 M LiCl was added, mixed by inversion and incubated at 4°C overnight. The next day the sample was centrifuged at 16000 ×*g* at 4°C for 30 min and the supernatant was discarded. The pellet containing RNA was washed in 500 µL of ice cold ethanol, centrifuged at 16000 ×*g*, air-dried, resuspended in 50-100 µL of nuclease-free water and stored in a freezer at -80°C until needed.

3.4.3 Spectrum kit RNA extraction

Total RNA was extracted from 200 mg of ground berry tissue (100 mg for seed samples) using the Spectrum™ Plant Total RNA Kit (Sigma-Aldrich, Auckland, NZ) according to the manufacturer's instructions.

The lysis buffer with 2-β-mercaptoethanol (2-BME) mixture was prepared by adding 10 µL of 2-BME to each 1 mL of lysis buffer (final concentration of 2-BME 1% v/v). Three to four berries were ground in liquid nitrogen, using mortar and pestle to a very fine powder. One mL of 1% v/v 2-BME containing lysis buffer was added to 200 mg of the finely ground berry material in 2 mL centrifuge tube and vortexed vigorously for at least 30 sec. The sample was then incubated at 56°C for 3-5 min and centrifuged for 3 min at 14000 ×g to pellet cellular debris.

Without disturbing the pellet, the supernatant was pipetted into a filtration column sitting in 2 mL collection tube and centrifuged at 14000 ×g for 1 min to remove residual debris. One millilitre of binding solution was added to the clarified solution and mixed immediately by inversion. Then the solution was transferred in 700 µL maximum portions onto a binding column seated in a 2 mL collection tube. Each portion was centrifuged at 14000 ×*g* for 30 sec with the flowthrough discarded after each centrifugation step. The column containing bound RNA was then washed by adding 500

µL of wash solution-1 and centrifuging at 14000*g* for 1 minute followed by two subsequent wash steps of 500 µL of wash solution-2 and subsequent centrifugation at 14000 ×*g* for 1 min. The flowthrough was discarded at each step. The column was then centrifuged at 14000 ×*g* for 1 minute to dry the column and the column was finally transferred to a new 2 mL collection tube. The bound total RNA was then eluted with 100 µL of nuclease-free water by application of centrifugation at 16000 ×*g* for 1 minute. The eluate containing purified RNA was stored in a freezer at -80°C.

3.4.4 DNaseI treatment

Purified RNA samples were treated with DNase I to remove traces of genomic DNA. The TURBO DNA-*free*™ Kit (Ambion, ABI, Auckland, New Zealand) was used accordingly to manufacturer's instructions. To the RNA sample, 0.1 volume 10× Turbo DNaseI Buffer and 1 µL of TURBO DNase were added, mixed gently and incubated at 37°C for 30 min. Then 0.1 volume of DNase Inactivation Reagent was added to the reaction, mixed and incubated at room temperature for 5 min, mixing occasionally. The sample was then centrifuged at 10000 ×*g* for 1.5 min and the supernatant was transferred to a fresh tube. The DNase-treated RNA was then precipitated using 1/10 sample volume of 3 M sodium acetate, 2 volumes of ethanol, washed with 70 % ethanol and resuspended in 30 µL of nuclease-free water.

3.4.5 Total RNA quantification

The concentration and quality of RNA was determined by measuring the absorbance of the sample at 230 nm, 260 nm and 280 nm using a NanoDrop® ND-1000 Spectrophotometer (Nanodrop Technologies, Montchanine, USA). The 260/280 nm and 260/230 nm ratios were used to estimate the purity of the isolated RNA and the concentration of the samples determined from the OD_{260} readings. The integrity of the extracted RNA was determined by running 1 µg aliquot on 1 % agarose denaturing gel (Sambrook and Russell 2001).

3.4.6 RNA denaturing gel

The integrity of RNA samples was checked by separation of a sample aliquot using a 1.5 % agarose denaturing gel.

To prepare 50 mL of gel solution, 0.75 ×*g* of agarose, and 5 mL of 10 x MOPS buffer were added to 37.5 mL of water and melted in a microwave oven. After cooling to approximately 60°C 7.5 mL of formaldehyde was added and mixed well by swirling. Immediately, the mixture was poured into a gel tray and left in a fume hood until solidified.

Sample denaturing buffer was prepared by mixing 500 µL 10 × MOPS buffer, 500 µL formamide, 150 µL formaldehyde and 2 µL ethidium bromide (10 mg/mL).

One volume of sample containing 1 µg of RNA was mixed with three volumes of sample denaturing buffer, incubated at 65°C for 5 minutes and snap-chilled on ice.

After adding RNA loading dye (80% v/v formamide, 10 mM EDTA, 0.1% w/v xylene cyanol, 0.1% w/v bromophenol blue), the samples were loaded on 1.5 % agarose denaturing gel submerged in RNA running buffer (1 x MOPS buffer). The samples were then fractionated by electrophoresis at 5 $V \cdot cm^{-1}$ for 50 min.

3.5 DNA extraction and preparation

Caution was taken when working with DNA in order to prevent DNA degradation and cross-contamination of samples.

3.5.1 Genomic DNA (gDNA) extraction

Genomic DNA was extracted from young Sauvignon blanc leaves collected at the Lincoln University research vineyard. Illustra Nucleon Phytopure Genomic DNA extraction Kit (GE Healthcare Life Sciences, Global Science, New Zealand) was used for extraction of gDNA according to the manufacturer protocols. Briefly, young leaves were collected and ground to a fine powder under liquid nitrogen using a mortar and pestle. Then, 0.1 mg of the ground tissue was transferred to a pre-chilled microcentrifuge tube and 600 µL of Reagent 1 was added and mixed thoroughly. Immediately, 200 µL of reagent 2 was added and the sample was inverted several times until a homogeneous mixture is obtained. The sample was incubated at 65°C in a shaking water bath for 10 min and then chilled on ice for 20 min. To extract DNA from the homogenate, 500 µL of ice-cold chloroform and then 100 µL of Nucleon PhytoPure DNA extraction resin were added and mixed well. The sample was centrifuged at 1300 ×*g* for 10 min and the upper phase containing DNA was carefully transferred to a fresh tube. To precipitate DNA, an equal volume of cold isopropanol was added and the tube was gently inverted until a precipitate was evident. The precipitated DNA was spooled out using a heat-sealed glass pipette formed into a hook, washed with 70% ethanol and dissolved in sterile water. To remove traces of RNA, the resuspended DNA was treated by adding RNaseA (Sigma-Aldrich, Auckland, New Zealand) at a final concentration of 20 µg/ml and incubating the sample at 37°C for 30 min.

3.5.2 Complementary DNA (cDNA) preparation

Complementary DNA was synthesized from total RNA using Oligo-dT primer and PrimeScript™ Reverse Transcriptase (Takara Bio Inc., Norrie Biotech, Auckland, New Zealand) according to the manufacturer's recommendations.

Up to 10 µg of total RNA was used in 40 µL the RT reaction. The RNA was incubated with Oligo-dT primer (5 µM final concentration of primer) in the presence of dNTPs (0.5 mM final concentration of each dNTP) at 65°C for 5 min and placed on ice for

1 min. Subsequently, 8 µL of 5×PrimeScript™ Buffer, 40 units RNase Inhibitor, and 200 units of PrimeScript™ Reverse Transcriptase and nuclease-free water were added to final volume of 40 µL. The reaction was incubated at 42°C for 60 min and heated at 70°C to deactivate the enzyme. Concentration and quality of cDNA was estimated using NanoDrop® ND-1000 Spectrophotometer (Nanodrop Technologies, Montchanine, USA).

3.6 PCR

3.6.1 PCR identification of berry expressed LOX and HPL genes

For the LOX and HPL genes identified *in silico*, specific PCR primers were designed in the 3'-region of the predicted coding sequence (Table 3.1 and Table 3.2). Complementary DNA, used in PCR reactions to isolate Sauvignon blanc specific cDNA amplicons, was prepared by pooling cDNA from berries of eight developmental stages. The Qiagen *Taq* DNA polymerase (Qiagen, Auckland, New Zealand) was used and, unless otherwise specified, the final concentration of reagents in a 50 µL PCR reaction was: 1× CoralLoad PCR Buffer, 1.5 mM $MgCl_2$, 200 µM of each dNTPs, 0.2 µM of each primer, 2.5 units of *Taq* DNA Polymerase and 2 µL cDNA. The reaction were performed in an iCycler thermocycler (BioRad, Auckland, NZ) using the following PCR parameters: 1 cycle at 94°C for 3 min, 40 cycles (94°C for 15 sec, 50-58°C for 15 sec, 72°C for 30-180 sec) and final extension at 72°C for 5 min. The reaction products were then separated on 1% agarose electrophoresis gel and analysed (see section 3.6.3). PCR products of the expected size were excised, gel-purified and sequenced directly.

Table 3.1 Oligonucleotide PCR primers used to identify predicted grape LOXs

Gene	Forward primer	Reverse primer
VvLOXA	5'-CCACGGAGATAGTCGAGCGAGAG-3'	5'- GCTCGCATCCTTGTAGAAGA -3'
VvLOXB/C/N	5'-CAAAGTATGCCATGGAAATGTCATCTG-3'	5'-TCAGGATTGGACTTGAGTTCTTCATAC-3'
VvLOXD	5'-AATCGTCCCACACTATGTCGACAATTC-3'	5'-GTACAAAAGTTTGTATGGTATCTTGG-3'
VvLOXE	5'-AAACACCCGACGACCTCATTGGAATTA-3'	5'-CAACTCCTCTAACTTTGCAGAAAACC-3'
VvLOXF	5'-GACAATAGTATGTGGGTGGCTCACGAC-3'	5'-GGAAATCATCTTTAACGTTAAGCAGGAGG-3'
VvLOXG	5'-GTGCAGATGGGGTCATTGAGAGTT-3'	5'-TTAATAATTTTTTCGAGTTCCTTTAAT-3'
VvLOXH	5'-TTGGGGCGATCGGTACTAGGTGGCAATG-3'	5'-GTCTACTGTCTTTGTTAGGAATGATGC-3'
VvLOXI	5'-GAATTTTCTGAGGTGAAGGAGGCT-3'	5'-TGGGCCATAGACATCAGGGGCCAGTCCA-3'
VvLOXJ/K	5'-CTCTTTGAAACCCCTGCAATGATCGAC-3'	5'-ACACTTGCTTCCACTGCAGCTTGTCAC-3'
VvLOXL	5'-TGTCTGCTGTGATTTATAAGAACTG-3'	5'-TTAGATTGAGACACTATTAGGAATT-3'
VvLOXM	5'-CAAGAGATGAACGATTTGGTCACCTCA-3'	5'-TCTTGGAGTAGACGGATGACAACAGGG-3'
VvLOXO	5'-ACAAGTGATTGGACTTGGAAGCTCGCA-3'	5'-GTAGTGGGCCACGTAGGTTTTGACCC-3'
VvLOXP	5'-AGAATGGGTAGAATCGTATGTTGATCA-3'	5'-CCACCAGGACTCATTACGCTTGTCATAG-3'
VvLOXR/S	5'-ACCGGAAAGCCTATGGAACACG-3'	5'-CCAATCTCGGTAGGCAGCACAA-3'

Table 3.2 Oligonucleotide PCR primers used to identify predicted grape HPLs

Gene	Forward primer	Reverse primer
VvHPLA	5'- AACTAGTCCACTCCGTCGTGTACGAAA -3'	5'- TCTCAGTTAGCTTTCTCAACGGCGG -3'
VvHPLB	5'-AACTTCAACAACATCGCCGACGG-3'	5'-GTCAACGACTTGAAAAGCACAGCG-3'
VvHPLC	5'-AACTTCAACGACATTGCCGATGA-3'	5'-GTCAACGACTTGAAAAGCAGAGAT-3'
VvHPLD	5'-AACTCGCTCCTCTCATCACACTTGGT-3'	5'-CTACGATACGTGCGTAATTGACTTG-3'
VvHPLE	5'-AACTCGCACCTCTCATCACGCTTGGA-3'	5'-CTACGATACGTGCGTAATTGACTTG-3'
VvHPLF	5'-CGATCTCAATTCATCTTCTTCATTG-3'	5'-CTGGGTCCTTGTGAACCGAGCGC-3'

3.6.2 Obtaining full-length coding sequences

Full-length coding sequences were predicted using bioinformatic interrogation of the Pinot noir genome sequence as described in section 3.2.1. PCR primers to the predicted translation initiation and termination sites were designed (Table 3.3. To facilitate subsequent directional cloning of PCR products encoding full-length CDSs into pENTR vectors, four nucleotides (CACC) were added at a 5' end of each forward primer.

Table 3.3 Oligonucleotide primers used to obtain full-length coding sequence of berry expressed LOX and HPL genes

TOPO overhand-forming sequence CACC is underscored; the predicted translation initiation site is marked in bold

Gene	Forward primer	Reverse primer
VvLOXA	5'-CACC**ATG**TTCAAGACTCAGGTCCA-3'	5'-**TCA**AATGGAGATACTGTATGGA -3'
VvLOXC	5'-CACC**ATG**ATTCATTCAATTGTTGGT-3'	5'-**TTA**GATGGAGACACTGTTGGGAATC-3'
VvLOXO	5'-CACC**ATG**GCAGTGGTTAAAGAAATCAT-3'	5'-**TCA**TATCGACACACTGTTTGGAATCCC-3'
VvHPLA	5'-CACC**ATG**TTGTCTTCCACGGTCATG-3'	5'-**TCA**GTTAGCTTTCTCAACGGCGG -3'

High-fidelity PrimeSTAR™ HS DNA Polymerase (Takara, Norrie Biotechniques, Auckland, New Zealand) was used to minimise any PCR derived sequence changes according to the manufacturer's recommendations. The final concentration of the reagents in a typical 50 µL PCR reaction was: 1× PrimeSTAR™ Buffer (Mg^{2+} Plus), 1.5 mM $MgCl_2$, 200 µM of each dNTPs, 0.2 µM of each primer, 1.5 units of PrimeSTAR™ HS DNA Polymerase and 2 µL cDNA. The reaction was placed in an iCycler thermocycler (BioRad, Auckland, New Zealand), and the PCR was conducted using the following reaction conditions: 1cycle at 98°C for 2 min, 30 cycles (98°C for 10 sec, 50-58°C for 15 sec, 72°C for 3.5 min) and final extension at 72°C for 7 min. The reaction products were then separated on 1% agarose electrophoresis gel and analysed (see section 3.6.3). PCR products of the expected size were excised, gel-purified, cloned into pENTR™/TEV/D-TOPO® vector (Invitrogen, Auckland, New Zealand) and transformed into One Shot® TOP10 competent *E. coli* cells (Invitrogen, Auckland, New Zealand) as described in section 3.7.

3.6.3 Agarose gel electrophoresis

Agarose gel electrophoresis was used to analyse PCR products and to separate a PCR product of a particular size from PCR products of other sizes.

Unless otherwise specified, 1% agarose-Tris-borate-EDTA (TBE) gels were used. The gels were prepared as follows. 1% (w/v) agarose was added to 1×TBE buffer (89 mM Tris base, 89 mM Boric acid, 2 mM EDTA, pH 8.0) and melted in a microwave until all agarose particles were dissolved. The melted agarose solution was then cooled down to 65°C and ethidium bromide dye was added to the final concentration 0.2 µg/mL, and the stock was stored at 55°C in a closed bottle until needed. When required, the warm agarose solution was poured into an assembled electrophoresis tray with an appropriately sized comb and left to solidify at room temperature. The gel was then submersed in 1× TBE running buffer in a suitable electrophoresis tank and the comb removed. DNA samples were then mixed with DNA loading dye (0.25% w/v bromophenol blue, 0.25% w/v xylene cyanol FF, 40% w/v sucrose in water) and loaded into the formed wells.

The electrophoresis was normally performed in 1×TBE buffer for at 8 $V \cdot cm^{-1}$ for 50-60 min. The DNA was visualised under UV light and the gel photographed using VersaDoc™ Imaging System (Bio-Rad, Auckland, New Zealand).

3.6.4 Purification of PCR products

Prior to further manipulations, PCR products were purified using the AxyPrep DNA Gel Extraction Kit (Axygen, Auckland, New Zealand). The PCR reaction products were separated on a 1% agarose gel as described in section 3.6.3. The product of expected size was excised from the gel and the gel slice weighed. The gel slice was then dissolved in three volumes per weight of Buffer DE-A by heating at 75°C for 6-8 min with regular mixing by vortexing. Buffer DE-B was then added to the agarose/DNA solution in the volume equivalent to half volume of used Buffer DE-A and mixed. The solubilised agarose was then transferred into a Binding column and the assembly centrifuges at 12000 ×*g* for 30 sec. The filtrate was discarded and 500 µL of washing Buffer W1 added to the Binding column and the assembly centrifuged at 12000 ×*g* for 30 sec. Then the column was washed twice with 700 µL of Buffer W2 in the same way as with Buffer W1. The purified DNA was eluted by adding 30 µL of eluent and centrifuging the assembly at 12000 ×*g* for 1 min. The column eluate from this step contained the purified PCR product and was either used directly or stored at -20°C.

3.6.5 Sequencing of DNA fragments

A typical 10 µL sequencing reaction consisted of 1×BigDye® Terminator v 3.1, 5×sequencing buffer, 1×ABI PRISM® BigDye® Terminator v3.1 premix, 0.3 µM sequencing primer, purified DNA template (purified PCR amplicon or plasmid DNA) and water. The sequencing reaction was performed at the following conditions: 1 cycle at 96°C for 1 min and 25 cycles (96°C for 10 sec, 50°C for 5 sec, 60°C for 4 min). The reaction was then submitted to the Lincoln University Bio-Protection Research Centre Sequencing Facility and was sequenced on an ABI Prism 3100-Avant Genetic Analyser with a 4 capillary 80 cm array installed and using Performance Optimized Polymer 6 (POP6).

3.6.6 Rapid amplification of cDNA 5' ends (5'-RACE)

5'-RACE experiments were performed in an attempt to obtain full-length sequence of *VvLOXD* gene using a technique described by Shi *et al*. (2002). A flowchart outlining major 5´-RACE steps is illustrated in Appendix A.1.4. Briefly, 5'-phosphorylated primer LOXDRT (Table 3.4) was designed based on the genomic sequence and used to generate first-strand (FS) cDNA using SuperScriptII™ reverse transcriptase (Invitrogen, Auckland, New Zealand) according to the manufacturer's recommendations. Terminal transferase activity of SuperScriptII incorporates C residues at the 3' termini of the first-strand cDNA complementary to 7-methylguanosine cap structures of mRNA molecule. A bridging oligo BOLOXD (Table 3.4), containing gene specific sequence and 5×G nucleotides at the 3´ end, was then ligated to the first strand cDNA by adding 10 pmol of BOLOXD oligo to the cDNA reaction, incubating at 95°C for 5 min, and then cooling to 25°C for 30 min. The poly-C tail of the first strand cDNA formed by terminal transferase activity of SuperScriptII was then ligated to poly-G overhand formed by ligation of BOLOXD using Mighty Mix DNA Ligation Kit (Takara, Norrie Biotech, Auckland, New Zealand) as per manufacturer's recommendations. One microliter of the ligated cDNA was then used in a standard PCR reaction with LOXDF1 and LOXDR1 primers (Table 3.4). The amplified DNA was purified and used as a template in a subsequent "nested" PCR reaction with LODF2 and LOXDR2 primers to increase specificity of the reaction (Table 3.4). The resulting PCR product was purified and sequenced as described in sections 3.6.3- 3.6.5.

Table 3.4 Oligonucleotide primers used in 5'-RACE experiment for VvLOXD

Primer name	Primer sequence
LOXDRT (5'-phosphorylated)	5'-CCAGAGTTTATGATGATA-3'
BOLOXD	5'-AGTATCATCATAAACTCTGGGGG-3'
LOXDF1	5'-CAGAAGGCAGTTAAGTGTGATG-3'
LOXDF2	5'-TGATGCACCCAGTCCACCGGCTA-3'
LOXDR1	5'-CTACTGCATGAGTGTTTAACCA-3'
LOXDR2	5'-TGACTGATTAATTGATGATAGG-3'

3.7 Cloning of PCR products

3.7.1 DNA ligation and bacterial transformation

Purified PCR products encoding partial and full-length CDSs of LOX and HPL genes were cloned into pENTR™/TEV/D-TOPO® vector (Invitrogen, Auckland, New Zealand) and transformed into One Shot® TOP10 competent *E. coli* cells (Invitrogen, Auckland, New Zealand) as follows.

PCR products (0.5-4.0 µL) were added to 1 µL of Salt Solution and 1 µL of TOPO® vector insuring 1:1 molar ratio PCR product:vector. The final reaction volume was adjusted to 6 µL with sterile water. The reaction was mixed gently and incubated for 5 min at room temperature (22-23°C). Two microlitres of the cloning reaction was then added into a vial containing One Shot® TOP10 Chemically Competent *E. coli* (Invitrogen, Auckland, New Zealand), mixed gently and incubated on ice for 30 min. The cells were then heat-shocked at 42°C for 30 sec and snap-chilled on ice. Two hundred and fifty microlitres of room temperature Luria Bertani (LB) medium (1 % w/v bacto-tryptone, 0.5% w/v yeast extract, 1% w/v sodium chloride in water, pH 7.5) was added to the vials containing DNA and *E. coli* cells, and incubated at 37°C with horizontal shaking (200 rpm) for 1 hour. Fifty microlitres of the transformation mixture was then spread on a LB-agar plate (solid media containing 1 % w/v bacto-tryptone, 0.5% w/v yeast extract, 1% w/v sodium chloride, 1.5% w/v bacto-agar, pH 7.5) supplemented with 50 µg/mL kanamycin and the plate was incubated overnight at 37°C.

3.7.2 Identifying positive clones by colony-PCR

A 25 µL PCR reaction using Qiagen *Taq* DNA polymerase (Qiagen, Auckland, New Zealand) was set up for each colony to be analysed essentially as described in chapter 3.6.1. All the reagents with exception of template were prepared on ice. In a laminar flow-hood, an individual colony was picked with a sterile pipette tip from the Petri dish containing colonies, and the tip was dipped into a tube containing PCR reaction. Immediately afterward, the pipette tip was placed into a labelled culture tube containing 3 mL LB medium complemented with 50 µg/mL kanamycin. A PCR reaction was then performed using conditions described in section 3.6.1. The products of the reaction were analysed by agarose gel electrophoresis and those reactions producing a PCR product of the expected size were identified. Bacterial cultures corresponding to the positive PCR

reactions were grown overnight at 37°C with vigorous shaking. Plasmid DNA was extracted from LB cultures of the positive clones and purified as in section 3.7.3.

3.7.3 Plasmid mini-preparation

Individual colonies from the plate containing transformation were grown overnight at 37°C with shaking at 250 rpm in 3 mL LB liquid cultures containing 50 µg/mL kanamycin. The cells were pelleted by centrifuging for 1 min at 14000 ×*g* in a microcentrifuge. Plasmid DNA was extracted in accordance with the method described in Sambrook and Russel (2001). The pelleted cells were resuspended in 250 µL Alkaline Lysis Solution I (50 mM glucose, 25 mM Tris-HCl (pH 8.0), 10 mM EDTA, pH 8.0) by vortexing. Then 250 µL Alkaline Lysis Solution II (0.2 N NaOH, 1% (w/v) SDS) was added and the sample was mixed by inversion 4-5 times followed by incubation at room temperature for 5 min until a cleared lysate was obtained. Immediately after this, 350 µL Alkaline Lysis Solution III (3M potassium acetate, 11% v/v glacial acetic acid) was added and the reaction was mixed by inversion 4-5 times. The tube was then centrifuged at 14000 ×*g* for 5 min at room temperature and the plasmid containing supernatant transferred to a fresh 1.5 mL eppendorf tube. Equal volume of isopropanol was added to the supernatant, mixed vigorously and centrifuged at 14000 ×*g* for 10 min to pellet plasmid DNA. The pellet was then washed with 75% ethanol, air-dried for 10-15 min and resuspended in 1×TE buffer containing RNaseA (Sigma-Aldrich, Auckland, New Zealand). After 15 min incubation at room temperature to remove RNA, an aliquot of the sample was taken for restriction endonuclease digestion analysis (see section 3.7.4) and the remaining sample was stored at -20°C until use.

3.7.4 Restriction endonuclease digestion

Unless otherwise specified, restriction endonucleases were purchased from Roche Diagnostics, Auckland, New Zealand and used according to the manufacturer's recommendation for the specific enzyme. A typical 20 µL reaction consisted of 1×SuRE/Cut Buffer, 10 Units of the restriction enzyme and up to 1 µg of DNA to be analysed. The reaction was incubated for 1 h at 37°C followed by an enzyme inactivation at 65°C for 15 min. The reaction products were analysed by separation of samples on 1% agarose gel containing ethidium bromide as described in section 3.6.3.

3.7.5 Long term storage of transformed *E. coli* cells

A single *E. coli* colony containing a construct of interest was used to inoculate 3 mL of LB medium supplemented with corresponding antibiotic and the culture was incubated at 37°C overnight with orbital shaking at 250 rpm. One millilitre of the fresh overnight culture was inoculated into a bead stock containing cryovial according to the manufacturer recommendations (Microbank™, Pro-Lab Diagnostics, Ngiao Diagnostics, Nelson, New Zealand). After the inoculation, excess of cryopreservative fluid was carefully discarded and the vial stored in a freezer at -80°C.

3.8 Quantitative real-time PCR (qPCR)

A Rotor-Gene™ 6000 real-time rotary analyser (Corbett, BioStrategy, Auckland, New Zealand) was used to study relative expression of Sauvignon blanc berry LOX and HPL transcripts. PCR primers for four berry expressed LOX genes, one HPL gene and four reference genes were designed using Vector NTI software (Invitrogen, Auckland, New Zealand) to unique regions within the 3'-end of their respective coding sequences. High levels of sequence similarity between *VvLOXA* and other closely related grape LOXs was taken into account when designing qPCR primers to avoid cross annealing of primers to these sequences.

Total RNA for qPCR analysis was extracted as described in section 3.4.3. cDNA templates were prepared and evaluated as described in section 3.5.2. A 100-well RotorDisc (Corbett, BioStrategy, Auckland, New Zealand) was used for each run, which contained a combination of cDNA template and non-template controls. Some runs included serial dilutions of standards as discussed in section 5.4.2.

To prepare serial dilutions of standards, an end-point PCR reaction for each gene was performed and PCR products isolated and purified as described in section 3.6.4. The identity of each PCR product was confirmed by sequencing. For each PCR product, DNA concentration was estimated and adjusted to 5×10^{-2} ng/µL, which was used in a series of eight 1:10 dilutions. Based on the results obtained from a qPCR run with a serial dilution of the standards, three dilutions (5×10^{-4}, 5×10^{-6} and 5×10^{-8}) were selected for use generating standard curves.

A typical 10 µL qPCR reaction consisted of 5 µL of 2 x SYBR® Premix Ex Taq ™ PCR Mix (Takara, Norrie Biotechniques, NZ), 1 µL of 2 µM primer mix (containing forward and reverse primers), 2 µL of diluted cDNA template and 2 µL of nuclease-free water. The PCR conditions were as follows: 1 cycle at 95°C for 30 sec, 40 cycles (95°C for 5 sec, 58°C for 15 sec, 72°C for 15 sec). A melt curve analysis was performed at the end of each run. The melt curves for each sample were then compared to the melt curves generated for corresponding standards in order to validate correctness of the products formed. Reference genes used and their GenBank accession numbers were as follows: *Actin* (actin 1, XM_002282480), *GAPDH* (glyceraldehyde-3-phosphate dehydrogenase, XM_002263109), *SAND* (SAND family protein, XM_002285134), *EF1* (elongation

factor-1 alpha, XM_002284888). The primers used in qPCR analysis are listed in Table 3.5

Table 3.5 Oligonucleotide primers used in real-time qPCR experiment

Gene	Forward primer	Reverse primer
Actin	5'-GCATCCCTCAGCACCTTCCAGCAG-3'	5'-CCACCTCAACACATCTCCATGTCAACC-3'
GAPDH	5'-ACTGCCTTGCTCCTCTTGCGAAG-3'	5'-CCAGTGCTGCTAGGAATGATGTTGAATG-3'
SAND	5'-TGCCTGTTGATACATCTCCTCGCTCTG-3'	5'-TGGTGGTGAGAACTCCGAAGATACATACTG-3'
EF1	5'-GTGCGTCATAGTTTTCTGCCTTCTTCCTTG-3'	5'-CTCAACCAGTTATCTGCCACCGCCTATC-3'
VvLOXA	5'-GCAAATCAAAGGGACAACGCTGTATGG-3'	5'-TGCTTCCACTGCGGCTTCC-3'
VvLOXC	5'-TGGTGGAAGGAAGTCAGGGAAGAG-3'	5'-TGGGCGGTTTGGGAGGTAGC-3'
VvLOXD	5'-ACCCACCAAATCGTCCCACACTATG-3'	5'-ACCTCTTCGTTGTCTGTCCACTCTG-3'
VvLOXO	5'-TTCCACCCACTCGCCTGATG-3'	5'-GCACCGCACCTGTTTCTTCG-3'
VvHPLA	5'-AACTAGTCCACTCCGTCGTGTACGAAA-3'	5'-AGTCCTTTCTGGCTCGAGCGTATTG-3'

The generated data from Rotor-Gene™ 6000 either was imported into Microsoft Excel and analysed using delta-delta-Ct method or quantified using two standard curves method as discussed in section 5.4.2. The output was normalised against a combination of reference genes which have been shown as most stable in grape berries, Actin, GAPDH, SAND and EF1 (Reid *et al.* 2006) using geNorm method (Vandesompele *et al.* 2002).

3.9 Recombinant protein expression

3.9.1 Designing protein expression constructs

To identify the presence and location of possible signal peptides, their cleavage sites and to predict possible subcellular localisation, the amino acid sequences of the predicted LOX and HPL proteins were submitted to TargetP 1.1 Server (http://www.cbs.dtu.dk/services/TargetP/) (Emanuelsson *et al.* 2007), ChloroP 1.1 Server (http://www.cbs.dtu.dk/services/ChloroP/) (Emanuelsson *et al.* 1999) and WoLF PSORT server (http://wolfpsort.org/) (Horton *et al.* 2007).

Based on predictions obtained from the software analysis, different set of PCR primers were designed for each gene (Table 3.6). Primers LOXAFL_TOPO and LOXATerm were used to amplify full-length VvLOXA coding sequence while LOXA-TP_TOPO in combination with LOXATerm were used to amplify a coding sequence with the putative chloroplast transit peptide removed. Primers LOXOFL_TOPO and LOXO-TP_TOPO were used in combination with LOXOTerm primer to amplify VvLOXO full-length and truncated (minus putative transit peptide) coding sequences respectively. A combination of LOXCFL_TOPO and LOXCTerm primers were used to amplify the full-length expression construct, as no transit peptide has been predicted from *in silico* analysis for VvLOXC. Primers HPLAFL_TOPO and HPLA-TP_TOPO were used in combination with HPLATerm primer to amplify VvHPLA full-length and truncated coding sequences respectively. Table 3.6 lists the primer sequences outlined above.

Table 3.6 PCR primers used to amplify fragments of VvLOXA, VvLOXC, VvLOXO and VvHPLA for cloning into pENTR™ TEV/D-TOPO® vectors

TOPO overhand-forming sequence CACC is underscored; the predicted translation initiation site is marked in bold

Primer name	Sequence
LOXAFL_TOPO	5'-CACCTTCAAGACTCAGGTCCAC-3'
LOXA-TP_TOPO	5'-CACCGTTGGCTACGTCCCTGCCAACAT-3'
LOXATerm	5'-**TCA**AATGGAGATACTGTATGGAACT-3'
LOXOFL_TOPO	5'-CACCGCAGTGGTTAAAGAAA-3'
LOXO-TP_TOPO	5'-CACCCCTGTTGCGGCTGTGA-3'
LOXOTerm	5'-**TCA**TATCGACACACTGTTTGGAATCCC-3'
LOXCFL_TOPO	5'- CACCATTCATTCAATTGTTGGT-3'
LOXCTerm	5'- **TTA**GATGGAGACACTGTTGGGAATC-3'
HPLAFL_TOPO	5'- CACCTTGTCTTCCACGGTCATG-3'
HPLA-TP_TOPO	5'- CACCAGGATCGACAAGTACAAGAGCAC-3'
HPLATerm	5'- TC**TCA**GTTAGCTTTCTCAACGGCGG-3'

Full-length clones of VvLOXA, VvLOXC, VvLOXO and VvHPLA (see section 3.7) were used as DNA templates to produce recombinant protein expression constructs. In order to reduce PCR-derived sequence errors, PCR reactions were performed with high-fidelity PrimeSTART™HS DNA Polymerase (Takara, Norrie Biotech, Auckland, New Zealand) according to the manufacturer instructions with the following PCR conditions: 1 cycle at 98°C for 2 min, 30 cycles (98°C for 10 sec, 50-58°C for 15 sec, 72°C for 3.5 min) and final extension at 72°C for 7 min. The PCR product was purified using AxyPrep kit (Axygen, Total Lab Systems, Auckland, New Zealand), cloned into pENTR™/TEV/D-TOPO® vector (Invitrogen, Auckland, New Zealand) and transformed into One Shot® TOP10 competent *E. coli* cells (Invitrogen, Auckland, New Zealand) as described in section 3.7. The resulted constructs were re-cloned from pENTR™/TEV/D-TOPO® vectors into the 6×His-tag containing Gateway® pDEST17 vector (Invitrogen, Auckland, New Zealand) using Gateway® LR Clonase™ II Enzyme Mix (Invitrogen, Auckland, New Zealand) according to the manufacturer instructions, and transformed into *E. coli* BL21(DE3) cells (Novagen, Merck Bioscience, Auckland, New Zealand).

Plasmids for each of the four constructs were extracted, checked by restriction digest and sequenced using an ABI Prism 3130xl Genetic Analyser from ABI Inc. (The Bio-Protection Research Centre, Lincoln University, New Zealand). The resulting constructs and their encoded proteins were designated as LOXAFL, LOXOFL and HPLAFL encoding full-length proteins; and LOXA-TP, LOXO-TP and HPLA-TP encoding

proteins without predicted transit peptides for VvLOXA, VvLOXO and VvHPLA respectively. As no transit peptide has been predicted for VvLOXC, only one construct, LOXCFL (encoding the full-length protein) was created for this enzyme.

The positive clones were prepared and stored as bead stocks at -80°C (described in section 3.7.5)

3.9.2 Heterologous expression of recombinant LOX proteins

Three mL of LB medium supplemented with ampicillin (100 μg/mL) was inoculated with a single colony or a bead containing the *E. coli* BL21(DE3) host cells containing a pDEST17 clone (see section 3.9.1). The culture was incubated in an orbital incubator overnight at 37°C at 250 rpm. A 50 μL aliquot of the overnight culture was used to inoculate a 50 mL LB culture (including 100 μg/mL ampicillin), and the culture grown in a orbital incubator at 37°C until OD_{600} = 0.6. Expression of the recombinant protein was induced by adding isopropyl β-D-1-thiogalactopyranoside (IPTG) to the final concentration of 1 mM. The incubation temperature was then decreased to 14°C and the culture was incubated for 18-20 h at 250 rpm. The cells were harvested by centrifugation at 5000 ×*g* for 10 min at 4°C and the cell pellet resuspended in 5 mL of 1×PBS (including 1× Complete EDTA-free Protease Inhibitor Cocktail) (Roche, Auckland, New Zealand). The resuspended cells were then sonicated (10×10 sec bursts with 10 sec breaks on ice at power 7 at 50% duty) using SONICATOR W-225 (Heat Systems-Ultrasonic Inc., Watson Victor Ltd., Auckland, New Zealand). The disrupted cells were centrifuged at 14000 ×*g* for 20 min at 4°C. The supernatant was transferred to a fresh tube and considered to be a soluble fraction. The remaining pellet was reconstituted in 5 mL of 8M urea, 10 mM sodium phosphate, pH 8.0 to solubilise insoluble proteins and spun again at 14000 ×*g* for 5 min at 4°C to pellet insoluble cellular debris. The resulting supernatant was considered as the insoluble protein fraction. Aliquots of both, soluble and insoluble fractions as well as their corresponding pre-induced fractions for each construct, were separated on NuPAGE® Novex 4-12% Bis-Tris Gel (Invitrogen, Auckland, New Zealand) according to the manufacturer instructions. The gel was stained with Fast Blue protein stain (Fisher biotech, Raylab, Auckland, New Zealand) and analysed.

Soluble fractions of the recombinant LOX proteins were analysed for LOX activity using α-linolenic acid (LnA), linoleic acid (LA) and AA (arachidonic acid) as substrates at various pH conditions as described in section 3.9.5.

3.9.3 Immobilised metal ion affinity chromatography (IMAC) purification of recombinant LOXA-TP and LOXO-TP

For isolation and partial purification of LOXA-TP and LOXO-TP constructs, 500 mL cell cultures were prepared as follows. A 3 mL of LB medium supplemented with ampicillin (100 μg/mL) was inoculated with a single colony or a bead containing either LOXA-TP or LOXO-TP construct in pDEST17 in *E. coli* BL21(DE3) host cells. The culture was incubated in an orbital incubator overnight at 37°C at 250 rpm. A 500 μL aliquot of the overnight culture was used to inoculate a 500 mL LB culture (including 100 μg/mL ampicillin), and the culture grown in an orbital incubator at 37°C until OD_{600} =0.6. Expression of the recombinant protein was induced by IPTG to the final concentration of 1 mM. The incubation temperature was then decreased to 14°C and the culture was incubated for 18-20 h at 250 rpm. The cells were then harvested by centrifugation at 5000 ×*g* for 10 min, washed with ice-cold 20 mM sodium phosphate buffer pH 7.4 and centrifuged again at 5000 ×*g*. The final cell pellet was resuspended in 40 mL of Binding/Wash buffer (20 mM sodium phosphate, 0.5 M NaCl, 20 mM imidazole, pH 7.4) to which one tablet of Complete EDTA-free Protease Inhibitor Cocktail (Roche, Auckland, New Zealand) was added. The sample was then sonicated (10×10 sec bursts with 10 sec breaks on ice at power 7 at 50% duty) using SONICATOR W-225 (Heat Systems-Ultrasonic Inc., Watson Victor Ltd., Auckland, New Zealand). The resulting slurry was centrifuged at 14000 ×*g* for 20 min at 4°C. The supernatant was filtered through a 45 μm filter prior to application to 3×1mL pre-equilibrated HisTrap™ FF Columns (GE Healthcare Life Sciences, Global Science, Auckland, New Zealand) connected in series. The columns were pre-equilibrated with Binding/Wash buffer according to the manufacturer's recommendations. The column assembly was attached to a Biologic DuoFlow 10 System and the samples loaded using a peristaltic pump (Bio-Rad, Auckland, New Zealand). The columns were then washed with the Binding/Wash buffer to remove unbound proteins. The eluate was monitored until absorbance at 280 nm returned to the baseline. Bound proteins were then eluted with the Elution buffer (20 mM Sodium phosphate, 0.5 M NaCl, 500 mM imidazole, pH 7.4).

The eluted His-purified fraction of the recombinant protein in Elution buffer was exchanged into 20 mM Tris-HCl buffer, pH8.0 (Buffer A) using 4×5 mL HiTrap™ Desalting columns (GE Healthcare Life Sciences, Auckland, New Zealand) connected in series, according to the manufacturer's recommendations. The desalted protein sample was then loaded on 2×1 mL DEAE Sepharose™ Fast Flow columns (GE Healthcare Life Sciences, New Zealand) connected in series, and the columns were washed with buffer A and eluted with step-gradient of buffer B (20 mM Tris-HCl buffer pH8.0, 1M NaCl) as per manufacturer's recommendations. Eluted proteins were monitored by recording the absorbance at 280 nm. Recombinant LOX proteins within eluted fractions were identified by SDS-PAGE analysis and LOX activity assay. The fractions containing LOX activity and acceptable purity were pooled together and buffer exchanged into 30 mM sodium phosphate, 50 mM NaCl (pH 7.5) using 4x5 mL connected in series Hi-Trap Desalt columns. Glycerol was then added to the final concentration of 30% (Storage buffer).

Due to the poor stability of the recombinant LOXO-TP, the ion-exchange purification step was excluded, and the His-purified LOXO-TP was buffer-exchanged into the Storage buffer as described above. The samples were analysed on NuPAGE® Novex 4-12% Bis-Tris Gel (Invitrogen, Auckland, New Zealand) according to the manufacturer instructions. The gel was stained with Fast Blue protein stain (Fisher biotech, Raylab, Auckland, New Zealand) and analysed. Protein concentration was estimated using Quant-iT™ Protein Assay Kit on Qubit fluorometer (Invitrogen, Auckland, New Zealand). The protein was stored in 50 µL aliquots at -80°C until required.

3.9.4 Heterologous expression and preparation of crude *E. coli* extract containing VvHPLA recombinant protein

Cultures for the preparation of recombinant VvHPLA protein were prepared in an identical manner to that described in section 3.9.2.

The partial purification of VvHPLA *E. coli* crude protein extract was based on the method described by Noordermeer *et al.* (2000b). Bacterial cells from a 50 mL liquid culture were harvested by centrifugation and the cell pellet was resuspended in 2.5 mL of 50 mM sodium phosphate buffer, pH 7.5 to which 1× Complete EDTA-free Protease Inhibitor Cocktail (Roche, Auckland, New Zealand) was added. The sample was then sonicated (10×10 sec bursts with 10 sec breaks on ice at power 7 at 50% duty) using

SONICATOR W-225 (Heat Systems-Ultrasonic Inc., Watson Victor Ltd., Auckland, New Zealand). The resulting slurry was spun at 14000 ×*g* for 20 min at 4°C and the supernatant was considered as total protein "soluble" fraction. The pellet was then resuspended in 50 mM of sodium phosphate buffer pH 7.5 containing 0.2% (w/v) Triton X-100 (membrane solubilisation buffer). The resuspended solution was re-centrifuged at 14000 ×*g* for 20 min at 4°C. The resulting supernatant considered to be a re-solubilised "membrane" fraction.

The remaining pellet was reconstituted in 5 mL of 8M urea, 10 mM Sodium Phosphate, pH 8.0 to solubilise any remaining insoluble proteins and centrifuged again at 14000 ×*g* for 5 min at room temperature to pellet cellular debris. The resulting supernatant was considered as the insoluble protein fraction. Aliquots of "soluble", "membrane" and "insoluble" fractions were separated on NuPAGE® Novex 4-12% Bis-Tris Gel (Invitrogen, New Zealand) according to the manufacturer instructions. Soluble fractions of the recombinant HPLAFL and HPLA-TP proteins were also subjected to HPL activity assays with PUFA-hydroperoxide substrates at various pH conditions as described in section 3.9.6.

3.9.5 Determination of LOX activity

Fatty acid substrates (α-linolenic [LnA], linoleic [LA], or arachidonic [AA] acids) (Sigma-Aldrich, Auckland, New Zealand) were prepared as described by Axelrod et al. (1981) and stored in small aliquots at a concentration of 5 mM. The formation of PUFA-hydroperoxides in LOX activity assay was measured as an increase in absorbance at 234 nm (for LA and LnA) and at 238 nm (for AA) as a result of conjugated double bond formation (Axelrod *et al.* 1981). For each reaction, a catalytic rate was determined from the linear part of the progression curve corresponding to the initial rate of the reaction and expressed as ΔA_{234} per second. All measurements for LOXA-TP characterisation were done in 3 ml quartz cuvettes (Starna, Australia) on T60 UV-Visible spectrophotometer (PG Instrument, Bio-Strategy, New Zealand). Most of LOXO-TP activity assays were performed in UV-Star microplates (Greiner bio-one, Alphatec, New Zealand) on FLUOstar Omega microplate reader (BMG Labtech, Alphatec, New Zealand) were used to measure the changes in absorbance at 234nm.

3.9.5.1 Determination of pH optima for LOXA-TP and LOXO-TP

Reaction buffers were prepared with 0.5 pH unit increment as follows, 100 mM sodium citrate (pH 3.0-3.5), 100 mM sodium acetate (pH 4.0-5.5), 100 mM sodium phosphate (pH 6.0-7.5), 100 mM sodium borate (pH 8.0-9.5). To estimate the pH optimum for each of the recombinant proteins, the reaction was run across the pH range 4.0-9.5 with 0.5 pH unit increment.

A typical assay with LOXA-TP consisted of 60 μM of either LnA, LA or AA substrate and 2.3 $\mu g \cdot mL^{-1}$ of purified protein. In experiments with LOXO-TP the final concentrations of FAs and partially purified LOXO-TP protein were 100 μM and 11.6 $\mu g \cdot mL^{-1}$ respectively. Tween 20 was added accordingly to the established for each pH detergent:substrate ratios (Table 3.7) as described in section 6.4.1.

Table 3.7 Empirically determined optimal detergent:substrate ratio

pH	Optimal Tween 20:FA ratio, % w/v:1 μM
≤5.0	0.000028
5.5	0.000131
6.0	0.000095
6.5	0.000061
≥7.0	0.000028

Reactions for both proteins were performed at 25°C in triplicates. Negative controls (no enzyme and no substrate) were included. Catalytic rates were determined from the linear part of the progression curves corresponding to the initial rate of the reactions and expressed as ΔA_{234} per second. The pH, at which the highest catalytic activity was detected, was considered as pH optimum for a particular protein.

3.9.5.2 Determination of temperature optima for LOXA-TP and LOXO-TP

Substrate and protein concentrations were the same as in the experiment described in section 3.9.5.1. Reactions with LOXA-TP and LOXO-TP were performed at pH 5.5 and 7.5 respectively. Tween 20 was added to each LOXA-TP reaction to obtain the optimal detergent:substrate ratio (at pH 5.5 - 0.000131% w/v for each 1 μM of the substrate added). No addition of Tween 20 was required for LOXO-TP reactions at its optimal pH

7.5 (as determined in section 6.4.1) and the final detergent:substrate ratio was 0.000028% w/v for each 1 µM of the substrate added (due to Tween 20 included during substrate stock preparation).

The temperature optimum was estimated by assaying LOX activity rate at temperatures 10-50°C. All reactions were conducted in 3 ml quartz cuvettes (Starna, Australia) on T60 UV-Visible spectrophotometer (PG Instrument, Bio-Strategy, New Zealand) equipped with a thermostatic cell holder connected to a constant-temperature water bath. The reaction buffer and thermostatic cell holder were equilibrated to a required temperature prior to the incubation, and the required temperature was maintained during the assay.

Each reaction was run in triplicate. Negative controls (no enzyme and no substrate) were included. Catalytic rates were determined from the linear part of the progression curves corresponding to the initial rate of the reactions and expressed as ΔA_{234} per second. The temperature at which the highest catalytic activity was detected had been considered as temperature optimum for a particular protein.

3.9.6 Determination of HPL activity

HPL activity were measured as a decrease in absorbance at 234 nm as a result of loss of conjugated double bonds during PUFA-hydroperoxides degradation, as originally suggested by Zimmerman and Vick (1970). 13(S)-hydroperoxides of LnA, LA and AA were prepared and purified using commercial soybean LOX-1 (Sigma-Aldrich, Auckland, New Zealand). Twenty microlitres of 1 mg/mL soybean LOX-1 was added to 150 µL of 5 mM stock of either LnA, LA or AA in 3 mL of sodium borate buffer pH 9.5. The reaction was incubated at RT for 10 min and then stopped by adjusting pH of the reaction to 3.5. Aliquots of the reaction were used immediately as substrates in experiments with VvHPLA recombinant proteins.

Measurements were done either in 3 ml quartz cuvettes (Starna, Australia) on T60 UV-Visible spectrophotometer (PG Instrument, Bio-Strategy, New Zealand) or in UV-Star microplates (Greiner bio-one, Alphatec, Auckland, New Zealand) on FLUOstar Omega microplate reader (BMG Labtech, Alphatec, Auckland, New Zealand). A typical HPL assay reaction consisted of either 13(S)-hydroperoxy-9Z,11E,15Z-octadecatrienoic acid

(13(S)-HPOTrE), or 13(S)-hydroperoxy-9Z,11E-octadecadienoic acid (13(S)-HPODE), or 15(S)-hydroperoxy-5Z, 8Z, 11Z, 13E-eicosatetraenoic acid (15(S)-HPETE) prepared as described above (final concentration 70 μM), 100 mM sodium acetate (pH 4.0-5.5), or 100 mM sodium phosphate (pH 6.0-7.5), or 100 mM sodium borate (pH 8.0-9.5) to which an aliquot of "membrane" *E. coli* fraction containing HPLAFL recombinant protein was added.

For each reaction, a catalytic rate was determined from the linear part of the progression curve corresponding to the initial rate of the reaction and expressed as ΔA_{234} per second.

3.9.7 Kinetic properties of the recombinant grape LOXs

Kinetic properties of the recombinant LOXs were determined by monitoring PUFA-hydroperoxide formation across a range of concentrations of LnA, LA and AA at the standard conditions. For LOXA-TP the standard assay consisted of 0-100 μM of FA substrate in 100 mM sodium acetate buffer (pH 5.5) at 25°C , 2.3 $\mu g.mL^{-1}$ of partially purified recombinant LOXA-TP protein and various final concentrations of Tween 20, depending on the substrate concentration (0.0001% (v/v) of Tween 20 per 1 μM of the substrate). For LOXO-TP the standard assay consisted of 0-160 μM of FA substrate in sodium phosphate buffer (pH 7.5) at 25°C, and 0.00003% (v/v) of Tween 20 per 1 μM of the substrate and 11.6 $\mu g.mL^{-1}$ of partially purified recombinant LOXO-TP. Each reaction was run in triplicate. Negative controls (no enzyme and no substrate) were included. The first order kinetic rates were estimated as changes in absorbance at 234 nm (for LnA and LA) and 238 nm (for AA) per sec and converted into $\mu mol \cdot min^{-1} \cdot mg^{-1}$, using extinction coefficients ε=23000 for LnA- and LA- hydroperoxides and ε=27000 for AA-hydroperoxides. The data was then exported into GraFit software (Erithacus Software Limited, East Grinstead, West Sussex, UK) and fitted using non-linear model and Lineweaver Burk plot to determine Michaelis constant (K_m) and maximum velocity (V_{max}) values for both enzymes.

3.9.8 HPLC analysis of LOX products

To determine identity of the LOXA-TP and LOXO-TP recombinant protein reaction products, the respective recombinant proteins were incubated in the presence of

saturating amounts of PUFA substrates at optimal assay conditions. Specifically, 60 μM of either LnA, LA or AA were incubated with either LOXA-TP or LOXO-TP in 50 mL reactions at 25°C for 15 min, and at pH 5.5 and 7.5 for LOXA-TP and LOXO-TP respectively. Enzyme reactions were stopped by adding 1.6 mL 2.5N HCL to adjust the pH of the reaction solution to 3.0. Extract-Clean ™ SPE C18 columns (Alltech, Grace Davison Discovery Sciences, Auckland, New Zealand) were used to purify the LOX metabolites essentially according to the manufacturer instructions. Briefly, the columns were conditioned with methanol and then with deionised water. The sample was then applied onto the column, washed with 10% acetonitrile and eluted with 5 mL of 100% acetonitrile. The volume of the sample was reduced to 1 mL by evaporation of the sample by flushing of the headspace with oxygen-free nitrogen. The concentrated hydroperoxide samples were stored under nitrogen in sealed vials at -80°C prior to analysis by reverse-phase high performance liquid chromatography (RP-HPLC).

To identify LOX products, RP-HPLC was performed on Agilent 1100 Series HPLC System (Agilent Technologies, Santa Clara, CA, USA), using a Luna 5μm C18(2) 100A column (250x4.60 mm); Phenomenex, Auckland, New Zealand). Authentic FA-hydroperoxide standards were obtained from Sapphire Biosciences, Waterloo, NSW, Australia, and included hydroperoxides of LnA (13(S)-HPOTrE and 9(S)-HPOTrE), LA (13(S)-HPODE and 9(S)-HPODE) and AA (5(S)-HPETE, 12(S)-HPETE and 15(S)-HPETE). LOX reaction products and authentic standards were resolved by isocratic elution with acetonitrile + 0.1% formic acid:H_2O + 0.1% formic acid (63:37) at a flow rate of 0.5 mL/min for 48 min at 25°C. The identity of LOX products was determined by comparison of retention times and UV-spectra of the reaction products with authentic standards.

3.9.9 GC-MS analysis of HPL products

To identify volatile products of reaction with the recombinant HPLAFL and HPLA-TP proteins, 9 mL reactions with LnA, LA and AA were performed in 20 mL gas tight screw cap SPME vials (Supelco, Sigma-Aldrich, Auckland, New Zealand) in a manner similar to that described in section 3.9.6. The reaction consisted of 6 mL of 0.1 mM sodium acetate buffer (pH 5.0), 2.5 mL of PUFA-hydroperoxide substrate prepared by incubation of soybean LOX-1 with a corresponding FA substrate (as described in

section 3.9.6) and 0.5 mL of "membrane" *E. coli* fraction containing HPLAFL recombinant protein. The reaction was then thoroughly mixed and incubated at 20°C for 30 min. In control samples, heat-inactivated recombinant protein sample were incubated with PUFA-hydroperoxides at the same conditions. Solid-phase microextraction (SPME) of the vial head space was then performed followed by a gas chromatography-mass spectrometry (GC-MS) analysis.

A CTC-Combi PAL autosampler (AOC-5000, Shimadzu, Kyoto Japan) was used to automate the capture of the headspace volatiles. Volatile components in the samples were adsorbed onto a Stableflex Divinylbenzene/Carboxen/Polydimethylsiloxane (DVB/CAR/PDMS; 50/30µm x 2cm) SPME fibre (SUPELCO, Bellefonte, PA,USA) placed into the headspace of the 20mL reaction vial held at 30°C for 30 minutes. The SPME fibre was initially conditioned at 250°C for 60 minutes and then twice each day (250°C for 10 minutes) prior to use.

Samples were analysed using a Shimadzu GCMS-QP2010 gas chromatograph mass spectrometer (Shimadzu, Kyoto Japan) fitted with two fused silica capillary columns of different polarity connected in series: a Rtx-Wax 30.0m x 0.25mm ID x 0.5µm film thickness (Polyethylene Glycol - Restek, Bellefonte, PA, USA) and a Rtx-1MS 15m x 0.25mm ID x 0.50µm (100% dimethyl polysiloxane - Restek, Bellefonte, PA, USA). Sample volatiles adsorbed on the SPME fibre were desorbed in the injection port of the GCMS at 250°C for 10 minutes. The column oven was held at 35°C for 3 minutes (during desorption of the SPME fibre), then heated to 250°C at 10°C min^{-1} where it was held at this temperature for 10 minutes.

Helium was used as the carrier gas with the constant linear velocity set at 32.2 cm sec^{-1} in splitless mode (1.20mL·min^{-1}). The mass spectrometer (MS) was operated in electron impact ionization mode with 70eV scanning across the mass range of 35 to 330 m/z. The temperature of the capillary interface was held at 250°C, with the source temperature set at 200°C. All analyses were carried out in scan mode. All compounds detected were identified by matching their mass spectra with the spectra of reference compounds in the NIST EPA/NIH Mass Spectral Library database (National Institute of Standards and Technology, NIST05).

Chapter 4
Identification of members of LOX and HPL gene families in grapevine

4.1 Introduction

Grapevines belong to the genus *Vitis* of the family Vitaceae. The evolution of the genus *Vitis* is proposed to involve the initial crossing of two diploid species, which formed a tetraploid (Jackson 2008). The subsequent crossing of the resulting tetraploid with another diploid species presumably led to the formation of the hexaploid ancestor of modern grapevine (Jackson 2008).

The beginning of the current project coincided with the release, in 2006 by the French-Italian Public Consortium, of the first drafts of the complete Pinot noir grape genome. Late in 2007 the 8× sequence of PN40024, a quasi-homozygous genotype of the Pinot noir cultivar, was released by the International Grape Genome Program (IGGP) (Jaillon *et al.* 2007).

Wine grape (*Vitis vinifera* L, 2n=38) has a relatively small genome of about 500 Mb. Availability of the full genome sequence shaped the strategy for the identification of grapevine members of both the LOX and HPL families. Thus, this sequence information became an invaluable tool in the identification of individual genes and also in determining size and structure of gene families within the genome.

In plants, lipoxygenases are represented by gene-families of various sizes. In the diploid model plant Arabidopsis (*Arabidopsis thaliana* L.) the LOX gene family consists of only six members, whereas larger family sizes have been reported from polyploidy plant species. Specifically, there are at least fourteen LOX members in potato (Liavonchanka and Feussner 2006), sixteen members in rice (Agrawal *et al.* 2004), fifteen members in *Medicago trancatula* and nineteen in soybean (Shin *et al.* 2008).

As described in section 2.5.1, HPL members belong to two groups of the CYP74 subfamily of the cytochrome P450 superfamily. Specifically, 13-HPLs members are regarded as CYP-74B enzymes while 9/13-HPLs are CYP74C enzymes. Based on the

existing genomic data from other plants, HPLs are normally represented by gene families, which are generally smaller than LOX gene families.

The following chapter will report and discuss the results of the mining of the grape genome, which was performed to identify members of grape LOX and HPL families.

4.2 Grape LOX family

4.2.1 Identification of grape LOX family members

Amino acid sequences of functionally characterised plant LOX proteins were used in BLAT and BLAST searches of the complete grape genome to identify grape LOXs as described in section 3.2.1. As a result, at least eighteen LOX-like sequences of various lengths have been identified since the beginning of the project and labelled with letters of the English alphabet from VvLOXA through to VvLOXS in order of their identification (Table 4.1). Recently, the automatic annotation of the Pinot noir genome was completed and the generated annotations were deposited into the GenBank. Those LOXs identified by earlier database mining were compared to the GenBank annotations and those matched sequences were assigned NCBI nucleotide and amino acid accession numbers (Table 4.1).

Twelve out of the eighteen identified grape LOX sequences encoded full- or nearly full-length functional proteins when compared with LOXs from other species. The remaining six LOX sequences either coded for truncated proteins, or there were present irresolvable gaps in the respective genomic DNA sequences which hampered their *in silico* analysis. Specifically, analysis of the *VvLOXF* sequence retrieved from Genoscope revealed a two-nucleotide insertion (GT) in exon 3, which leads to a shift in the open reading frame and would potentially result in a premature termination of the encoded protein. However, a homologous sequence of *VvLOXF* obtained from GenBank (XR_078140) lacked such insertion and encoded a fully functional protein. The predicted coding sequence of *VvLOXK* was 504 bp shorter than its close homologue *VvLOXJ* and possessed two single-nucleotide substitutions within its coding sequence (C/T in exon 4 and G/A in exon 7), which resulted in the generation of two premature stop-codons. The 5'-region of *VvLOXM* coding sequence was interrupted by a transposon-like sequence, and only 267 bp of *VvLOXN* coding sequence could be retrieved from the available Pinot noir genome resources. Genomic sequences of *VvLOXD* and *VvLOXR* possessed a number of irresolvable gaps in the retrievable genomic DNA sequence data and therefore their full structure and functionality could not be predicted. It is worth mentioning here that although analysis in Pinot noir genome shows that *VvLOXD* is most likely to be a pseudogene, it has been found

expressed in Sauvignon blanc tissues, and was therefore included in a more detailed study, which is described in later chapters.

Table 4.1 Identified grape LOXs and their predicted characteristics

ID	NCBI nucleotide	Predicted	Chromosome	NCBI protein	Predicted	Predicted
VvLOXA	XM_002285538	2,706	Chr 6 (-)	XP_002285574	901	13-LOX
VvLOXB	XM_002280615	2,601	Chr 14 (-)	XP_002280651	866	9-LOX
VvLOXC	XM_002284499	2,580	Chr 14 (-)	XP_002284535	859	9-LOX
VvLOXD	N/A	2,177	Chr Un Random	N/A	725	Unknown
VvLOXE	XM_002283130	2,718	Chr 6 (+)	XP_002283166	905	13-LOX
VvLOXF	XR_078140	2,607	Chr 6 (+)	N/A	869	Pseudogene
VvLOXG	XM_002283111	2,712	Chr 6 (+)	XP_002283147	903	13-LOX
VvLOXH	XM_002283099	2,610	Chr 6 (+)	XP_002283135	869	13-LOX
VvLOXI	XM_002283087	2,511	Chr 6 (+)	XP_002283123	836	13-LOX
VvLOXJ	XM_002263818	2,712	Chr 13 (+)	XP_002263854	903	13-LOX
VvLOXK	XR_077340	2,208	Chr 13 (+)	N/A	736	Pseudogene
VvLOXL	XM_002277971	2,631	Chr 5 (+)	XP_002278007	876	9-LOX
VvLOXM	N/A	1,062	Chr 6 (-)	N/A	353	Pseudogene
VvLOXN	N/A	267	Chr 14 (-)	N/A	89	Pseudogene
VvLOXO	XM_002273222	2,751	Chr 9 (+)	XP_002273258	916	13-LOX
VvLOXP	XM_002265469	2,763	Chr 1 Random (+)	XP_002265505	920	13-LOX
VvLOXR	XM_002265785	1,847	Chr Un Random (-	XP_002265821	614	Pseudogene
VvLOXS	XM_002275232	2,760	Chr Un Random (-	XP_002275268	919	13-LOX

The sequences of those LOX genes identified from searching the Genoscope resources and had no corresponding annotations in the GenBank are presented in Appendix A.2.1. Specifically, partial sequences of *VvLOXM* and *VvLOXN* were mined from the Pinot noir genome using GenScan and did not have any corresponding accessions in the GenBank. Furthermore, the 5′-region of *VvLOXD* sequence was identified within a genomic contig in the region with a number of sequence gaps. Therefore, the complete sequence of *VvLOXD* could not be predicted from these resources. The sequence information available was used in 5' RACE experiments on Sauvignon blanc berry cDNA as described in section 3.6.6. As a result of these experiments, a partial coding region of 2,177 bp was isolated and used in subsequent analysis named *VvLOXD* (Appendix A.2.1).

4.2.2 Chromosomal localisation

Figure 4.1 schematically illustrates chromosomal location of fourteen out of eighteen identified grape LOX sequences and their orientation with respect to double-stranded genomic DNA.

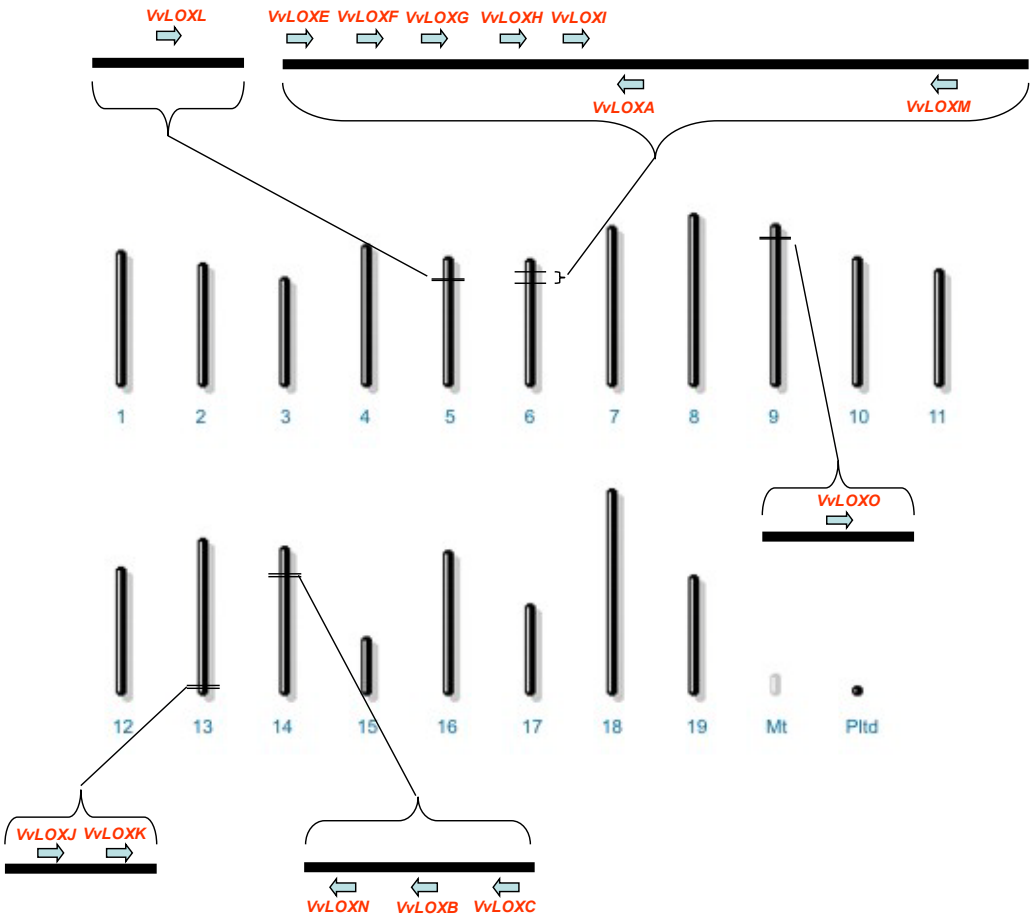

Figure 4.1 Schematically represented chromosome location of the predicted grape LOX genes

Fourteen out of eighteen identified in the grape genome LOX genes were mapped with respect to the predicted grape chromosomes. The sequences of the other three genes, *VvLOXD*, *VvLOXP* and *VvLOXR* could not be linked to any of the existing chromosomes. Nineteen nuclear chromosomes, mitochondrial (Mt) and plastidial (Pltd) sub-genomes are schematically depicted. The arrows indicate 5' to 3' direction for the predicted coding sequences.

Chromosome 6 possesses the largest collection of the LOX sequences. *VvLOXA, VvLOXE, VvLOXF, VvLOXG, VvLOXH* and *VvLOXI* are located within a 100 kb region on chromosome 6 and share between 70% and 90% nucleotide sequence identity. Similarly, *VvLOXB*, *VvLOXC* and the partial sequence for *VvLOXN* are located on chromosome 14 and also share a high degree of similarity (between 75 and 95% sequence identity). The sequence of *VvLOXL* was linked with chromosome 5; *VvLOXO*, with chromosome 9; and *VvLOXJ* and *VvLOXK*, with chromosome 13.

Not all identified LOX sequences, however, could be clearly linked to a particular linkage group/chromosome at this time. Specifically, the sequences of *VvLOXD,*

VvLOXP, *VvLOXR* and *VvLOXS* were found within genomic sequence that could not be associated with any of the currently defined grape chromosomes.

4.2.3 Phylogenetic relationship of grape LOXs

As has been described in section 2.4.4, plant lipoxygenases are categorised into three groups based on their catalytic activity (the positional specificity of insertion of the hydroperoxide group) and the presence or absence of an N-terminal chloroplast-transit peptide. Dependant on the position of oxygenation on the fatty acid backbone (either at carbon-9 or carbon-13), LOXs can be divided into 9-LOX or 13-LOX subclasses respectively (Liavonchanka and Feussner 2006). 13-LOXs, in turn, can be further split into sub-groups with respect to their protein structure. Type I LOXs lack plastid transit peptides and share over 75% sequence similarity among themselves, whereas type II LOXs possess a plastid-transit peptide and exhibit low sequence similarity with members of the sub-group (Shibata and Axelrod 1995). To predict regiospecificity and potential subcellular location, the putative amino acid sequences of the identified grape LOXs were aligned to biochemically characterised members of other plant LOXs (Table 4.2) and analysed using ClustalW as described in section 3.2.2 (the complete alignment is attached in Appendix A.2.2).

Table 4.2 Characterised plant LOXs used in the multiple alignment and phylogenetic tree reconstruction

Species	ID	NCBI nucleotide accession	UniProt or NCBI protein accession
Arabidopsis thaliana	LOX1_At_1	AY093104	Q06327
	LOX1_At_2	AJ302043	Q9LUW0
	LOX2_At_1	AY062611	P38418
	LOX2_At_2	AY075625	Q9LNR3
	LOX2_At_3	AY056166	Q9FNX8
	LOX2_At_4	AC011020;F12B7.11	Q9CAG3
Arachis hypogaea	LOX1_Ah_1	AF231454	Q9M5D3
Brassica napus	LOX2_Bn_2	AY162143	Q8GV01
Glycine max	LOX1_Gm_1	J02795	P08170
	LOX1_Gm_2	J03211	Q39870
	LOX1_Gm_3	X13302	P09186
	LOX1_Gm_4	D13999	P38417
	LOX1_Gm_5	U50075	Q43446
	LOX1_Gm_6	U26457	Q43440
	LOX1_Gm_7	X56139	P24095
Hordeum vulgare	LOX1_Hv_1	L35931	P29114
	LOX2_Hv_1	U56406	P93184
Lens culinaris	LOX1_Lc_1	X71344	P38414
Nicotiana tabacum	LOX1_Nt_1	X84040	Q43800
Oryza sativa	LOX1_Os_1	X64396	P29250
	LOX2_Os_1	D14000	P38419
	LOX2_Os_2	AJ270938	Q9FSE5
Pisum sativum	LOX1_Ps_2	X78580	P14856
	LOX1_Ps_3	X78581	P09918
Populus deltoides	LOX2_Pod_1	DQ131178	Q45HK7
	LOX2_Pod_2	DQ131179	Q45HK6
Populus trichocarpa	PtLOX	XM_002320535	XP_002320037
Prunus dulcis	LOX1_Prd_1	AJ418043	Q8W4X6
Ricinus communis	RcLOX	XM_002527220	XP_002527266
Solanum tuberosum	LOX1_St_1	X79107	P37831
	LOX1_St_2	U24232	O49150
	LOX2_St_1	X96405	O24370
	LOX2_St_2	X96406	O24371
Zea mays	LOX1_Zm_1	DQ335760	Q9LKL4
	LOX1_Zm_3	AF329371	Q9AXG8
	LOX2_Zm_1	DQ335768	A1XCI5
	LOX2_Zm_6	NM_001112506	A1XCI1

With the exception of VvLOXD, all sequences used in the alignment derived from the Pinot noir genome. The coding sequence of VvLOXD experimentally determined from Sauvignon blanc berry was significantly longer than the available corresponding sequence from the Pinot noir genome. Therefore, the former was translated into amino acid sequence and used in the alignment. Sequences of VvLOXM and VvLOXN were

removed from the alignment due to the truncated short sequences that were retrieved for these two genes.

As determined by protein structural studies in plant LOXs, five amino acid residues are involved in binding the atom of catalytic iron, namely three conserved histidines together with two more conserved amino acids, either His/Asn/Ser and the C-terminal isoleucine (Minor *et al.* 1996). Most of the predicted grape LOX proteins contained specific PLAT and LOX domains and conserved residues required for iron-binding (highlighted in yellow, Appendix A.2.2). Exceptions were VvLOXI, which had an aspartic acid residue in the place of a histidine, which is critical for iron binding (position 900, Appendix A.2.2), and VvLOXR and VvLOXS which possessed a terminal valine rather than the highly conserved isoleucine typical of plant LOXs (position 1066, Appendix A.2.2).

The resulting alignment was used to construct an unrooted tree using neighbour-joining method (Figure 4.2).

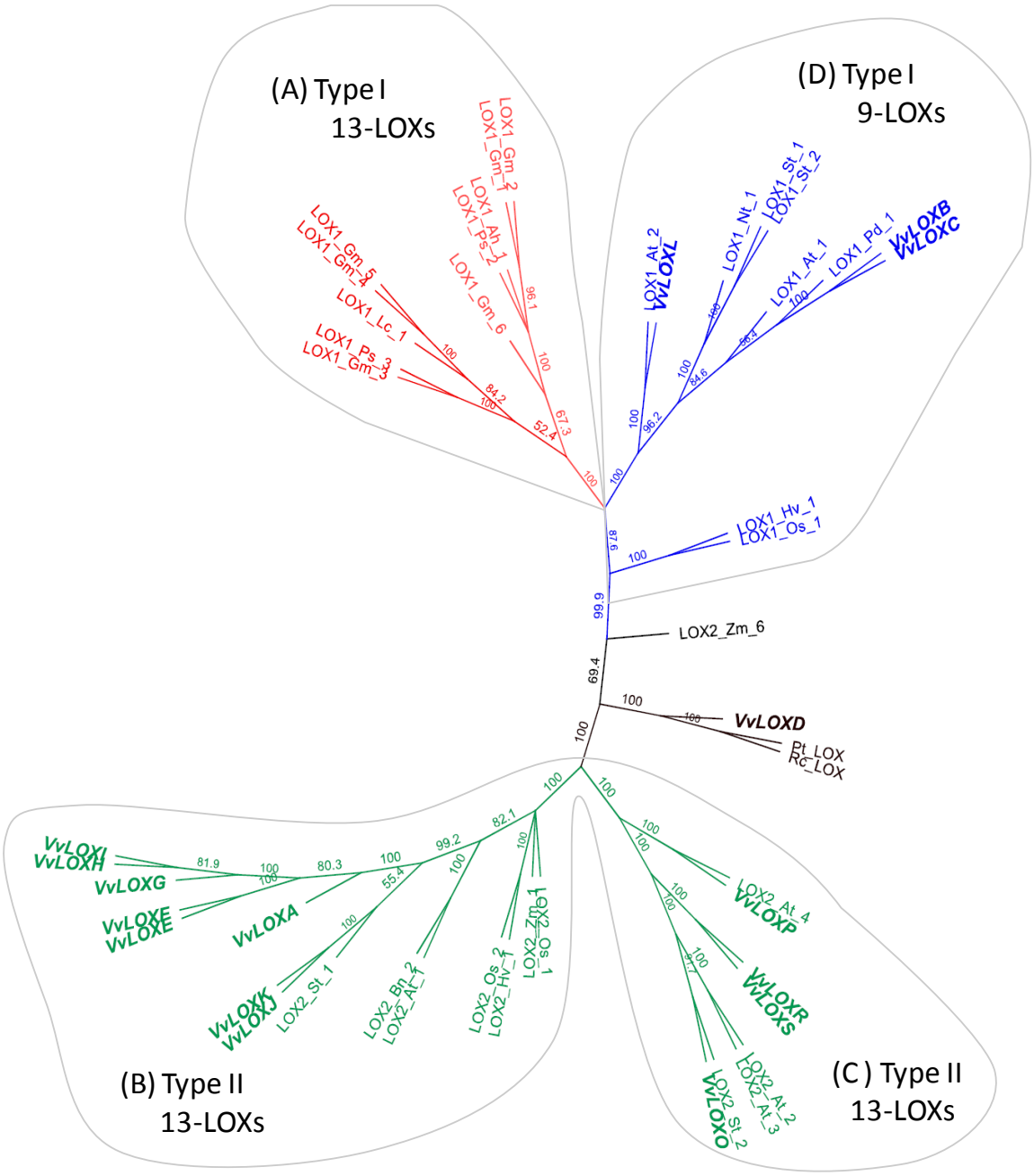

Figure 4.2 Phylogenetic analysis of the predicted grape LOXs (emphasised in bold italic) and biochemically characterised plant LOXs

The evolutionary relationships were inferred using the neighbour-joining method (Saitou and Nei 1987). The bootstrap consensus tree was generated from 1000 replicates and branch consensus support (%) is shown on individual branches (Felsenstein 1985). All positions containing alignment gaps and missing data were eliminated only in pairwise sequence comparisons. Phylogenetic analyses were conducted using Geneious 4.8 software package (Biomatters Ltd., Auckland, New Zealand).

Table 4.1 and Table 4.2 contain gene IDs and accession names for the LOXs used in the alignment construction. According to the previous classification, members of different groups are outlined and shown in different colours as follows: A (red) - type I 13-LOXS, B and C (green) – two clusters of Type II 13-LOXs, D (blue) – Type I 9-LOXs and black – unclassified.

Phylogenetic analysis placed all identified grape LOXs, with exception of VvLOXD, within either the 13-LOX type II or 9-LOX groups (Figure 4.2). No predicted grape LOXs were classified as type I 13-LOX.

VvLOXC, VvLOXB, and VvLOXL grouped with characterised 9-LOX members (Figure 4.2.D) and possessed the conserved valine residues typical for this class of LOX (position 763, highlighted in green, Appendix A.2.2). The remaining LOXs, with the exception of VvLOXD, possessed the conserved phenylalanine residue involved in determining regiospecificity typical for 13-LOXs (position 763, highlighted in green, Appendix A.2.2) and were placed in two separate clusters of type II 13-LOXs (Figure 4.2. B and C). VvLOXD possessed a leucine residue at this site (position 763, highlighted in green, Appendix A.2.2) which was found in only these other uncharacterised putative LOXs: Pt_LOX from poplar and Rc_LOX from castor bean. Both, Pt_LOX and Rc_LOX were generated as automated genome annotation sequences. They shared 65-70% pairwise identity with VvLOXD at amino acid level and were placed in a distinct branch of the tree (Figure 4.2). Further to these significant differences, VvLOXD was the only LOX protein in the alignment that possessed a serine, rather than an alanine, at the position determining LOX stereospecificity (position 738, Appendix A.2.2). As mentioned in section 2.4.2, the alanine residue at this position is highly conserved amongst plant LOXs and is responsible for the production of (S)-enantiomers of PUFA-hydroperoxides.

In order to check whether missing sequence data in the N-terminal region of VvLOXD in the original alignment affected the grouping and relationship between the other grape LOX members, a further alignment and tree were constructed containing only conserved LOX domain regions. This analysis resulted in the construction of an almost identical tree that did not change the relative position of its members (see Appendix A.2.3).

4.3 Grape CYP74 family

4.3.1 Identification of grape CYP74 members

Due to the high levels of sequence similarity amongst different members of CYP74 family (namely AOS, HPL and DES), the decision was made to mine the Pinot noir genome for members of the entire CYP74 family, rather than just HPLs.

Similarly to the identification of the LOX family (section 4.2.1), protein sequences of known CYP74 members (Table 4.3) were used in Genoscope BLAT and BLAST searches in order to identify CYP74 homologues in the Pinot noir genome.

Table 4.3 Characterised plant CYP74 members

Species	ID	NCBI Protein accession
Arabidopsis thaliana	AtHPL	AAC69871
	AtAOS	CAA63266
Capsicum annum	CaHPL	AAA97465
	CaDES	ABH03632
Cucumis melo	CmHPL	AAK54282
Cucumis sativus	CsHPL2	AAF64041
Hordeum vulgare	HvAOS1	CAB86384
	HvHPL	CAC82980
Lycopersicum esculentum	LeHPL	AAF67142
	LeAOS1	CAB88032
	LeAOS2	AAF67141
	LeDES	AAG42261
Linum usitatissimum	LuAOS	AAA03353
Musa acuminata	MaHPL	CAB39331
Medicago sativa	MsHPL1	CAB54847
	MsHPL2	CAB54848
	MsHPL3	CAB54849
Medicago trunculata	MtHPL1	CAC86898
	MtHPL2	CAC86899
	MtAOS	CAC86897
Nicotiana tabacum	NtDES	AAL40900
Parthenium argentatum	PaAOS	CAA55025
Psidium gujava	PgHPL	AAK15070
Solanum tuberosum	StHPL	CAC44040
	StAOS	CAD29735
	StDES	CAC28152

As a result of the genome mining of the Pinot noir genome, seven genes coding for CYP74-like proteins were identified. Based on their sequence similarity with the characterised CYP74 members, six out of the seven identified genes were regarded as HPLs (VvHPLA-F) and one gene as AOS (VvAOS) (Table 4.4). No putative DES genes were identified as a result of the mining. The identified proteins were submitted to NCBI and their corresponding nucleotide and protein accession numbers were determined (Table 4.4).

Table 4.4 Identified grape CYP74 members

ID	NCBI nucleotide accession	Predicted CDS length, bp	Chromosome (strand)	NCBI protein accession	Predicted protein length, aa	Predicted functionality
VvHPLA	XM_002272955	1464	Chr 12 (+)	XP_002272991	487	13-HPL
VvHPLB	XM_002281123	1452	Chr 3 (+)	XP_002281159	483	9/13-HPL
VvHPLC	XM_002281154	1452	Chr 3 (+)	XP_002281190	483	9/13-HPL
VvHPLD	XM_002281165	1497	Chr 3 (+)	XP_002281201	499	9/13-HPL
VvHPLE	XM_002281177	1497	Chr 3 (+)	XP_002281213	499	9/13-HPL
VvHPLF	XM_002281190	1464	Chr 3 (+)	XP_002281226	487	9/13-HPL
VvAOSA	XM_002283744	1563	Chr 18 (-)	XP_002283780	520	13-AOS

All the predicted HPLs were similar in size, encoding typical HPL proteins, ranging from 483 to 499 aa long (Table 4.4). With the exception of *VvHPLA*, all identified HPLs had a single-exon predicted genomic structure. The coding sequence of *VvHPLA* spanned two exons. The putative AOS, *VvAOSA* encoded a 520 aa protein and its coding sequence consisted of a single exon.

4.3.2 Chromosomal localisation

Using the genome browser provided by the Genoscope, the identified CYP74 members were positioned on the predicted grape chromosomes (Figure 4.3). *VvHPLA* was predicted to be located on chromosome 12, while five other identified HPL genes were tandemly located on chromosome 3 and the predicted *VvAOSA* was localised to chromosome 18 (Figure 4.3).

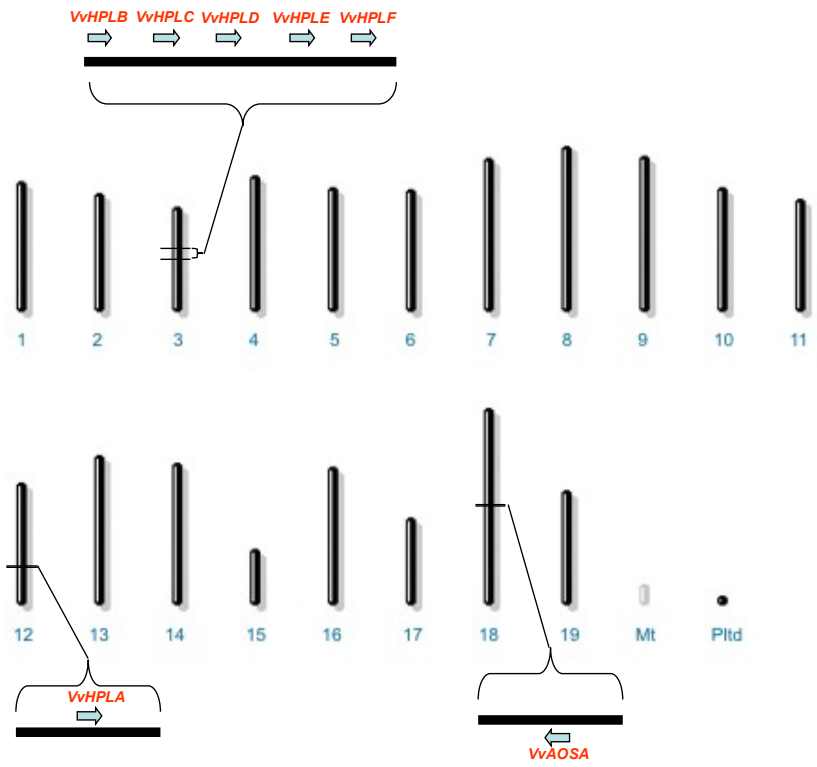

Figure 4.3 Schematically represented chromosome location of the predicted grape CYP74 genes

Identified in the grape genome members of the CYP74 family were mapped with respect to the predicted grape chromosomes. Nineteen nuclear chromosomes, mitochondrial (Mt) and plastidial (Pltd) sub-genomes are schematically depicted. The arrows indicate 5' to 3' direction for the predicted coding sequences.

4.3.3 Phylogenetic relationship of grape CYP74 members

In order to predict biochemical properties of the identified grape CYP74 members, their amino acid sequences were aligned to the reported members of AOS, HPL and DES families from other plant species (see Table 4.3) using ClustalW as described in section 3.2.2 (Appendix A.2.4). The alignment was used to construct an unrooted phylogenetic tree using the neighbour-joining algorithm with 1000 replicates (Figure 4.4). As shown in Figure 4.4, only one predicted grape HPL, VvHPLA grouped with characterised 13-HPLs (CYP74B subfamily shown in red), while VvHPLB, C, D, E and F formed a cluster with 9/13-HPL members (CYP74C subfamily shown in blue). As predicted,

VvAOSA grouped with characterised 13-AOS members (CYP74 subfamily shown in green) and no predicted grape CYP74s was clustered with DES members (CYP74 shown in green and yellow for AOS and DES respectively, Figure 4.4).

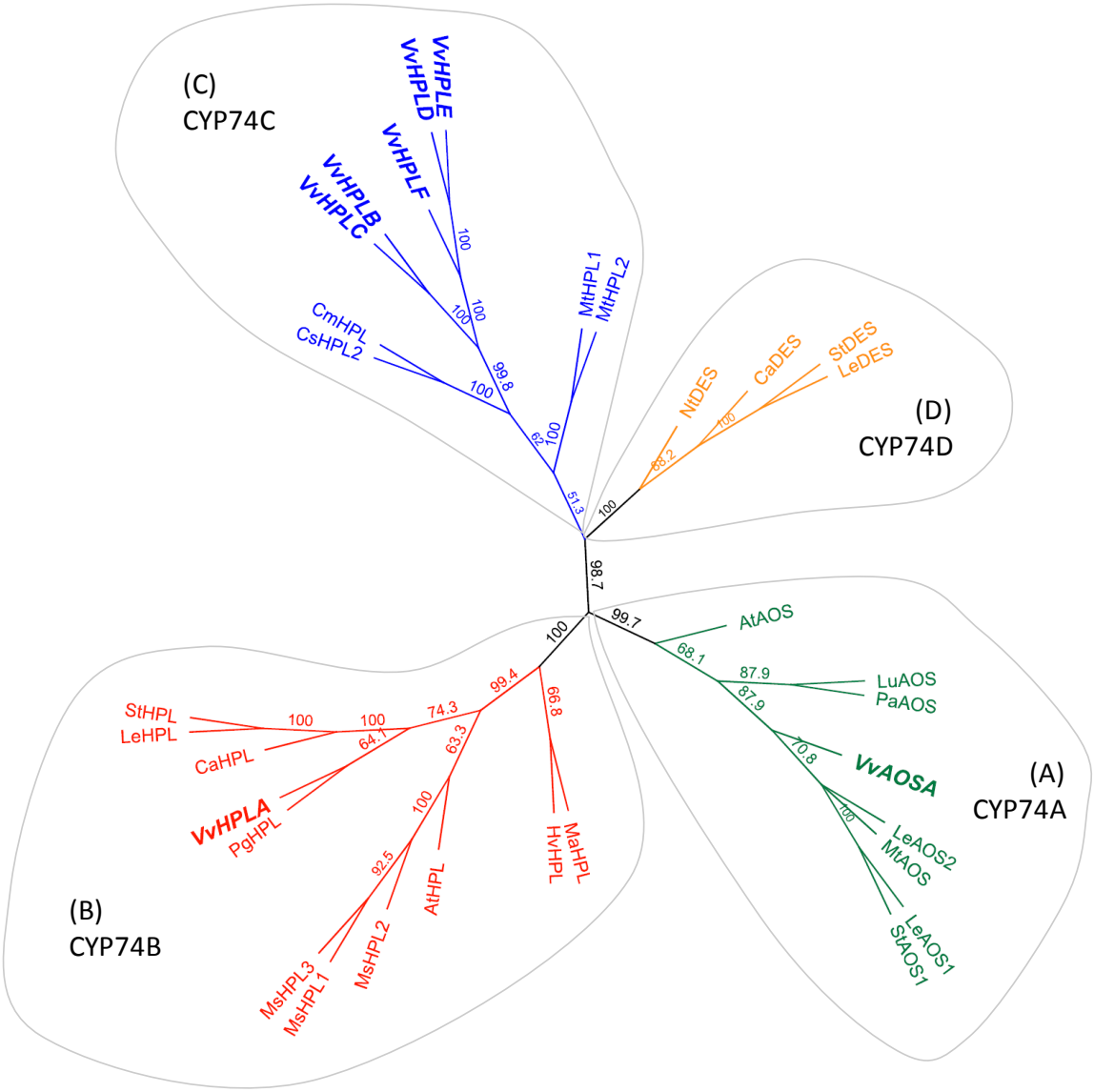

Figure 4.4 Phylogenetic analysis of the predicted grape CYP74 enzymes and CYP74 members reported from other species.

The evolutionary relationships were inferred by using the neighbour-joining method (Saitou and Nei 1987). The bootstrap consensus tree was generated from 1000 replicates and branch labels represent the consensus support (%) (Felsenstein 1985). All positions containing alignment gaps and missing data were eliminated only in pairwise sequence comparisons. Phylogenetic analyses were conducted in Geneious software package (Biomatters Ltd., Auckland, New Zealand). Table 4.3 and Table 4.4 contain gene IDs and accession names for the genes used in the alignment. Subfamilies of CYP74 family are outlined and shown in different colours as follows: A (green) – CYP74A, B (red) – CYP74B, C (blue) – CYP74C, D (yellow) – CYP74D.

Detailed analysis of the important functional domains within the primary structure of the identified grape CYP74 proteins further supports the functional division predicted by phylogenetic relationships with characterised CYP74s (Appendix A.2.4). The position and functional importance of such domains have been reviewed and studied by Lee *et al.* (2008). All aligned sequences contained typical CYP74 insertions in the $FxxGx_3CxG$ cytochrome P450 signature motif (Appendix A.2.4, highlighted in red). All sequences in the alignment contained strictly conserved residues that bind the catalytic molecule of haem by interacting with haem propionates (highlighted in blue, Appendix A.2.4). Furthermore, all sequences contained an invariant cysteine residue serving as a protein contributing ligand of the Fe(III) molecule (highlighted in orange, Appendix A.2.4).

The study by Lee *et al*. (2008) also identifies CYP74 active site residues important for substrate binding and determining the mechanism of catalysis. One of such important residues (for reference, Phe-137 in Arabidopsis AtAOS) has been proposed to interact with C11 carbon of the substrate during radical and carbocation formation and to determine the fate of intermediate compounds (Lee *et al.* 2008). The research also reported that all AOSs studied contained a phenylalanine at this position, while HPLs and DESs contained a leucine. In agreement with this observation, all except one of the predicted grape HPLs contained a leucine at this position, while the predicted VvAOS contained a phenylalanine residue (Appendix A.2.4, position 161 highlighted in yellow). The sole exception was VvHPLC, which instead of leucine contained a phenylalanine at this position, a residue typical for AOSs (Appendix A.2.4, position 161).

Another important residue (for reference, Ser-155 in Arabidopsis AtAOS) is reported to be important for stabilisation of the epoxyallylic intermediate (Lee *et al.* 2008). In most of the characterised HPLs and DESs serines at the position corresponding to S-155 in AtAOS are substituted to either alanines or valines. This was also true for five identified grape HPLs. VvHPLA, B, D, E and F possessed an alanine at the position corresponding to Ser-155 in AtAOS (position 179 of the alignment, Appendix A.2.4). The exception, again, was VvHPLC, which had a proline residue at this position. As was expected, VvAOS possessed a serine at the conserved position, which supported its classification as an AOS member (position 179 of the alignment, Appendix A.2.4).

4.4 Discussion

4.4.1 Grape LOXs

4.4.1.1 Expansion of grape LOX gene family is likely to be attributed to multiple duplication events

Sequence analysis of *Vitis vinifera* genome has identified the presence of at least eighteen LOX-like sequences. LOX gene families of a similar size have been reported for potato (at least 14 members (Liavonchanka and Feussner 2006)), rice (at least 16 members (Agrawal *et al.* 2004)), Medicago (15 reported members) and soybean (at least 19 members (Shin *et al.* 2008)). The expansion of the LOX gene family in legume plants has been attributed to ancient polyploidy events with subsequent duplication and/or tandem duplication (Shin *et al.* 2008). It has also been proposed that the genome of modern grape has been formed by merging three ancestral genomes either by a true polyploidy event or through successive genome duplications (Jaillon *et al.* 2007). This theory is supported by the existence within the grape genome of clusters of paralogous genes located on different chromosomes. For example, Jaillon and colleagues (2007) report that grape chromosomes 6, 8 and 13 carry a number of genes that share a high degree of sequence similarity and form paralogous clusters on each of these three chromosomes. Similarly, the present investigation indicates that *VvLOXJ* and *VvLOXK*, which are located on chromosome 13, have high sequence similarity with *VvLOXE*, *F*, *G*, *H*, *I* and *A*, located on chromosome 6 (Figure 4.1). Phylogenetic analysis (Figure 4.2) also clusters these LOX family members together. Furthermore, *VvLOXL*, located on chromosome 5, is highly similar to sequences of *VvLOXB*, *C* and *N*, located on chromosome 14. The chromosomes 5 and 14 have also been identified as containing paralogous regions (Jaillon *et al.* 2007). In contrast, the partial sequence of *VvLOXM*, which also shares 90 to 95% nucleotide sequence identity with *VvLOXB* and *VvLOXC*, has been located on chromosome 6, which does not contain any definite paralogous regions with neither chromosome 5, nor chromosome 14.

The further expansion of the LOX gene family can also be explained by tandem gene duplication events. For example, six LOX genes (*VvLOXE*, *F*, *G*, *H*, *I* and *A*) share between 60 and 80% nucleotide sequence identity and have been found to be located within 100 Kbp on chromosome 6 (Figure 4.1).

It has been determined, that after the duplication paralogous genes over time undergo functional differentiation, which often increases plant adaptability and stress-resistance (Ober 2005). Similarly, duplicated LOX genes, despite their high sequence similarity, may have acquired redundancy in biochemical terms and may be involved in multiple independent physiological processes within the plant.

Further functional and biochemical characterisation of the members of the LOX gene family is required to confirm which members are functional and which represent pseudogenes. As discussed in section 4.2.1, sequence analysis of some of the identified grape LOXs indicates that they are likely to have lost function and may be considered pseudogenes. However, it is also important to take into account that the published genome sequence belongs to a highly homozygous genotype, while most cultivated grape cultivars are highly heterozygous and derive from quite different ancestral genetic backgrounds. It is likely therefore, that in a heterozygous background some alleles identified in this study as non-functional retained their functionality. It is also likely, that more members of the LOX gene family will be identified as genome sequence and annotation progresses to fill gaps in the existing the genome sequence.

4.4.1.2 Grape LOX gene family is represented by 13- and 9-LOX members

The present classification separates LOX proteins into three groups based on their regiospecificity and presence/absence of plastid transit peptide as described in section 2.4.4. This classification, however, is not perfect and has a number of exceptions. Firstly, many LOXs possess dual regiospecificity and in *in vitro* experiments have shown these LOXs are able to produce either hydroperoxide forms to a greater or lesser extent (Porta and Rocha-Sosa 2002). Secondly, apart from being localised to the cytoplasm and plastids, LOXs have also been found in a range of cellular organelles, such as the vacuole, peroxisomes, lipid bodies, plasma membranes and microsomal membranes (reviewed in Liavonchanka and Feussner 2006). Furthermore, there are studies indicating, that despite the absence of recognisable targeting peptides and predicted cytosolic localisation, some LOXs have been found to be localised within the chloroplast (Gao *et al.* 2008). Despite shortcomings, the proposed classification is useful as the first step in predicting potential function and localisation of individual members of large LOX families.

Three of the conserved histidines together with one His/Asn/Ser at the conserved position, and the C-terminal isoleucine are responsible for binding an atom of a catalytic iron (Minor *et al.* 1996). As mentioned in section 4.2.3, VvLOXI, VvLOXR and VvLOXS have non-conservative amino acid substitutions at these important positions. It has been reported, that a single amino acid substitution in one of the iron-binding histidines deactivates soybean LOX2 (Wang *et al.* 1994). These findings suggest that the $His_{900}Asp$ substitution (Appendix A.2.2) in the amino acid sequence of VvLOXI may result in the loss of one of the catalytic iron ligands, and will subsequently affect VvLOXI catalytic properties or possibly lead to its complete deactivation. Moreover, the predicted sequences of VvLOXR and VvLOXS both have isoleucine residues replaced by valines at the important C-terminal amino acid position. An identical substitution was observed in an unusual LOX from maize, ZmLOX6 (LOX2_Zm6). This substitution was listed as one of the potential reasons that recombinant ZmLOX6 protein, expressed in *E. coli* , failed to convert PUFAs into either 13- or 9-hydroperoxides but instead displayed hydroperoxide lyase activity. The products of this reaction were an odd-chain ω-oxo fatty acid and a C5 compound (Gao *et al.* 2008).

The phylogenetic analysis of the grape LOX gene family places all of the identified grape LOXs into two groups, type II 13-LOXs and cytosolic 9-LOXs (Figure 4.2). The exception is VvLOXD, which was placed in a separate group together with the functionally uncharacterised LOXs from *Populus trichocarpa* (Pt_LOX) and *Ricinus communis* (Rc_LOX), which were included in the alignments as these sequences represent the nearest VvLOXD sequence matches (Figure 4.2).

As mentioned earlier, the predicted classification of the grape LOXs (i.e. type II 13-LOX or 9-LOX) can be supported by conserved positions of amino acids that are thought to provide the positional 13- or 9-LOX specificity. In the region that contains the substrate binding domain, 13-LOXs contain conserved phenylalanine or histidine residues, whereas all 9-LOXs contain valines (position 763, highlighted in green, Appendix A.2.2). The physical size of these amino acids at the conserved position has been suggested to affect the substrate orientation or penetration depth inside the binding pocket (Liavonchanka and Feussner 2006). With the exception of VvLOXD, all the predicted grape 13-LOXs contained phenylalanine, while the predicted 9-LOXs contained valine at this position. Interestingly, VvLOXD, as well as its closest matches

Pt_LOX and Rc_LOX, contained a leucine at this critical position. The effect of such substitution is unknown, but a tyrosine substitution at this position has been observed in ZmLOX6 and possibly contributed to its unusual catalytic properties mentioned earlier.

Most of plant LOXs exhibit a high level of product stereospecificity and convert PUFAs almost exclusively into (*S*)-enantiomers. This feature has been ascribed to a single alanine residue within the LOX domain (Coffa and Brash 2004). With the exception of VvLOXD, all predicted grape LOXs possessed a conserved alanine as the stereodeterminant. VvLOXD possessed a serine residue at this position. In contrast, Pt_LOX and Rc_LOX, the nearest matches to VvLOXD, retained specific alanine at the stereodetermining position. Previous research indicates, that the substitution of alanine to glycine in (*S*)-lipoxygenases results in the production of (*R*)-enantiomers by these LOXs (Coffa and Brash 2004). To date there has been no alanine-to-serine substitutions, such as that found in VvLOXD, that have been functionally characterised and the effect of such a substitution on VvLOXD functionality remains unclear.

The high number of substitutions in the predicted amino acid sequence of VvLOXD, (in particular those at functionally important conserved positions) may indicate that VvLOXD gene encodes an inactive LOX protein. The existence of homologous gene sequences in other plant species suggests that at least some of the substitutions observed in VvLOXD are also present in LOX genes from other plants and most likely occurred much earlier in the evolution. Furthermore, as will be shown in Chapter 5, transcripts of VvLOXD were detected in Sauvignon blanc berries. These observations make VvLOXD an interesting candidate for further detailed study, and if functional, it is likely to have unique properties, not previously reported for plant LOXs.

It is evident from Figure 4.2, that type II 13-LOXs form two separate clusters within this group (Figure 4.2 B, C). Sequence analysis revealed that the basis for forming two separate groups is likely to be based on sequence variation in both PLAT and LOX domains, although members of both type II clusters possess typical 13-LOXs residues. Members of both type II clusters typically possess N-terminal sequences encoding chloroplast targeting peptides (Feussner and Wasternack 2002). However, the sequence divergence and reported properties of the characterised members of both clusters indicate that these enzymes can be localised in different compartments of the chloroplast. For instance, GFP-tagged LOXH1 (LOX2_St_1, cluster B, Figure 4.2) and

LOXH3 (LOX2_St_2, cluster C, Figure 4.2) were localised respectively in stroma and thylakoids of potato leaf chloroplasts (Farmaki *et al.* 2007).

Furthermore, the developmental and stress-induced gene expression patterns of members of the two type II clades appear to be different. For instance, expression of potato *LOXH3* transcripts was transiently induced by leaf wounding, while there was no significant changes in expression levels of *LOXH1* (Farmaki *et al.* 2007). However, wound-induced gene expression seems not to be limited to members of the C-cluster only. Specifically, Arabidopsis mutants with reduced levels of AtLOX-2 (LOX2_At_1, Figure 4.2. B) failed to accumulate JA in response to leaf wounding, while wounded wild-type plants exhibited a seven-fold increase in the JA levels in four hours after wounding indicating the importance of AtLOX-2 in stress-related JA biosynthesis (Bell *et al.* 1995).

As the results indicate, while *in silico* prediction and phylogenetic analysis are useful tools for an initial characterisation of LOX function, further functional analysis such as those presented in Chapters 5 and 6, are required to characterise the identified grape LOXs.

4.4.2 Grape CYP74s

Although the goal of this project was to characterise only those members of HPL branch of the LOX pathway in grapevine, the initial screen of genomic resources for putative HPLs also included putative members of AOS and DES families similar to those identified in other plants. This was due to high sequence similarity amongst the CYP74 family members, which resulted in ambiguous results during preliminary BLAST searches. As a result, the initial genome mining resulted in identification of a potentially complete CYP74 family in the grape genome, including HPL, AOS and DES members.

The results obtained during the initial mining were somewhat unexpected. Out of the seven putative CYP74 members identified, six genes encoded HPLs, one gene encoded AOS and there was no evidence of the existence of DES-like genes (Table 4.4). Absence of DES sequences in the grape genome implies that the DES-branch of the LOX pathway does not exist in this species. Published data supports this, indicating that DES enzymes seem to be restricted to some algae and to a few genera of higher plants, namely *Solanum*, *Ranunculus* and *Allium* (Stumpe and Feussner 2006).

The predominance of HPL members suggests that the metabolism of PUFA-hydroperoxides in grapevine occurs primarily via the HPL branch of the LOX pathway (GLV-pathway). Furthermore, five out of six identified grape HPLs phylogenetically group with functionally characterised 9/13-HPLs, predicting that these enzymes possess dual specificity and that these proteins are likely to be localised outside of plastids. Only one grape HPL, VvHPLA grouped with members of the 13-HPL subfamily. This enzyme possessed a longer N-terminal peptide than the other grape HPLs (Appendix A.2.4), and *in silico* localisation analysis predicted for this enzyme to be localised to the chloroplast.

It would be appealing to suggest that the existence of five members of the 9/13-HPL sub-family and corresponding 9-LOXs will result in high content of C9 products (aldehydes and their derivatives) in grape juice and subsequently wine. Indeed, the presence of a range of C9 aldehydes and alcohols has been reported in musts of both red and white cultivars (Hashizume and Samuta 1997). However, most of these compounds derived from macerated stems and leaves, while the content of berry-derived C9 compounds was relatively small (Hashizume and Samuta 1997). In contrast, the content of C6 compounds was much higher in all organs, exceeding levels of C9 compounds in berries by up to ten-fold, and in leaves up to a thousand-fold (Hashizume and Samuta 1997). These data indicate, that in macerated grapes significantly larger proportion of PUFAs are being metabolised via the 13-HPL pathway. Low abundance of C9 compounds in macerated grapes can be due to a number of reasons.

For instance, as discussed earlier, the number of putative 9-LOX genes in the grape genome is relatively less than the number of putative 13-LOXs. It is possible therefore that the lower abundance of C9 compounds is limited by the low number of 9-LOXs present and/or low activities of 9-LOXs, which would ultimately result in a lower concentration of 9-hydroperoxide substrates available for further metabolism. Alternatively, 9-LOXs, and therefore their reaction products, the 9-hydroperoxides, may be physically separated from the corresponding HPL enzymes inside the cell. Therefore, insufficient cell disruption could potentially prevent or limit the amount of 9-hydoperoxide substrates available for 9/13-HPL enzymes and could potentially result in low amounts of C9 volatiles produced in crushed grapes.

Finally, the conditions formed by maceration of grapes, such as pH or temperature, might not be suitable for 9-LOX and/or 9/13-HPL proteins, limiting their activity, and subsequently resulted in lower levels of C9 compounds produced in grape musts.

Furthermore, it is not clear whether the high level of C6 compounds in grapes is due only to high VvHPLA activity. It is possible that in the absence of 9(S)-hydroperoxides and in the excess of 13(S)-hydroperoxides, at least some of 9/13-HPLs will participate in the metabolism of the latter substrates and therefore contribute to the amount of C6 GLVs produced. This is an important question, which should be addressed in future investigations.

Chapter 5
Gene expression analysis of berry localised LOXs and HPLs

5.1 Introduction

The first step chosen for characterisation of the GLV pathway was the study of gene expression of the genes potentially involved in this pathway. Although studying of gene expression does not take into account a number of other factors such as post-transcriptional, post-translational modifications and enzyme activity of each individual member involved in the biochemical pathway, levels of gene expression often correlates with the level of metabolites produced via this pathway.

As mentioned before, the ultimate goal of the current project was identification of LOX and HPL members involved in the formation of short-chain volatiles in Sauvignon blanc grape berries. Berries are the major component of the grape must that directly determine the quality of the wines. Therefore, the assumption was made that grape berry GLV compounds are synthesized directly in the berry by berry-expressed LOX and HPL enzymes, and changes in LOX and HPL gene expression reflect changes in level of secondary metabolites produced by corresponding enzymes.

Due to the initial unavailability of the full grape genome, the initial plan called for identification of candidate LOX and HPL members utilising existing grape berry EST databases. As a result of such screening, ESTs of two grape LOX genes (which were later designated as *VvLOXA* and *VvLOXC*) and one HPL gene (*VvHPLA*) were identified from these EST databases and were eventually also found to be expressed in Sauvignon blanc berries. These initial findings coincided with the release of first drafts of the Pinot noir genome. Subsequently, a more thorough mining of the genomic resource was undertaken in order to identify all possible candidates.

As described in Chapter 4, sequences of eighteen putative LOXs and six putative HPLs have been identified. Due to time constraints, it proved impossible to characterise all 24 identified genes and the decision was made to characterise only selected members with a focus on the members potentially involved in the formation of short-chain volatiles.

The following chapter describes and discusses gene expression patterns of the LOXs and HPL selected for study in Sauvignon blanc berries.

5.2 Identification of berry expressed LOXs and HPLs from Sauvignon blanc

Total RNA was extracted from Sauvignon blanc berries from eight developmental stages using CTAB extraction method as described in section 3.4.2. Berries for the initial analysis were collected in the 2006 season (see sections 3.3.1 and 3.3.3 for the details). The integrity of the extracted RNA was determined visually using denaturing agarose gel electrophoresis as described in section 3.4.6 (Figure 5.1).

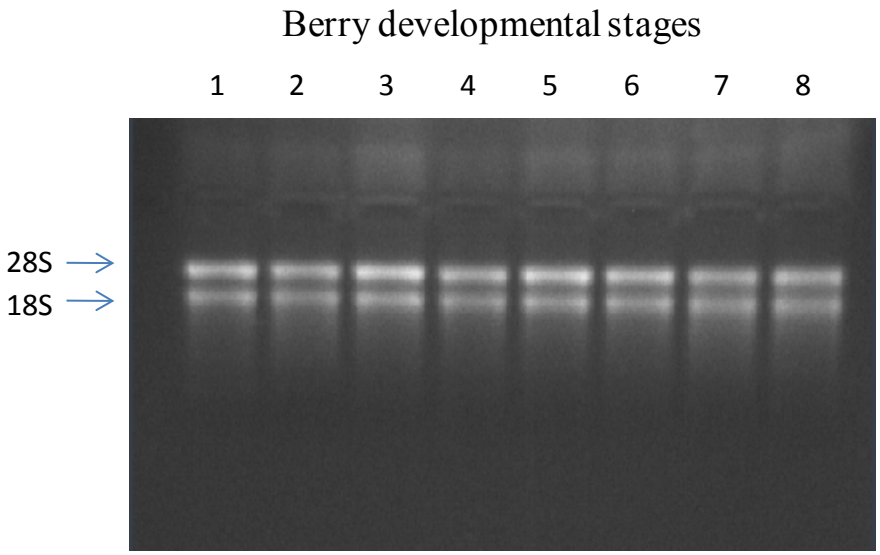

Figure 5.1 RNA denaturing gel analysis.

One microgram of total RNA, extracted from berries of eight developmental stages (lanes 1-8 correspond to stages 1-8), were separated using an RNA denaturing agarose gel. The arrows indicate bands corresponding to 28S and 18S sub-units of plant ribosomal RNA.

The purified total RNA was then converted into complementary DNA (cDNA) using an oligo-dT primer to prime the synthesis reaction as described in section 3.5.2. Synthesised cDNA of individual berry developmental stages was then pooled together and the resulting pool used for subsequent experiments.

As mentioned earlier, *VvLOXA*, *VvLOXC* and *VvHPLA* were the first genes identified, as their sequences were available in berry EST databases. *VvLOXA*, *VvLOXC* and *VvHPLA* were also found to be expressed in Sauvignon blanc berries (Figure 5.2). Based on their phylogenetic relationship with functionally characterised members from other plants, *VvLOXA* and *VvHPLA* had been identified as putative type II 13-LOX and 13-HPL respectively (Figure 4.2.B and Figure 4.4) and therefore were selected as initial candidates for the further biochemical investigation. Upon the release of the first full

genome drafts, other LOX and HPL family members were identified and *VvLOXO* was added to the selected genes as a representative member of a sub-cluster of type II 13-LOXs (Figure 4.2. C). Furthermore, a representative of the 9-LOX clade, *VvLOXC* (Figure 4.2. D), and an unclassified LOX, *VvLOXD* (Figure 4.2), were added to the group of selected enzymes for comparison. As a result, expression of four LOX genes, *VvLOXA*, *C*, *D* and *O*, and one HPL gene, *VvHPLA* were studied in Sauvignon blanc berries. Figure 5.2 summarises the results of an initial end point PCR analysis with the selected genes for further expression analyses.

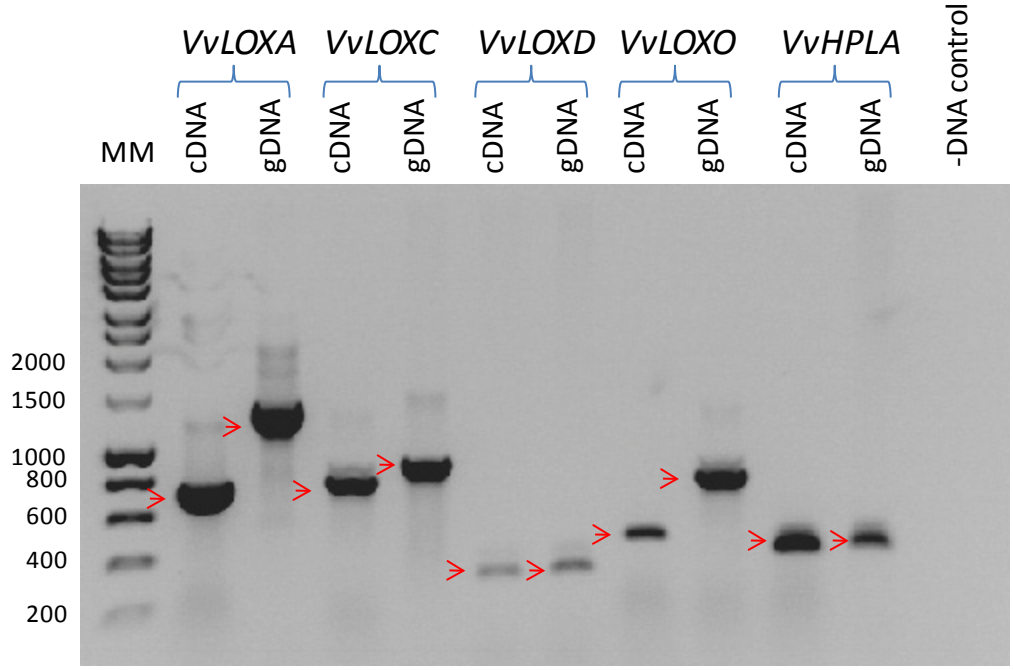

Figure 5.2 End-point PCR analysis of grape LOX and HPL genes identified for detailed characterisation in Sauvignon blanc

10 µL of each PCR reaction were separated on a 1% agarose gel and examined under UV-light. The primers used in the reactions are listed in Table 3.1. The samples were run in pairs after amplification with complementary (cDNA) and genomic (gDNA) DNA as template (MM – molecular marker). Arrows indicate the predicted size of the corresponding cDNA and genomic fragments.

Amplification with cDNA and genomic DNA templates produced PCR products of the predicted sizes (Figure 5.2).Varying intensity of PCR products was observed in the end-point PCRs with identical template concentrations (Figure 5.2). It is likely that the observed variation was either due to differences in the copy number of specific genes present in the template pool or due to differences in PCR efficiency of different sets of primers.

The expression of the remaining LOXs and HPLs in Sauvignon blanc berries was also checked (Figure 5.3 and Figure 5.4). However, due to time constraints, this study was limited to identifying their presence in the total RNA pool (in which eight berry developmental stages were combined) using end-point PCR.

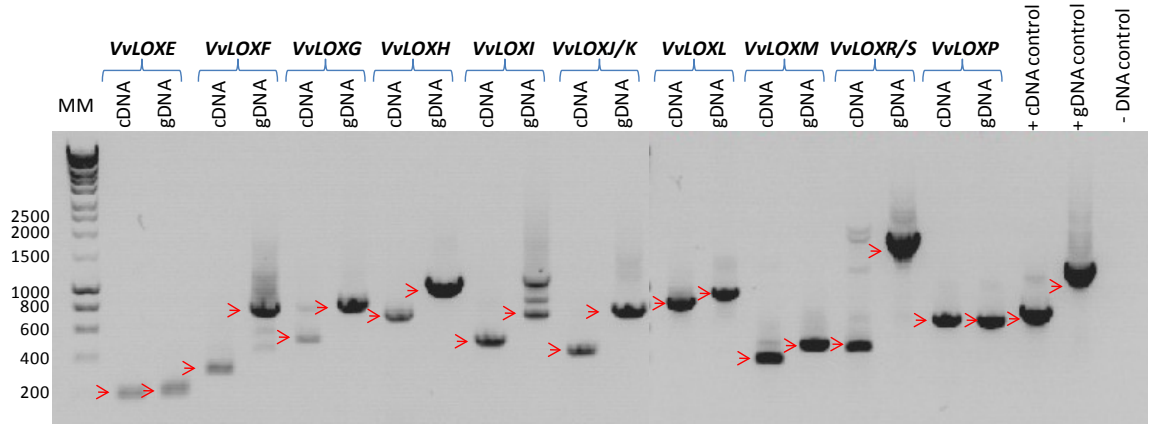

Figure 5.3 Determination of presence/absence of expression of grape LOX gene family in Sauvignon blanc berries

10 µL of each PCR product was run on 1% agarose gel and examined under UV-light. The primers used in the reactions are listed in Table 3.1. The samples were run in pairs after amplification with cDNA and gDNA (MM – molecular marker). Arrows indicate the predicted by *in silico* analysis size of the corresponding cDNA and genomic fragments.

Figure 5.3 illustrates results of the PCR analysis performed on the total pool of transcripts extracted from berries of eight developmental stages. Although all primer combinations produced PCR products of the expected sizes, subsequent sequencing of the PCR products revealed that some of the PCR products did not correspond to the expected LOX sequence. Specifically, PCR products with primer combinations designed to amplify regions of *VvLOXB*, *F*, *G*, *K*, *M*, *N* and *R* genes, were identified as sequences of other closely related genes. Closer analysis revealed that this was most likely due to cross-annealing of some primer pairs to closely-related genes.

A similar experiment was performed for the remaining five putative 9/13-HPLs and the results are shown in Figure 5.4.

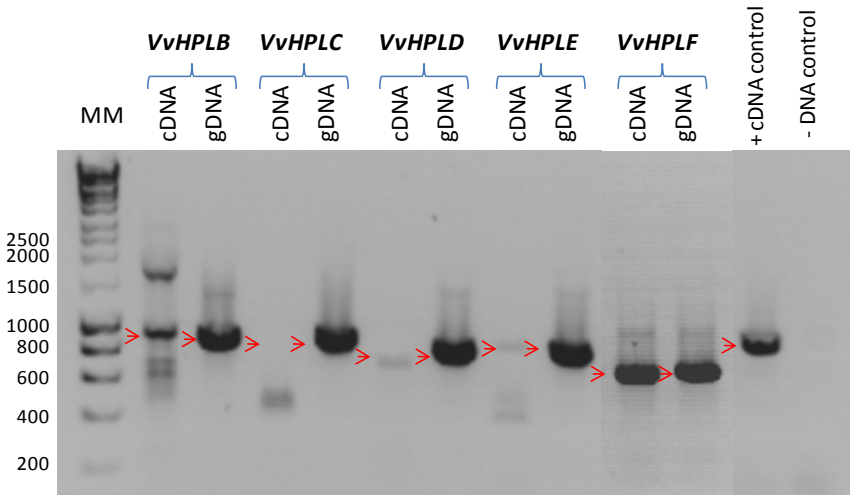

Figure 5.4 Electrophoresis analysis of the remaining HPLs

10 µL of each PCR product was run on 1% agarose gel and examined under UV-light. The primers used in the reactions are listed in Table 3.2. The samples were run in pairs after amplification with cDNA and gDNA (MM – molecular marker). Arrows indicate the predicted size of the corresponding cDNA and genomic fragments.

As can be seen in Figure 5.4, four of the five putative 9/13-HPL genes (*VvHPLB*, *D*, *E* and *F*) were expressed in Sauvignon blanc berry at different levels. Using Sauvignon blanc genomic DNA as a template, PCR products of the expected size were obtained for all 9/13-HPLs. Sequence analysis of cloned PCR products confirmed the identity of each PCR amplicon indicating the chosen primers were capable of distinguishing between genes with high sequence similarity.

Overall, eleven LOX genes and five HPL genes were found to be expressed in Sauvignon blanc berries at various levels. Transcripts of seven LOX genes and one HPL gene were not detected in pooled RNA of different Sauvignon blanc berry developmental series. It is worth mentioning that these results do not preclude expression of the remaining LOXs and HPLs in berries that have been grown in differing conditions to those studied here.

5.3 Cloning of full-length coding sequences of the selected LOXs and HPL

As mentioned in the previous section, four LOX genes and one HPL gene were selected for further molecular and biochemical analysis. To obtain full-length coding sequences (CDS) of the selected genes, PCR primers to the translation initiation and termination sites of *VvLOXA*, *C*, *O* and *VvHPLA* were designed using Pinot noir genomic annotations and used in PCR reactions with Sauvignon blanc cDNA template as described in section 1.1.1. Segment of the 5′ region of *VvLOXD* could not be retrieved from existing genomic resources. Accordingly, a 5′-RACE experiment approach was used in an attempt to deduce the full-length CDS for Sauvignon blanc *VvLOXD* as described in section 3.6.6.

Full-length PCR products for VvLOXA, C, O and VvHPLA were isolated, purified and cloned into the pENTR™/TEV/D-TOPO® vector (Invitrogen, NZ) and transformed into One Shot® TOP10 competent *E. coli* cells (Invitrogen, NZ) as described in section 3.7. For each construct, twenty randomly selected colonies from a plate containing transformants were analysed using colony-PCR (see section 3.7.2 for description). Six positive colonies were subsequently selected, plasmid DNA isolated (section 3.7.3) and this DNA submitted for sequence analysis (section 3.6.5).

For each gene, the sequence data obtained for six randomly selected clones were aligned and analysed. The analysis revealed a number of putative single nucleotide polymorphisms (SNPs) found within coding sequences of different clones for each gene. The highest number of SNPs was found within the CDS of *VvLOXA*. Sequence variation has also been observed in individual clones of *VvLOXO*, *VvLOXC* and *VvHPLA*, however at much lower frequency.

The alignment shown in Appendix A.3.1 highlights 32 SNPs identified in the 2708 bp coding sequence of the *VvLOXA*. In order to confirm that the variation seen in the *VvLOXA* transcript pool was not a technical artefact, an 80 bp region of *VvLOXA* CDS containing 4 putative SNPs was PCR-amplified using gDNA from six different vines (region is outlined with a red box, Appendix A.3.1). The genomic sequences obtained were aligned with the previously sequenced 6 transcript clones and their chromatograms were compared.

The analysis of the aligned chromatograms revealed that 2 of the 4 SNPs identified from transcript pool (marked positions 2 and 3, Appendix A.3.2) were present in all six genomic samples. All six genotypes were heterozygous for these SNP positions. In comparison, only one genotype (SB12) appeared to have C/T variation (marked position 1, Appendix A.3.2) and none of the sequenced genotypes had any variation at the fourth polymorphic position identified in the transcript pool (marked position 4, Appendix A.3.2). It is unclear whether the later polymorphism is a polymerase-introduced error or a rare polymorphism. Sequencing of more individual genotypes is required to answer this question.

To determine whether the identified 32 SNPs affect the tertiary structure of VvLOXA protein variants, the deduced amino acid sequences were used to model their spatial configuration using Swiss-PDB viewer software (http://spdbv.vital-it.ch/, accessed 20 May 2010) developed by Guex and Peitsch (1997), with crystal structure of soybean LOX-1 as template. The predicted 3D models of six *VvLOXA* variants were then superimposed in order to deduce structural alignments and compare their active sites. The obtained results predicted no major changes in the active site and LOX domain of the putative proteins (Appendix A.3.3). The positions of iron-binding ligands were the same in all variants. Some misalignments between the variants however were observed in the PLAT-domain region (Appendix A.3.3). Although observed changes in the PLAT domain are unlikely to affect LOX activity, further experiments are required to confirm this. Although a comparison of *VvLOXA* variants was unachievable within the current project due to time constraints, all six variants were cloned into protein expression vectors for later characterisation.

The full-length sequences of identified Sauvignon blanc LOXs and HPL genes have been submitted to the GenBank with the following accessions numbers: *VvLOXA* (FJ858255), *VvLOXC* (FJ858256), *VvLOXO* (FJ858257) and *VvHPLA* (FJ861082).

Characterising the *VvLOXD* gene was more challenging than for the other selected genes. Due to a gap in the Pinot noir genomic sequence, it was impossible to predict the full-length coding sequence for *VvLOXD*. To circumvent this issue, a series of 5'-RACE PCR experiments were performed as described in section 3.6.6. As a result, a PCR fragment of 2177 bp was obtained, which was approximately 500 bp larger than the predicted sequence information from the Pinot noir genome.

The identified *VvLOXD* sequence was used in a BLAST search and the closest matches outside of *Vitis* were found to be *Rc_LOX* (XM_002527220) from castor bean (*Ricinus communis*) and *Pt_LOX* (XM_002320535) from black cottonwood (*Populus trichocarpa*). Both, *Rc_LOX* and *Pt_LOX* were generated as a result of an automatic annotation of the corresponding genomes, but have not yet been characterised functionally.

The three sequences were aligned using ClustalW and analysed (Appendix A.3.4). The sequence of *VvLOXD* had 75% pairwise identity with *Pt_LOX* and 76% with *Rc_LOX*. The identified *VvLOXD* fragment was 60 bp shorter from the predicted translation initiation site of PtLOX and 381 bp shorter than *Rc_LOX* (Appendix A.3.4). Further experiments will be required to determine whether the sequence information obtained represents the full extent of the coding sequence for *VvLOXD,* or whether there is still a short portion of the coding sequence missing. Due to time constraints, no further attempts were undertaken as part of the current investigation and the largest *VvLOXD* fragment was used in phylogenetic and gene transcript analyses.

5.4 Expression study of berry LOXs and HPLs

Quantitative real-time PCR (qPCR) analyses were undertaken to study relative expression of LOX and HPL genes in grape berries using the method described in section 3.8 during development and upon wounding or chemical treatments. These experiments included berry wounding and spraying with a solution of methyl jasmonates (MeJA). Transcript levels of LOX and HPL genes were also compared in healthy berries with berries infected with the common grape pathogen *Botrytis cinerea*. A detailed description of sampling conditions and elicitation trials is described in section 3.3.

5.4.1 Selection of reference genes

Four grapevine genes were selected as reference genes in this study based on the previous research by Reid *et al*. (2006). These genes were *Actin* (actin 1, XM_002282480), *GAPDH* (glyceraldehyde-3-phosphate dehydrogenase, XM_002263109), *SAND* (SAND family protein, XM_002285134) and *EF1* (elongation factor-1 alpha, XM_002284888). The geNorm VBA applet for Microsoft Excel (Vandesompele *et al.* 2002) was used to evaluate expression stability of the four genes in samples from different experiments.

Appendix A.3.5 presents results of testing for each particular set of samples. Based on the M-value obtained for each tested gene, the decision was made on which genes were used for that particular experiment as described in later sections.

Specifically, *Actin* and *GAPDH* were to be the most stable genes in the sample sets representing Sauvignon blanc developmental series, samples from wounding and MeJA treatment experiments (Appendix A.3.5, A, C, D), and these two genes were selected as reference genes in the corresponding experiments. Expression of *SAND* and *EF1* genes varied the least between different tissues of Sauvignon blanc berry (Appendix A.3.5, B) and they were used as reference genes of choice for calculating transcript distribution of selected LOXs and HPL within the berry.

5.4.2 Establishing qPCR method and post-run analysis

Premix Ex Taq ™ PCR Mix (Takara, Norrie Biotechniques, Auckland, New Zealand) was chosen for performing qPCR analysis. This mix utilises SYBR® Green I

intercalating dye that fluoresces once bound to double-stranded DNA. PCR cycling and real-time measuring of fluorescence intensity was performed on Rotor-Gene™ 6000 real-time rotary analyser (Corbett, BioStrategy, Auckland, New Zealand).

Primers for qPCR analysis were designed according to the guidelines set out in Premix Ex Taq ™ PCR Mix manual. Extra care was taken when designing primers for *VvLOXA*. As mentioned earlier, there are five other LOX genes in the grape genome, which are highly similar to *VvLOXA*. These sequences were aligned and PCR primers specific to *VvLOXA* were selected, avoiding regions where such primers could cross-anneal with other LOX gene family members. Primers used in the gene expression study are listed in Table 3.5. To check quality of the designed primers, they were initially used in end-point PCR analysis using PCR conditions as similar as possible to the conditions considered for qPCR experiments. End-point PCR products were analysed on a 1% low-range agarose gel due to the small size of the amplicons (Figure 5.5). All primer pairs produced single-band products of the expected size. Subsequent sequencing of the purified PCR products confirmed their sequence identity and therefore the specificity of the PCR reaction.

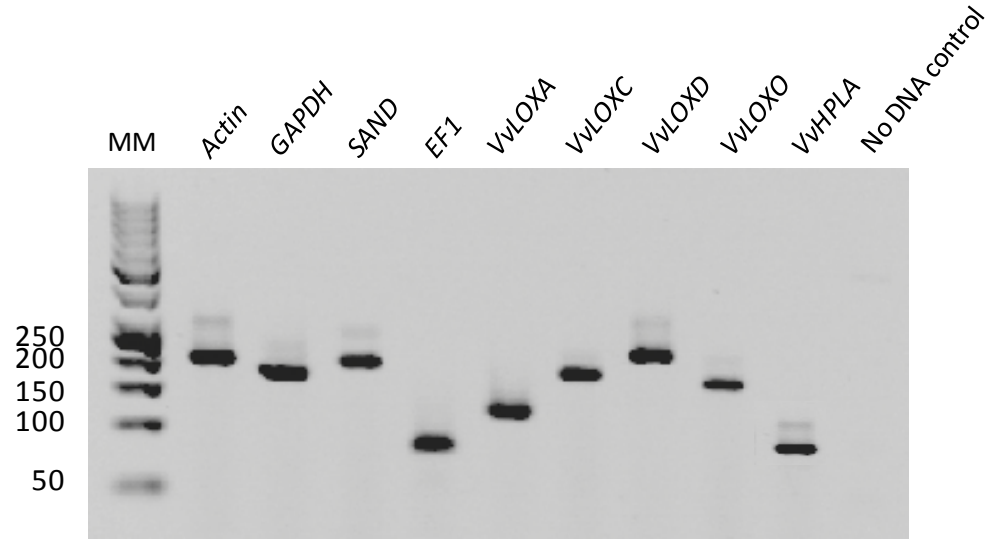

Figure 5.5 End-point PCR with primer pairs designed for real-time qPCR experiments

10 µL of each PCR product was run on 1% low-range agarose gel and examined under UV-light. The primers used in the reactions are listed in Table 3.5. MM – molecular marker.

The purified PCR products were quantified using a NanoDrop® ND-1000 Spectrophotometer and used for preparation of serial dilutions of standards and generating standard curves for all genes studied as described in section 3.8. The initial standard curves were generated using eight Ct points obtained from running qPCR reactions with 1:10 serial dilutions of the standard template (an example of a standard curve generated for *Actin* is shown in Appendix A.3.6).

Three points on each standard curve were then selected for using in subsequent qPCR runs, representing samples containing 1×10^{-4}, 1×10^{-6} and 1×10^{-8} ng/µL of PCR product respectively (Figure 5.6). These three points were selected from the linear parts of the initial eight-point standard curves ensuring that all experimental data points fall between the two outer points of the standard curve. Generated three-point standard curves were used for relative quantification using a two standard curve (TSC) analysis, which is part of Rotor-Gene™ 6000 post-run analysis software.

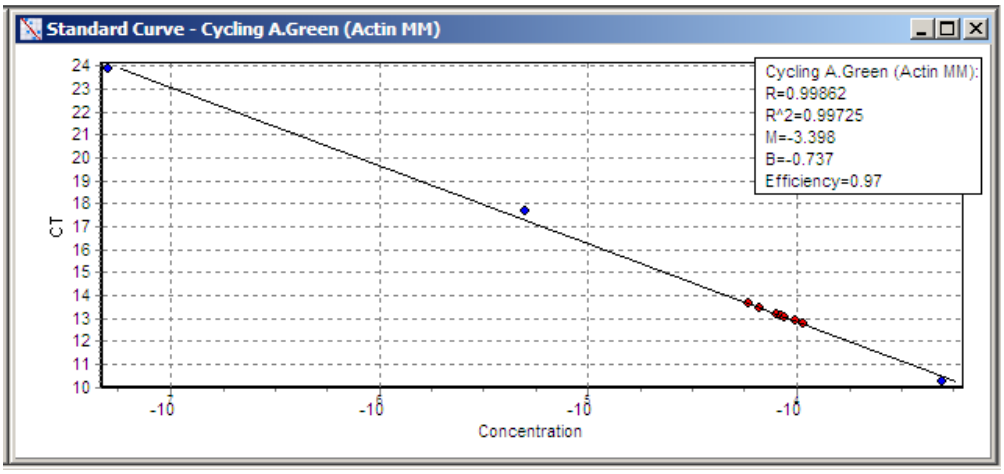

Figure 5.6 An example of a standard curve window displaying main amplification characteristics for *Actin*

Blue dots correspond to serial dilution of standards (1×10^{-4}, 1×10^{-6} and 1×10^{-8} ng/µL of PCR product respectively) and red tots represent unknown cDNA samples.

Although standard curves generated using serial dilution of PCR products are a good estimator of the amplification efficiency for a given set of primers, this method often does not take into account sample-to-sample variation in amplification efficiency for the same set of primers. To overcome this problem, amplification efficiency for each sample were calculated using second derivative maximum algorithm, which is part of "Comparative Quantitation Analysis" module of the Rotor-Gene™ 6000 software.

Figure 5.7 illustrates the screenshot of "Comparative Quantitation Analysis" software with amplification efficiency values generated for a number of samples and standards with a set of primers amplifying *Actin* gene. As can be seen from the figure, amplification values ranged from 1.92 to 1.98 within the same run using the same PCR conditions.

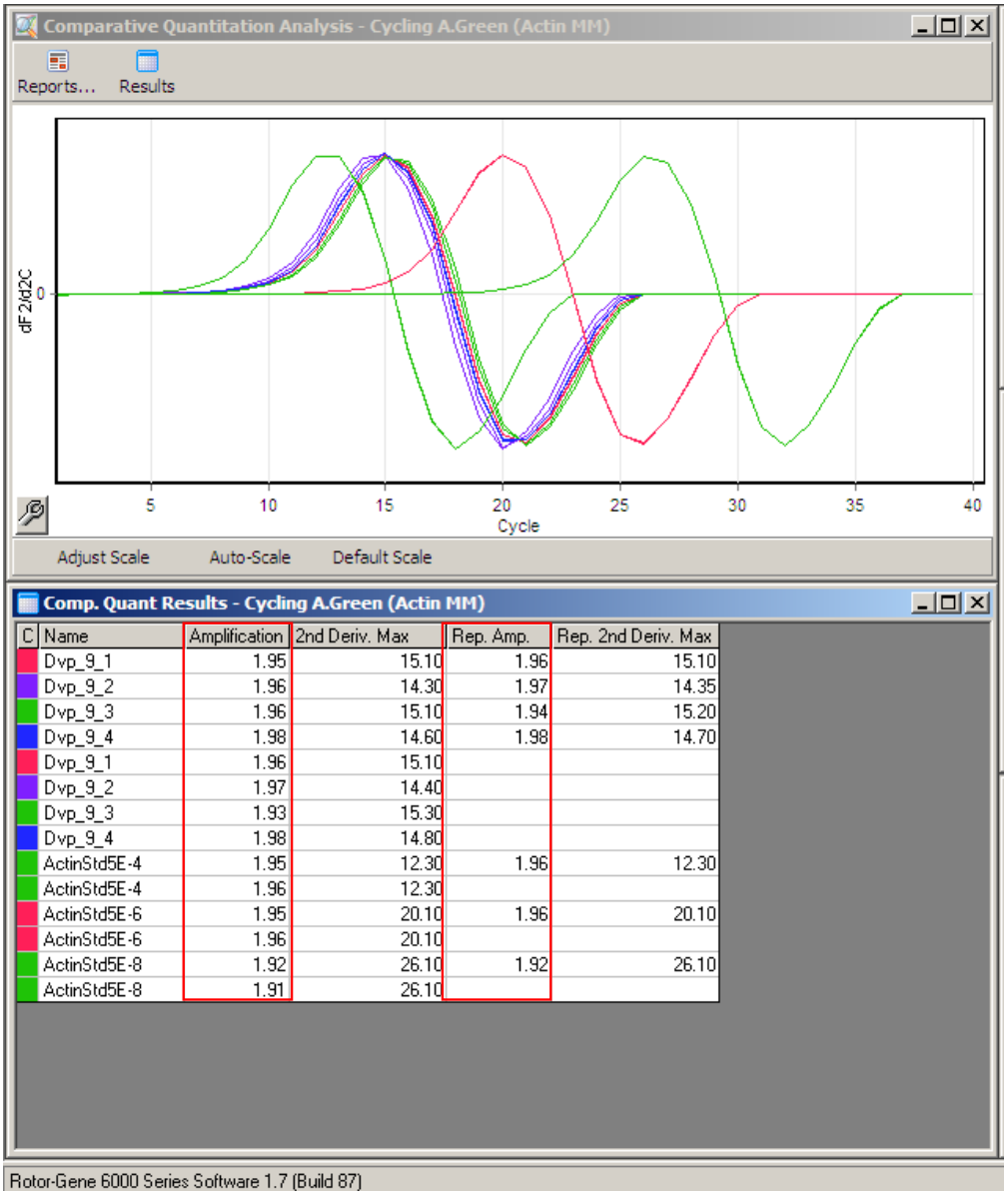

C	Name	Amplification	2nd Deriv. Max	Rep. Amp.	Rep. 2nd Deriv. Max
	Dvp_9_1	1.95	15.10	1.96	15.10
	Dvp_9_2	1.96	14.30	1.97	14.35
	Dvp_9_3	1.96	15.10	1.94	15.20
	Dvp_9_4	1.98	14.60	1.98	14.70
	Dvp_9_1	1.96	15.10		
	Dvp_9_2	1.97	14.40		
	Dvp_9_3	1.93	15.30		
	Dvp_9_4	1.98	14.80		
	ActinStd5E-4	1.95	12.30	1.96	12.30
	ActinStd5E-4	1.96	12.30		
	ActinStd5E-6	1.95	20.10	1.96	20.10
	ActinStd5E-6	1.96	20.10		
	ActinStd5E-8	1.92	26.10	1.92	26.10
	ActinStd5E-8	1.91	26.10		

Figure 5.7 An example of a typical post-run analysis window using "Comparative Quantitation" analysis

The amplification efficiency values were calculated using the second derivative maximum method. Amplification values for each sample and average for two replicates are outlined by red boxes.

Further calculations of relative transcript abundance were then performed using ΔΔCt method (Livak and Schmittgen 2001), with modifications described below.

Amplification efficiency and Ct values for each sample were exported into MS Excel™ spreadsheet and used in calculations of relative transcript abundance for each gene using formula:

$$\mathbf{Q = E^{\Delta Ct}} \qquad (1)$$

Q = gene transcript abundance in a sample relative to the sample with highest expression;

E = amplification efficiency estimated for each sample using second derivative maximum algorithm in "Comparative Quantitation Analysis" module of the Rotor-Gene™ 6000 software;

ΔCt = Ct of the sample – Ct of the sample with the highest expression.

Geometric mean of Q values of multiple reference genes were then used for calculation of normalisation factor (N) for each sample using "GEOMEAN" function in MS Excel:

$$\mathbf{N="GEOMEAN" (Q1, Q2, ...Qn)} \qquad \mathbf{(2)}$$

N – normalisation factor;

"GEOMEAN" – function of MS Excel calculating geometric average for multiple values;

$Q_1, Q_2, ...Q_n$ – relative transcript quantity values obtained for reference genes 1, 2, ... n (see formula 1).

The normalised expression levels for each gene of interest (GOI) were then calculated using formula:

$$\mathbf{Q_{GOI(norm)} = \frac{Q_{GOI}}{N}} \qquad (3)$$

QGOI(norm) = normalised relative GOI transcript abundance;

QGOI = GOI transcript abundance in a sample relative to the sample with the highest expression (see formula 1);

N = normalisation factor obtained by geometric averaging of expression levels of multiple reference genes (formula 2).

All gene expression studies conducted for LOX and HPL genes within this project, were carried out using modified ΔΔCt method described above taking into account amplification efficiency values generated by Rotor-Gene™ 6000 using second derivative maximum algorithm. Some runs also included serial dilutions of standards for genes studied, and the results were also analysed using a TSC method.

Both methods generated compatible results, but the modified ΔΔCt method was a method of choice for further analysis as it accounted for sample-to-sample variation in amplification efficiency.

5.4.3 Changes in LOX and HPL gene expression throughout berry development

The changes in LOXs expression during berry development were studied in the 2007, 2008 and 2009 growing seasons.

The geNorm applet was downloaded from http://medgen.ugent.be/~jvdesomp/genorm/ and used for testing *Actin*, *GAPDH*, *SAND* and *EF-1* as described in section 5.4.1. Appendix A.3.5.A demonstrates the results of geNorm analysis, indicating that *Actin* and *GAPDH* were the two most stable genes (M=0.17), followed by *SAND* (M=0.18) and less stable *EF-1* (M=0.26). Therefore, a geometrical mean of *Actin* and *GAPDH* gene expression was used as a normalisation factor in further experiments studying changes in LOX and HPL gene expression during berry development.

Relative gene expression was studied using qPCR experiments as described in section 3.8. The data for each of the five genes studied in the three seasons were exported into MS Excel spreadsheet and analysed using ΔΔCt method. The initial experiment included analysis of berry developmental stages collected in 2007 season. At each developmental stage, the same cDNA batch was used for all five genes, which allowed comparison their relative comparison. The expression levels of all five genes were normalised to a geometrical mean of *Actin* and *GAPDH* expression and recalculated relative to a sample with the smallest level of expression level taken as 1 (Figure 5.8).

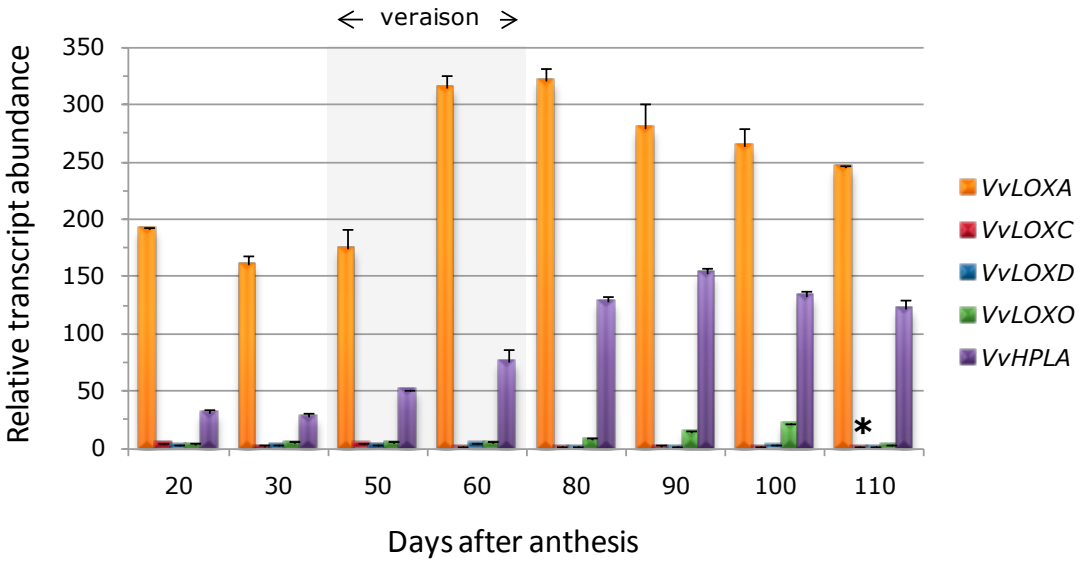

Figure 5.8 Relative expression of LOX and HPL genes during berry development in 2007 season

The relative expression of grape berry LOX and HPL genes across development was studied in the 2007 growing season. The expression levels of all five genes were normalised to a geometrical mean of *Actin* and *GAPDH* expression and recalculated relative to a sample with the smallest level of expression level taken as 1 (labelled with an asterix). The error bars represent a standard deviation of the mean for technical replicates and propagated by normalisation against two reference genes. Veraison took place approximately 50 to 60 days after anthesis (highlighted by shaded area).

As can be noted from Figure 5.8, *VvLOXA* had the highest level of expression amongst five genes studied. Depending on developmental stage, transcript abundance of *VvLOXA* exceeded the abundance of other LOXs between 10 and 300 fold.

To study seasonal variability in expression patterns for each individual LOX and HPL gene across development over a 3 years period, a further gene expression analysis was performed individually for each gene in three seasons. For each gene, a sample with the lowest expression transcript abundance of this gene was selected as a calibrator (expression level 1, marked with an asterisk on the graph, Figure 5.9) and transcript abundance for a given gene in all other samples was expressed relatively to the calibrator (Figure 5.9).

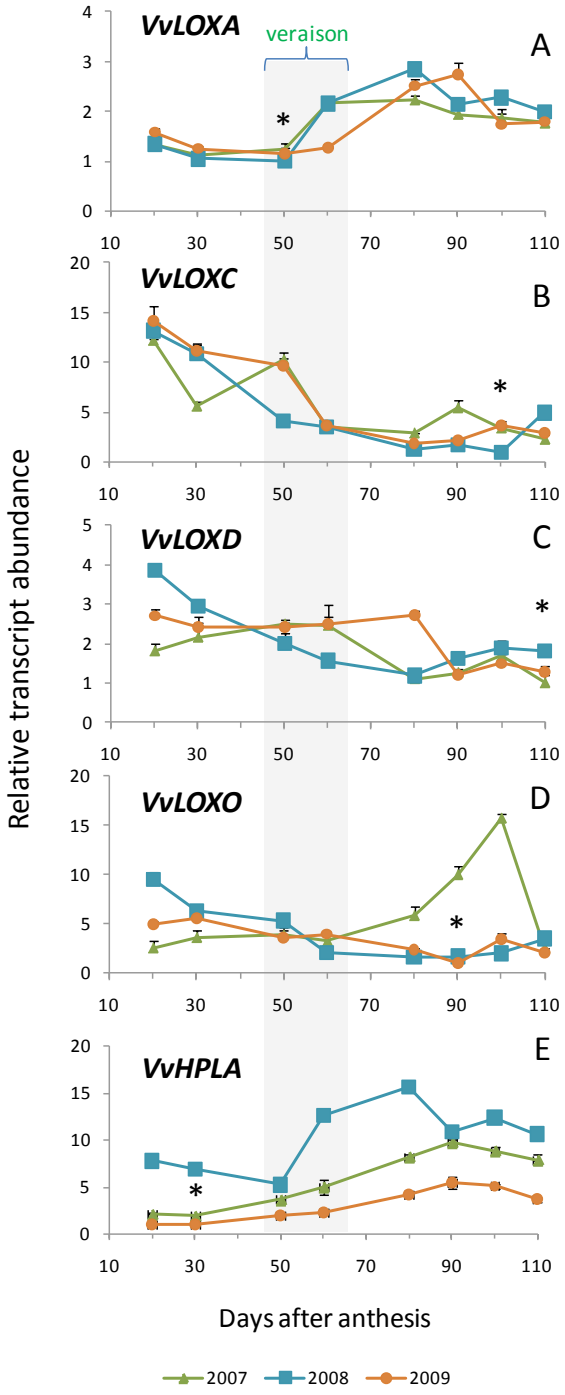

Figure 5.9 Changes in LOX and HPL gene expression throughout berry development

The relative expression of grape berry LOX and HPL genes across development was studied in the 2007, 2008 and 2009 growing seasons. For each gene berry transcript abundance levels are displayed relative to the sample with the lowest level of expression for that experiment (labelled with an asterix). The geometrical mean of *Actin* and *GAPDH* reference genes was used as a normalisation factor. The error bars represent a standard deviation of the mean for technical replicates and propagated by normalisation against two reference genes. Veraison in each season took place approximately 50 to 60 days after anthesis (highlighted by shaded area).

As can be seen from Figure 5.9, across three seasons *VvLOXA* displayed a similar pattern of expression typified by an increase in transcript abundance around veraison, which subsequently remained at a relatively constant level through to harvest (Figure 5.9. A). In contrast, *VvLOXC* transcript abundance steadily declined during initial stages of berry development and stayed low during the post-veraison stages (Figure 5.9. B). *VvLOXD* expression was comparatively stable across development (Figure 5.9. C). Seasonally, *VvLOXO* exhibited a more variable pattern of transcript abundance. Expression of *VvLOXO* decreased from earlier to later stages in the 2008 and 2009 seasons. However, in the 2007 season expression levels remained low during earlier stages of development, with an increase that started shortly post-veraison, reaching a maximum around the pre-harvest stage (Figure 5.9. D). Expression of *VvHPLA* decreased slightly in the pre-veraison stages, however started to increase around veraison and continued to rise through to the pre-harvest stage (100 daa) (Figure 5.9. E). Notably, while patterns of expression of *VvHPLA* were similar in the 2007 and 2009 seasons, there was an increase in expression of VvHPLA post veraison. Specifically, *VvHPLA* expression increased during veraison, and remained high through to 90 daa , whereupon it returned to levels similar to those observed in the 2007 and 2008 seasons (Figure 5.9. E).

5.4.4 Transcript distribution in different tissues of the berry

In order to determine the spatial distribution of *VvLOXA*, *C*, *D*, *O* and *VvHPLA* transcripts within grape berry, expression patterns for these genes were investigated using qPCR analysis in separate berry tissues.

Berries at a late stage developmental (80-90 daa) were used for the analysis as described in section 3.3.4. RNA was extracted from skins, pulp and seed of berries and converted into cDNA.

Prior to the main experiment, a geNorm evaluation of reference genes was performed as described in section 5.4.1. The results of the test (Appendix A.3.5. B) indicated that the least variable reference genes amongst the three fractions of the berry were *SAND* and *EF-1*(M=0.05), followed by *GAPDH* (M=0.38) and *Actin* (M=0.52). Based on these results, a geometrical mean of *SAND* and *EF-1* gene expression was chosen as the

normalisation factor for a further use in the determination of spatial distribution of LOX and HPL transcript in Sauvignon blanc berries.

For each gene, relative abundance in the three fractions was first calculated using ΔΔCt method as described in section 3.8. Assuming that the sum of transcript abundance in each individual berry tissue represents the total transcript abundance (100%) for a given gene in the whole berry, transcript abundance in each individual berry tissue was expressed as portions of the total transcript abundance for this gene in the whole berry (Figure 5.10).

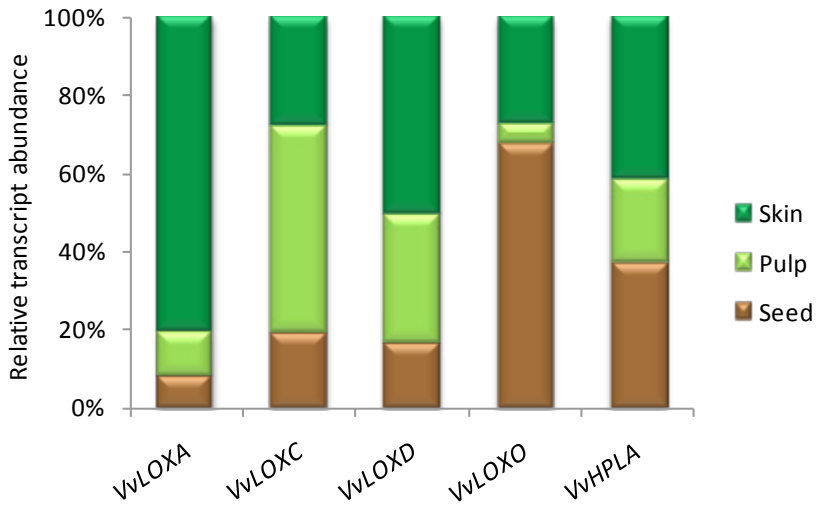

Figure 5.10 Transcript distribution of LOX and HPL genes in different berry tissues

The distribution of LOX and HPL gene transcripts was studied in three berry fractions: skin, pulp and seeds. Geometrical mean of expression of *SAND* and *EF1* reference genes was used as a normalisation factor between samples.

The majority of *VvLOXA* transcripts, 80% of total *VvLOXA* expression in berries, were found to be located in berry skins with the remainder of the expression almost equally distributed between pulp and seed (Figure 5.10). Transcripts of *VvLOXC*, the predicted 9-LOX, were found predominantly in pulp (52 %), with the remaining expression split equally between the skin and seeds (Figure 5.10). *VvLOXD* transcripts were found to be split relatively evenly among all compartments with the bulk of transcripts located in skin (Figure 5.10). In contrast to *VvLOXA*, the majority of *VvLOXO* transcripts were found to be localised in seeds (67 %), followed by skins (28 %). Only a small portion of

VvLOXO transcripts (5%) were detected in the pulp (Figure 5.10). Skins and seeds had higher transcript levels of *VvHPLA* (42 and 37 % respectively) than pulp, which had 22% of the total *VvHPLA* transcript content (Figure 5.10).

5.4.5 Expression of grape berry LOX and HPL genes in response to wounding

Investigation of gene expression in response to mechanical damage of grape tissues is an important aspect of the current investigation for two main reasons. Firstly, LOX pathways, including the GLV-pathway, are known to be induced by wounding in plants as part of signalling or defensive mechanisms. Therefore, it is important to address whether grapevine LOX and HPL genes are responsive to mechanical damage such as wounding or herbivore feeding. The second, more practical question is how mechanical damage as a result of viticultural and winemaking operations pre- and post-harvest may change levels of LOX and HPL genes and subsequently levels of short-chain volatile compounds in grape juices and wines. Therefore, an experiment involving berry wounding was designed and executed as described in section 3.3.6. Three biological replicates were collected for unwounded (control) berries and for each time point after wounding. The RNA extracted from the wounded and unwounded berries was subsequently extracted and processed into cDNA as described in sections 3.4 and 3.5.2.

Determination of suitable reference genes using geNorm was conducted as described in section 5.4.1. The results of this analysis indicate that the most stable genes for a given set of samples were *Actin* and *GAPDH* (M=0.04), followed by *SAND* (M=0.21) and *EF-1* (M=0.83) (Appendix A.3.5.C). Therefore, a geometrical mean of Actin and GAPDH reference genes was chosen as a normalisation factor in wounding-related experiments as the two most stable genes amongst the four genes tested.

Relative changes in expression levels of LOX and HPL genes were studied using ΔΔCt method as described in section 5.4.2. Transcript abundance in unwounded berries was taken as 1 and changes in the transcript abundance in each individual gene upon wounding was expressed as a fold change relative to the unwounded control (Figure 5.11).

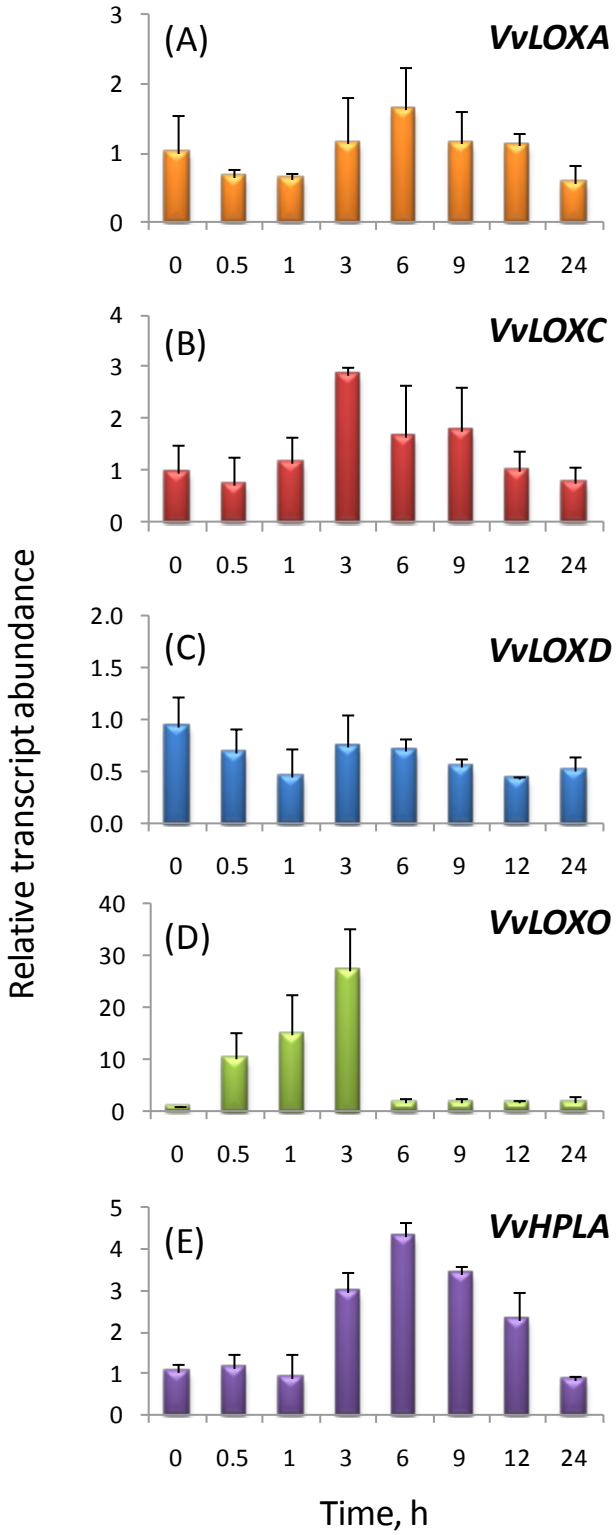

Figure 5.11 Expression of grape LOX and HPL genes in wounded berries

The results for each gene are displayed relative to the unwounded control (0 h). The geometrical mean of *Actin* and *GAPDH* reference genes was used as a normalisation factor. Three independent biological replicates were analysed for each time point. Each bar represents the mean for the replicated values and the error bars represent standard deviation of the mean.

As is evident from Figure 5.11, the genes studied exhibited varied responsiveness to mechanical damage (Figure 5.11. A-E). *VvLOXA* transcript abundance did not change significantly during the first hour after wounding, but its expression started to increase after one hour reaching the highest levels in 6 hours after wounding (Figure 5.11. A). There was a gradual decline trend observed in the expression of *VvLOXA* gene after 6 hours, and after 24 hours *VvLOXA* transcript levels were slightly below the levels observed in the pre-wounded berries (Figure 5.11. A).

VvLOXC did not respond to wounding during the first hour after the treatment. However, 3 hours post wounding a three-fold increase in the abundance of its transcripts was evident (Figure 5.11. B). The expression of *VvLOXC* tended to decline after the peak at 3 hours, although there was a large variation between replicates at 6 and 9 hours after wounding (Figure 5.11. B).

There were no significant changes observed in expression of *VvLOXD* in response to the wounding treatment (Figure 5.11. C).

A clear response to wounding was observed for *VvLOXO*. A rapid accumulation of transcripts was observed as soon as 30 minutes after wounding. A peak of expression occurred at 3 hours post wounding (an approximately 30-fold increase over basal levels of expression), followed by a rapid decline back to basal levels of expression within six hours post wounding (Figure 5.11. D).

The pattern of VvHPLA gene expression (Figure 5.11. E) was similar to that one of VvLOXA (Figure 5.11. A). Similarly to VvLOXA, there was little or no change in the expression of VvHPLA during the first hour upon wounding. A three-fold increase in transcript abundance was observed after three hours, reaching a maximum level (almost five-fold increase) six hours after wounding (Figure 5.11. E). Also, similar to VvLOXA, levels of VvHPLA expression steadily declined after 6 hours and by 24 hours after wounding its expression returned to the basal level (Figure 5.11. E).

5.4.6 Effect of MeJA treatment on LOX and HPL gene expression

To test whether jasmonates are able to induce expression of LOX and HPL genes in the same way as wounding, an elicitation trial with MeJA was set up using fruiting cuttings as described in sections 3.3.2 and 3.3.5.

Two groups of fruiting cuttings ("treated" and "control") were spatially separated to prevent exposure of control plants to highly volatile MeJA. Plants in the "treated" group were then sprayed with MeJA solution, containing 822.4 µmol/L MeJA, 0.2% ethanol and 1% Triton X-100. Ethanol was added to assist solubility of lipophilic MeJA and Triton X-100 was added as a surfactant to assist penetration of the elicitor through the cuticle layers of leaves and berries. The sprayed bunches and leaves were collected at the same time intervals as in the wounding experiment described in section 5.4.5. "Control" plants were sprayed with "control" solution (0.2% ethanol, 1% Triton X-100) and collected at the same time intervals as "treated" plants. Plant material from three independent "treated" plants were collected for each time point and analysed as biological replicates. For "control" plants, berries and leaves were collected at each corresponding time point from two independent plants. Although berries and leaves were collected during the experiment, only berry material was further processed and analysed by qPCR experiments. Since the experimental material and time course were similar to that used in the wounding experiments, the same reference genes (namely *Actin* and *GAPDH*) were used in the MeJA-elicitation experiment to normalise gene expression data.

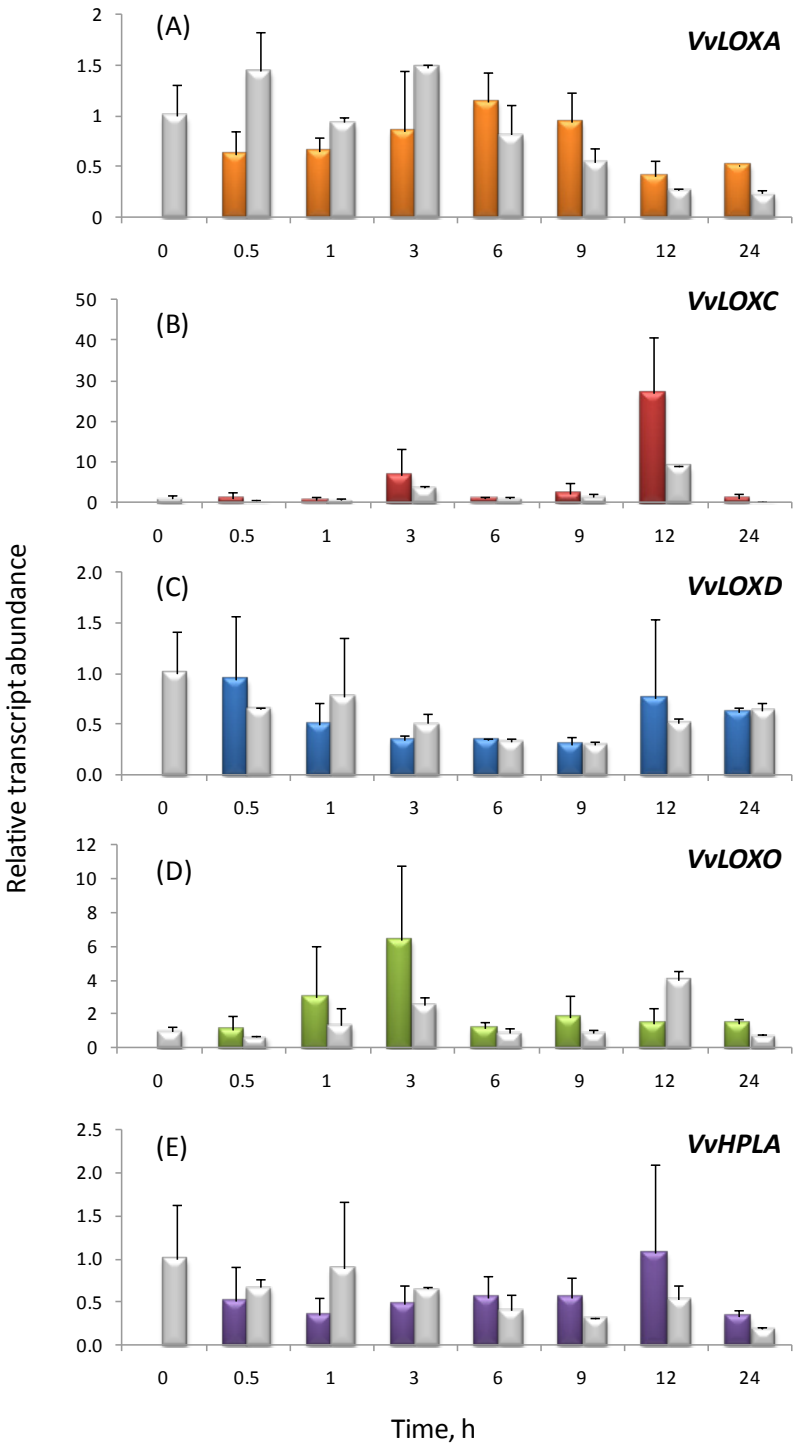

Figure 5.12 Expression of grape LOX and HPL genes upon treatment with MeJA

The results for each gene are displayed as colour bars representing gene expression in plants sprayed with MeJA-solution and grey bars, representing expression levels in control plants sprayed with "control" solution at the corresponding time points (see above for detailed experimental conditions). The expression levels are presented relative to the untreated control (0 hr). The geometrical mean of *Actin* and *GAPDH* reference genes was used as a normalisation factor. Three independent biological replicates were analysed at each time point for MeJA treated plants and two replicates were analysed for control plants. Each bar represents the mean for the replicated values and the error bars represent standard deviation of the mean.

As can be seen from Figure 5.12, variation in LOX and HPL gene expression between biological replicates of MeJA-treated and "control" berries was substantial for many time points. This observation has to be taken into account while interpreting the results obtained from the MeJA-treatment experiment. Despite the large variability between the replicates, some trends in gene expression were observed for each gene, which will be described below.

The expression pattern of *VvLOXA* in berries treated with MeJA (Figure 5.12. A) was similar to the expression pattern observed in wounded berries (Figure 5.11. A). Upon elicitation, there was a slight decrease in *VvLOXA* transcript levels during the first hour, then a gradual increase which reached its maximum in approximately six hours after the treatment. After six hours, the expression of *VvLOXA* was declining again and in twelve hours after the treatment was only half of the expression level of the pre-treated berries. Interestingly, a similar pattern of changes was observed in "control" berries (Figure 5.12. A). The pattern differed from the "treated" berries only in 0.5 hours after spraying, where unlike a 2-fold decrease observed in treated berries, a 1.5-fold increase in expression occurred in berries sprayed with the "control" solution.

MeJA treatment imparted a bimodal pattern of induction of gene expression to *VvLOXC* (Figure 5.12. B). The first spike of expression was observed at 3 hours post treatment and resulted in up to a 10-fold increase in transcript abundance after which the expression returned to basal levels in 6 hours. A subsequent peak of induction was observed in 12 hours after spraying, which was approximately 30-fold higher than the pre-induced expression levels. After a further 12 hours (24 hours post treatment), the *VvLOXC* expression returned to the basal level. Similarly to *VvLOXA*, expression of *VvLOXC* gene in berries sprayed with "control" solution followed the pattern observed in MeJA-treated berries, but with lower magnitude. At the 3-hour mark, expression of *VvLOXC* in "control" berries increased 4-fold and at 24-hour mark – almost 9-fold.

Expression of *VvLOXD* in MeJA-treated berries seemed to decline over the initial 9 hours after treatment and then started to return to the preinduced levels. As with the previous two genes, expression pattern in control berries were similar to the treated one.

Expression of *VvLOXO* in MeJA-treated berries exhibited a similar trend to that observed for this gene in wounded berries (section 5.4.5). A gradual rise of expression shortly after the treatment reached a maximum 3 hours post treatment and returned back

to basal level 6 hours post treatment (Figure 5.12. D). However, unlike the almost 30-fold increase in *VvLOXO* expression levels observed 3 hours post wounding (Figure 5.11. D), spraying of the berries with MeJA resulted in only a 6-10-fold increase compared to the untreated control (Figure 5.12.D). Consistent with the previous observations, the pattern of *VvLOXO* gene expression in "control" berries was similar to the "treated" berries with lower magnitude (gray bars, Figure 5.12.D). The exception was observed 12 hours after the spraying, where *VvLOXO* transcript abundance in "control" berries was almost two-fold higher than in MeJA-treated.

Somewhat surprising results were observed in expression of *VvHPLA* (Figure 5.12.E). Unlike in the wounding experiment, where transient expression induction was observed over the period from 3 to 12 hours after wounding (Figure 5.11.E), no clear induction was detected upon MeJA treatment (Figure 5.12.E).

5.4.7 Expression of LOX and HPL genes in berries infected with *Botrytis cinerea*

To determine how grape berries LOXs and HPL respond to pathogen infection, Sauvignon blanc healthy bunches and bunches partially infected with *Botrytis cinerea* were collected. Infected berries within a bunch (indicated by red arrow, Appendix A.1.3.B) were separated from the berries which had no obvious signs of the infection located adjacent to infected grapes within the same bunch (indicated by yellow arrow, Appendix A.1.3.B). Levels of LOX expression in these two groups were compared with the levels of expression in healthy berries, collected from non-infected bunches (Figure 5.13).

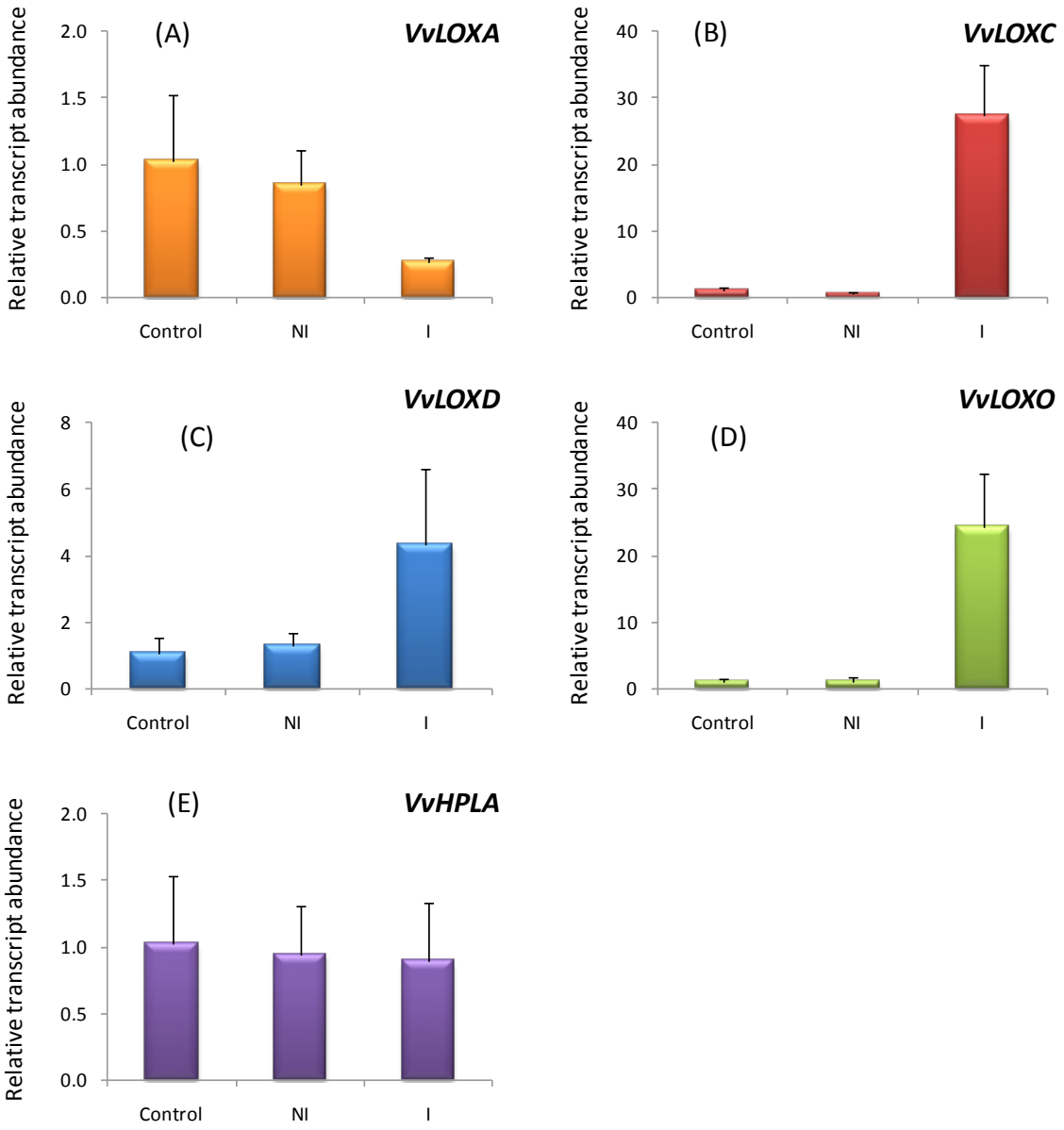

Figure 5.13 Effect of pathogen infection on LOX and HPL gene expression was studied in grape berries infected with the pathogen *Botrytis cinerea*.

Effect of pathogen infection on expression of *VvLOXA* (**A**), *VvLOXC* (**B**), *VvLOXD* (**C**), *VvLOXO* (**D**) and *VvHPLA* (**E**) genes was studied as described earlier. Intact healthy berries were used as a control. Relative to the control, changes in gene expression were quantified in berries with visible signs of infection (**I**) and in berries with no visible signs of infection (**NI**) taken from the same bunch as infected berries. The geometrical mean of *Actin*, *GAPDH* and *SAND* reference genes was used as a normalisation factor. Three independent biological replicates were analysed. Each bar represents a mean for the replicated values and error bars represent standard deviation of the mean.

As illustrated in Figure 5.13, expression of *VvLOXA* in the infected berries was reduced approximately 2-fold compared to the healthy control berries (Figure 5.13. A). In contrast, the expression of *VvLOXC*, *VvLOXD* and *VvLOXO* increased approximately

27-, 4- and 25-fold respectively (Figure 5.13, B-D). Surprisingly, there was no change in expression of *VvHPLA* in response to pathogen infection (Figure 5.13. E). Furthermore, there seemed to be no systemic response to the infection in non-infected berries adjacent to infected berries. Expression levels of all five genes in the berries located closely to the infected ones (NI) were the same as in control berries, collected from the healthy plants (Figure 5.13.A-E).

5.5 Discussion

As reviewed earlier, enzymes involved in the LOX pathway in plants play a fundamental role in lipid and FA metabolism, which in turn is related to many biological processes and physiological functions. These include metabolism of storage lipids during germination, turnover of membranes and plastids, formation of signalling molecules such as jasmonates and GLVs in response to biotic and abiotic stress, and antimicrobial compounds in response to pathogen attack. Such a versatility of functions, in turn, is determined by a range regulatory mechanisms at all levels, including transcriptional, post-transcriptional, translational and pos-translational regulation of enzyme activity. These regulatory mechanisms will be activated differently depending on localisation within the plant, subcellular localisation, developmental stage, environmental conditions as well as a range of other biotic and abiotic factors. Within this context, the initial research into grapevine LOX pathway was focused primarily on developmental and stress-related changes in transcriptional regulation of LOX and HPL genes in grape berries.

Grape berries are non-climacteric fruits and feature a distinctive stage during development known as veraison. During veraison, the berries undergo significant physical and physiological changes, which include berry softening, accumulation of sugars, reduction in acids and changes in colouration in red varieties that signal the onset of ripening (Coombe 1992). These changes are associated with an oxidative burst and changes in cell structure. At this stage of berry development, cell division ceases and berry enlargement occurs due mainly to cell expansion. It is sensible to assume therefore, that the changes in the berry cell structure will lead to changes in lipid metabolism and will subsequently be reflected in changes in transcription of the genes participating in different branches of the LOX-pathway including the GLV-pathway. Furthermore, the importance of the GLV-pathway in berry development can also be deduced from the observed developmentally driven evolution of berry oxylipins (Kalua and Boss 2009; Peña-Cortés *et al.* 2004).

The results of preliminary end-point PCR experiments indicate that several LOX and HPL genes are expressed in intact Sauvignon blanc grape berries throughout development (Figure 5.2, Figure 5.3 and Figure 5.4). Furthermore, it is likely that other LOX and HPL members will be expressed in other plants organs and/or under other

developmental or environmental conditions. Due to the time constraints, characterisation of these two families was restricted to four LOX genes and one HPL gene.

Based on the phylogenetic relationship with functionally characterised plant LOXs, *VvLOXA* and *VvLOXO* represent two-subclasses of type II 13-LOXs. Comparison of functionally characterised plant HPLs with putative grapevine HPLs, indicated that *VvHPLA* was the only grape member predicting exclusively 13-HPL activity (Figure 4.4). Therefore, out of five selected genes, *VvLOXA*, *VvLOXO* and *VvHPLA* were the most likely candidates participating in the formation of C6 volatiles. In addition, *VvLOXC* (a putative 9-LOX) and *VvLOXD* with unknown properties were included further as representatives of the major LOX subdivisions for comparative analysis.

Analysis of full-length nucleotide sequences of the cloned Sauvignon blanc genes revealed high sequence similarity with the respective sequences retrieved from the Pinot noir genome resource. Furthermore, the variation observed between homologous sequences in two cultivars was not greater than the sequence variation between a number of Sauvignon blanc sequences, isolated from different vines. As described in section 5.3, randomly isolated and cloned SB LOX coding sequences had a number of polymorphisms with the highest number of polymorphisms observed in the sequence of *VvLOXA*. The reason for the intraspecific sequence variation can be explained first of all by heterozygosity of the existing grape genotypes as discussed in section 5.3. Furthermore, the grapevine is a vegetatively propagated plant, which further promotes distribution and accumulation of mutations. Therefore, most of the existing clonally propagated grape cultivars are in fact populations of genetically heterogeneous genotypes. Effect of such variation on performance of each particular enzyme is an interesting question and requires further investigation. Therefore, each of the identified *VvLOXA* variants has been cloned into a protein expression vector in order to assess the biochemical properties of each of the recombinant proteins. Time constraints have unfortunately prevented the in-depth analysis of the biochemical activity of these variants.

Amongst the five genes selected for detailed characterisation, *VvLOXD* was the most unusual and also the most challenging to work with. Firstly, a large portion of *VvLOXD* genomic sequence remains unknown even after the release of the latest iteration of Pinot

noir genome sequence. The nature and extent of these sequence gaps remains unknown. The existence of sequence gaps may indicate either difficulties in sequencing of the particular region, or issues related to contig assembly. Another possible reason is the existence in the grape genome of two structurally different haplotypes for a certain locus (Wendl and Yang 2004). Even though the highly homozygous grape genotype PN40024 was used for sequencing, it retained approximately 7% of residual heterozygosity (Jaillon *et al.* 2007). It is likely therefore, that structural difference in some heterozygous regions of the genome might have caused ambiguities during the assembly process. This, in turn, could lead to inability of the assembling software to find overlapping regions and such regions were represented as sequence gaps.

In an attempt to identify the missing sequence information of *VvLOXD*, a 5'-RACE experiment was conducted on RNA extracted from Sauvignon blanc berries. The result of these experiments however were inconclusive. Although the sequence obtained for *VvLOXD* by the 5'-RACE experiment did reveal some missing sequence information, it was shorter than its predicted homologues from castor bean (*Ricinus communis*) and black cottonwood (*Populus trichocarpa*) and was lacking a translation initiation site sequence (section 5.3., Appendix A.2.1). One possible explanation is that *VvLOXD* is a pseudogene and the 5'-RACE DNA fragment represents the actual *VvLOXD* sequence transcribed in Sauvignon blanc.

Another possible reason for the difficulties in obtaining the 5' coding region could be the same reason that caused gaps in the published genomic sequence of *VvLOXD*. This phenomenon can be caused by formation of secondary structures in a particular region of DNA, thereby inhibiting DNA polymerases and possibly reverse transcriptases employed in these experiments. Such examples have been reported for sequences interrupted with transposon insertions (Viswanathan *et al.* 1999). Future direction for elucidation of the full-length sequence of *VvLOXD* are discussed in Chapter 7.

Despite missing putative sequence information in the 5′-region corresponding to the N-terminus of *VvLOXD*, a pair of primers was designed in the 3' region of *VvLOXD* coding sequence and used in quantitative PCR (qPCR) experiments to determine its expression patterns.

5.5.1 Selection of reference genes for normalisation of gene expression

In order to normalise the results obtained by qPCR analyses, the expression level of gene(s) of interest (GOI) is normally related to the expression level of a chosen reference gene or a number of genes. Historically, a single gene was selected arbitrarily from a number of "classic" plant housekeeping genes (HKGs) and used without any further validation of the appropriateness for qPCR analyses. Recently, significant attention have been given to issues surrounding the selection of appropriate reference genes for qPCR analyses in plants (reviewed by Guénin *et al.* 2009; Gutierrez *et al.* 2008). The studies revealed that none of the commonly used plant HKGs is absolutely stable in terms of expression levels, and the extent of variation of HKG expression varies depending on the particular experiment or trial.

For instance, a study of 15 HKGs in berries of red grape cultivar Cabernet sauvignon revealed that, although several genes were more stable than the others, any single gene could be used as a reference gene on its own (Reid *et al.* 2006). In addition to the observed variation within a particular developmental season, the authors report interseasonal difference it terms of gene expression at a particular berry developmental stage.

Variation in transcript abundance of a gene being used as a reference gene will ultimately lead to inaccurate interpretation of qPCR analysis. Such variation however can be reduced by performing preliminary expression evaluation experiments with several HKGs, and selecting the most stable genes as reference genes for a particular set of samples (Gutierrez *et al.* 2008). To further reduce inaccuracy due to HKG variation, at least two most stable reference genes should be used in combination to generate a normalisation factor.

Vandesompele et al. (2002) developed an algorithm which enables testing of a number of candidate reference genes to determine the most stable gene for a given set of samples (Vandesompele *et al.* 2002). This algorithm has been used by the authors to create geNorm VBA applets for Microsoft Excel. Based on average pairwise variation of a given reference gene with all other tested reference genes, geNorm determines the gene expression stability value (M) for the gene. The tested reference genes are then ranked accordingly to their M values, with the lower M value-genes demonstrating lower variation in a given set of samples.

The study by Reid et al. (2006) utilised geNorm for ranking grape reference genes over grape berry development. The study identifies four most stable genes namely Actin (actin 1, XM_002282480), GAPDH (glyceraldehyde-3-phosphate dehydrogenase, XM_002263109), SAND (SAND family protein, XM_002285134), EF1 (elongation factor-1 alpha, XM_002284888). Expression stability of these four genes was evaluated and the most stable reference genes were selected for generating a normalisation factor in corresponding sets of samples (see section 5.4.1).

5.5.2 Methods used for relative qPCR data analysis

Several methods have been developed over the years for analysing the output of qPCR analysis. Selection of a particular method depends greatly on experimental questions and quantification strategies selected to address these questions.

Generally, two strategies can be applied to analyse gene expression: absolute or relative qPCR. Absolute quantification estimates copy number of a particular GOI in a sample using a standard curve generated with series of standards, copy number of which is known. Relative quantification measures changes in the GOI expression levels in one sample relative to expression levels of the same gene in another sample. In order to normalise the expression results for the template input, the GOI expression levels in both samples are also related to the expression of a reference gene (or a combination of reference genes) in these samples. Relative quantification was chosen for LOX and HPL gene expression studies, as this approach provides a simpler way of monitoring gene expression changes in a large number of samples. Two methods of relative quantification were evaluated and used in this study: the two standard curve method (TSC) and comparative Ct method (or ΔΔCt (delta-delta Ct) method).

The two standard curve (TSC) method is a convenient and relatively accurate method for analysing gene expression using one reference gene as a normaliser. The method requires a standard curve for each gene included in the run. The standard curves are then used to quantify concentrations of each gene and normalise these concentrations to a reference gene of choice and to an assigned normaliser within a sample set. TSC method is also incorporated into Rotor-Gene™ 6000 software package and represents a convenient way of analysing the data without the need of exporting the data into a third-party software.

TSC method however has also a number of disadvantages. First of all, this method is based on the assumption that amplification efficiency for all samples is the same as for the standards used for generation of standard curves. Furthermore, when multiple reference genes are used for normalisation, this method requires generation of standard curves for each of the gene and occupies a significant number of wells in each run. This, in turn, reduces a number of wells available for samples to be analysed and increases the cost of consumables used.

An alternative method of relative gene quantification is the comparative Ct method (Livak and Schmittgen 2001). In contrast to TSC method, the comparative Ct method does not require running of standard curves in each run. Instead, in each sample the Ct (crossing threshold) value for the gene of interest (GOI) is first compared to the Ct value of the reference gene. The normalised values are further normalised relative to a calibrator sample assigned within a sample set. The essential condition of the comparative method is that the amplification efficiencies of the GOI and the reference gene should be either identical, or the difference between the two genes has to be taken into account during the calculations.

Theoretically, each cycle of a PCR reaction doubles the amount of DNA present at the beginning of the cycle and is said to be 100% efficient, or to have amplification efficiency of 2. However, in reality the efficiency of the reaction is always lower than 100% due to a number of factors such as primer binding efficiency, cycle conditions, presence of inhibiting components in the reaction, etc. Therefore, it is important to determine and take into account amplification values for samples analysed.

There are several methods exist for estimating amplification efficiency for a given gene. If the TSC method is used for the analysis, the amplification efficiency for a given gene (or a set of primers) can be estimated by measuring a slope of the curve which in Corbett Rotor-Gene™ 6000 is expressed as M value (Figure 5.6). The optimal M value is -3.322 which indicates 100% reaction efficiency.

Another useful feature of the Rotor-Gene™ 6000 software is its ability to calculate amplification efficiency for each sample as part of "Comparative Quantitation" analysis. This calculation is based on second derivative maximum method (Tichopad *et al.* 2003).

The advantage of this method is that it estimates amplification efficiencies individually for each sample and takes into account the differences which can potentially be introduced by the factors discussed above. Therefore, amplification efficiencies value generated for each sample by Rotor-Gene™ 6000 software were used to correct expression levels of LOX and HPL genes using comparative Ct method as described in section 5.4.2.

5.5.3 Changes in LOX and HPL gene expression over berry development

The initial quantitative gene expression experiments indicate that amongst the four LOXs studied, *VvLOXA* is the most highly expressed LOX at all times during development (Figure 5.8). Transcript abundance of the other three LOXs in intact berries are significantly lower. The high levels of *VvLOXA* expression compared to the other LOXs studied may indicate an important role of *VvLOXA* in general cell metabolism and berry development.

Analysis of the gross spatial localisation of LOX transcripts in ripe berries indicated that *VvLOXA* has the highest levels of expression in berry skins (Figure 5.10.A). The high abundance of *VvLOXA* expression and localisation of transcripts in berry skins suggests that VvLOXA protein is possibly involved in the increase of 13-LOX activities observed in grape musts after prolonged skin contact (Ferreira *et al.* 1995). Furthermore, taking into account the high level of *VvLOXA* expression in skin and its predicted chloroplastic location, it is appealing to implicate *VvLOXA* involvement in a "housekeeping" role linked to important processes such as plastid turnover and membrane metabolism in berry skin. As mentioned earlier, during veraison the grape berry undergoes significant physiological and structural changes associated with the switch to berry ripening. The *VvLOXA* expression data collected over the three seasons data are consistent and indicate that *VvLOXA* expression increases during veraison (Figure 5.9.A).

Gene expression data also suggests that *VvLOXA* is a likely candidate involved in the formation of GLVs. First of all, the expression data shows that the patterns of changes in expression of *VvLOXA* resemble changes observed in expression of *VvHPLA*, the only predicted 13-HPL in grapevine. For both genes, the increase in expression begins around veraison and reaches its maximum in around 80-90 daa, followed by a gradual

decrease (Figure 5.9.A and E). Furthermore, a similar pattern was observed by Kalua and Boss (2009) in evolution of the most abundant berry localised Cabernet Sauvignon GLVs, (*E*)-2-hexenal and hexanal. The authors observed little change in (*E*)-2-hexenal abundance pre-veraison, followed by a 3-fold increase immediately after veraison and decrease at around 100 daa (Kalua and Boss 2009). A similar trend was observed for another GLV aldehyde, hexanal, although the concentrations of hexanal were smaller than those reported for (E)-2-hexenal (Kalua and Boss 2009).

As mentioned earlier, *VvLOXA* and *VvLOXO* genes were identified as 13-LOX genes and were considered in this study as two potential candidates involved in GLVs formation. However, as discussed in section 2.4, products of 13-LOX enzymes can also be converted by AOS and subsequent enzymes into jasmonates. It is therefore important to take into account the potential involvement of *VvLOXA* and *VvLOXO* in the jasmonate biosynthesis

A previous study of jasmonate accumulation in grape berries reported that the concentration of JA and MeJA in seeds is higher than in the skin and pulp (Kondo and Fukuda 2001). The report also suggested that jasmonates influence grape seed development and dormancy (Kondo and Fukuda 2001). Although most of *VvLOXO* basal expression in a late stage berry was detected in berry seeds (Figure 5.10.D), it is yet to be determined whether *VvLOXO* is responsible for the high concentration of jasmonates reported in grape berry seeds. Moreover, in contrast to the consistent seasonal pattern of expression of *VvLOXA*, *VvLOXO* developmental expression was found to be both season- and stage-dependent (Figure 5.9.D). These data may indicate that the role of *VvLOXO* in berry development may not be limited to the seed development, as suggested by the spatial localisation of gene expression, and that *VvLOXO* expression may be influenced by external cues in grape tissues.

While the 13-LOXs, *VvLOXA* and *O* were found to be predominately expressed in the skin and seed respectively, almost half of the total transcripts of the putative 9-LOX, *VvLOXC* were identified in berry pulp (Figure 5.10.B). Although the presence of C9 aldehydes and alcohols has been reported in grape musts and wine (Clarke and Bakker 2004), there no clear evidence of 9-LOX activity in intact or crushed grape berries published to date. The gradual decrease in *VvLOXC* transcripts across berry development may indicate that 9-LOXs are more important at early stages of the

development and become less important after veraison. A similar pattern was observed in expression of *TomLoxA*, a putative 9-LOX gene from tomato fruit. The abundance of *TomLoxA* transcripts was the highest in mature green fruits and decreased gradually through to ripeness (Griffiths *et al.* 1999b).

5.5.4 Effect of wounding on LOX and HPL gene expression

As mentioned earlier, LOX enzymes can be involved in plant responses to wounding, most commonly by activating the AOS and/or HPL branches of the LOX pathway. Generally, wounding response in plants is associated with herbivore feeding. In viticulture this response can also be initiated by mechanical damage that occurs during fruit/leaf thinning and during mechanical harvesting and transportation of the grapes to the winery. It has been shown in a range of plants that individual LOX transcripts rapidly accumulate in response to wounding which subsequently results in increased levels of volatile jasmonates and/or GLVs that are released from the wounded plant tissue (Feussner and Wasternack 2002; Matsui 2006).

The results of the berry wounding experiment clearly identifies at least one LOX gene that is responsive to mechanical damage. An almost 10-fold increase in the *VvLOXO* transcript abundance was observed 30 min after wounding, reaching a 30-fold peak in expression at 3 hrs post-wounding, which returned to pre-wounded levels of expression 6 hours after wounding. Likewise, the closest homologue to *VvLOXO*, potato LOX-gene *LOX-H3* was shown to respond rapidly to wounding of leaves by increasing its expression level 30 min after wounding and reducing to almost undetectable levels 6 hours post wounding.

As mentioned previously, the majority of *VvLOXO* transcripts in intact berries appeared to be located predominantly in seeds. Since RNA extracted from the whole berry (including seeds) was used for the transcript analysis in wounded berries, a further investigation is required in order to determine which berry tissue (skin, berry or pulp) is the main source of accumulation of *VvLOXO* transcripts upon wounding.

The response of the other 13-LOX gene, *VvLOXA*, to wounding was not as apparent as for *VvLOXO*. As described in section 5.4.5, wounding of berries resulted in a slight initial decrease in transcriptional levels of *VvLOXA*, following by a gradual increase, which at 6 hours after wounding was approximately two-fold higher than in the pre-

wounded berries. Although the highest increase in the level of expression of *VvLOXA* observed was only two-fold, this increase can have a significant influence taking into account that *VvLOXA* is by far the most abundant LOX amongst the four identified (Figure 5.8).

A similar increase at 6 hours post wounding was observed for the closest *VvLOXA* homologues *AtLOX2* (Bell and Mullet 1993) and *LOX-H1* (Royo *et al.* 1996). Both authors implicated *AtLOX2* and *LOX-H1* in wound-induced JA biosynthesis on the basis of their patterns of gene expression in response to wounding. However, it has been shown lately that *AtLOX2* is not essential for the rapid accumulation of JA in Arabidopsis. It has since been suggested *AtLOX2* was involved in the production of JA-precursors which accumulate throughout plant development and are rapidly released upon wounding (Glauser *et al.* 2009).

Alternatively, *VvLOXA* and its homologues from other plant species may be involved in GLV-, rather than in jasmonate-generating pathway. In their recent study, Halitschke *et al.* (2004) suggested that 13-hydroperoxides involved in formation of GLVs and jasmonates in leaves of *Nicotiana attenuata* are produced by two different LOXs, *NaLOX2* and *NaLOX3* respectively. Interestingly, *NaLOX2* is highly similar to *VvLOXA* while *NaLOX3* shares high sequence similarity with *VvLOXO*. Similarly to *VvLOXO*, *NaLOX3* was strongly induced by wounding and herbivore feeding, while relatively little changes were observed in transcript levels of *NaLOX2* (Halitschke and Baldwin 2003). Furthermore, upon wounding, *N. attenuata* mutant impaired in *NaLOX3* transcripts had reduced levels of jasmonate, but had the same levels of hexanal and (*Z*)-3-hexenal compared to the wild-type (Halitschke and Baldwin 2003).

It is likely, that *NaLOX2*, *AtLOX2* and *LOX-H1* respond to jasmonates as part of the secondary response and their products are further metabolised by HPL leading to the formation and release of GLVs. In much the same way, it can be suggested that in grape berry *VvLOXO* is involved in a prompt response to wounding generating jasmonates, which can further activate *VvLOXA* and *VvHPLA* genes to initiate the GLV-pathway as a signalling or defence mechanism.

Patterns of *VvHPLA* expression after wounding tend to support this hypothesis. As can be seen from Figure 5.11, temporal changes in expression of *VvHPLA* had a delayed induction profile compared to *VvLOXO* and were almost identical to that observed for

VvLOXA. In a manner similar to the pattern observed for *VvHPLA*, expression of *N. attenuate* HPL gene, *NaHPL*, in wounded leaves began to increase 75 min after wounding reaching its maximum levels around 8 hours and reducing back to basal levels at 16 hours after wounding (Halitschke *et al.* 2004). The changes in *NaHPL* transcripts however did not correlate with the pattern of wounding-induced release of corresponding GLVs, which indicates the complexity of the oxylipin regulatory mechanism at different levels (Halitschke *et al.* 2004).

Adding further to the observed intricacy of the molecular regulation of oxylipin formation, is the fact that FA-hydroperoxide metabolising enzymes often compete for the same substrate. It has been shown for instance, that wounding of *N. attenuata* leaves with silenced AOS activity results in reduced levels of jasmonates, but at the same time increases production of GLVs (Halitschke *et al.* 2004). This observation may indicate NaHPL's ability to compensate for a loss of NaAOS activity and metabolise increased amounts of FA-hydroperoxides. This, in turn, can lead to a suggestion that FA-hydroperoxides, despite been produced by different LOXs within different subcellular compartments, are localised at sites, where they are available to both, AOSs and HPLs.

To prove the relationship of grape LOXs and subsequent enzymes in response to wounding, further detailed characterisation of the pathway and interaction between individual enzymes is required. The most straightforward experiment would require post-treatment monitoring of the end-products of each particular branch of the LOX pathway and relating this information back to the changes in the observable gene expression patterns. However, for a more complete investigation, a set of experiments involving LOX and HPL transgenic or mutant plants would be required.

In addition to the observed changes in 13-LOX and 13-HPL gene expression, a 3-fold increase in *VvLOXC* (a putative 9-LOX) expression was also observed in 3 hr after wounding. The response of 9-LOX genes to wounding is not well documented. However, Royo and colleagues (1996) report an increase in abundance of *StLox1* (the nearest match of *VvLOXC* from potato), transcripts 24 hours after potato roots were wounded. It appears that wounding may induce expression of 9-LOX genes, but the reason for such induction is yet to be elucidated.

No apparent change in *VvLOXD* expression was observed at any point after wounding, suggesting that this gene is not responsive to wounding, at least during the initial 24 hour period investigated.

5.5.5 Effect of MeJA treatment on LOX and HPL gene expression

Jasmonic acid (JA) and methyl jasmonate (MeJA) are well known inducers of the LOX pathway (reviewed in Wasternack 2007). The derivatives of JA and MeJA (collectively known as jasmonates) are involved in regulating plant growth and development, and are the key components in plant response to various biotic and abiotic stresses. In particular, jasmonates have been reported as major signalling molecules responsible for activating wound-induced gene expression (Wasternack *et al.* 2006). One might therefore reasonably expect that treatment of grape tissues with jasmonates might mimic wound and pathogen responses by changing steady-state levels of LOX and HPL gene expression.

In contrast to the "wounding" experiment, however, much larger variation in gene expression levels was observed between the biological replicates for some time points (Figure 5.12). The variation was observed in MeJA-treated as well as in "control" berries. Such spread of data has to be taken into account while interpreting these results. The observed variation in expression levels could be due to a number of reasons. It is possible some of the differences in expression levels between the replicates are due to potential differences in the developmental stage of each of the individual fruiting cuttings used as a biological replicates. Although all cuttings were propagated at the same time, some developmental differences were visually observed for bunches grown on different plants.

Differences in the berry developmental stages however are unlikely to explain the even greater variation in expression of *VvLOXC* in 3 and 12 hours and *VvLOXO* in 1 and 3 hours after spraying with MeJA solution (Figure 5.12. B, D). The reason for such differential response by different plants remains unclear and requires further investigation.

Despite greater variation between the biological replicates, spraying berries with MeJA solution resulted in similar patterns of changes in expression of *VvLOXA* and *VvLOXO*

compared to physical wounding, however the magnitude of the changes was lower for both genes (Figure 5.12. A,D).

Some unexpected differences were observed between the two treatments in the expression of *VvLOXC*. In addition to a 3-hour induction of expression after spraying with MeJA (which was also observed in wounded berries), a second, much stronger induction, was observed around 12 hours after the spraying (Figure 5.12. B). In contrast, in 12 hours after wounding, expression of VvLOXC returned to its steady-state levels (Figure 5.11. B).

Due to the high degree of variation between the biological replicates and relatively low magnitude of changes in the gene expression of VvLOXD, it is difficult to deduce if this gene changed levels of its espression in response to spraying with MeJA solution (Figure 5.12. C).

Unlike after wounding, where expression of *VvHPLA* followed the pattern of *VvLOXA*, no major changes in transcript abundance of *VvHPLA* was observed upon spraying with MeJA (Figure 5.12. E). Similar responses have been reported in cucumber, where the HPL gene studied was induced by wounding, but not by MeJA treatment (Matsui *et al.* 2006). These results may indicate that the wounding response is not limited to activation of MeJA pathway, and additional signals are required to initiate members of the GLV pathway, namely HPL genes. This is in agreement with the proposed mechanisms of plant response to wounding, which involve multiple biochemical pathways and signalling cascades (León *et al.* 2001). The mechanisms of wound signalling may also be different in different plant species (León *et al.* 2001).

Another unexpected observation has been made as a result of the MeJA experiment. In particular, it was observed that expression of LOX genes in berries sprayed with "control" solution resembles the pattern of expression observed in plants sprayed with MeJA solution.

One of the arguments explaining the similarity of gene expression patterns in MeJA treated and "control solution" treated berries might be that the studied genes change their expression during the day, and the observed expression patterns reflect diurnal nature of the changes. Although this assumption cannot be ruled out completely without further experiments, the observed expression patterns for at least one LOX gene,

VvLOXA, does not support the diurnal hypothesis. In case of diurnal expression, the expected levels of *VvLOXA* transcripts at 0 h and 24 h time points would presumably be the same as samples for these time point were collected at exactly same time of the day. In contrast, the data presented in Figure 5.12. A illustrate that expression levels of *VvLOXA* were 2-fold lower in the berries sprayed with MeJA-solution and 3-fold lower in berries sprayed with "control" solution compared to untreated berries collected at the same time the day before.

Another possibility is that chemical components of the "control" solution, can induce changes in gene expression in "control" berries in a similar way to MeJA-treated berries. As described in section 3.3.5, the "control" solution contained the same constituents as the MeJA-solution with the exception of MeJA. Specifically, the "control" solution contained 0.2% ethanol and 1% Triton X-100, which were added in order to increase solubilisation of water-insoluble MeJA and to facilitate the penetration of the solution through the cuticle layer of grape berries.

A further exploration of the existing literature revealed that detergents can indeed induce expression of some genes. In particular, non-ionic detergent Tween 20 has been found to induce expression of *OPR3* gene in Arabidopsis leaves (Müssig *et al.* 2000). Interestingly, the *OPR3* gene encodes 12-oxophytodienoic acid reductase, which is involved in the AOS branch of LOX pathway. OPR enzymes catalyse reduction of cyclopentanone ring of oxophytodienoic acid (OPDA) and are also induced by wounding and JA (Wasternack 2007). Similarly, induction of at least some LOXs in grape berries sprayed with "control" solution can be explained by presence of Triton X-100 within the solution, which mimics the response to other stimuli such as wounding and jasmonates. In this case, the changes in expression observed in MeJA-treated berries most likely induced by cumulative action of MeJA and Triton X-100, which explains the higher expression levels in "treated" berries relative to "control" berries (Figure 5.12).

The effect of synthetic non-ionic detergents and their natural analogues on LOX and HPL gene expression needs to be studied in greater details in order to validate the observations and explanations described above. If grape plants indeed respond to non-ionic detergents by activating defence pathways, analogous forms of such detergents obtained from natural sources might potentially be used as cost-effective and eco-

friendly elicitors to increase plant's resistance to pests and diseases. Furthermore, the activation of grapevine defence systems may also influence the levels of some important aroma and flavour compounds and their precursors in the grape berry, which may ultimately affect flavour and aroma of wines produced from these grapes.

5.5.6 Levels of LOX and HPL gene expression in Sauvignon blanc berries infected with *Botrytis cinerea*

Botrytis cinerea is a necrotrophic fungal pathogen that commonly infects grape leaves and fruits, bringing significant losses in yield and quality to the harvested grapes. It has been previously shown in the white grape cultivar Chardonnay that inoculation of leaves with *B. cinerea* can both stimulate and repress pathogen-related genes (Chong *et al.* 2008). In Arabidopsis, the inoculation of leaves with *B. cinerea* results in elevated levels of C6 volatiles (Kishimoto *et al.* 2008). These C6 volatiles have been found to have direct fungicidal activities (Kishimoto *et al.* 2008).

Aside from the direct defensive role, GLVs and jasmonates, produced in response to pathogen infection, are known to induce systemic responses either through the vascular system or through a cascade of airborne signals (reviewed by Shah 2009). For instance, Arabidopsis plants treated with GLVs showed increased resistance to *B. cinerea* compared to untreated plants (Kishimoto *et al.* 2005). It would be reasonable to expect therefore that the abundance of LOX and HPL transcripts in the berries infected with *B. cinerea* will be different from the levels of corresponding genes in healthy berries. Furthermore, if a systemic response is part of the defensive strategy in grapes, it might be expected that there would be observable changes in LOX and HPL gene expression in uninfected berries that were grown adjacent to infected berries.

To test this, Sauvignon blanc bunches partially infected with the pathogen were collected and obviously infected berries were separated from the berries without visual signs of infection as described in section 3.3.7. Levels of LOX expression in these two groups were compared with the levels of expression in healthy berries, spatially separated from infected berries and considered to be "control" berries.

As described in section 5.4.7, *VvLOXA* exhibited an almost 4-fold reduction in transcript abundance in infected berries compared to the control. The reasons for such a reduction of *VvLOXA* are unknown, but it may be related to termination of normal cell

metabolism as part of initiated programmed cell death (PCD). Such response have been reported for some plant and animal lipoxygenases upon pathogen infection (reviewed in Maccarrone *et al.* 2001). Another possibility is that some LOXs are regulated by the same transcription factors, and an increase in expression of some members was a result in reduction of others.

In contrast to the observed decrease of *VvLOXA* expression, other LOX genes had elevated levels of transcripts in the berries infected with *B. cinerea*. In particular, *VvLOXC*, the putative 9-LOX, was found to be highly expressed in the infected berries (Figure 5.13.B). Similarly, a putative LOX from Chardonnay, which shares significant sequence similarity with *VvLOXC* was investigated in leaves inoculated with a spore suspension of *B. cinerea* and showed an increase in transcription 72 hours after inoculation (Chong *et al.* 2008). It has been proposed, that 9-LOXs are involved in pathogen response by producing anti-microbial compounds or by activating PCD to isolate the site of infection (Göbel *et al.* 2002; Göbel *et al.* 2003).

Unlike in previous experiments, where no major changes were observed for *VvLOXD* expression, up to a 6 fold increase in expression of this gene was observed in the pathogen infected berries. Such an increase suggests a potential role of *VvLOXD* in post-infection processes, although the nature of these processes and *VvLOXD* involvement in them are yet to be determined.

VvLOXO, which showed a strong transient induction upon wounding and MeJA treatment, had also elevated levels in *B. cinerea* infected berries (Figure 5.13.D). However, unlike in the wounding and MeJA experiments, where expression of *VvLOXO* occurred transiently over a relatively short period of time, in *B. cinerea* infected berries elevated expression of *VvLOXO* seemed to be continuous.

Levels of *VvHPLA* gene expression did not change between infected and uninfected berries. These results were unexpected as increased levels of HPL activities and elevated levels of GLVs have been reported upon *B. cinerea* infection in other plants (Matsui *et al.* 2006; Shiojiri *et al.* 2006). Despite the suggested role of GLV products in plant's response to pathogen infection, there has been no clear evidence showing increased levels of HPL gene expression upon infection in other plants. It is possible that *VvHPLA* gene expression is only induced during the initial stages of the infection, producing the required amount of the corresponding HPL enzyme. One of the other

possibilities is that VvHPLA does not participate in response to *B. cinerea* infection and generation of GLVs is accomplished by other HPL members.

Surprisingly, with the exception of a slight change in *VvLOXA* transcription there was little or no alteration in LOX and HPL gene transcription in the non-infected berries growing adjacent to infected berries on the same bunch. It is yet to be determined whether the absence of systemic response between the adjacent berries, or the transient nature of the systemic response is responsible for the observed difference in the transcription levels of LOX and HPL genes in such sample sets.

As can be seen from the discussion above, the qPCR experiments studying LOX and HPL gene expression in Sauvignon blanc berries do not give complete answers to questions regarding the roles of these genes *in vivo*. These experiments however are very useful for identifying further directions for studying LOX and HPL genes as well as the corresponding proteins. Some further experiments will be suggested and discussed in Chapter 7.

Chapter 6
Heterologous expression and biochemical characterisation of individual LOXs and HPLs

6.1 Introduction

Phylogenetic relationships with functionally characterised LOX and HPL members from other plant species as well as identification of important functional residues were a major focus of the initial investigation into the grape LOX and HPL gene families. Based on the phylogenetic analysis, putative functional properties were assigned to the identified grape LOX and HPL members as discussed in Chapter 4. However, to validate the predicted functionality for the identified enzymes, biochemical analysis for individual proteins was necessary. To facilitate this type of investigation, purification and characterisation of individual enzymes from the organism of interest is required. Such a task, however, becomes complicated with the presence of closely related gene family members being expressed at the same time. The presence of isozymes with similar molecular weight and isoelectric point often hampers the purification of individual isozymes directly from the plant and prevents determination of their individual functions.

A more convenient and reliable way to characterise such enzyme family members is to clone the cDNA encoding an individual protein into a protein expression vector and express the protein heterologously in a non-native host such as *E. coli* (reviewed by Makrides 1996). This approach has become a routine tool for *in vitro* biochemical characterisation of proteins.

Heterologous protein expression of selected LOX and HPL genes in *E. coli* was chosen as the method of choice for determining *in vitro* functionality of these genes. As discussed in earlier chapters, VvLOXA and VvLOXO were selected as representatives of the two 13-LOX sub-clades, while VvLOXC was selected as a representative member of the 9-LOX clade. VvHPLA was selected for *in vitro* characterisation as the only putative representative of 13-HPL enzymes identified in the Pinot noir genome.

The subsequent sections in this chapter will describe the results of these experiments and discuss the importance of these results in the context of this investigation.

6.2 Construction of heterologous vectors for recombinant protein expression

6.2.1 Amino acid sequence analysis of VvLOXA, VvLOXC, VvLOXO and VvHPLA to predict their localisation

As reviewed in Chapter 2, some plant LOXs and HPLs have been found to be localised to particular organelles within the plant cell, while others are localised in the cytoplasm. Localisation of proteins to a particular organelle is often facilitated by regions of the proteins known as transit peptides (TPs) (reviewed by Patron and Waller 2007). TPs are integral parts of newly produced proteins that serve for delivery and sometimes for anchoring the mature proteins to a particular membrane within the organelle. In some other instances, TPs are processed and removed once the protein is delivered to the correct organelle (reviewed by Patron and Waller 2007). The presence of a TP in the sequence of the recombinant protein can also result in targeting of the expressed protein into *E. coli* inclusion bodies (IBs) (Jonasson *et al.* 2002). Proteins, which are incorporated into inclusion bodies, in most cases, lose their functionality and therefore are not well suited for biochemical characterisation (Jonasson *et al.* 2002).

In order to identify whether the selected LOX and HPL proteins contain TPs, and to predict potential subcellular localisation of the corresponding mature proteins, LOX and HPL amino acid sequences were analysed using a number of different prediction software packages as described in section 3.9.1. The prediction confidence for these analyses is rated based on a reliability class (RC) value. RC value ranges 1 to 5, where 1 indicates the strongest and 5 – the lowest prediction confidence.

Table 6.1 summarises results obtained after analysis of VvLOXA, VvLOXC, VvLOXO and VvHPLA amino acid sequences using the TargetP 1.1 Server (http://www.cbs.dtu.dk/services/TargetP/) (Emanuelsson *et al.* 2007). Similar results were obtained when the sequences were submitted to other web-based software tools such as the ChloroP 1.1 Server (http://www.cbs.dtu.dk/services/ChloroP/) (Emanuelsson *et al.* 1999) and WoLF PSORT server (http://wolfpsort.org/) (Horton *et al.* 2007).

Table 6.1 Output of the signal sequence and cleavage site prediction analysis for selected grape LOX and HPL proteins using TargetP 1.1 Server

Len – sequence length, aa; **cTP** (chloroplast transit peptide), **mTP** (mitochondrion transit peptide), **SP** (signal peptide), **other** – final scores on which final prediction is made; **Loc** – prediction of localisation (**C** – chloroplast, **M** – mitochondrion, **S** – secretory pathway, **-** – any other location); **RC** – reliability class (from 1 to 5, where 1 indicates the strongest prediction confidence); **TPlen** – length of the predicted peptide.

Name	Len	cTP	mTP	SP	other	Loc	RC	TPlen
VvLOXA	901	0.577	0.126	0.033	0.119	C	3	47
VvLOXC	859	0.126	0.103	0.070	0.922	-	2	-
VvLOXO	916	0.563	0.040	0.082	0.475	C	5	60
VvHPLA	487	0.776	0.121	0.134	0.158	C	2	64

The combined results indicate that VvLOXA and VvHPLA proteins most likely possess transit peptides (RC values are 3 and 2 respectively for VvLOXA and VvHPLA) which are predicted to target these proteins to the chloroplast. The lengths of the predicted chloroplast targeting peptides (cTPs) for VvLOXA and VvHPLA were 47 and 64 aa respectively. The TargetP software did not identify any TPs in the sequence of VvLOXC (RC=2), while the existence of a 60 aa cTP at the N-terminus of VvLOXO was predicted, but with low confidence (RC=5).

To avoid the potential targeting of the heterologously expressed protein into IBs the sequence that encodes the predicted TP can be removed during designing of the expression construct. This approach has also proven to be successful in experiments with recombinant LOXs (Terp *et al.* 2006) and HPLs (Noordermeer *et al.* 2000b). Therefore, for heterologous expression of VvLOXA, VvLOXO and VvHPLA (for which transit peptides had been predicted) two protein expression constructs (one encoding a full-length protein and one, in which predicted TP has been removed) were designed (Appendix A.4.1). As no TP had been predicted for VvLOXC protein, only one construct encoding the full-length protein was prepared for VvLOXC.

6.2.2 Preparation of recombinant constructs

The recombinant LOX and HPL constructs were prepared using Gateway® recombination cloning technology (Invitrogen, Auckland, New Zealand). Gateway® cloning system allows generation of a vast range of desired recombinant constructs in a time- and cost-efficient manner by replacing restriction endonucleases and DNA-ligase enzymes with site-specific recombination. Usually, the generation of a recombinant protein expression construct via Gateway® technology involves directional insertion of the coding sequence (CDS) of the gene of interest (GOI) into an "entry" vector, which can be subsequently used for re-cloning GOI's CDS into various "destination" vectors. The system used in current investigation utilised the pENTR™/TEV/D-TOPO® vector (Invitrogen, Auckland, New Zealand) as an entry vector, and Gateway® pDEST17 (Invitrogen, Auckland, New Zealand) as a destination vector.

The Gateway® pDEST17 is a N-terminal fusion destination vector, which contains a translation initiation codon upstream of a 6 × histidine tag (His-tag). The presence of a 6 × His-tag in the recombinant protein facilitates its isolation from the host cell matrix utilising Immobilised Metal Ion Affinity Chromatography (IMAC) as will be discussed later. The general workflow for preparation of recombinant constructs is schematically represented in Appendix A.4.1.

The earlier constructs of VvLOXA, C, O and VvHPLA (sections 1.1.1 and 3.7), were used as templates with a combination of primers listed in Table 3.6 to PCR-amplify DNA amplicons representing full-length CDS constructs for VvLOXA, C, O and VvHPLA as described in section 3.9.1. Initial ATG sequences encoding a translation initiation site in the new constructs were removed using a PCR-based strategy. The removal of the initial ATG from the native sequence had been performed in order to ensure that protein expression initiates at the pDEST17 vector specific ATG and all recombinant proteins contain 6xHis tag at their N-termini.

Section 3.9.1 also describes the procedures, by which the predicted TP sequences were removed from the sequences of VvLOXA, O and VvHPLA, thereby creating truncated versions of the corresponding proteins.

All reverse primers used in the PCR amplification included in-frame translation termination codon (stop-codon) to ensure the produced proteins contain only gene specific amino acids Table 3.6.

The amplicons for full-legth CDS and truncated (-TP) CDS of the LOX and HPL genes were purified and cloned into pENTR™/TEV/D-TOPO® vectors as described in section 3.9.1. These vectors were then used in a subsequent LR recombination reaction in order to re-clone the DNA fragments into Gateway® pDEST17 destination vectors according to manufacturer's instructions. The constructs were then sequenced and analysed as described in section 3.9.1 to confirm that no PCR or cloning errors were incorporated into the expression constructs. As an example, Appendix A.4.2 schematically represents constructs of VvLOXA (with and without TP) cloned into pDEST17 vector. Expression of the recombinant transcripts is controlled by T7 polymerase promoter and the resulting transcripts contain gene-specific sequence and sequences encoding important translation regulatory sites (Appendix A.4.2). These include a ribosomal binding site (RBS), translation initiation site, sequences encoding 6×His-tag, a TEV protease cleavage recognition site and transcription termination sites (Appendix A.4.2). As a result, each recombinant protein produced from pDEST17 constructs contained a 38 aa long N-terminal extension containing a 6xHis tag (Appendix A.4.2)

The prepared constructs were transformed into *E. coli* BL21(DE3) cells (Novagen, Merck Bioscience, Auckland, New Zealand) as described in section 3.9.1 and used in subsequent protein expression experiments.

6.3 Heterologous expression and purification of recombinant LOX and HPL proteins

6.3.1 Heterologous expression of full-length LOX and HPL constructs

To check if the protein expression constructs carrying full-length sequences of LOXAFL, LOXCFL, LOXOFL and HPLAFL were able to produce recombinant proteins, these constructs were transformed into BL21 (DE3) cells and expressed as described in sections 3.9.2 and 3.9.4. Trial expression experiments were initiated by addition to IPTG of a final concentration of 1 mM and incubation at either 37°C for 6 hours or at 14°C for 18 hours. Figure 6.1 represents a typical example of analysis of recombinant proteins extracted from these experiments and fractionated using polyacrylamide gel.

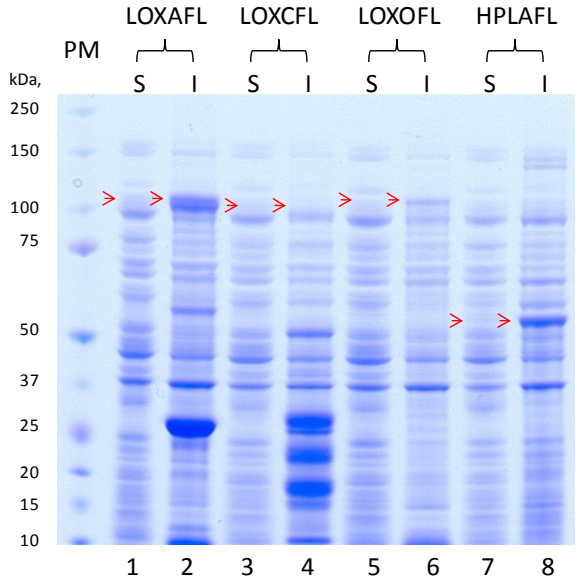

Figure 6.1 SDS-PAGE gel analysis of recombinant full-length LOX and HPL proteins produced in initial expression experiments

30 µg of each protein sample were run on NuPAGE® 4-12% Bis-Tris gel (Invitrogen, Auckland, New Zealand) and stained with Fast Blue protein stain (Fisher biotech, Raylab, Auckland, New Zealand). Soluble (**S**) and insoluble (**I**) fractions of each recombinant protein were extracted as described in section 3.9.2. The constructs were as follows: LOXAFL (lanes 1 and 2), LOXCFL (lanes 3 and 4), LOXOFL (lanes 5 and 6), HPLAFL (lanes 7 and 8). Arrows indicate the expected band positions for corresponding proteins as predicted from amino acid sequence analysis. **PM** – Precision Plus Protein standard (BioRad, Auckland, New Zealand).

As can be seen from Figure 6.1, no protein band of the expected size was evident in the soluble protein fractions of LOXAFL and HPLAFL expression, although bands corresponding to the predicted proteins were detected in the corresponding insoluble fractions. Similar results were observed for LOXOFL construct, although band intensity for the expected protein in the insoluble fraction was lower, than those observed for LOXAFL and HPLAFL. No distinct bands were observed in any of the fractions for LOXCFL. Similar results were obtained when the proteins were expressed at 37°C for 6 hours after induction with 1mM IPTG.

To further check whether the isolated soluble fractions contain functional recombinant proteins, these fractions were used in appropriate LOX and HPL assays as described in sections 3.9.2-3.9.6. These experiments failed to detect any activities in the crude soluble fractions (data not shown). Therefore, only truncated versions (with removed transit peptides) of the corresponding enzymes were subsequently analysed.

6.3.2 Expression and purification of recombinant LOXA-TP

In contrast to LOXAFL, LOXA-TP recombinant protein was detectable in the soluble fraction of protein extracts isolated from cultures, which were incubated at 14°C for 18 hours after induction with 1 mM IPTG.

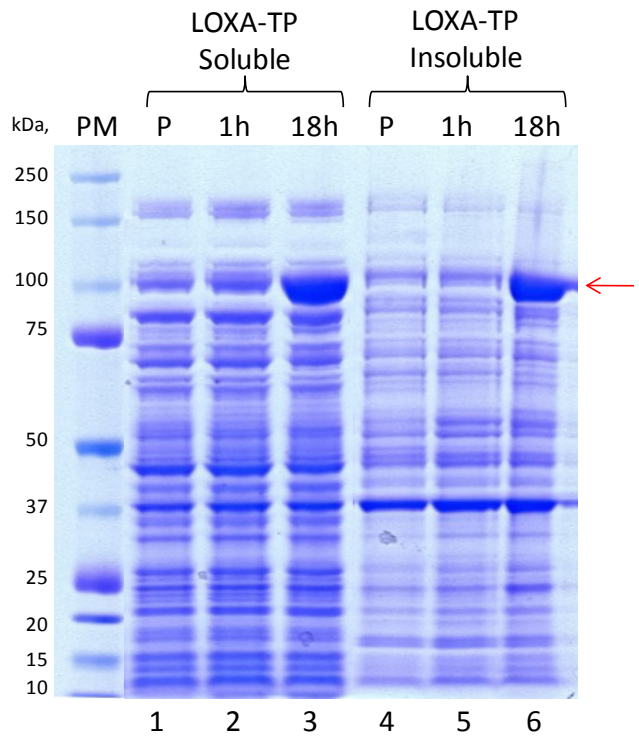

Figure 6.2 SDS-PAGE gel analysis of recombinant LOXA-TP

30 µg of each protein sample were run on NuPAGE® 4-12% Bis-Tris gel (Invitrogen, Auckland, New Zealand) and stained with Fast Blue protein stain (Fisher biotech, Raylab, Auckland, New Zealand). BL21(DE3) cells containing LOXA-TP protein expression construct were grown at 37°C until OD600~0.6. The cultures were then induced with 1 mM IPTG and incubated at 14°C for 18 hours. The samples for analysis were collected just before the induction (**P**) , after 1 hour (**1h**) and 18 hours (**18h**) of post-induction incubation. Soluble (lanes 1, 2 and 3) and insoluble (lanes 4, 5 and 6) fractions for each collected sample were analysed. Red arrow indicates expected band positions for the recombinant LOXA-TP protein. **PM** – Precision Plus Protein standard (BioRad, Auckland, New Zealand).

As shown in Figure 6.2, 18 hours after the induction both the soluble and the insoluble fractions of crude *E. coli* protein extract contained significant amounts of the recombinant protein (lanes 3 and 6), compared to the cultures collected before the induction (lanes 1 and 4) and in one hour after induction (lanes 2 and 5).

Ten micrograms of total soluble protein was then incubated with FA substrates with monitoring changes in the absorbance at 234 nm as described in section 3.9.5. The incubation of soluble protein extract with FA substrate caused a significant increase in absorbance at 234 nm indicating that there was present an active recombinant protein. (Appendix A.4.3). The ability of the protein extract to give an increase in absorbance at 234 nm disappeared after the protein sample was incubated at 90°C for 10 min (Appendix A.4.3). Moreover, no activities were detected when the same amount of

protein from the preinduced sample was used in the assay (Appendix A.4.3). These results indicated that the increase in absorbance at 234 nm was most likely due to LOX activity derived from the recombinant LOXA-TP protein.

Purification of the recombinant LOXA-TP was performed using IMAC chromatography with subsequent ion exchange chromatography as described in section 3.9.3. IMAC chromatography is based on affinity of recombinant proteins that contain polyhistidine tags for metal ions. This affinity allows covalent binding of the His-tagged proteins to the metal ions immobilised in the stationary fraction of the purification column, while most of the endogenous *E. coli* proteins pass through the column unbound. The bound His-tagged proteins can be subsequently eluted with either imidazole (which has higher affinity to the bound metal ions than the histidine containing recombinant protein) or with a low pH buffer.

HisTrap™ FF columns (GE Healthcare Life Sciences, Global Science, Auckland, New Zealand) prepacked with precharged Ni^{2+} Sepharose™ and connected to Biologic DuoFlow 10 Chromatographic System (Bio-Rad, Auckland, New Zealand) were used for purification of the recombinant LOXA-TP protein as described in section 3.9.3. Lanes 1-4 in Figure 6.3 illustrate the results of IMAC purification.

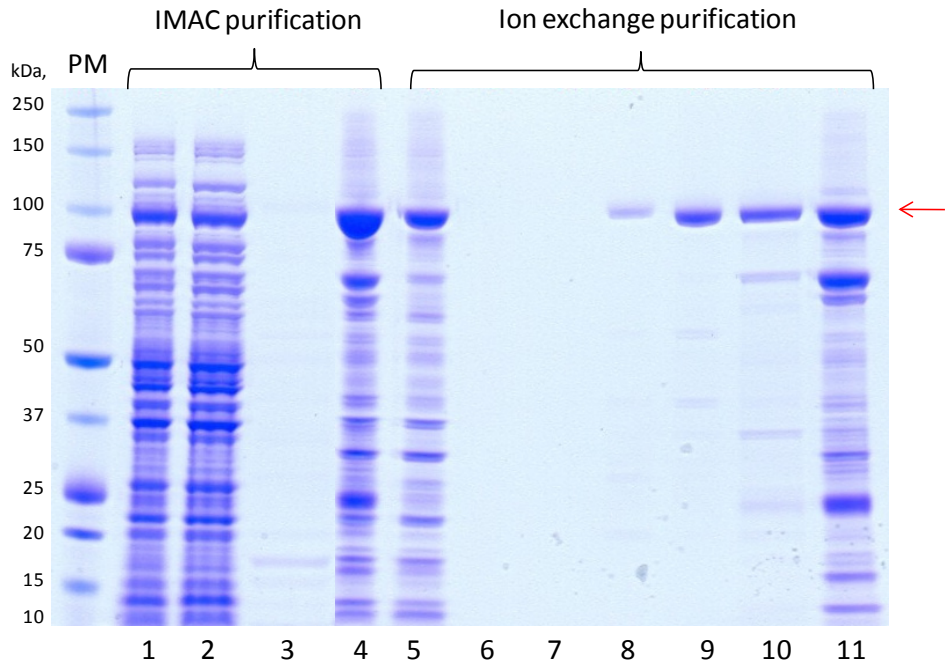

Figure 6.3 SDS-PAGE gel analysis of IMAC and ion-exchange (DEAE) purification of LOXA-TP

Eluted protein fractions were run on NuPAGE® 4-12% Bis-Tris gel and stained with Fast Blue protein stain. The first four lanes represent different stages of IMAC purification and the rest of the lanes represent different fractions of ion-exchange (DEAE) purification. The lanes are labeled as follows: **1** - total soluble fraction, **2** – HisTrap flowthrough fraction, **3** – column wash fraction, **4** –500 mM imidazole elution fraction; **5** – DEAE flowthrough fraction, **6** – 20 mM NaCl elution fraction, **7** – 40 mM NaCl elution fraction, **8** – 80 mM NaCl elution fraction, **9** – 100 mM NaCl elution fraction, **10** – 120 mM NaCl elution fraction, **11** – 200 mM NaCl elution fraction. Red arrow indicates expected band positions for the recombinant LOXA-TP protein. **PM** – Precision Plus Protein standard.

As can be seen from Figure 6.3, post-IMAC purification fraction (lane 4) contained the recombinant LOXA-TP protein of approximately 100 kDa as a major band as well as a number of contaminating bands. These contaminating proteins most likely represent histidine-rich proteins that are endogenous to *E. coli* proteins, and which compete for binding sites on the column with His-tagged LOXA-TP. Moreover, some of the contaminating proteins may represent products of proteolysis of LOXA-TP. Although all precautions were taken during protein extraction and processing to prevent endogenous protease activities, it is possible that some proteolysis occurred during the expression or prior to recombinant protein purification. In order to improve the purity of the recombinant LOXA-TP, an experiment that included a stepwise increase concentration of imidazole in the wash buffer was performed. Although column washes with higher imidazole concentration improved to some extent the purity of the eluted

protein fraction, they also resulted in significant loss of recombinant LOXA-TP (Appendix A.4.4). Therefore, ion-exchange chromatography was employed to further purify the IMAC-purified fractions.

Ion-exchange chromatography is based on the ability of charged protein molecules to bind to oppositely charged groups attached to an insoluble matrix. Binding of the proteins occurs in the presence of buffers with low salt concentration (hence low ionic strength). Linear increase in the ionic strength of the buffer passing through the insoluble matrix will result in a gradual elution of the proteins based on their overall charge.

HiTrap™ DEAE FF anion exchange columns (GE Healthcare Life Sciences, Global Science, Auckland, New Zealand) were chosen for further purification of recombinant LOXA-TP. Based on *in silico* prediction, the isoelectric point (pI) of the recombinant LOXA-TP protein was 6.4. Therefore, at pH 8.0 LOXA-TP should bind to weak anion exchanger medium of DEAE column.

The IMAC-purified fraction containing recombinant LOXA-TP was exchanged into 20 mM Tris-HCl buffer, pH8.0 (Buffer A) using 4x5 mL HiTrap™ Desalting columns. The buffer exchanged protein was then loaded on HiTrap™ DEAE FF column and eluted with step-gradient of buffer containing 1M NaCl as described in section 3.9.3. Eluted fractions were analysed on SDS-PAGE gel (lanes 5-11, Figure 6.3) and checked for LOX activity. The fractions with acceptable purity and exhibiting LOX activities were pooled together and buffer-exchanged into storage buffer as described in section 3.9.3. The aliquoted fractions were stored at -80°C till further analysis.

6.3.3 Expression and purification of recombinant LOXO-TP

As mentioned earlier LOXOFL recombinant protein accumulated in the insoluble fraction of the total *E. coli* protein extract (Figure 6.1). Moreover, the soluble fractions collected from LOXOFL-expressing cultures lacked LOX activities across the pH 4.0-9.5 range. Reduction of temperature during the induction period and induction with lower IPTG concentrations did not give any improvement.

In contrast to the full-length LOXO recombinant protein construct (LOXOFL), the truncated version (LOXO-TP) construct produced protein of expected size in both

soluble and insoluble fractions at 37°C and 14°C incubation during the expression (Figure 6.4).

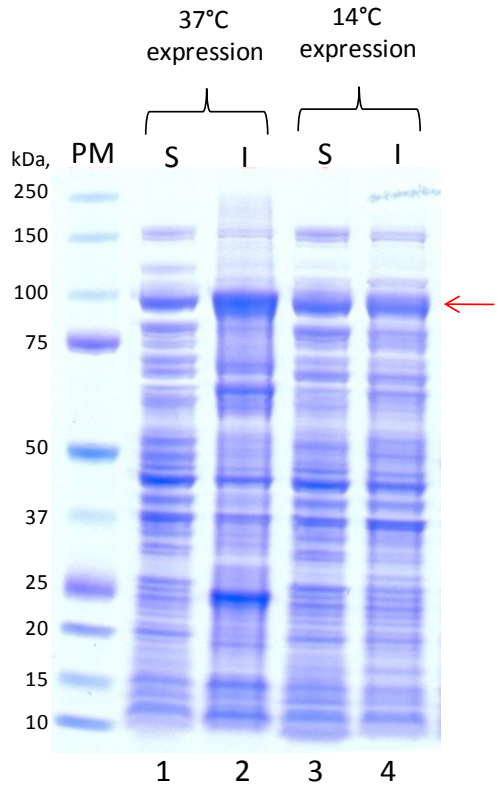

Figure 6.4 SDS-PAGE gel analysis of recombinant LOXO-TP

30 µg of each protein sample were run on NuPAGE® 4-12% Bis-Tris gel and stained with Fast Blue protein stain. BL21(DE3) cells containing LOXO-TP protein expression construct were grown at 37°C until OD600~0.6. The cultures were then induced with 1 mM IPTG and incubated either at 37°C for 6 hours or at 14°C for 18 hours. Soluble (**S**) and insoluble (**I**) fractions of crude protein extracts were analysed from cultures incubated at 37°C (lanes 1 and 2) and at 14°C (lanes 3 and 4). Red arrow indicates expected band positions for the recombinant LOXO-TP protein. **PM** – Precision Plus Protein standard.

Although no significant difference was observed in the amount of the protein expressed at either 37°C or 14°C (Figure 6.4), the soluble fraction of the crude protein extract from the culture incubated at 14°C exhibited much higher LOX activities based on changes in absorbance at 234 nm (Appendix A.4.3). Therefore all subsequent expressions were performed at 14°C.

Similar to LOXA-TP, further purification of the recombinant LOXO-TP was conducted by applying a combination of IMAC and ion-exchange chromatography (Figure 6.5).

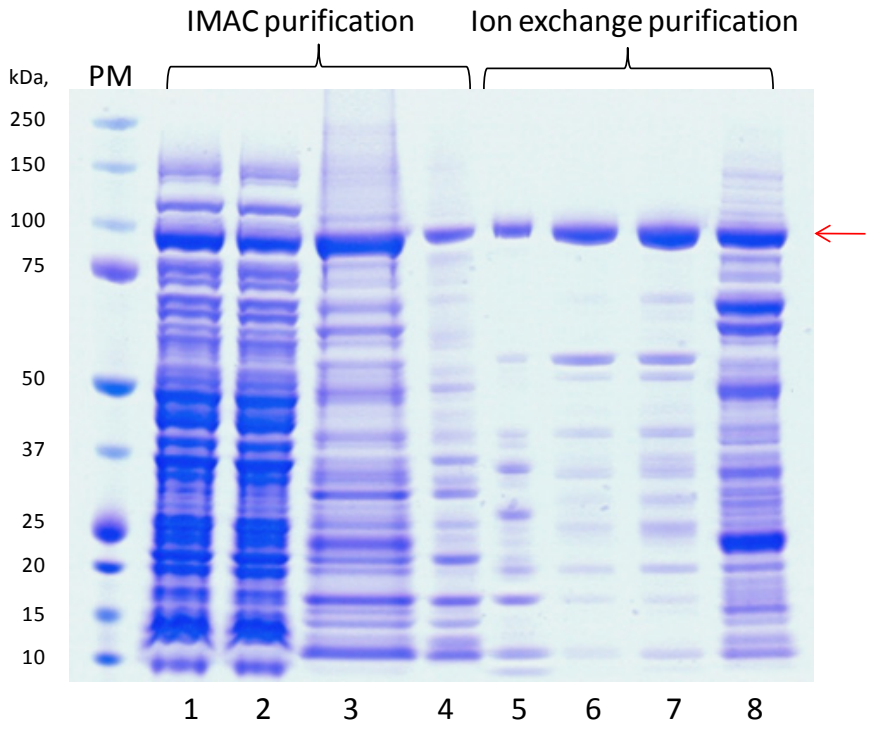

Figure 6.5 SDS-PAGE gel analysis of IMAC and DEAE purificatoion of LOXO-TP

Eluted protein fractions were run on NuPAGE® 4-12% Bis-Tris gel and stained with Fast Blue protein stain. First four lanes represent different stages of IMAC purification and the remainder of the lanes represent different fractions of ion exchange purification. The lanes are labeled as follows: **1** - total soluble fraction, **2** – HisTrap flowthrough fraction, **3** – eluted with 500 mM imidazole fraction, **4** – eluted fraction after desalting; **5** – DEAE flowthrough fraction, **6** – 80 mM NaCl elution fraction, **7** – 100 mM NaCl elution fraction, **8** – 200 mM NaCl elution fraction. Red arrow indicates expected band positions for the recombinant LOXO-TP protein. **PM** – Precision Plus Protein standard.

All LOXO-TP eluted fractions were subjected to a LOX activity assay. However, despite relatively high recovery of the recombinant LOXO-TP in the ion exchange-purified fractions (lanes 6 and 7, Figure 6.5), these fractions generated only small changes in absorbance at 234 nm compared to the freshly prepared crude protein extract observed before. Further investigation revealed that other fractions, including total crude extract and IMAC-purified fractions rapidly lost LOX activities, indicating that recombinant LOXO-TP was highly unstable. Addition of stabilising agents such as glycerol and dithiothreitol (DTT) at various concentration failed to improve the stability of the purified protein samples.

The most stable form of recombinant LOXO-TP was found to be freshly eluted IMAC-purified protein extract. When exchanged into a storage buffer, aliquoted and kept at -80°C, the IMAC-purified fraction of recombinant LOXO-TP retained similar levels of activities for months. Freshly-thawed samples kept on ice were found to lose

approximately 30% of activity after one hour, but retained approximately 95% of activity within 15 min of thawing (Appendix A.4.5).

Therefore, after the IMAC-purification, the eluted fraction was buffer-exchanged into storage buffer, aliquoted into 50 µL aliquots and stored at -80°C as described in section 3.9.3. Subsequent biochemical characterisations of the recombinant LOXO-TP were conducted within 5-10 minutes of thawing the protein sample to prevent variation due to protein instability.

6.3.4 Expression of recombinant LOXCFL

As shown in Figure 6.1, initial expression experiments with recombinant LOXCFL failed to produce any detectable levels of proteins of the expected size. As no transit peptide had been predicted for VvLOXC, only full-length constructs were prepared for this protein.

In order to obtain soluble LOXCFL, various expression temperatures and IPTG concentrations were tried. Furthermore, in order to overcome potential codon-bias issues associated with expression of a plant protein in *E. coli*, the LOXCFL construct was re-transformed into the Rosetta-gami(DE3)pLysS (Novagen, Merck Bioscience, Auckland, New Zealand) expression host and induction experiments at various temperatures and IPTG concentrations carried out.

The *E. coli* Rosetta-gami(DE3)pLysS strain supplies tRNA for six codons which are relatively abundant in eukaryotic cells, but production of which is deficient in *E. coli* cells (such as the BL21(DE3) strain). Furthermore, the Rosetta-gami(DE3)pLysS strain is complemented with pLysS plasmid encoding T7 lysozyme, a feature that allows most stringent control of the recombinant protein at the preinduced stage. In addition, Rosetta-gami(DE3)pLysS strains possess *lacY* mutation, which allows precise control over expression when altered amounts of inducer (IPTG) are added to the cultures.

Figure 6.6 illustrates the results of the experiment where both, BL21(DE3) and Rosetta-gami(DE3)pLysS containing LOXCFL constructs were incubated at 12°C (rather than 14°C as used in previous experiments) for 24 hours after induction with 1 mM IPTG to further reduce rates of protein synthesis.

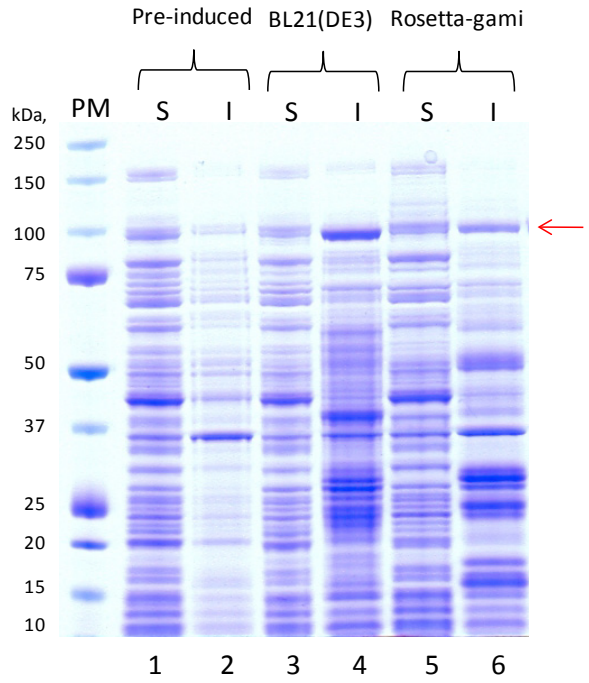

Figure 6.6 SDS-PAGE gel analysis of recombinant LOXCFL in different host strains

Protein samples were run on NuPAGE® 4-12% Bis-Tris gel and stained with Fast Blue protein stain. BL21(DE3) and Rosetta-gami(DE3)pLysS cells containing LOXCFL protein expression construct were grown at 37°C until OD_{600}~0.6. The cultures were then induced with 1 mM IPTG and incubated at 12°C for 24 hours. Soluble (**S**) and insoluble (**I**) fractions of crude protein extracts were analysed from preinduced fraction of Rosetta-gami(DE3)pLysS (lanes 1 and 2), and induced with 1 mM IPTG fractions of BL21(DE3) strain (lanes 3 and 4) and Rosetta-gami(DE3)pLysS strain (lanes 5 and 6) after 24 hour incubation . Red arrow indicates expected band positions for the recombinant LOXCFL protein. **PM** – Precision Plus Protein standard.

As can be seen from Figure 6.6, the prolonged incubation at lower temperature resulted in the expression of a protein of the expected size in insoluble fractions of both strains (lanes 4 and 6, Figure 6.6). However, no visible expression was observed in soluble fractions of either strain (lanes 3 and 5, Figure 6.6). Furthermore, no changes in absorbance at 234 nm were observed when the soluble fractions were incubated with LnA, LA and AA at various pH conditions indicating absence of LOX activities.

To check if reduced IPTG concentration can induce production of soluble LOXCFL, Rosetta-gami(DE3)pLysS cultures containing LOXCFL constructs were induced with either 0.5, 0.25, 0.1 or 0.05 mM of IPTG (final concentration) and incubated at 37°C for 4 hours (Figure 6.7).

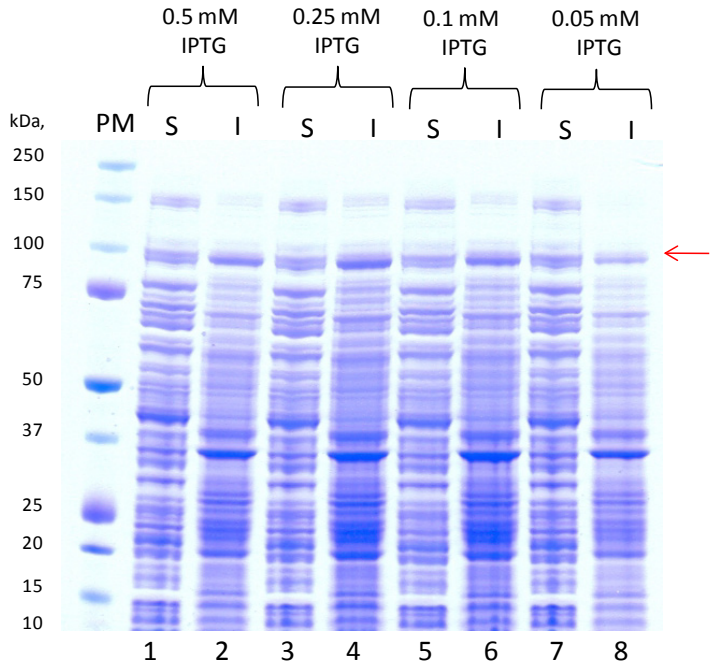

Figure 6.7 SDS-PAGE gel analysis of recombinant LOXCFL expressed after induction with different concentrations of IPTG

30 µg of protein samples were run on NuPAGE® 4-12% Bis-Tris gel and stained with Fast Blue protein stain. Rosetta-gami(DE3)pLysS cells containing LOXCFL protein expression construct were grown at 37°C until OD600~0.6. The cultures were then induced with different concentrations of IPTG and incubated at 37°C for 4 hours. Soluble (**S**) and insoluble (**I**) fractions of crude protein extracts induced at final 0.5 mM (lanes 1 and 2), 0.25 (lanes 3 and 4), 0.1 (lanes 5 and 6), and 0.05 mM (lanes 7 and 8) were analysed. Red arrow indicates expected band positions for the recombinant LOXCFL protein. **PM** – Precision Plus Protein standard.

As illustrated in Figure 6.7, changes of the inducer concentration resulted in some changes in levels of recombinant protein produced in insoluble fractions, with the highest levels of recombinant LOXCFL observed at 0.25 mM IPTG (lane 4, Figure 6.7). However, no recombinant protein accumulation was observed in the corresponding soluble fractions (lanes 1, 3, 5 and 7, Figure 6.7). Furthermore, none of the soluble fractions exhibited LOX activities. Prolonged expression at the lower temperatures and lower IPTG concentration also failed to produce any soluble and functional LOXCFL (data not shown).

Due to a combination of the time constraints, and also because VvLOXC represented a putative 9-LOX and was unlikely to participate in the formation of C6 and C5 compounds, there were no further attempts undertaken to obtain soluble active VvLOXC protein within this project.

6.3.5 Expression of recombinant HPLAFL and HPLA-TP

Initial expression of recombinant HPLAFL and HPLA-TP was performed as for LOX constructs described in section 3.9.2. Similar to LOXA and LOXO, recombinant protein expression of the full-length recombinant protein of HPLA resulted in accumulation of recombinant protein only within the insoluble fractions (lane 8, Figure 6.1 and lanes 2 and 4, Figure 6.8). Expression of the HPLA-TP construct (in which the putative chloroplast transit peptide had been removed) however resulted in production of recombinant protein of the expected size in both soluble and insoluble fractions, at 37°C as well as at 14°C (lanes 5-8, Figure 6.8).

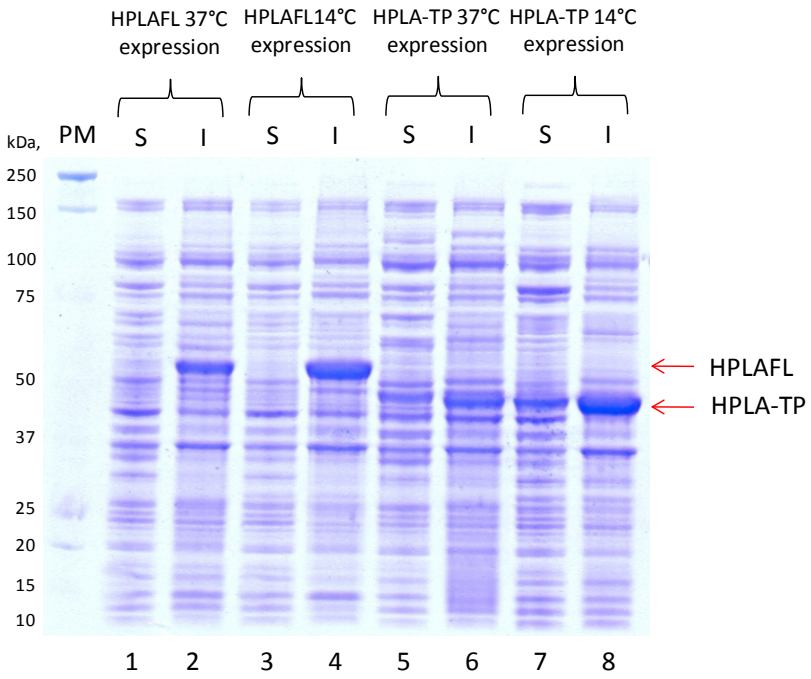

Figure 6.8 SDS-PAGE gel analysis of recombinant HPLAFL and HPLA-TP

30 µg of each protein sample were run on NuPAGE® 4-12% Bis-Tris gel and stained with Fast Blue protein stain. BL21(DE3) cells containing HPLAFL and HPLA-TP protein expression construct were grown at 37°C until OD600~0.6. The cultures were then induced with 1 mM IPTG and incubated either at 37°C for 6 hours or at 14°C for 18 hours. Soluble (**S**) and insoluble (**I**) fractions of crude protein extracts were analysed from cultures incubated at 37°C (lanes 1, 2 and 5, 6 for HPLAFL and HPLA-TP) and at 14°C (lanes 3, 4 and 7, 8 for HPLAFL and HPLA-TP). Red arrows indicates expected band positions for HPLAFL and HPLA-TP recombinant proteins. **PM** – Precision Plus Protein standard.

However, when HPLAFL or HPLA-TP soluble fractions were subjected to HPL-assays as described in section 3.9.6, no activity as determined by changes in absorbance at 234 nm was observed for any of the HPLA fractions. The absence of HPL activities in the

soluble fractions of HPLAFL-expressing cultures could possibly be explained by lack of the soluble HPLAFL protein, which is also supported by the SDS-PAGE analysis of crude protein extracts (lanes 1 and 3, Figure 6.8). However, it was not clear why there was an absence of HPL activity in soluble fractions of HPLA-TP-expressing cultures, as clearly bands of expected sizes were present within the crude protein fractions analysed by the SDS-PAGE analysis (lanes 5 and 7, Figure 6.8).

Several authors have recently raised questions concerning the importance of the presence of detergents for activation of certain HPLs (Hughes *et al.* 2006; Noordermeer *et al.* 2000b; Noordermeer *et al.* 2001b). According to Hughes et al. (2006), the presence of non-ionic detergents such as Triton X-100 or Emulphogene *in vitro* emulates a "membrane" environment, which is required for *in vivo* functioning of HPLs. Furthermore, Noordermeer *et al.* (2000b) were able to solubilise active HPL recombinant protein from insoluble bacterial pellets by applying a detergent-containing buffer. To check if application of a detergent during extraction effects activity of the VvHPLA recombinant proteins, the extraction method was modified according to the method proposed by Noordermeer *et al.* (2000b).

As described in section 3.9.4, after the initial extraction of soluble HPLAFL and HPL-TP protein fraction, the remaining bacterial pellets were re-constituted in the membrane solubilisation buffer, containing 0.2% (w/v) Triton X-100. Subsequent centrifugation recovered "membrane" protein fractions, which along with soluble fractions were SDS-PAGE analysed and assayed for HPL activities.

It was not possible to detect any distinct bands of the expected size in the "membrane" fraction of HPLAFL after SDS-PAGE analysis (lane 2, Figure 6.9), although a weak band of expected size was present in the "membrane" fraction of HPLA-TP (lane 4, Figure 6.9). When aliquots of soluble and "membrane" fractions of HPLAFL and HPLA-TP were incubated with LnA-hydroperoxide substrate, only HPLAFL fractions induced decrease in absorbance at 234 nm, indicating presence of active HPL proteins in these fractions (Appendix A.4.7). Furthermore, although undetectable on SDS-PAGE gel, the membrane fraction of HPLAFL exhibited much higher rate of conversion compared to the soluble fraction (Appendix A.4.7).

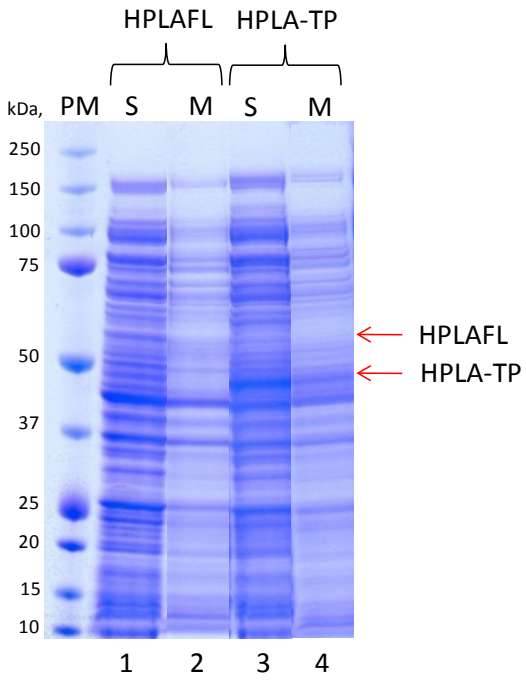

Figure 6.9 SDS-PAGE gel analysis of soluble and "membrane" fractions of recombinant HPLAFL and HPLA-TP

Protein sample were run on NuPAGE® 4-12% Bis-Tris gel and stained with Fast Blue protein stain. BL21(DE3) cells containing HPLAFL and HPLA-TP protein expression construct were grown at 37°C until OD600~0.6. The cultures were then induced with 1 mM IPTG and incubated either at 14°C for 18 hours. Soluble (**S**) and membrane (**M**) fractions of crude protein extracts were extracted as described in section 3.9.4 and analysed from HPLAFL-expressing cultures (lanes 1 and 2) and HPLA-TP-expressing cultures. Red arrows indicates expected band positions for HPLAFL and HPLA-TP recombinant proteins. **PM** – Precision Plus Protein standard.

Hughes et al. (2006) report that activity of water-soluble detergent-free recombinant HPL from *Medicago trancatula* can be recovered by adding detergent above its critical micelle concentration (CMC). In order to check if addition of detergent would re-activate soluble fractions of HPLAFL and HPLA-TP expressing cultures with 13(S)-HPOTrE, TritonX-100 (CMC=0.2-0.9 mM) was added to the corresponding reactions at concentrations 0-3.2 mM. However, none of the reactions with soluble HPLAFL displayed an increase in activity upon addition of detergent compared to the detergent-free reactions. Moreover, there was no lyase activity observed at any detergent concentration when soluble HPLA-TP fraction was incubated with 70 µM of 13(S)-HPOTrE (data is not shown).

Time allocated for the completion of the current research did not allow for complete purification and biochemical characterisation of HPLA enzyme. However, the

membrane fraction of HPLAFL extract was used in a set of preliminary experiments to identify pH optimum and product specificity of recombinant VvHPLA (see sections 6.4.6-6.4.8).

6.4 Biochemical characterisation of recombinant LOXA-TP and LOXO-TP

As in the preliminary experiments described earlier, LOX activities were measured as changes in absorbance at 234 nm. LOXA-TP characterisation was conducted in 3 ml quartz cuvettes on T60 UV-Visible spectrophotometer (PG Instrument, Bio-Strategy, Auckland, New Zealand). Later availability of FLUOstar omega microplate reader (BMG Labtech, Alphatec, Auckland, New Zealand) allowed LOX assays to be performed in smaller volumes using microplates, which increased throughput. The majority of LOXO-TP assays were performed using FLUOstar omega microplate reader, with the exception of LOX assays to determine temperature optima, in which case T60 UV-Visible spectrophotometer equiped with a temperature controlled cuvette holder was used.

6.4.1 Effect of Tween 20 on LOX activity

To determine the optimal pH for recombinant LOXA-TP and LOXO-TP, LOX assays were conducted in various buffers over a pH range of 3.5-9.5 as described in section 3.9.5. The results of preliminary experiments indicated that recombinant LOXA-TP was active in an acidic environment and no LOX activities for LOXA-TP were observed at above pH 6.5. Below pH 3.5, LOXA-TP protein precipitated and consequently no LOX activity was detected.

Performing a series of negative controls (no enzyme added) in LOX assays at pHs below 7.5 revealed that when FA substrate was mixed with buffer, significant changes in absorbance at 234 nm were observed even in the absence of enzyme (Appendix A.4.8). These changes are most likely due to autooxidation of FA-substrates. Furthermore, when recombinant LOXA-TP protein was incubated with various LnA substrate concentrations, an unusual pattern of changes in LOXA-TP catalytic rates was observed with the increase of substrate concentration in the assay (blue line, Figure 6.10). An initial increase in the catalytic rates was observed when concentration of the substrate increased from 0 to 10 μM. When concentration of LnA increased from 10 to 60 μM, a gradual decline in the conversion rate was observed, and an increase again at concentrations higher than 60 μM (blue line, Figure 6.10). When changes in absorbance at 234 nm were monitored at corresponding concentrations of the substrate in reactions where no enzyme was added, a constant increase in the conversion rate was observed

with increasing LnA concentration (dark red line, Figure 6.10). At concentration of the substrate higher than 350 µM, the conversion rates in the reactions with and without enzyme were the same. This suggested that the autooxidation of LnA is most likely to be responsible for the unusual changes in conversion rates observed in the preliminary LOXA-TP assays.

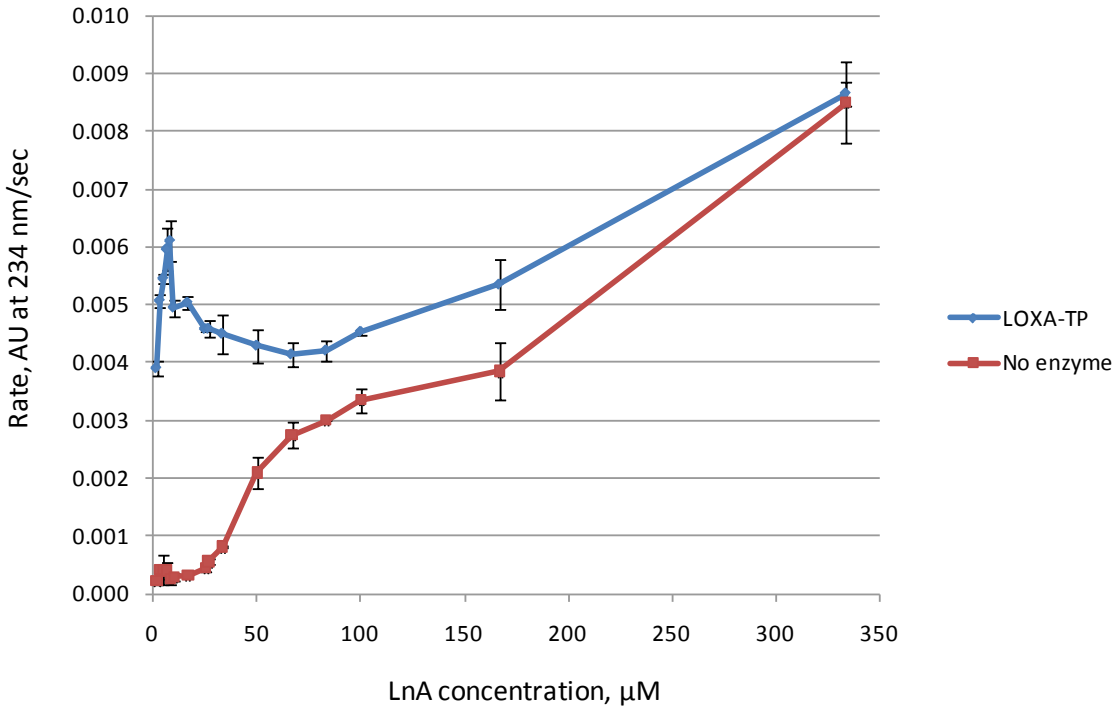

Figure 6.10 Effect of substrate concentration on LOX assay at pH 5.5

Seven micrograms of purified LOXA-TP protein was incubated at various concentrations of LnA in 3 mL of sodium acetate buffer (pH 5.5) and its initial kinetic rate was determined from the linear part of the curves (data not shown). Similarly, autooxidation rates were established at the corresponding concentrations of LnA to which no enzyme was added. The established rates were then plotted against final concentrations of LnA. Blue and red lines correspond to changes in catalytic rates in samples with and without LOXA-TP respectively.

Addition of a non-ionic detergent Tween 20 at concentration less than 1% eliminated self-oxidation of FA substrates. It was also observed, that the addition of Tween 20 to LOXA-TP reactions affected the conversion rates compared to the reactions, where no detergent was added.

To determine if detergent:substrate ratio affects conversion rates at a given concentration of FA substrate, a series of LOX assays were performed with recombinant

LOXA-TP at the determined optimum pH (pH 5.5) at various LnA concentrations, to which various amounts of Tween 20 were added. Analysis of Tween 20 titration curves (Appendix A.4.9) revealed that for each particular concentration of the substrate, there was an optimum Tween 20 concentration, outside of which the detergent had an inhibiting effect on conversion rates. The optimal Tween 20 concentrations for each of a series substrate concentrations were then plotted against the corresponding substrate concentrations Figure 6.11. The resulting graph displayed strong positive correlation (R^2>0.99) between an increase in concentration of LnA and an increase in optimum concentration of Tween 20 required for LOXA-TP to convert the substrate at maximum rate (Figure 6.11). The optimal detergent:substrate ratio was then determined from the slope of the curve and was 0.000131% for each 1 µM of LnA.

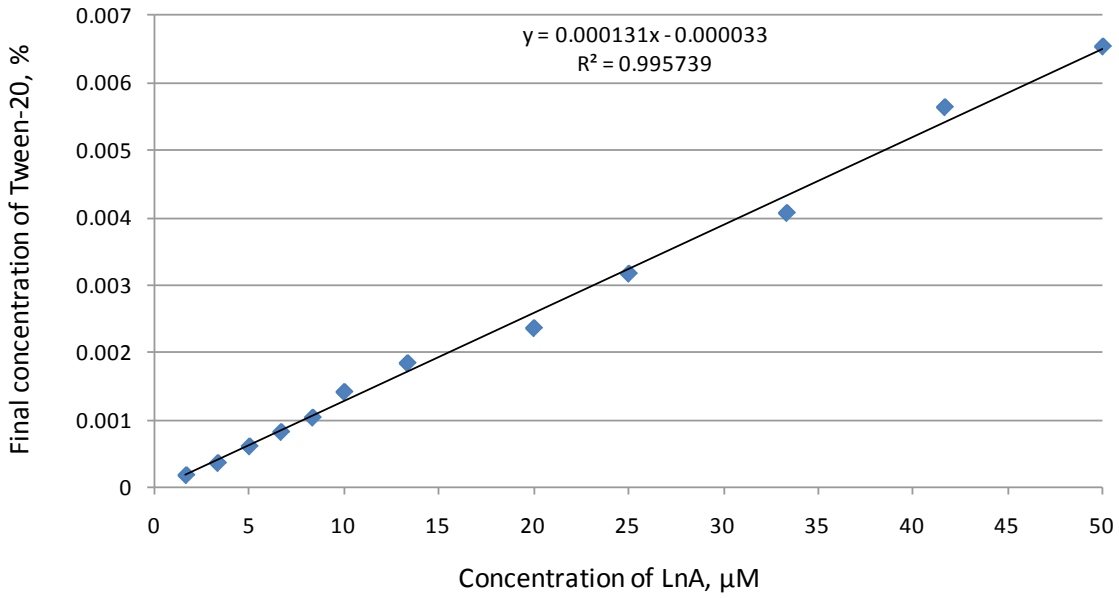

Figure 6.11 Correlation between LnA concentration and optimum concentration of Tween 20 required for maximum LOXA-TP conversion rate

Optimum concentrations of Tween 20 for a number of substrate concentrations were determined in a series of LOX assays with recombinant LOXA-TP as described above and in Appendix A.4.9. The empirically determined optimal Tween 20 concentrations were then plotted against the corresponding substrate concentrations and the data points were fitted using a linear regression model. The optimal detergent:substrate ratio was determined from the slope of the curve.

The optimal detergent:substrate ratio determined for LOXA-TP only held true for LOX assays conducted at pH 5.5. When LOXA-TP was incubated with constant

concentration of LnA at different pHs the optimal detergent:substrate ratios for particular pH were found to change (Figure 6.12).

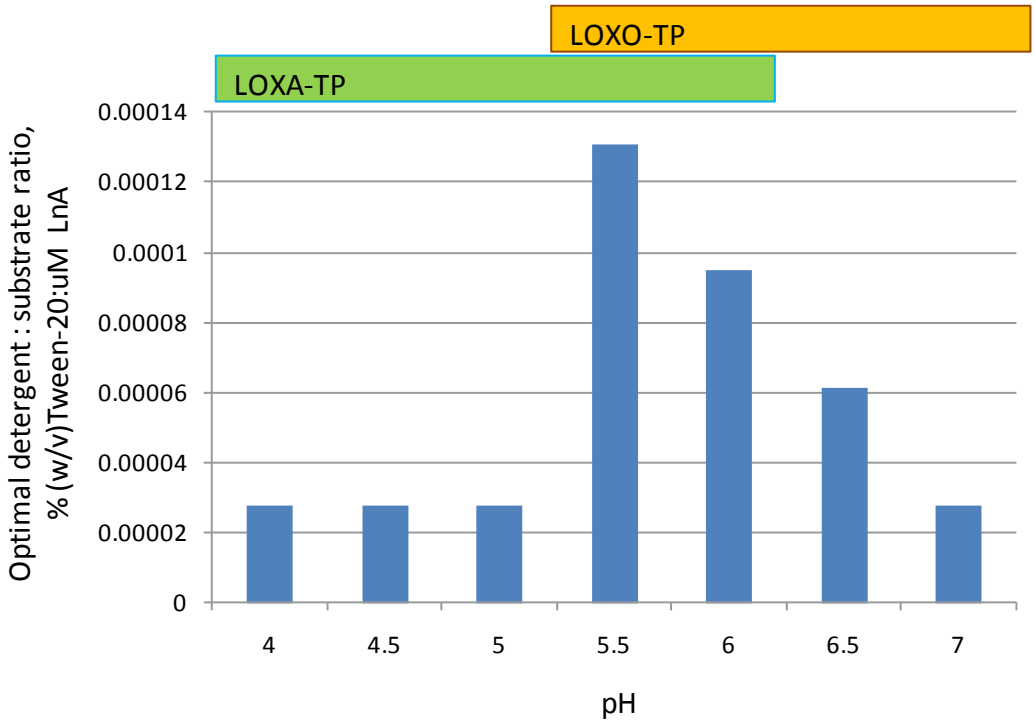

Figure 6.12 Effect of pH on Tween 20 requirements for recombinant LOXA-TP and LOXO-TP to perform the reaction at maximum rate

Recombinant LOXA-TP or LOXO-TP enzymes were incubated with LnA substrate (final concentration 60 µM) in 3 mL of either sodium acetate (pH 4.0-5.5) or sodium phosphate (pH 6.0-7.0) buffer in presence of various concentration of Tween 20. The ratio of detergent:substrate at which the catalytic rate was the highest for a given pH was accepted as the optimal ratio for the particular pH, and displayed as bar graph. The horizontal bars at the top indicate a pH range at which LOXA-TP and LOXO-TP were assayed.

As can be seen from Figure 6.12, at pHs below 7.5 the requirements for Tween 20 increased in a linear fashion with its maximum at pH 5.5 (0.000131% (w/v) for each 1 µM of LnA added), after which the highest catalytic LOX activities were observed at a ratio of 0.000028. It should be noted here that detergent:substrate ratio of 0.000028 was obtained without adding any extra detergent into the reaction due to the presence of Tween 20 in FA substrate stocks. As explained in section 3.9.5, Tween 20 was added to FAs during substrate stock preparation in order to increase its solubility. Therefore, it is possible that at pHs 4.0-5.0 the optimum detergent:substrate ratio is below 0.000028. As was mentioned earlier, no effect of detergent addition was observed on activities of

LOXA-TP or LOXO-TP at pH<7.5. Similar results were obtained for substrates of LA and AA (data not shown).

Empirically determined optimal Tween 20:FA ratios were used in the subsequent experiments for determining pH optima of the recombinant LOXA-TP and LOXO-TP. There was no change in LOX activity plus or minus Tween 20 at pHs above 7.5, thus no detergent was added in LOX assays at pHs above 7.5.

6.4.2 Effect of pH on activity of the recombinant LOXA-TP and LOXO-TP

The assays for determining optimum pH of LOXA-TP and LOXO-TP were performed at 25°C with saturating concentrations of LnA, LA or AA substrate as described in section 3.9.5.

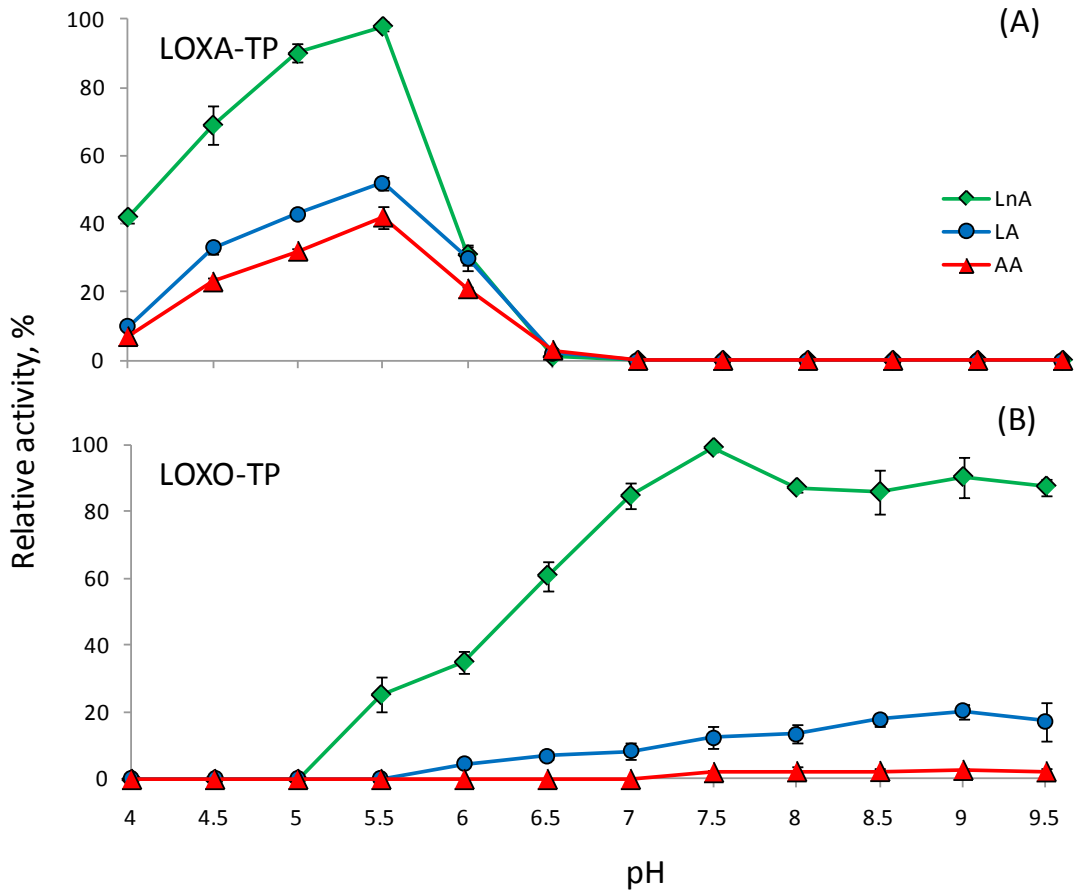

Figure 6.13 Effect of pH on activity of LOXA-TP and LOXO-TP

Recombinant LOXA-TP protein **(A)** and LOXO-TP protein **(B)** were incubated with 60 µM or 100 µM (final concentrations) of either LnA, LA or AA substrate respectively at pH 4.0-9.5 at 25°C. Catalytic rates were determined as changes in absorbance at 234 nm per second. The highest catalytic rate observed for each of the proteins was expressed as 100% and remaining data points were expressed as a percentage of this. Error bars represent standard deviation of the mean for three replicates.

As shown in Figure 6.13.A, LOXA-TP oxidised all three FAs in an acidic environment (pH 4.0-6.5) with its maximum activity observed at pH 5.5. Utilising LnA as a substrate LOXA-TP retained approximately 40% of its maximum activity at pH 4.0 and no activities were observed at pH>6.5 with any of the three substrates. At pH 5.5 the highest catalytic rate of LOXA-TP was observed with LnA, while the catalytic rates with LA and AA were around 50% and 40% of the maximum activity respectively. However, as displayed in Figure 6.13.A, the relative LOXA-TP activity with the three different substrates was pH dependent. At pH 6.0, for example, the conversion rate of LOXA-TP with LnA was the same as with LA and differed only slightly from the

conversion rate with AA (Figure 6.13.A). At pH 3.5 or lower, precipitation of LOXA-TP occurred.

In contrast to LOXA-TP, LOXO-TP preferred neutral and alkaline conditions with its maximum activities observed at pH 7.5 with LnA, and pH 9. 0 with LA (Figure 6.13.B). Recombinant LOXO-TP was found to precipitate when the reaction pH was below pH 5.0. Catalytic activity of LOXO-TP was higher with LnA across the whole pH range. The conversion rates were substantially lower for LA (5-20% of LnA), and with AA (below 5% of the total rates detected with LnA) (Figure 6.13.B).

6.4.3 Effect of temperature on activity of the recombinant LOXA-TP and LOXO-TP

To determine the optimum temperature for both recombinant LOXs, enzyme activities were measured over a range of temperatures (10-50°C) with saturated (60 μM for LOXA-TP and 100 μM for LOXO-TP) concentrations of all three FA substrates (LnA, LA and AA) as described in section 3.9.5.2.

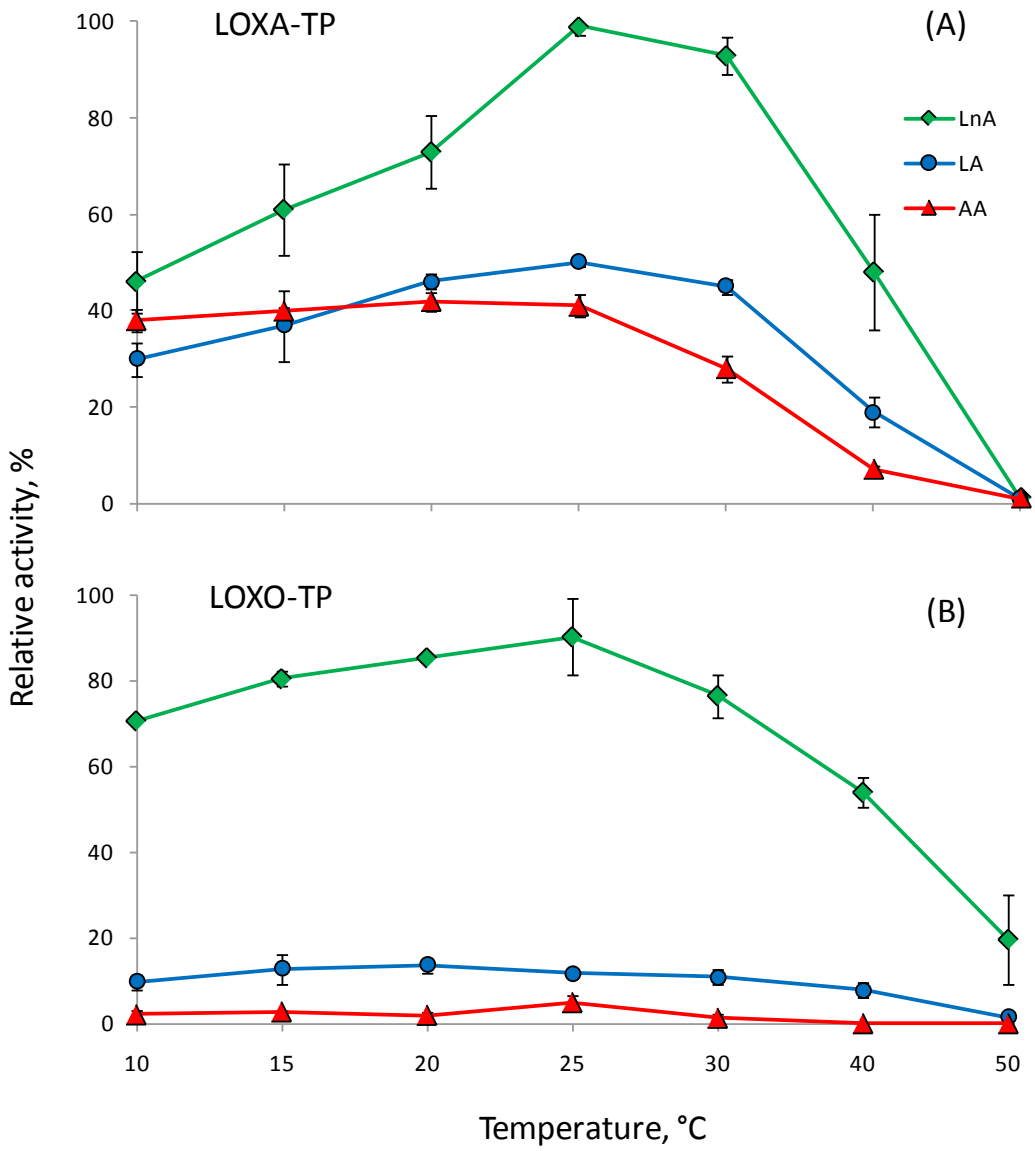

Figure 6.14 Effect of temperature on activity of recombinant LOXA-TP and LOXO-TP

Recombinant LOXA-TP protein **(A)** and LOXO-TP protein **(B)** were incubated with 60 µM or 100 µM (final concentration) of either LnA, LA or AA substrate at temperatures between 10 and 50°C. Catalytic rates were determined as changes in absorbance at 234 nm per second. The highest catalytic rate observed for each of the proteins was expressed as 100% and remaining data points were expressed as a percentage of this. Error bars represent standard deviation of the mean for three replicates.

Maximum activities for both recombinant proteins with LnA were observed at 25°C (Figure 6.14). Activities of LOXA-TP with all substrates were abolished at 50°C, while at 10°C LOXA-TP retained approximately 30-50% of its maximum activity depending on the substrate used in the assays (Figure 6.14.A). Interestingly, the decrease in temperature did not seem to affect LOXA-TP activity with LA and AA to the same extent as with LnA (Figure 6.14.A).

LOXO-TP was more temperature tolerant and when incubated with LnA retained approximately 20% of maximal activity at 50°C and at 10°C retained approximately 70% of its maximum activity (Figure 6.14.B).

6.4.4 Kinetic properties of recombinant LOXA-TP and LOXO-TP

To determine basic kinetic characteristics of the recombinant LOXA-TP and LOXO-TP proteins, the velocity of the substrate conversion was studied across a range of concentrations of LnA, LA and AA fatty acids using standard conditions as described in section 3.9.7. The kinetic data for recombinant LOXA-TP and LOXO-TP were fitted with non-linear fit model described by the Michaelis-Menten equation using GraFit software (Erithacus Software Limited, East Grinstead, West Sussex, UK) (Figure 6.15) and these data used for calculating Michaelis constant (K_m) and maximum velocity (V_{max}) values for both enzymes (Table 6.2).

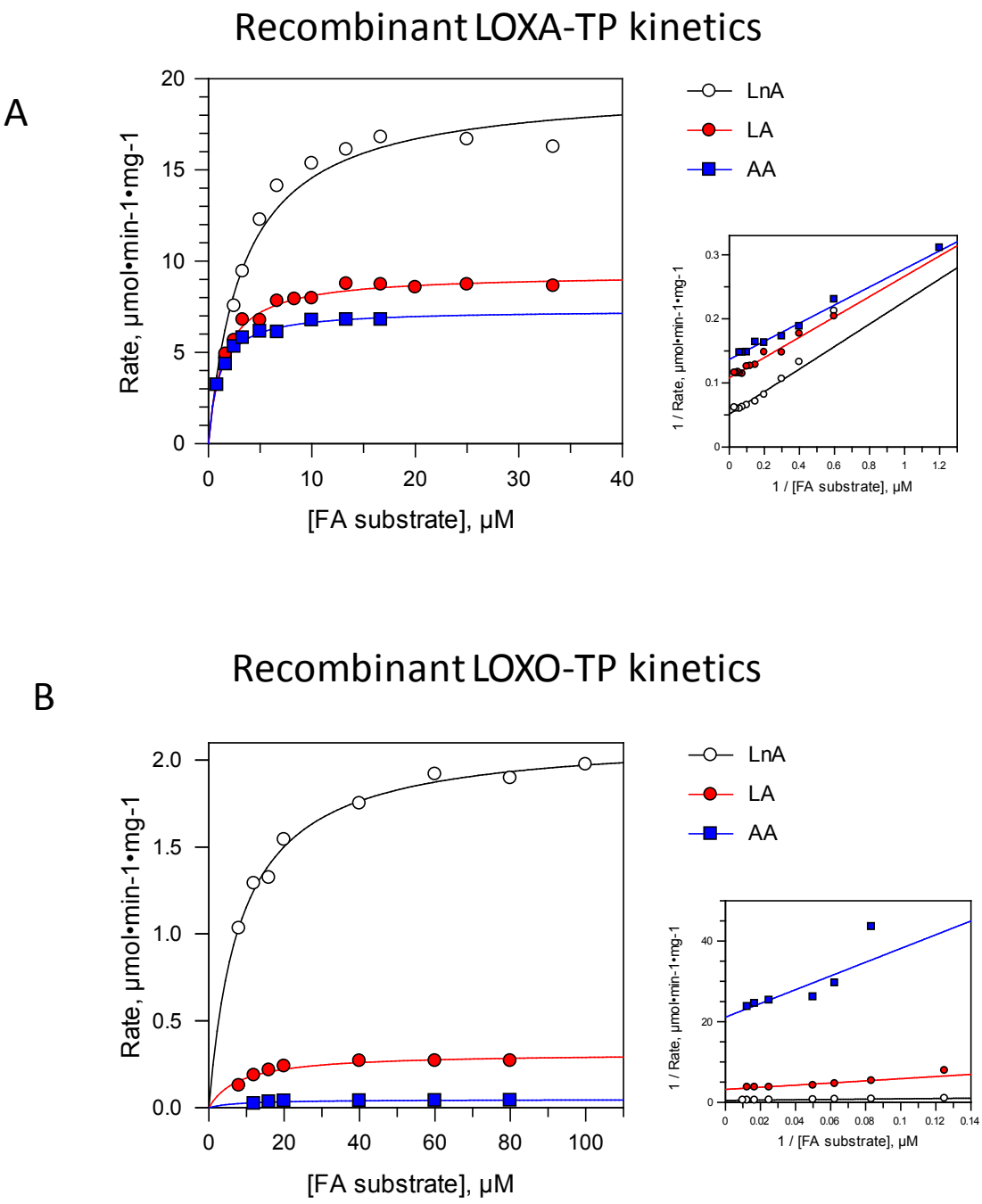

Figure 6.15 Kinetic properties of recombinant LOXA-TP and LOXO-TP

A series of LOX assays with recombinant LOXA-TP and LOXO-TP on a range of concentration of LnA, LA and AA fatty acids were performed as described in section 3.9.7. The kinetic data for recombinant LOXA-TP (A) and LOXO-TP (B) were fitted with non-linear fit model described by Michaelis-Menten equation using GraFit software (Erithacus Software Limited, East Grinstead, West Sussex, UK). The fitted data were used to determine Michaelis constant (K_m) and maximum velocity (V_{max}) values for both enzymes (Table 6.2).

Table 6.2 Biochemical properties and optimum assay conditions of recombinant LOXA-TP and LOXO-TP enzymes

Enzyme	Optimum pH	Optimum temperature, °C	Specific activity, U·mg^{-1} total protein	Substrate	V_{max}, µmol·min^{-1}·mg^{-1}, ±SE	K_m (µM), ±SE	V_{max}/K_m	Products formed
LOXA-TP	5.5	25	19.56	LnA	19.56 ± 0.93	3.4 ± 0.6	5.70	13(S)-HPOTrE
				LA	9.29 ± 0.15	1.5 ± 0.1	6.32	13(S)-HPODE
				AA	7.32 ± 0.11	1.0 ± 0.1	7.10	15(S)-HPETE
LOXO-TP	7.5	25	2.14	LnA	2.14 ± 0.04	8.5 ± 0.6	0.25	13(S)-HPOTrE
				LA	0.30 ± 0.02	8.4 ± 1.8	0.04	13(S)-HPODE
				AA	0.05 ± 0.01	8.1 ± 3.1	0.01	15(S)-HPETE

The K_m values for both LOXA-TP and LOXO-TP were in the low micromolar range indicating a very high affinity of both enzymes for all three substrates (Table 6.2).

Comparison of K_m and V_{max} values indicates that LOXA-TP has higher affinity for AA (1.5-fold and 3-fold higher than for LA and LnA respectively), but converts LnA over 2-fold faster than LA and 3-fold faster than AA. In comparison, LOXO-TP had the highest catalytic efficiency with LnA (V_{max}/K_m for LnA was 7- and 29-fold higher than for LA and AA respectively), although K_m values for all three fatty acids were very similar (Table 6.2).

6.4.5 Product identification of recombinant LOXA-TP and LOXO-TP

The identity of LOXA-TP and LOXO-TP products was determined using reverse-phase high performance liquid chromatography (RP-HPLC) by comparing the products with authentic standards as described in section 3.9.8.

The HPLC analysis of the reaction products produced by LOXA-TP and LOXO-TP revealed that both enzymes convert LnA exclusively into 13(S)-HPOTrE, LA – into 13(S)-HPODE and AA – into 15(S)-HPETE (Figure 6.16, Table 6.2).

These results confirm the predicted classification of VvLOXA and VvLOXO as 13-LOX enzymes.

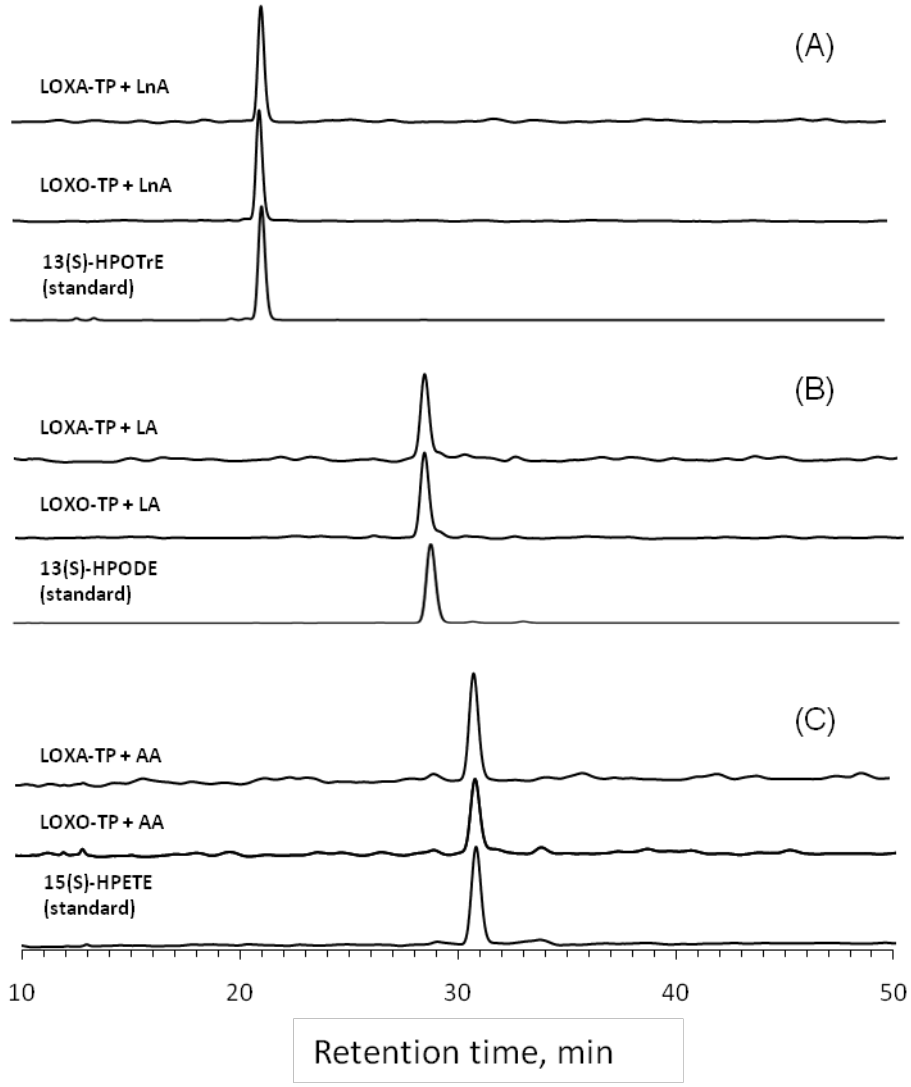

Figure 6.16 Product identification of the recombinant LOXA-TP and LOXO-TP

Purified reaction products of LOXA-TP and LOXO-TP activity against LnA, LA and AA were resolved by RP-HPLC and their retention times were compared with authentic standards 13(S)-HPOTrE, 13(S)-HPODE and 15(S)-HPETE. RP-HPLC was performed on Agilent 1100 Series HPLC System (Agilent Technologies, Santa Clara, CA, USA), using a Luna 5µm C18(2) 100A column (250x4.60 mm) (Phenomenex, Auckland, New Zealand). LOX reaction products and authentic standards were resolved by isocratic elution with acetonitrile + 0.1% formic acid:H_2O + 0.1% formic acid (63:37) at a flow rate of 0.5 mL/min for 48 min at 25°C, monitoring the eluted compounds at 234 nm.

6.4.6 Biochemical characterisation of recombinant HPLAFL

Preliminary HPL assays with crude *E. coli* extracts containing recombinant HPLAFL and HPLA-TP enzymes revealed that only the "membrane" fraction of HPLAFL-expressing constructs exhibited sufficient levels of activities required for further biochemical characterisation (section 6.3.5). Due to time constraints, only partial

biochemical characterisation of HPLAFL recombinant protein was performed. This included determination of pH optimum and identification of the reaction products of HPLAFL activity. The preliminary experiments indicated that HPLAFL prefers 13(S)-HPOTrE as the substrate. Although HPLAFL has also showed some activity against 13(S)-HPODE and 15(S)-HPETE, the catalytic rates of HPLAFL against these substrates were insufficient for their accurate comparison with the HPLAFL activities against 13(S)-HPOTrE. Therefore, only 13(S)-HPOTrE substrate was used in determining the pH optimum for the recombinant HPLAFL enzyme as described below.

6.4.7 Effect of pH on activity of recombinant HPLAFL

In order to determine the effect of pH conditions on HPLAFL activity, 40 µL of the "membrane" *E. coli* fraction containing HPLAFL protein was incubated with 70 µM (final concentration) of 13(S)-HPOTrE in 250 µL total volume at various pHs as described in section 3.9.6.

As shown in Figure 6.17, HPAFL preferred acidic environment and its highest activity with 13(S)-HPOTrE was observed at pH 5.0. At pH 4.0 HPLAFL retained around 60% of its maximum activity, but formed a precipitate at pH 3.5. HPLAFL retained 10-20% of its maximum activity at pH 6.5-9.5.

Atwal *et al*. (2005) report differential pH optima for the recombinant LeHPL from tomato fruit. The authors showed that LeHPL's highest activity with LnA-hydroperoxide was at pH 5.0. At pH 7.0, however, the recombinant LeHPL preferred LA-hydroperoxides as substrate and showed no activity towards LnA-hydroperoxides (Atwal *et al.* 2005). To check if similar phenomenon is true for the recombinant HPLAFL, LA- and AA-hydroperoxides were used as substrates in reactions with HPLAFL at a wider range of pH conditions, but no activation was observed compared to activities with LnA-hydroperoxides.

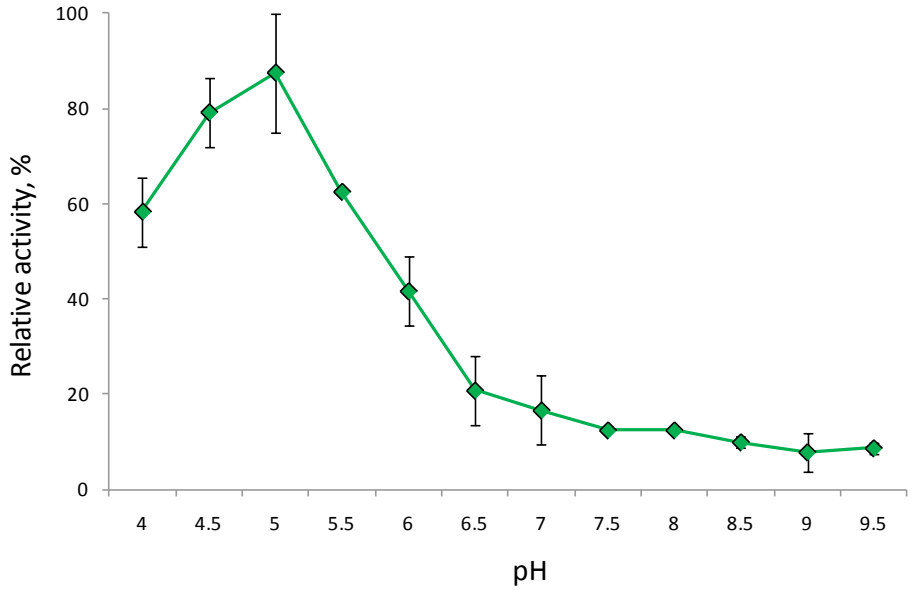

Figure 6.17 Effect of pH on HPLAFL activity

Recombinant HPLAFL protein was incubated with 70 µM 13(S)-HPOTrE at pH 5.0 at 25°C. Catalytic rates were determined as decrease in absorbance at 234 nm per second. The highest catalytic rate was expressed as 100% and remaining data points were expressed as a percentage of this. Error bars represent standard deviation of the mean for three replicates.

6.4.8 Product identification of recombinant HPLAFL

To identify volatile products of HPLAFL catalysis, the "membrane" *E. coli* fraction containing recombinant HPLAFL was incubated with FA-hydroperoxides (namely 13(S)-HPODE, 13(S)-HPOTrE and 15(S)-HPETE) and the headspace of the reaction was analysed using GC-MS as described in section 3.9.9.

To confirm the absence of HPL activity in the *E. coli* fraction containing recombinant HPLA-TP protein observed earlier (section 6.3.5), this fraction was also incubated with FA-hydroperoxides and analysed as described above. The results of GC-MS analysis of HPLAFL and HPLA-TP products, as well as controls for each substrate are attached in Appendices A.4.10 - A.4.12.

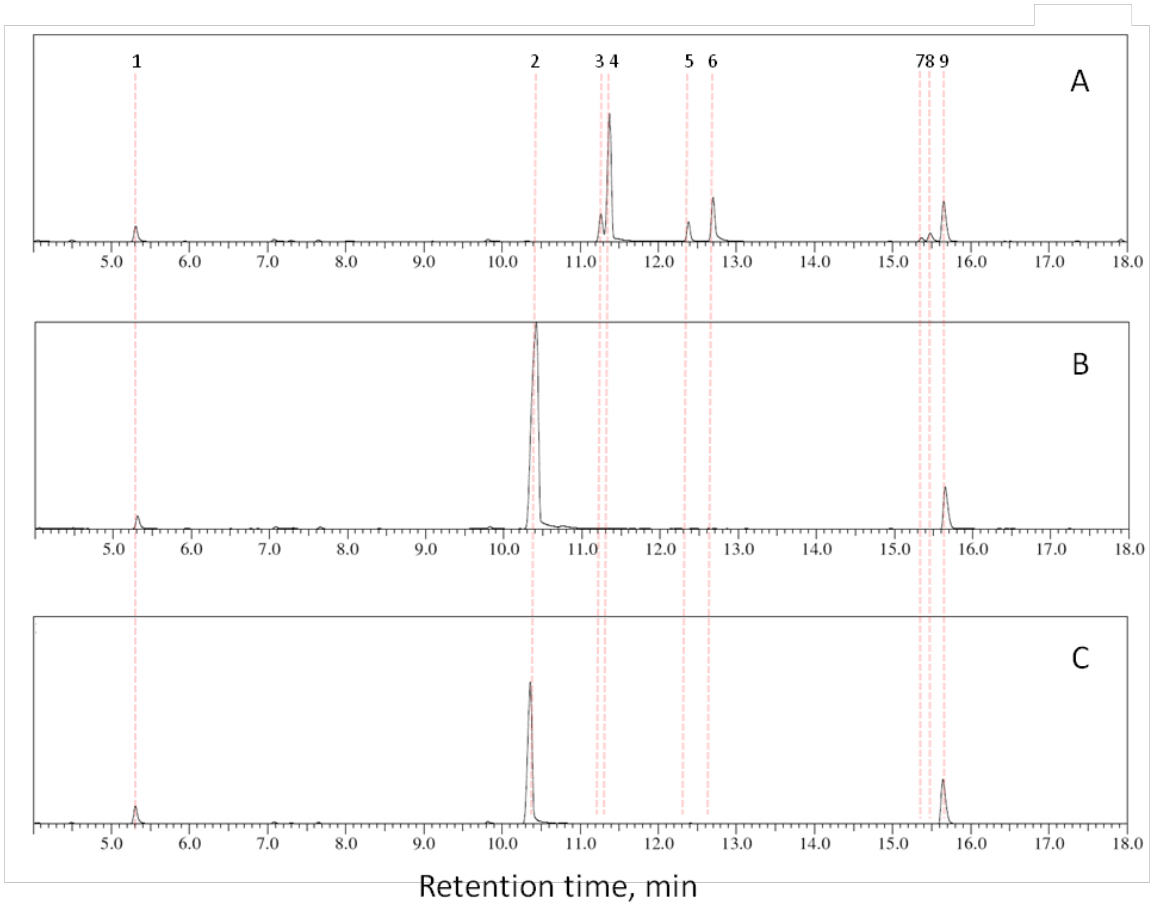

Figure 6.18 GC-MS analysis of HPLAFL products

"Membrane" fraction containing recombinant HPLAFL protein was incubated in sealed vials with soybean LOX1 derived FA-hydroperoxides. The headspace of the vials were analysed using GC-MS as described in section 3.9.9. Panels A, B and C represent chromatograms of the HPLAFL volatile reaction products obtained in reactions with 13(S)-HPOTrE, 13(S)-HPODE and 15(S)-HPETE respectively. The detected peaks were labelled 1-9 in order of their elution. The corresponding to each peak compounds were identified by matching their mass spectra with the mass spectra of reference compounds in the NIST EPA/NIH Mass Spectral Library (National Institute of Standards and Technology, NIST05).Based on their closest maches, the identified compounds were identified as follows: 1 – acetone; 2 – hexanal; 3 – 2-methyl-4 pentanal; 4 – (*Z*)-3-hexenal; 5 – (*E*)-2-hexenal ; 6 – (*E*)-2-hexenal ; 7 – 2(*E*), 4(*E*)-hexadienal; 8 – 2(*E*), 4(*E*)-hexadienal and 9 – acetic acid. The corresponding spectra for the identified compounds are attached in Appendix A.4.13. Acetone (peak 1) and acetic acid (peak 9) in each sample were introduced from the reaction buffer and are not products of the reaction.

Figure 6.18 illustrates the results obtained by analysis of vial headspace volatile composition after incubation of "membrane" *E. coli* fraction containing recombinant HPLAFL with three FA-hydroperoxide substrates. The detected peaks were labelled 1-9 in order of their elution. The tentative identity of each peak was determined by matching their mass spectra with the mass spectra of reference compounds in the NIST EPA/NIH Mass Spectral Library (National Institute of Standards and Technology,

NIST05). It is important to note that several HPLAFL volatile reaction products had at least two high-scoring matches in the Mass Spectral Library (Appendix A.4.13). The identity of the library compound that gave the highest match score based on the mass spectra to the unknown compound was assigned to the compound to be identified. These identities however need to be further validated by using more detailed types of analysis.

As can be seen from Figure 6.18, all samples contained acetone (peak 1) and acetic acid (peak 9). These peaks are also present in control runs, where no enzymes were added (Appendix A.4.10). These compounds most likely derive from sodium acetate buffer used for incubation and therefore should be ignored.

As shown in Figure 6.18.(A), there were six peaks formed as a result of HPLAFL activity with 13(S)-HPOTrE substrate (peaks 3, 4, 5, 6, 7 and 8). These products were absent when no active enzyme was present in the reaction (Appendix A.4.10). Matching individual spectra of the six new unidentified compounds with the existing library predicted their possible identity.

Based on the overall score, the compound corresponding to peak 3 was identified as 2-methyl-4-pentanal, a C5 compound (Figure 6.18.(A), Appendix A.4.13 (3)). However, the spectrum of the compound corresponding to peak 3 was also almost identical to the spectrum of (*Z*)-3-hexenal (Appendix A.4.13 (3)). Therefore, further analysis would be required to confirm the identity of this compound.

Peak 4 represented the bulk of the isolates, indicating that this compound is likely to be the main reaction product of HPLAFL activity with 13(S)-HPOTrE substrate Figure 6.18.(A). Based on comparison with compounds in the library, the compound corresponding to peak 4 was identified as (*Z*)-3-hexenal, although the next closest match from the library was 2-methyl-4-pentanal (Appendix A.4.13 (4)).

Furthermore, some of the peaks, although well separated chromatographically, were identified as the same compound. Particularly, peaks 5 and 6 were both identified as (*E*)-2-hexenal (Figure 6.18.(A), Appendix A.4.13 (5 and 6)) and peaks 7 and 8 were identified as 2(*E*), 4(*E*)-hexadienal (Figure 6.18.(A), Appendix A.4.13 (7 and 8).

In contrast to the number of volatile products identified as a result of HPLAFL driven 13(S)-HPOTrE metabolism, the metabolism of 13(S)-HPODE and 15(S)-HPETE with

HPLAFL resulted in formation of a single volatile compound, hexanal (Figure 6.18.(B and C), Appendix A.4.13 (2)). Interestingly, residual amounts of hexanal were also identified in control samples, where inactive or no enzyme was added to either 13(S)-HPODE and 15(S)-HPETE containing reactions (Appendices A.4.11 and A.4.12).

6.5 Discussion

Identification of basic biochemical characteristics of the LOX and HPL genes is an essential part of their overall functional characterisation. The *in vitro* biochemical assays allow the prediction of optimal conditions, substrate and product specificity as well as basic kinetic characteristics for each individual enzyme. Moreover, individual products obtained as a result of *in vitro* assays can be isolated and identified.

6.5.1 Preparation of recombinant LOX and HPL proteins for further biochemical characterisation

6.5.1.1 Presence of TPs affects solubility and activity of recombinant LOX and HPL proteins

As previously discussed, VvLOXA, VvLOXO, VvLOXC and VvHPLA genes were selected for functional characterisation by means of expressing the corresponding recombinant proteins and subjecting the recombinant proteins to *in vitro* biochemical analysis. However, the initial protein expression experiments with LOXAFL, LOXCFL, LOXOFL and HPLAFL failed to produce soluble functional full-length recombinant proteins for any of the selected genes (section 6.3.1). For all constructs however, varying levels of recombinant proteins were observed in the crude insoluble fractions.

It is well known, that many recombinant proteins expressed in prokaryote host such as *E. coli* can aggregate in the form of inclusion bodies (IBs) due to a high production rate, incorrect folding, presence of targeting peptides or the hydrophobic nature of the proteins synthesised (Jonasson *et al.* 2002). Once incorporated into IBs, the expressed proteins cannot be extracted in the soluble form and therefore cannot be used in biochemical assays without further processing. The inclusion body-incorporated proteins can be solubilised using denaturants and subsequently re-folded into their native form by removing the denaturant. This method however is more expensive and often results in low protein yields.

Amino-acid analysis of the selected LOXs and HPL predicted the presence of transit peptides (TPs) within VvLOXA, VvLOXO and VvHPLA coding sequences that predicted targeting of these proteins to the chloroplast (section 6.2.1). The presence of TPs in the native forms of these enzymes may explain the inability of these proteins to remain in the soluble fraction when they are expressed in *E. coli* cells. To overcome this

problem, the gene section encoding the predicted TP can be excluded during construction of the protein expression vector, as has been reported in earlier studies of plant LOXs (Padilla *et al.* 2009; Terp *et al.* 2006). Therefore, in addition to the full-length constructs, constructs expressing recombinant VvLOXA, VvLOXO and VvHPLA without TPs were designed and designated as (LOXA-TP, LOXO-TP and HPLA-TP) (section 6.2.2).

As predicted, the removal of TPs resulted in soluble functional forms of VvLOXA and VvLOXO recombinant proteins being able to be recovered (sections 6.3.2 and 6.3.3). LOXA-TP and LOXO-TP were therefore further purified using affinity chromatography. These partially purified fractions were used to functionally characterise the recombinant proteins as will be discussed in section 6.5.2.

In contrast, removing the predicted TP sequence from the coding sequence of VvHPLA, resulted in expression of soluble, but inactive protein (see section 6.3.5). Further analysis of the related literature indicated that some HPLs (namely the CYP74C HPL from *Medicago truncatula*) exhibited low activities in the water-soluble form, but were re-activated by adding a non-ionic detergent (Emulphogene) at concentrations above its critical micelle concentration (CMC) (Hughes *et al.* 2006). Unfortunately, Emulphogene was not available at the time of performing the experiments describe here, and it was impossible to validate its ability to re-activate soluble fractions of the recombinant VvHPLA protein. However, the addition of another non-ionic detergent, TritonX-100, to the soluble fractions of HPLAFL and HPLA-TP at concentrations up to 10-fold higher than TritonX-100 CMC, failed to increase activities of the recombinant HPLAFL and HPLA-TP fractions as described in section 6.3.5. Further experiments would be required to establish if detergent re-activation of soluble HPL proteins is specific to Emulphogene.

Although unable to re-activate soluble fractions of HPLAFL and HPLA-TP recombinant proteins, addition of TritonX-100 during protein extraction had a positive effect on HPLAFL activities. As described in section 6.3.5, when the pellet recovered after the separation of the HPLAFL soluble fraction was re-constituted in a buffer containing 0.2% TritonX-100 (as had been proposed by (Noordermeer *et al.* 2000b)), substantial lyase activities were observed in this “membrane” fraction. In contrast, no HPL activities in HPLA-TP “membrane” fraction were detected.

One of the possible reasons explaining the absence of functional activities of HPLA-TP is an incorrectly predicted length of its TP. It is likely, that all or a part of the removed VvHPLA TP is required for the functional lyase activities.

In contrast to VvLOXA, VvLOXO and VvHPLA, analysis of amino acid sequence of VvLOXC did not identify any putative transit peptides (section 6.2.1). Various attempts to obtain soluble recombinant VvLOXC protein were not successful and the expressed protein was associated with the insoluble fraction of the bacterial extracts (section 6.3.1).

As discussed in section 2.4, most of the characterised plant 9-LOXs lack N-terminal transit peptides and have been found to be localised in the cytosol. However, a putative tomato 9-LOX, TomLoxA, has been found to be associated with the membrane fraction of tomato fruits crude extract (Bowsher *et al.* 1992; Ferrie *et al.* 1994). It is possible, therefore, that grape VvLOXC *in vivo* is associated with a membrane fraction despite the lack of an obvious targeting peptide for such association.

A number of further experiments, which could potentially help to obtain functional soluble recombinant VvLOXC protein are discussed in Chapter 7.

6.5.1.2 Tween 20 effects *in vitro* LOX assay conditions

When performing initial experiments with recombinant LOXA-TP and LOXO-TP a number of technical issues were encountered such as pH-dependent substrate self-oxidation and substrate inhibition of LOX activities (section 6.4.1). These issues were closely studied and led to a number of observations and modifications to the standard LOX assay methods.

Autooxidation of lipids and free fatty acids is a well known process as it is one of the main causes of quality deterioration of many food products (reviewed by Frankel 1991). It is also known that autooxidation mechanisms of oils in water emulsions can be substantially different from the mechanisms determining oxidation of bulk lipids (reviewed by McClements and Decker 2000). The behaviour of lipids and free FAs in aqueous solutions is complicated and depends on factors such as FA concentration, temperature of the solution and ionisation state of carboxyl groups of free FAs (Cistola *et al.* 1988; McClements and Decker 2000; Ponginebbi *et al.* 1999). It has been shown that the addition of non-ionic detergents such as Tween 20 above CMC protects FAs

from autooxidation (Ponginebbi *et al.* 1999). It is likely that Tween 20 forms mixed micelles with free FAs, creating a protective layer at the water:FA interface thereby making the internal content of the micelle less accessible to radical attack (Ponginebbi *et al.* 1999). However, the micelle and phase formation of free FAs in aqueous solutions is further complicated by factors such as pH and temperature of the reaction (Cistola *et al.* 1988; Verhagen *et al.* 1978). For example, at pH 10, CMC value for LA is 167 μM, whereas at pH 9 and 8 formation of acid-soap dimers starts at concentrations of 60 μM and 21 μM respectively (Verhagen *et al.* 1978). Subsequently, it is expected that the rate of FA autooxidation at different pHs will vary due to amount of free FA substrate accessible to radical attack.

These findings support the observed substrate autooxidation at low pHs in the early experiments with recombinant LOXA-TP (section 6.4.2). During these experiments changes in absorbance at 234 nm were observed at pH below 7.5 even in the absence of added enzyme, indicating chemical oxidation of the FA substrate (Appendix A.4.8). Furthermore, the autooxidation rates at constant substrate concentration varied at different pH conditions with the highest rate observed at pH 5.5. An addition of non-ionic surfactant Tween 20 at a final concentration <1% prevented autooxidation across the FA concentration range investigated.

The addition of Tween 20 to LOX assays, however, not only prevented substrate autooxidation but also affected the catalytic rates of the recombinant LOXs added to reactions. For example, in the absence of detergent, the conversion rates with LOXA-TP at pH 5.5 were greatly affected by the substrate autooxidation and at LnA concentrations >300 μM were almost equal with the autooxidation rates (Figure 6.10). Dependant on the amount of Tween 20 added, the observed conversion rates were either induced or inhibited (Appendix A.4.9).

The effect of detergents on LOX activities have been previously reported by a number of authors (Schilstra *et al.* 1994; Srinivasulu and Rao 1993; Zimmerman and Snyder 1974), however the controversy exists of whether the detergents interact directly with the enzyme or indirectly, affecting the substrate availability. Supporting the later theory Galpin and Allen (1977), have shown that LOXs interact preferably with monomeric forms of FAs and suggested that all inhibition and stimulation effects observed in LOX

assays depend directly on the amount of monomeric substrate available for a LOX enzyme to act upon.

The results obtained by titrating Tween 20 in reactions with LOXA-TP at different concentrations of LnA support the later hypothesis (Appendix A.4.9). Such conclusion can also be drawn based on observations that at constant LOX enzyme concentration, increased LnA concentrations require proportionally increased Tween 20 amounts for maximal enzyme activity (Figure 6.11). Further experiments with LOXA-TP and LOXO-TP at pH 4.0-7.0 revealed that the optimum detergent:substrate ratio is also pH dependent (Figure 6.12). Specifically, the optimum detergent:substrate ratio increased in a linear fashion from pH 7.0 to pH 5.5, and at pH<5.5 the maximum activities were observed when no extra Tween 20 was added to reactions (Figure 6.12). However, it is important to take into account that Tween 20 was used in the initial substrate stock preparation and was present in all reactions at the ratio 0.000028% (w/v) Tween 20 for each 1 μM of FA substrate.

The observations above indicate the complexity of factors influencing optimal *in vitro* LOX assay conditions. The factors such as optimal detergent concentration are often overlooked when estimating basic biochemical and kinetic properties of LOX enzymes. In particular, it is clear that correct adjustment of detergent concentration is critical for assays carried out at low pH. For recombinant LOXA-TP and LOXO-TP optimal detergent:substrate ratios were determined and used in the subsequent assays. The issues surrounding the complexity of LOX assays at different experimental conditions however need to be studied in greater detail for accurate estimation of LOX properties. Some suggestions for determining optimal LOX assay conditions will be discussed in Chapter 7.

6.5.2 Functional *in vitro* characterisation of recombinant LOXA-TP and LOXO-TP

As explained earlier, VvLOXA and VvLOXO are of particular interest for the current investigation as representative members of two sub-groups of 13-LOXs (Figure 4.2), and subsequently are potential candidates involved in formation of C6 and C5 volatiles. It was important therefore to determine the detailed biochemical properties of recombinant LOXA-TP and LOXO-TP in order to predict their functionality.

6.5.2.1 LOXA-TP and LOXO-TP, two 13-LOXs with different properties

As predicted, LOXA-TP and LOXO-TP were confirmed to be 13-LOXs by HPLC analysis of their reaction products (section 6.4.5, Figure 6.16). Both recombinant proteins possessed 13-LOX activity, producing exclusively 13(S)-HPOTrE and 13(S)-HPODE from LnA and LA respectively (Figure 6.16. A, B).

Along with LnA(18:3) and LA (18:2), the two major plant PUFAs, LOXA-TP and LOXO-TP were assayed with AA (20:4) as a substrate. Although absent in plants, AA is common to micro-organisms including common plant pathogens such as pathogenic fungi and oomycetes (reviewed by Oliw 2002). It has been shown, that during pathogen infection, plant LOXs are able to metabolise pathogen derived AA, producing signalling compounds and consequently activating plant defence mechanisms (Bostock *et al.* 1992; Shewe and Nigam 1997). Several plant LOXs have been shown to be able to metabolise AA in *in vitro* biochemical experiments producing a range of FA-hydroperoxides (5(S)-, 8(S)-, 11(S)-, 12(S)- or 15(S)-HPETE) (reviewed by Shewe and Nigam 1997). The best studied higher plant LOX, soybean LOX-1, for example converts AA preferentially into 15(S)-HPETE (Oliw 2002). Similarly, Sauvignon blanc recombinant LOXA-TP and LOXO-TP converted AA exclusively into 15(S)-HPETE (Figure 6.16. C), which classifies these two enzymes as 15-LOXs with respect to AA.

Both, LOXA-TP and LOXO-TP, preferred LnA as a substrate, but their ability to metabolise LA and AA differed at their respective optimal assay conditions. The metabolic rates were also affected by changes in pH and temperature (Figure 6.15, Figure 6.13, Figure 6.14). While at optimal assay conditions, LOXA-TP was able to oxygenate LA and AA at 50% and 40% of the rates observed for LnA, the catalytic rates of LOXO-TP with LA and AA were below 10% of the rates observed with LnA (Figure 6.15). Similar substrate specificity has been observed when the closest matches of VvLOXO from Arabidopsis, AtLOX-3 and AtLOX-4, were expressed and assayed *in vitro* (Bannenberg *et al.* 2009). Furthermore, the observed LOXA-TP substrate specificity pattern was similar to the substrate specificity of AtLOX-2, the closest Arabidopsis match to VvLOXA (Bannenberg *et al.* 2009).

Although capable of producing the same reaction products, LOXA-TP and LOXO-TP exhibited significantly different kinetic properties and preferred different *in vitro* reaction conditions for maximal activity (Table 6.2).

In particular, the two enzymes reacted differently at different temperatures. Although both enzymes displayed the highest catalytic rates at 25°C, recombinant LOXO-TP protein was more tolerant to high temperatures, retaining around 20% of its maximal activity at 50°C, while at this temperature recombinant LOXA-TP protein was inactive (Figure 6.14). Furthermore, LOXO-TP was also less sensitive to low temperatures and at 10°C retained, around 70% of its maximum activity when incubated with LnA.

A similar effect of temperature has also been observed in olives, where temperatures above 25°C during malaxation resulted in a decline of both, LOX and HPL activities, and subsequently resulted in low amounts of C6 volatiles released from milled olive fruits (Sanchez and Harwood 2002).

In contrast to LOXO-TP, which preferred alkaline-to-neutral assay conditions with the maximum activities recorded at pH 7.5 (Figure 6.13.B), LOXA-TP preferred an acidic environment, being most active at pH 5.5 and completely inactive at pH 6.5 (Figure 6.13.A).

6.5.2.2 Different pH optima suggest differential subcellular localisation of VvLOXA and VvLOXO proteins

The difference in pH optimum of LOXA-TP and LOXO-TP suggests differential compartmentalisation of the corresponding native enzymes *in vivo*. Although *in silico* analysis predicts targeting of both proteins to the chloroplast (Table 6.1), the confidence score predicting a cTP for VvLOXO (RC=5) is very low, compared to VvLOXA and VvHPLA predictions (RC=3 and 2 respectively). Moreover, based on the prediction score, VvLOXO could be targeted to a compartment other than the chloroplast or mitochondrion (Table 6.1).

Another possible explanation for the different pH optima of the recombinant LOXA-TP and LOX-TP results is potential targeting of corresponding native VvLOXA and VvLOXO to different compartments within the chloroplast. For example, the normal pH of the chloroplast's stroma is around 7.5, whereas pH of the lumen has been reported to be around 5.5 under normal light conditions and as low as 3.5 pH units at high light stress conditions (Kramer *et al.* 1999). Thus, if the predicted chloroplast localisations

for VvLOXA and VvLOXO are correct, it is possible that these proteins may be targeted to the lumen and stroma of the chloroplast respectively.

Alternatively, VvLOXO might be localised to lipid-like globules mentioned earlier that are located within the plastids of grape berry pericarp (Hardie *et al.* 1996b). Structures similar to the lipid-like globules have been observed in the plastids of other plants and have been termed plastoglobules (PGs) (Austin *et al.* 2006). Plastoglobules have been long considered to be passive storage compartments. However, recently they have the focus of increased attention due to their proposed involvement in stress-related metabolic pathways (reviewed by Bréhélin and Kessler 2008). Active participation of PGs in metabolic pathways can be attributed to the action of proteins associated with the outer monolayer of polar lipids that enclose the content of the lipid globule. In Arabidopsis, for example, 34 proteins of known and unknown function have been found associated with the outer layer of the PG (Ytterberg *et al.* 2006). Four out of thirty four identified Arabidopsis PG proteins have been suggested to be involved in lipid metabolism, but specific functions of three of them have been deduced only from *in silico* analyses (Ytterberg *et al.* 2006). The fourth protein was characterised as an AOS enzyme (Laudert *et al.* 1996). In addition, Padham *et al*. (2007) identified a triacylglycerol lipase, which was found to be co-localised with plastoglobular neutral lipids.

Identification of AOS, lipase and other lipid metabolism-related enzymes suggests at least partial participation of PGs in generation of jasmonates. Although there has been no reports on identification of LOXs within the PG's proteome yet, the presence of LOXs is evident in lipid bodies of germinating cucumber seeds (Feussner and Kindl 1992; Feussner *et al.* 2001) and in lipid-like globules in cells of ripening strawberry fruit (Leone *et al.* 2006). Furthermore, lipid body-associated LOX activity has been implicated in the production of C6 volatiles in strawberry fruits (Leone *et al.* 2006) and carnation petals (Hudak and Thompson 1997), which in turn implies the involvement of HPLs capable of metabolising 13(S)-hydroperoxides.

The findings outlined above are in agreement with a suggested localisation of VvLOXO to lipid-like structures found in grape berry plastids and in grape berry seeds. These results can also potentially explain the high levels of VvLOXO transcripts found in seeds of intact grape berry. Furthermore, recombinant LOXO-TP prefers neutral and

alkaline conditions, which also fits with the reported pH optima for other lipid body LOXs (Feussner *et al.* 1996; Feussner *et al.* 2001). Finally, LOXs localised to lipid bodies also require N-terminal β-barrel peptide for correct targeting (May *et al.* 2000). This can potentially explain ambiguous results obtained as a result of transit peptide analysis (section 6.2.1).

Although the existing literature discussed above may support localisation of VvLOXO to the lipid bodies of seeds, some other results may challenge this proposed hypothesis. Particularly, biochemical experiments with LOXO-TP indicate that the preferred substrate for this enzyme is LnA, and ability to metabolise LA is 7-fold lower than LnA (Table 6.2, Figure 6.15. B). However, the LnA content in seeds of Cabernet Sauvignon has been reported to be more than 100-times lower than LA (Miele *et al.* 1993). In comparison, concentration of LnA-derived jasmonates in seeds is high and exceeds concentration of jasmonate content in pulps and skins at any time of berry development (Kondo and Fukuda 2001).

The results of this study and those reported by other authors, clearly are insufficient for a confident localisation prediction of VvLOXA and VvLOXO. Further experiments have been initiated within our research group to begin addressing this issue. Some future directions for localisation of grape LOXs and HPLs will also be discussed in Chapter 7.

6.5.2.3 Potential implication of the existence of LOXs with different properties in winemaking

The ability of LOXA-TP to retain its activity at pH as low as 4 suggests that VvLOXA might be responsible for the formation of C6 compounds in acidic conditions (pH 3.2-3.5) that are found in grape musts. Moreover, the principal localisation of *VvLOXA* transcripts in the grape berry skin suggests that the skins are the main source of VvLOXA enzyme activity in the grape must. Similarly, in musts of the white grape variety Chardonnay, skin contact has been reported to be responsible for an increase in the levels of C6 volatiles (Ferreira *et al.* 1995). Assaying LOXA-TP *in vitro* at pH 3.5 however resulted in precipitation of the recombinant LOXA-TP. The observed precipitation can be due to removal of the N-terminal peptide and incorporation of a

vector-specific peptide to facilitate IMAC purification as described in section 6.2.2. Another potential explanation of how native VvLOXA may retain its functionality in must without precipitation, may be due to its potential capability to associate with micelle-like structures present in musts after grape crushing. Further experiments with the native form of VvLOXA would be necessary to tests these hypotheses and to check if VvLOXA is the main enzyme responsible for the rapid formation of GLV-volatiles upon grape crushing.

In contrast to VvLOXA, VvLOXO is unlikely to be directly involved in the formation of GLVs in the grape must environment, mainly due to its preference for neutral-to-alkaline conditions (Figure 6.13.B). In *in vitro* experiments precipitation of LOXO-TP observed at pH<5.0 and it is unlikely to remain functional in the low-pH environment of the grape must. However, the potential participation of VvLOXO enzyme in the formation of GLVs upon crushing cannot be ruled out completely at this stage, considering the rapid accumulation of *VvLOXO* transcripts upon wounding (section 5.4.5). For instance, VvLOXO can be involved in damage signalling during the harvest, thereby increasing levels of LOXs directly responsible for production of GLVs. It is also possible that VvLOXO produces 13-hydroperoxides prior to berry disruption, thereby contributing to the total substrate pool, which becomes available to other LOXs upon crushing.

6.5.3 Characterisation of recombinant HPLAFL

Due to time constraints and difficulties associated with obtaining functional recombinant VvHPLA, mostly qualitative results were obtained with recombinant HPLAFL and no quantitative conclusions except for pH optima with 13(S)-HPOTrE can be drawn at this time.

6.5.3.1 Recombinant HPLAFL possesses 13-HPL activities and prefers LnA as a substrate

Analysis of the reaction products of recombinant HPLAFL confirmed that the putative grape 13-HPL, VvHPLA is able to metabolise 13(S)- and 15(S)-hydroperoxides into C6 and possibly C5 volatiles (Figure 6.18). HPLAFL metabolism of LA- and AA-

hydroperoxides produced the expected for these substrates reaction products, namely hexanal (Figure 6.18. B,C). However, as shown in Figure 6.18.A, when LnA-hydroperoxides were incubated with HPLAFL, the volatile content of the headspace of the reaction contained typical for 13-HPLs (*Z*)-3-hexenal and (*E*)-2-hexenal as well as a number of other compounds. Preliminary matching of these later compounds against available libraries tentatively identified them as 2-methyl-4 pentanal, (*E*)-2-hexenal and two peaks corresponding to 2(*E*), 4(*E*)-hexadienal. However, a more detailed analysis involving authentic standards of these compounds would be required to confirm the identity of unknown peaks. To unambiguously identify the compounds, a more detailed analysis involving comparison of retention time and mass spectra of the authentic standards will be required.

Another interesting observation was the presence of a peak corresponding to hexanal in samples where LA- and AA-hydroperoxides where incubated in the absence of HPLAFL (Appendices A.4.11 and A.4.12). In comparison, in reactions containing LnA-hydroperoxides, only volatile buffer constituents were observed in the absence of the enzyme (Appendix A.4.10). The most likely explanation for the observed phenomenon is that LA- and AA-hydroperoxides can be metabolised to hexanal spontaneously at low rate.

As discussed in section 6.4.8, the major products of HPLAFL-catalysed metabolism of LnA-hydroperoxide were (*Z*)-3-hexenal and (*E*)-2-hexenal . It is known, that (*Z*)-3-hexenal is an unstable compound and isomerises rapidly to (*E*)-2-hexenal or reduced to (*Z*)-3-hexenol by the action of alcohol dehydrogenase (ADH) (Matsui 2006). This therefore suggests that (*Z*)-3-hexenal is the primary product of HPLAFL metabolism, and formation of (*E*)-2-hexenal is likely to occur as a result of spontaneous isomerisation of (*Z*)-3-hexenal.

Interestingly, (*E*)-2-hexenal has been reported as the major C6 volatile aldehyde in grape musts with (*Z*)-3-hexenal proving to be undetectable (Ferreira *et al.* 1995; Iyer *et al.* 2010). These reports suggest that the conversion of (*Z*)-3-hexenal into (*E*)-2-hexenal in crushed grapes is much quicker than in the *in vitro* experiments with HPLAFL and possibly requires action of alkenal isomerase as discussed in section 2.5.2.4.

The volatile content of aldehydes released from berries of red grape varieties during their development also contains predominantly (*E*)-2-hexenal and excludes (*Z*)-3-

hexenal (Kalua and Boss 2009; Salinas *et al.* 2004). Furthermore, in intact berries during development, as well as in crushed berries, amounts of (*E*)-2-hexenal always exceeded amounts of hexanal (Iyer *et al.* 2010; Kalua and Boss 2009).

The higher abundance of (*E*)-2-hexenal over hexanal can be explained by a higher concentration of LnA compared to LA. Alternatively, the higher (*E*)-2-hexenal amount can be attributed to the preference of LOX and HPL enzymes to LnA and LnA-hydroperoxides respectively. The latter hypothesis is supported by the observed preference of recombinant VvLOXA and VvLOXO towards LnA and VvHPLA towards LnA-hydroperoxides, as discussed earlier.

6.5.3.2 Recombinant HPLAFL prefers acidic conditions for its maximum activity with LnA-hydroperoxides

Preliminary experiments with the recombinant HPLAFL and LnA-hydroperoxide revealed that the enzyme remains active across a wide range of pH, but prefers acidic conditions with pH optimum of 5.0 (Figure 6.17). To date, such a low pH optimum has only been reported for the recombinant tomato HPL (LeHPL) with LnA-hydroperoxide as a substrate (Atwal *et al.* 2005). At the same time, pH optimum of the recombinant LeHPL with LA-hydroperoxide was around 7.0 (Atwal *et al.* 2005). It is worth noting however, that even at pH 5.0, the activity of LeHPL with LnA-hydroperoxides was only around 1% of its activity with LA-hydroperoxides at the same pH conditions (Atwal *et al.* 2005). In comparison, pH optima of other plant HPLs preferring LnA-hydroperoxides as substrate are higher than pH 5.0. Specifically, bell pepper HPL has been reported to have an optimum of pH 5.5 (Shibata *et al.* 1995), sugarbeet - pH 6.7 (Rabetafika *et al.* 2008) and Arabidopsis - pH 7.2 from (Kandzia *et al.* 2003).

Low pH optimum of VvHPLA suggests its potential involvement, along with VvLOXA, in the formation of C6 volatiles in acidic conditions of grape must. Furthermore, the subcellular localisation of VvHPLA proteins in grape berries can be similar to that of VvLOXA, with VvHPLA likely to be localised in subcellular compartments with an acidic environment such as the lumen of the chloroplast. In potato leaves and in leaves of *M. trancatula,* for instance, 13-HPLs have been found associated with thylakoid membranes of chloroplasts (De Domenico *et al.* 2007; Farmaki *et al.* 2007).

In vivo association of VvHPLA with membranes is further supported by the observed increased HPL activity in the "membrane" fraction of *E. coli* expression cultures (described in section 6.3.5). Further analysis of the amino acid sequence of VvHPLA identifies a predicted transmembrane region, also supporting a membrane association. It is likely, that association with a membrane is required for a conformational activation of VvHPLA enzyme as has been suggested by Hughes *et al.* (2009) for other plant HPLs.

It is clear from the above observations that VvHPLA is a likely candidate involved in the formation of C6 and possibly C5 volatiles in grape berries *in vivo* as well as in grape must upon crushing. Certain results, such as pH optimum of the recombinant HPLAFL, indicate that the native VvHPLA possesses unique properties, that have not been reported for this type of enzymes to date. These preliminary results point out directions for a future characterisation of VvHPLA, which will be discussed in Chapter 7.

Chapter 7
Final conclusions and future research

The current work was initiated in 2006 as part of the Sauvignon Blanc Programme. The ultimate goal of the Sauvignon Blanc Programme was to identify flavour and aroma compounds that determine the unique properties of New Zealand Sauvignon blanc wine. One of the main objectives of the Programme was the delineation of the biochemical processes leading to the formation of important aroma compounds, volatile thiols, and studying of the processes affecting the levels of volatile thiols in wine. Based on the existing knowledge, it was hypothesised that the precursors of volatile thiols are formed in grape berries as a result of glutathionation of either straight-chain or branched-chain C6 and C5 aliphatic compounds. The analysis of the grape metabolome suggested that the C6 (and possibly C5) aliphatic compounds most likely to be formed as a result of the enzymatic degradation of polyunsaturated fatty acids (PUFAs) via green leaf volatile (GLV) pathway. Further literature research revealed that GLVs may themselves affect flavour and aroma of grape juices and wines. Subsequently, this project was set up to study the GLV biochemical pathway in Sauvignon blanc grape berries as a potential contributor of GLVs on wine quality and as a likely source of C6 and C5 precursors of volatile thiols. At the same time, another project was initiated to study glutathionation of the C6 and C5 compounds.

Although it is generally accepted that the GLV pathway is a major source of aliphatic volatile compounds in plants, there has been no identification or functional characterisation studies reported to date characterising the pathway and its individual members in the grapevine.

This thesis describes and discusses the results of identification and initial characterisation of lipoxygenase (LOX) and hydroperoxide lyase (HPL) members of the GLV pathway in grape berries with the focus on those members potentially involved in the formation of C6 and C5 compounds. In addition, identification and an initial characterisation was attempted for grape LOXs and HPLs potentially involved in the formation of C9 compounds, which also contribute to flavour and aroma of wines.

The outcome of this research, however, has a much greater application than the contribution of the GLV pathway to wine aroma alone. As reviewed in Chapter 2, LOX and HPL members of the GLV pathway are involved in many important developmental and stress-response processes in grapes and other plant species. Accumulation of GLVs occurs in response to herbivore feeding, wounding or pathogen attack. GLVs serve as signalling molecules in plant-plant, plant-pathogen and plant-herbivore communications; activate plant local and systemic responses to both biotic and abiotic stresses. GLVs also possess antimicrobial properties and their accumulation inhibits the pathogen growth during the earlier stages of the infection. In addition, the by-product of the GLV production, the wound hormone traumatin, is involved in callus growth and wound healing of damaged plants.

Furthermore, as mentioned in section 2.4.6, the GLV-pathway represents only one of the few possible branches of the LOX pathway. Another branch of the LOX pathway, namely the AOS pathway, is often activated by the same stress stimuli as the GLV pathway and produces a range of important phytohormones, known as jasmonates. Aside from being important stress-related hormones, jasmonates are also involved in plant growth and development.

The GLV and AOS pathways are very similar in terms of the participating enzymes and in the way they metabolise PUFAs. For the reasons mentioned above, the results presented in this thesis are often discussed in a context of the potential involvement of either of the two pathways in the processes studied.

The subsequent section will summarise the key findings and discuss the potential future direction for the research.

<u>The key objectives of this work were:</u>

- To identify LOX and HPL gene members in the grape genome.
- To study gene expression of Sauvignon blanc grape berry expressed LOXs and HPLs.
- To study biochemical properties of selected recombinant LOX and HPL proteins.

7.1 Identification of LOX and HPL genes in grape genome

7.1.1 Key findings

This research reveals the complexity of the genetic makeup of the GLV metabolic pathway in grapes. 18 LOX genes and 6 HPL genes were identified in the Pinot noir grape genome. Phylogenetic analysis of the identified grape LOXs classifies them as members of two groups, type II 13-LOXs and 9-LOXs. Phylogenetic analysis of the identified grape HPLs classifies them as 13-HPLs (CYP-74B) and 9/13-HPLs (CYP-74C). The identified LOX and HPL genes were mapped to the predicted grape chromosomes.

7.1.2 Future work

The existing genomic sequence information can be used further for identification of members and predicting functions of biochemical pathways including the GLV pathway. For example, genomic regions corresponding to the promoters of LOX and HPL genes can be analysed in order to predict their roles and identify transcription factors responsible for expression of these genes.

The data used in this work was obtained from the homozygous Pinot noir line, a genotype that is not used in commercial viticulture. Sequencing of genomes from commercially grown grapevine clones will potentially identify additional members of LOX and HPL families. Availability of massively parallel sequencing platforms such as Illumina® (Illumina, Inc.), 454 pyrosequencing (454 Life Sciences) and SOLiD™ (Applied Biosystems) allows cost effective re-sequencing and *de novo* sequencing of whole genomes. Re-sequencing may also potentially identify sequence variation amongst the genes identified here, which may explain phenotypic variation in the GLV profiling of different varietals.

7.2 Study of gene expression of Sauvignon blanc berry expressed LOX and HPL genes

7.2.1 Key findings

Several LOX and HPL genes have been found to be expressed at different levels in Sauvignon blanc berries. Four LOX genes (*VvLOXA*, *C*, *D* and *O*) and one HPL gene (*VvHPLA*) were selected for gene expression studies as representative members of the major phylogenetic groups identified for grape LOX and HPL families respectively. DNA fragments corresponding to the full-length coding sequences of Sauvignon blanc *VvLOXA*, *C*, *O* and *VvHPLA*, and a partial DNA fragment corresponding to almost full-length coding sequence of *VvLOXD* were isolated from the berry transcript pool and cloned.

A study of selected LOX and HPL gene expression revealed different levels of basal expression and differential tissue distribution of individual LOX and HPL genes within the berry. The studied genes also displayed different patterns of expression across various stages of berry development, upon wounding and in berries infected with *Botrytis cinerea*. Amongst the four LOX gene studied, transcripts of *VvLOXA* were the most abundant at all stages during berry development. *VvLOXO* was induced transiently upon berry piercing and is a clear candidate involved in berry response to wounding. Expression levels of *VvLOXC* and *VvLOXO* in berries infected with *Botrytis cinerea* were significantly increased compared to uninfected berries.

7.2.2 Future work

Gene expression studies presented in this thesis were the first step in characterisation of multiple members involved in the GLV pathway and other branches of the LOX pathway. Due to the large number of LOX and HPL genes expressed in the Sauvignon blanc berries, characterisation of all members was beyond the resources and timeline allocated for this project. Therefore, only 4 LOX genes and 1 HPL gene, representative of major phylogenetic groups for these gene families, were used in the gene expression studies in this work. It is important to continue to study the gene expression of other LOX and HPL genes expressed in grape berry but not included in this study. Further work also needs to be done to determine the expression patterns of LOX and HPL genes in other grape organs such as leaves, stems, roots and flowers.

Further attempts are required to determine the full-length sequence of *VvLOXD* and other grape LOX genes, sequence of which could not be retrieved from the genome sequence. This can be achieved using techniques different from the described here 5 - RACE in combination with modification to the existing cDNA preparation in order to improve reverse-transcription efficiency and obtain full-length template. Alternatively, molecular techniques such as genome walking could be employed to obtain the unknown 5′ genomic regions of the incomplete genes.

Sequence variation in the coding sequence of *VvLOXA* transcripts (described in section 5.3) can also be further explored. As mentioned in section 5.3, six protein expression constructs containing coding sequences of representative *VvLOXA* variants have been prepared and can be further analysed to compare their biochemical properties.

The current research raised an important question about localisation of transcripts of individual LOX and HPL genes within grape berry. The experiments comparing LOX and HPL gene expression levels in three different tissues of grape berry indicated that some LOXs might preferentially be expressed in specific tissue types (see section 5.4.4). This should be taken into account in further gene expression experiments.

To better understand LOX and HPL transcript distribution within grape berry, *in situ* hybridisation using RNA-labelled probes can be employed. Furthermore, to detect localisation of the corresponding LOX and HPL proteins within the berry, immunohistochemsitry can be used using antibodies specific to an individual protein of interest, or to a group of closely related proteins. To get further insights into *in vivo* functions of LOXs and HPLs, the subcellular localisation studies of LOX and HPL proteins are essential. To address the question of subcellular localisation of a particular LOX or HPL protein, fluorescent reporter genes such as green fluorescent protein (GFP) can be attached to the C-terminus of the protein of interest. This can be done by creating a GFP-fusion construct, in which coding sequence of the gene is cloned in frame and upstream of the sequence encoding GFP. The GFP fusion can be then expressed transiently in the plant and localisation of the fused protein can be detected using confocal microscopy. This technique has proven to be efficient for determining subcellular localisation of LOXs and HPLs from other plant species (Chen *et al.* 2004; Farmaki *et al.* 2007; Mita *et al.* 2005).

In section 5.5.5 a question about possible diurnal regulation of expression of some LOX and HPL genes was raised. To date, there is no clear evidence that LOX and HPL genes follow strict diurnal patterns of expression. Therefore, experiments addressing this question should be performed. For example, berry samples could be collected at frequent (2-3 hours) time intervals in normal field conditions and gene expression of various LOX and HPL genes evaluated. It is also important to conduct this experiment on berries of at least three different developmental stages.

As discussed in section 5.5.5, it is likely that non-ionic detergents such as Tween 20 and Triton X-100 are able to induce gene expression of some LOXs in the manner similar to MeJA induction. This is a potentially interesting area of research with possible practical applications in viticulture. Exogenous MeJA application to other plants has been shown to induce plant's systemic resistance to herbivores (McConn *et al.* 1997), pathogens (Vijayan *et al.* 1998), increase shelf life of fruits by inducing resistance against pathogen and chilling injury (González-Aguilar *et al.* 2003; Zhang *et al.* 2006b). Furthermore, the activation of defence-related genes can potentially change composition of flavour and aroma compounds in grapes, and subsequently may affect flavour and aroma of wines produced from these grapes. With a cost of production of non-ionic detergents being only a fraction of the price of MeJA or JA, the detergents can become a cost-effective substitution of jasmonates in some applications. Important consideration in experiments with non-ionic detergents are their potential impact on the surrounding environment and food quality of grapes. These should be carefully evaluated and only safe biodegradable compounds selected.

This work revealed that representative members of type II 13-LOX sub-clades (namely VvLOXA and VvLOXO) despite producing the same reaction products, have different gene expression patterns during development as well as upon wounding and pathogen infection. *VvLOXA* and *VvLOXO* also have differential spatial transcript distribution within the berry and differ significantly in relative levels of transcript abundance in the intact berry. As was suggested earlier, it is likely that these two LOX genes direct fatty acid metabolism into separate fluxes of the LOX pathway such as HPL and AOS branches. To test this hypothesis a number of experiments can be performed. As an initial experiment, changes in gene expression can be related to changes in the emission of volatile compounds to a particular elicitor, for example wounding. A more complex study would involve measuring volatile profiles in mutant plants, impaired in

expression of either HPL or AOS genes. This approach however may be complicated with respect to HPL expression as more than one HPL gene have been found to be expressed in grape berry.

7.3 Biochemical characterisation of recombinant grape LOXs and HPLs

7.3.1 Key findings

In vitro biochemical analysis of the reaction products of recombinant VvLOXA and VvLOXO confirmed that these two enzymes are 13-LOXs. Both enzymes preferred α-linolenic acid (LnA) as substrate. Both enzymes had the same temperature optima of 25°C, but preferred different pH conditions. Recombinant VvLOXA preferred an acidic environment and had pH optimum of pH 5.5, while VvLOXO preferred neutral-to-basic conditions and had pH optimum of pH 7.5.

Preliminary experiments with recombinant VvHPLA confirmed the ability of this enzyme to metabolise 13(S)-hydroperoxides, releasing C6 volatile aldehydes. Recombinant VvHPLA exhibited maximum activity with 13(S)-hydroperoxides of LnA as substrate at pH 5.0.

7.3.2 Future work

As described in section 6.4.1, LOX assays with the recombinant LOXA-TP (truncated version of VvLOXA) revealed significant effects of low pH conditions on FA substrate stability and LOXA-TP activity. A number of experiments conducted here suggested that the observed effect is most likely attributed to substrate availability at pHs below pH 7.5. To overcome the issue of substrate availability, optimal detergent:substrate ratio was determined for LOXA-TP at pH 5.5. However, the ratio determined at pH 5.5 was not optimal at other pH conditions. These findings indicate that behaviour of FA substrate at different pH conditions is complex and requires further investigation. The determination of the optimal LOX assay conditions is particularly important for enzymes operating at low pH conditions such as VvLOXA. A series of experiments should be set up to determine optimal detergent:substrate ratio at various pHs, different types of substrates and substrate concentrations and at various operating temperatures. The results should be carefully analysed in order to determine parameters which could be used in further LOX assays at these conditions. The experiments should be performed using a number of different LOX enzymes in order to validate results.

Further work needs to be done in order to obtain soluble functional VvLOXC protein and determine its biochemical properties. In order to increase the solubility and functionality of VvLOXC, an expression construct may be created, in which VvLOXC coding sequence is fused to highly soluble fusion tags such as NusA-tag or GST-tag. Alternatively, recombinant VvLOXC protein can be purified from inclusion bodies and refolded. Furthermore, VvLOXC can also be transiently expressed in and subsequently purified from a plant host such as *Nicotiana benthamiana* (Sheludko *et al.* 2007).

Partial purification of the recombinant VvHPLA protein has been achieved in this work and some biochemical properties have been determined for this enzyme (see sections 6.4.6-6.4.8). However, further experiments are required in order to improve the isolation and purification of this and other HPL enzymes. Initially, the length of the predicted chloroplast targeting peptide (cTP) should be reviewed, and alternative truncated points should be selected for removing the cTP. However, as discussed in section 6.5.3.2, it is possible that the presence of the cTP is essential for VvHPLA in order to be catalytically active. In this case, the efforts should be focused on the improvement of the purification of VvHPLA using detergents as described in this work. For example, Triton X-100 detergent used here for purification of "membrane" VvHPLA fraction can be substituted with Emulphogene detergent, which has been found to be highly efficient according to Hughes et al. (2006). In addition, a transient expression in a plant host can be employed as suggested for expression of VvLOXC.

Other identified grape LOXs and HPLs require biochemical characterisation in the way similar to the methods described in this work. Particular interest for the further characterisation of the GLV pathway in grapes represents a group of identified closely related putative 9/13-HPLs (see section 4.4.2). For example, the predicted sequence variation in important functional residues of highly similar VvHPLB and VvHPLC may potentially result in significant difference in the substrate and product specificity of these two closely related enzymes. This and other important question need to be addressed in order to fully characterise the GLV pathway in grapes.

7.4 Concluding remarks

The current work is the first extensive investigation of the GLV pathway biochemical in the grapevine at the molecular level. This work set the ground for a number of potentially interesting areas of basic science and applied research related to the production of GLVs and other important LOX-related compounds.

The existence of large LOX and HPL gene families, which are involved in the formation of GLVs in grapes suggests the complexity of the GLV biochemical pathway and potential intricacy of its regulation. To determine the functional roles of each enzyme in the pathway, detailed characterisation of each member, as well as interactions between the members, will be required. This is particularly important in relation to the LOX enzymes. As previously discussed, only some grape LOXs will take part in the GLV pathway, while others will participate in other LOX pathway branches such as AOS and DES pathways. This work identifies only one member of AOS and no DES members in the grape genome. It would be beneficial therefore to include the grape AOS into the future studies, providing much wider scope on the PUFA metabolism via the LOX pathway in the grapevine.

The current work used gene expression studies as an indicator of the functional role that each of the LOX or HPL enzymes may be fulfilling *in vivo*. The next steps in the functional characterisation of each member would require detailed protein expression studies, analysis of the reaction products and using genetic tools in order to alter expression levels of each gene (protein).

The extensive knowledge about the functional properties of each enzyme and the pathway as a whole will help to establish the genotype-environment interactions that drive the expression of phenotypic traits. The ability to regulate the expression of phenotypic traits, such as chemical composition of grapes or resistance of vines to pathogens, is the ultimate goal of the modern day viticulture.

This work will add significantly to the body of knowledge about molecular aspects of the grapevine physiology and to the overall knowledge of the GLV pathway in plants. The obtained knowledge can also be applied for developing viticultural tools to aid winegrowers and winemakers to produce grapes and wines of the desired quality.

References

Agrawal GK, Tamogami S, Han O, Iwahashi H, Rakwal R. (2004). Rice octadecanoid pathway. *Biochemical and Biophysical Research Communications,* **317**(1), 1-15.

Allen MS, Lacey MJ. (1999). Methoxypyrazines of grapes and wines. In *Chemistry of Wine Flavour* (pp. 31-38): American Chemical Society.

Andreou A, Brodhun F, Feussner I. (2009). Biosynthesis of oxylipins in non-mammals. *Progress in Lipid Research,* **48**(3-4), 148-170.

Angerosa F, Mostallino R, Basti C, Vito R. (2000). Virgin olive oil odour notes: Their relationships with volatile compounds from the lipoxygenase pathway and secoiridoid compounds. *Food Chemistry,* **68**(3), 283-287.

Atwal AS, Bisakowski B, Richard S, Robert N, Lee B. (2005). Cloning and secretion of tomato hydroperoxide lyase in *Pichia pastoris*. *Process Biochemistry,* **40**(1), 95-102.

Austin JR, II, Frost E, Vidi P-A, Kessler F, Staehelin LA. (2006). Plastoglobules are lipoprotein subcompartments of the chloroplast that are permanently coupled to thylakoid membranes and contain biosynthetic enzymes. *Plant Cell*, 1693-1703.

Axelrod B, Cheesborough TM, Laakso S. (1981). Lipoxygenase from soybean. *Methods Enzymol.,* **71**, 441-451.

Bannenberg G, Martínez M, Hamberg M, Castresana C. (2009). Diversity of the enzymatic activity in the lipoxygenase gene family of *Arabidopsis thaliana*. *Lipids*.

Bate NJ, Sivasankar S, Moxon C, Riley JMC, Thompson JE, Rothstein SJ. (1998). Molecular characterization of an Arabidopsis gene encoding hydroperoxide lyase, a cytochrome P-450 that is wound inducible. *Plant Physiol.,* **117**(4), 1393-1400.

Bauman JA, Gallander JF, Peng AC. (1977). Effect of maturation on the lipid content of Concord grapes. *Am. J. Enol. Vitic.,* **28**(4), 241-244.

Baumes R, Bayonove C, Barillère JM, Escudier JL, Cordonnier R. (1988). La macération pelliculaire dans la vinification en blanc. Incidence sur la composante volatile des moûts *Connaissance de la Vigne et du Vin,* **32**(3), 209–223.

Baysal T, Demirdöven A. (2007). Lipoxygenase in fruits and vegetables: A review. *Enzyme and Microbial Technology,* **40**(4), 491-496.

Bell E, Creelman RA, Mullet JE. (1995). A chloroplast lipoxygenase is required for wound-induced jasmonic acid accumulation in Arabidopsis. *Proceedings of the National Academy of Sciences of the United States of America,* **92**(19), 8675-8679.

Bell E, Mullet JE. (1993). Characterization of an Arabidopsis lipoxygenase gene responsive to methyl jasmonate and wounding. *Plant Physiology,* **103**(4), 1133-1137.

Berna AZ, Trowell S, Clifford D, Cynkar W, Cozzolino D. (2009). Geographical origin of Sauvignon blanc wines predicted by mass spectrometry and metal oxide based electronic nose. *Analytica Chimica Acta,* **648**(2), 146-152.

Blee E. (2002). Impact of phyto-oxylipins in plant defense. *Trends in Plant Science,* **7**(7), 315-322.

Blée E. (1998). Phytooxylipins and plant defense reactions. *Progress in Lipid Research,* **37**(1), 33-72.

Bonner J, English J, Jr. (1938). A chemical and physiological study of traumatin, a plant wound hormone. *Plant Physiol.,* **13**(2), 331-348.

Bostock RM, Yamamoto H, Choi D, Ricker KE, Ward BL. (1992). Rapid stimulation of 5-lipoxygenase activity in potato by the fungal elicitor arachidonic acid. *Plant Physiol.,* **100**(3), 1448-1456.

Bowsher CG, Ferrie BJM, Ghosh S, Todd J, Thompson JE, Rothstein SJ. (1992). Purification and partial characterization of a membrane-associated lipoxygenase in tomato fruit. *Plant Physiol.,* **100**(4), 1802-1807.

Bramley RGV. (2005). Understanding variability in winegrape production systems 2. Within vineyard variation in quality over several vintages. *Australian Journal of Grape and Wine Research,* **11**(1), 33-42.

Brash AR. (2009). Mechanistic aspects of CYP74 allene oxide synthases and related cytochrome P450 enzymes. *Phytochemistry,* **70**(13-14), 1522-1531.

Bréhélin C, Kessler F. (2008). The plastoglobule: A bag full of lipid biochemistry tricks. *Photochemistry and Photobiology,* **84**(6), 1388-1394.

Buonaurio R, Servili M. (1999). Involvement of lipoxygenase, lipoxygenase pathway volatiles, and lipid peroxidation during the hypersensitive reaction of pepper leaves to *Xanthomonas campestris* pv. *vesicatoria*. *Physiological and Molecular Plant Pathology,* **54**(5-6), 155-169.

Chehab EW, Raman G, Walley JW, Perea JV, Banu G, Theg S*, et al.* (2006). Rice hydroperoxide lyases with unique expression patterns generate distinct aldehyde signatures in Arabidopsis. *Plant Physiol.,* **141**(1), 121-134.

Chen G, Hackett R, Walker D, Taylor A, Lin Z, Grierson D. (2004). Identification of a specific isoform of tomato lipoxygenase (TomLoxC) involved in the generation of fatty acid-derived flavor compounds. *Plant Physiology,* **136**(1), 2641-2651.

Cheng Q, Zhang B, Zhuge Q, Zeng Y, Wang M, Huang M. (2006). Expression profiles of two novel lipoxygenase genes in *Populus deltoides*. *Plant Science,* **170**(6), 1027-1035.

Chong J, Le Henanff G, Bertsch C, Walter B. (2008). Identification, expression analysis and characterization of defense and signaling genes in *Vitis vinifera*. *Plant Physiology and Biochemistry,* **46**(4), 469-481.

Cistola DP, Hamilton JA, Jackson D, Small DM. (1988). Ionization and phase behavior of fatty acids in water: application of the Gibbs phase rule. *Biochemistry,* **27**(6), 1881-1888.

Clarke RJ, Bakker J. (2004). *Wine flavour chemistry*. Oxford, UK: Blackwell Pub.

Coffa G, Brash AR. (2004). A single active site residue directs oxygenation stereospecificity in lipoxygenases: Stereocontrol is linked to the position of oxygenation. *Proceedings of the National Academy of Sciences of the United States of America,* **101**(44), 15579-15584.

Coombe BG. (1992). Research on development and ripening of the grape berry. *American Journal of Enology and Viticulture,* **43**(1), 101-110.

Croft KPC, Juttner F, Slusarenko AJ. (1993). Volatile products of the lipoxygenase pathway evolved from *Phaseolus vulgaris* (L.) leaves inoculated with *Pseudomonas syringae* pv *phaseolicola*. *Plant Physiol.,* **101**(1), 13-24.

da Silva FG, Iandolino A, Al-Kayal F, Bohlmann MC, Cushman MA, Lim H*, et al.* (2005). Characterizing the grape transcriptome. Analysis of expressed sequence tags from multiple Vitis species and development of a compendium of gene expression during berry development. *Plant Physiology,* **139**(2), 574-597.

Darriet P. (1993). *L'arôme et Les Précurseurs d'Arôme du Sauvignon*. Unpublished Thèse de Doctorat, Université de Bordeaux II.

Darriet P, Lavigne V, Dubourdieu D. (1991). Caractérisation de l'arôme variétal des vins de Sauvignon par couplage CPG-Olfactométrie. *J. Int. Sci. Vigne Vin,* **25**(3), 167-174.

Darriet P, Tominaga T, Demole E, Dubourdieu D. (1993). Mise en évidence dans le raisin de *Vitis vinifera* (var. Sauvignon) d'un précurseur de la 4-mercapto-4-methylpentan-2-one. *C. R. Acad. Sci. Paris, Biol. Pathol. végétale,* **1993**(316), 1332-1335.

De Domenico S, Tsesmetzis N, Di Sansebastiano G, Hughes R, Casey R, Santino A. (2007). Subcellular localisation of *Medicago truncatula* 9/13-hydroperoxide lyase reveals a new localisation pattern and activation mechanism for CYP74C enzymes. *BMC Plant Biology,* **7**(1), 58.

Deluc L, Quilici D, Decendit A, Grimplet J, Wheatley M, Schlauch K*, et al.* (2009). Water deficit alters differentially metabolic pathways affecting important flavor and quality traits in grape berries of Cabernet Sauvignon and Chardonnay. *BMC Genomics,* **10**(1), 212.

Duan H, Huang MY, Palacio K, Schuler MA. (2005). Variations in CYP74B2 (hydroperoxide lyase) gene expression differentially affect hexenal signaling in the Columbia and Landsberg erecta ecotypes of Arabidopsis. *Plant physiology.,* **139**(3), 1529-1544.

Dyrlov Bendtsen J, Nielsen H, von Heijne G, Brunak S. (2004). Improved prediction of signal peptides: SignalP 3.0. *Journal of Molecular Biology,* **340**(4), 783-795.

Emanuelsson O, Brunak S, von Heijne G, Nielsen H. (2007). Locating proteins in the cell using TargetP, SignalP and related tools. *Nat. Protocols,* **2**(4), 953-971.

Emanuelsson O, Nielsen H, von Heijne G. (1999). ChloroP, a neural network-based method for predicting chloroplast transit peptides and their cleavage sites. *Protein Sci,* **8**(5), 978-984.

Farmaki T, Sanmartin M, Jimenez P, Paneque M, Sanz C, Vancanneyt G*, et al.* (2007). Differential distribution of the lipoxygenase pathway enzymes within potato chloroplasts. *J. Exp. Bot.*, erl230.

Felsenstein J. (1985). Confidence limits on phylogenies: An approach using the bootstrap. *Evolution,* **39**(4), 783-791.

Ferreira B, Hory C, Bard MH, Taisant C, Olsson A, Le Fur Y. (1995). Effects of skin contact and settling on the level of the C18:2, C18:3 fatty acids and C6 compounds in burgundy chardonnay musts and wines. *Food Quality and Preference,* **6**(1), 35-41.

Ferrie BJ, Beaudoin N, Burkhart W, Bowsher CG, Rothstein SJ. (1994). The cloning of two tomato lipoxygenase genes and their differential expression during fruit ripening. *Plant Physiol.,* **106**(1), 109-118.

Feussner I, Hause B, Nellen A, Wasternack C, Kindl H. (1996). Lipid-body lipoxygenase is expressed in cotyledons during germination prior to other lipoxygenase forms. *Planta,* **198**(2), 288-293.

Feussner I, Kindl H. (1992). A lipoxygenase is the main lipid body protein in cucumber and soybean cotyledons during the stage of triglyceride mobilization. *FEBS Letters,* **298**(2-3), 223-225.

Feussner I, Kuhn H, Wasternack C. (2001). Lipoxygenase-dependent degradation of storage lipids. *Trends in Plant Science,* **6**(6), 268-273.

Feussner I, Wasternack C. (2002). The lipoxygenase pathway. *Annual Review of Plant Biology,* **53**, 275-297.

Frankel EN. (1991). Review. Recent advances in lipid oxidation. *Journal of the Science of Food and Agriculture,* **54**(4), 495-511.

Froehlich JE, Itoh A, Howe GA. (2001). Tomato allene oxide synthase and fatty acid hydroperoxide lyase, two cytochrome p450s involved in oxylipin metabolism, are targeted to different membranes of chloroplast envelope. *Plant Physiol.,* **125**(1), 306-317.

Gallander JF, Peng AC. (1980). Lipid and fatty acid compositions of different grape types. *Am. J. Enol. Vitic.,* **31**(1), 24-27.

Galpin JR, Allen JC. (1977). The influence of micelle formation on lipoxygenase kinetics. *Biochimica et Biophysica Acta (BBA) - Lipids and Lipid Metabolism,* **488**(3), 392-401.

Gao X, Stumpe M, Feussner I, Kolomiets M. (2008). A novel plastidial lipoxygenase of maize (*Zea mays*) ZmLOX6 encodes for a fatty acid hydroperoxide lyase and is uniquely regulated by phytohormones and pathogen infection. *Planta,* **227**(2), 491-503.

Gardner H. (1998). 9-Hydroxy-traumatin, a new metabolite of the lipoxygenase pathway. *Lipids,* **33**(8), 745-749.

Gardner HW. (1989). Soybean lipoxygenase-1 enzymically forms both (9S)- and (13S)-hydroperoxides from linoleic acid by a pH-dependent mechanism. *Biochimica et Biophysica Acta - Lipids and Lipid Metabolism,* **1001**(3), 274-281.

Gardner HW. (1991). Recent investigations into the lipoxygenase pathway of plants. *Biochimica et Biophysica Acta - Lipids and Lipid Metabolism,* **1084**(3), 221-239.

Gardner HW. (1995). Biological roles and biochemistry of the lipoxygenase pathway. *Hortscience,* **30**(2), 197-205. Article.

Gardner HW, Grove MJ. (1998). Soybean lipoxygenase-1 oxidizes 3Z-nonenal: a route to 4S-hydroperoxy-2E-nonenal and related products. *Plant Physiology,* **116**(4), 1359-1366.

Gardner HW, Grove MJ, Salch YP. (1996). Enzymic Pathway to Ethyl Vinyl Ketone and 2-Pentenal in Soybean Preparations. *Journal of Agricultural and Food Chemistry,* **44**(3), 882-886.

Gardner HW, Hamberg M. (1993). Oxygenation of (3Z)-nonenal to (2E)-4-hydroxy-2-nonenal in the broad bean (Vicia faba L.). *Journal of Biological Chemistry,* **268**(10), 6971-6977.

Glauser G, Dubugnon L, Mousavi SAR, Rudaz S, Wolfender J-L, Farmer EE. (2009). Velocity estimates for signal propagation leading to systemic jasmonic acid accumulation in wounded Arabidopsis. *Journal of Biological Chemistry,* **284**(50), 34506-34513.

Göbel C, Feussner I, Hamberg M, Rosahl S. (2002). Oxylipin profiling in pathogen-infected potato leaves. *Biochimica et Biophysica Acta (BBA) - Molecular and Cell Biology of Lipids,* **1584**(1), 55-64.

Göbel C, Feussner I, Rosahl S. (2003). Lipid peroxidation during the hypersensitive response in potato in the absence of 9-lipoxygenases. *The Journal of Biological Chemistry,* **278**(52), 52834-52840.

González-Aguilar GA, Buta JG, Wang CY. (2003). Methyl jasmonate and modified atmosphere packaging (MAP) reduce decay and maintain postharvest quality of papaya 'Sunrise'. *Postharvest Biology and Technology,* **28**(3), 361-370.

Grechkin AN. (1998). Recent developments in biochemistry of the plant lipoxygenase pathway. *Progress in Lipid Research,* **37**(5), 317-352.

Grechkin AN, Bruhlmann F, Mukhtarova LS, Gogolev YV, Hamberg M. (2006). Hydroperoxide lyases (CYP74C and CYP74B) catalyze the homolytic isomerization of fatty acid hydroperoxides into hemiacetals. *Biochimica et Biophysica Acta (BBA) - Molecular and Cell Biology of Lipids,* **1761**(12), 1419-1428

Grechkin AN, Kuramshin RA, Latypov SK, Safonova YY, Gafarova TE, Ilyasov AV. (1991). Hydroperoxides of α-ketols. Novel products of the plant lipoxygenase pathway. *European Journal of Biochemistry,* **199**(2), 451-457.

Griffiths A, Barry C, Alpuche-Solis A, Grierson D. (1999a). Ethylene and developmental signals regulate expression of lipoxygenase genes during tomato fruit ripening. *J. Exp. Bot.,* **50**(335), 793-798.

Griffiths A, Prestage S, Linforth R, Zhang J, Taylor A, Grierson D. (1999b). Fruit-specific lipoxygenase suppression in antisense-transgenic tomatoes. *Postharvest Biology and Technology,* **17**(3), 163-173.

Guénin S, Mauriat M, Pelloux J, Van Wuytswinkel O, Bellini C, Gutierrez L. (2009). Normalization of qRT-PCR data: the necessity of adopting a systematic, experimental conditions-specific, validation of references. *J. Exp. Bot.,* **60**(2), 487-493.

Guex N, Peitsch MC. (1997). SWISS-MODEL and the Swiss-Pdb Viewer: An environment for comparative protein modeling. *Electrophoresis,* **18**(15), 2714-2723.

Gutierrez L, Mauriat M, Guénin S, Pelloux J, Lefebvre J-F, Louvet R*, et al.* (2008). The lack of a systematic validation of reference genes: a serious pitfall undervalued in reverse transcription-polymerase chain reaction (RT-PCR) analysis in plants. *Plant Biotechnology Journal,* **6**(6), 609-618.

Halitschke R, Baldwin IT. (2003). Antisense LOX expression increases herbivore performance by decreasing defense responses and inhibiting growth-related transcriptional reorganization in *Nicotiana attenuata*. *Plant Journal,* **36**(6), 794-807.

Halitschke R, Ziegler J, Keinänen M, Baldwin IT. (2004). Silencing of hydroperoxide lyase and allene oxide synthase reveals substrate and defense signaling crosstalk in *Nicotiana attenuata*. *The Plant Journal,* **40**(1), 35-46.

Hardie WJ, Aggenbach SJ, Jaudzems VG. (1996a). The plastids of the grape pericarp and their significance in isoprenoid synthesis. *Australian Journal of Grape and Wine Research,* **2**(3), 144-154.

Hardie WJ, O'Brien TP, Jaudzems VG. (1996b). Morphology, anatomy and development of the pericarp after anthesis in grape, *Vitis vinifera* L. *Australian Journal of Grape and Wine Research,* **2**(2), 97-142.

Hashizume K, Samuta T. (1997). Green odorants of grape cluster stem and their ability to cause a wine stemmy flavor. *Journal of Agricultural and Food Chemistry,* **45**(4), 1333-1337.

Hause B, Weichert H, Hoehne M, Kindl H, Feussner I. (2000). Expression of cucumber lipid-body lipoxygenase in transgenic tobacco: Lipid-body lipoxygenase is correctly targeted to seed lipid bodies. *Planta,* **210**(5), 708-714.

Heitz T, Bergey DR, Ryan CA. (1997). A gene encoding a chloroplast-targeted lipoxygenase in tomato leaves is transiently induced by wounding, systemin, and methyl jasmonate. *Plant Physiology,* **114**(3), 1085-1093.

Higgins PA, Peng AC. (1976). Lipid composition of `Concord' grapes. *Am. J. Enol. Vitic.,* **27**(1), 32-35.

Horton P, Park K-J, Obayashi T, Fujita N, Harada H, Adams-Collier CJ*, et al.* (2007). WoLF PSORT: protein localization predictor. *Nucl. Acids Res.,* **35**(suppl_2), W585-587.

Howe GA, Lee GI, Itoh A, Li L, DeRocher AE. (2000). Cytochrome P450-dependent metabolism of oxylipins in tomato. Cloning and expression of allene oxide synthase and fatty acid hydroperoxide lyase. *Plant Physiol.,* **123**(2), 711-724.

Howe GA, Schilmiller AL. (2002). Oxylipin metabolism in response to stress. *Current Opinion in Plant Biology,* **5**(3), 230-236.

Hudak KA, Thompson JE. (1997). Subcellular localization of secondary lipid metabolites including fragrance volatiles in Carnation petals. *Plant Physiology,* **114**(2), 705-713.

Hughes R, Domenico SD, Santino A. (2009). Plant cytochrome CYP74 family: biochemical features, endocellular localisation, activation mechanism in plant defence and improvements for industrial applications. *Chembiochem,* **10**(7), 1122-1133.

Hughes RK, Belfield EJ, Muthusamay M, Khan A, Rowe A, Harding SE*, et al.* (2006). Characterization of *Medicago truncatula* (barrel medic) hydroperoxide lyase (CYP74C3), a water-soluble detergent-free cytochrome P450 monomer whose biological activity is defined by monomer-micelle association. *Biochem J,* **395**(3), 641-652.

Hughes RK, West SI, Hornostaj AR, Lawson DM, Fairhurst SA, Sanchez RO*, et al.* (2001). Probing a novel potato lipoxygenase with dual positional specificity reveals primary determinants of substrate binding and requirements for a surface

hydrophobic loop and has implications for the role of lipoxygenases in tubers. *Biochem. J.,* **353**(2), 345-355.

Iglesias JLM, Dabila FH, Marino JIM, Gorrdillo CdM, Exposito JM. (1991). Biochemical aspects of the lipids in *Vitis vinifera* grapes (Macabeo variety). Part 1. Linoleic and linolenic acids as aromatic precursors. *Food / Nahrung,* **35**(7), 705-710.

Iyer MM, Sacks GL, Padilla-Zakour OI. (2010). Impact of harvesting and processing conditions on green leaf volatile development and phenolics in Concord grape juice. *Journal of Food Science,* **75**(3), C297-C304.

Jackson RS. (2000). *Wine Science. Principles, Practice, Perception* (2 ed.). USA: Academic Press.

Jackson RS. (2008). *Wine science: principles and applications* (3rd ed.): Elsevier.

Jaillon O, Aury JM, Noel B, Policriti A, Clepet C, Casagrande A*, et al.* (2007). The grapevine genome sequence suggests ancestral hexaploidization in major angiosperm phyla. *Nature,* **449**(7161), 463-467.

Jakoby WB, Stevens J, Duffel MW, Weisiger RA. (1984). The terminal enzymes of mercapturate formation and the thiomethyl shunt. *Rev. Biochem. Toxicol.,* **6**, 97-115.

Jonasson P, Liljeqvist S, Nygren P-A, Stahl S. (2002). Genetic design for facilitated production and recovery of recombinant proteins in Escherichia coli. *Biotechnol Appl Biochem,* **35**(Pt 2), 91-9105.

Kalua CM, Boss PK. (2009). Evolution of volatile compounds during the development of Cabernet sauvignon grapes (*Vitis vinifera* L.). *Journal of Agricultural and Food Chemistry,* **57**(9), 3818-3830.

Kandzia R, Stumpe M, Berndt E, Szalata M, Matsui K, Feussner Ivo. (2003). On the specificity of lipid hydroperoxide fragmentation by fatty acid hydroperoxide lyase from *Arabidopsis thaliana*. *Journal of Plant Physiology,* **160**(7), 803-809.

Kishimoto K, Matsui K, Ozawa R, Takabayashi J. (2005). Volatile C6-aldehydes and allo-ocimene activate defense genes and induce resistance against *Botrytis cinerea* in *Arabidopsis thaliana*. *Plant Cell Physiol.,* **46**(7), 1093-1102.

Kishimoto K, Matsui K, Ozawa R, Takabayashi J. (2008). Direct fungicidal activities of C6-aldehydes are important constituents for defense responses in Arabidopsis against *Botrytis cinerea*. *Phytochemistry,* **69**(11), 2127-2132.

Kondo S, Fukuda K. (2001). Changes of jasmonates in grape berries and their possible roles in fruit development. *Scientia Horticulturae,* **91**(3-4), 275-288.

Kramer DM, Sacksteder CA, Cruz JA. (1999). How acidic is the lumen? *Photosynthesis Research,* **60**(2), 151-163.

Kühn H, Eggert L, Zabolotsky OA, Myagkova GI, Schewe T. (1991). Keto fatty acids not containing doubly allylic methylenes are lipoxygenase substrates. *Biochemistry,* **30**(42), 10269-10273.

Laudert D, Pfannschmidt U, Lottspeich F, Holländer-Czytko H, Weiler EW. (1996). Cloning, molecular and functional characterization of *Arabidopsis thaliana* allene oxide synthase (CYP 74), the first enzyme of the octadecanoid pathway to jasmonates. *Plant Molecular Biology,* **31**(2), 323-335.

Lee D-S, Nioche P, Hamberg M, Raman CS. (2008). Structural insights into the evolutionary paths of oxylipin biosynthetic enzymes. *Nature*.

León J, Rojo E, Sánchez-Serrano JJ. (2001). Wound signalling in plants. *Journal of Experimental Botany,* **52**(354), 1-9.

Leone A, Bleve-Zacheo T, Gerardi C, Melillo MT, Leo L, Zacheo G. (2006). Lipoxygenase involvement in ripening strawberry. *Journal of Agricultural and Food Chemistry,* **54**(18), 6835-6844.

Liavonchanka A, Feussner I. (2006). Lipoxygenases: occurrence, functions and catalysis. *Journal of Plant Physiology,* **163**(3), 348-357.

Livak KJ, Schmittgen TD. (2001). Analysis of relative gene expression data using real-time quantitative PCR and the $2^{-\Delta\Delta C_T}$ method. *Methods,* **25**(4), 402-408.

Lund CM, Thompson MK, Benkwitz F, Wohler MW, Triggs CM, Gardner R*, et al.* (2009). New Zealand Sauvignon blanc distinct flavor characteristics: sensory, chemical, and consumer aspects. *American Journal of Enology and Viticulture,* **60**(1), 1-12.

Lund S, Peng F, Nayar T, Reid K, Schlosser J. (2008). Gene expression analyses in individual grape (*Vitis vinifera* L.) berries during ripening initiation reveal that pigmentation intensity is a valid indicator of developmental staging within the cluster. *Plant Molecular Biology,* **68**(3), 301-315.

Lutteke T, Krieg P, Furstenberger G, von der Lieth CW. (2003). LOX-DB - a database on lipoxygenases. *Bioinformatics,* **19**(18), 2482-2483.

Maccarrone M, Melino G, Finazzi-Agro A. (2001). Lipoxygenases and their involvement in programmed cell death. *Cell Death Differ,* **8**(8), 776-784.

Makrides SC. (1996). Strategies for achieving high-level expression of genes in *Escherichia coli*. *Microbiol. Rev.,* **60**(3), 512-538.

Matsui K. (2006). Green leaf volatiles: hydroperoxide lyase pathway of oxylipin metabolism. *Current Opinion in Plant Biology,* **9**(3), 274-280.

Matsui K, Fukutomi S, Wilkinson J, Hiatt B, Knauf V, Kajwara T. (2001). Effect of overexpression of fatty acid 9-hydroperoxide lyase in tomatoes (*Lycopersicon esculentum* Mill.). *Journal of Agricultural and Food Chemistry,* **49**(11), 5418-5424.

Matsui K, Minami A, Hornung E, Shibata H, Kishimoto K, Ahnert V*, et al.* (2006). Biosynthesis of fatty acid derived aldehydes is induced upon mechanical wounding and its products show fungicidal activities in cucumber. *Phytochemistry,* **67**(7), 649-657.

Matsui K, Miyahara C, Wilkinson J, Hiatt B, Knauf V, Kajiwara T. (2000a). Fatty acid hydroperoxide lyase in tomato fruits: Cloning and properties of a recombinant enzyme expressed in *Escherichia coli*. *Bioscience, Biotechnology and Biochemistry,* **64**(6), 1189-1196.

Matsui K, Shibutani M, Hase T, Kajiwara T. (1996). Bell pepper fruit fatty acid hydroperoxide lyase is a cytochrome P450 (CYP74B). *FEBS Letters,* **394**(1), 21-24.

Matsui K, Ujita C, Fujimoto S-h, Wilkinson J, Hiatt B, Knauf V*, et al.* (2000b). Fatty acid 9- and 13-hydroperoxide lyases from cucumber. *FEBS Letters,* **481**(2), 183-188.

Matsui K, Wilkinson J, Hiatt B, Knauf V, Kajiwara T. (1999). Molecular cloning and expression of Arabidopsis fatty acid hydroperoxide lyase. *Plant and Cell Physiology,* **40**(5), 477-481.

May C, Höhne M, Gnau P, Schwennesen K, Kindl H. (2000). The N-terminal β-barrel structure of lipid body lipoxygenase mediates its binding to liposomes and lipid bodies. *European Journal of Biochemistry,* **267**(4), 1100-1109.

McClements DJ, Decker EA. (2000). Lipid oxidation in oil-in-water emulsions: Impact of molecular environment on chemical reactions in heterogeneous food systems. *Journal of Food Science,* **65**(8), 1270-1282.

McConn M, Creelman RA, Bell E, Mullet JE, Browse J. (1997). Jasmonate is essential for insect defense in Arabidopsis. *Proceedings of the National Academy of Sciences of the United States of America,* **94**(10), 5473-5477.

Melan MA, Dong X, Endara ME, Davis KR, Ausubel FM, Peterman TK. (1993). An *Arabidopsis thaliana l*ipoxygenase gene can be induced by pathogens, abscisic acid, and methyl jasmonate. *Plant Physiology,* **101**(2), 441-450.

Miele A, Bouard J, Bertrand A. (1993). Fatty acids from lipid fractions of leaves and different tissues of Cabernet Sauvignon grapes. *American Journal of Enology and Viticulture,* **44**(2), 180-186.

Minor W, Steczko J, Stec B, Otwinowski Z, Bolin JT, Walter R*, et al.* (1996). Crystal structure of soybean lipoxygenase L-1 at 1.4 Å resolution. *Biochemistry,* **35**(33), 10687-10701.

Mita G, Quarta A, Fasano P, De Paolis A, Di Sansebastiano GP, Perrotta C*, et al.* (2005). Molecular cloning and characterization of an almond 9-hydroperoxide lyase, a new CYP74 targeted to lipid bodies. *J. Exp. Bot.,* **56**(419), 2321-2333.

Mullins MG, Rajasekaran K. (1981). Fruiting cuttings: Revised method for producing test plants of grapevine cultivars. *Am. J. Enol. Vitic.,* **32**(1), 35-40.

Müssig C, Biesgen C, Lisso J, Uwer U, Weiler EW, Altmann T. (2000). A novel stress-inducible 12-oxophytodienoate reductase from *Arabidopsis thaliana* provides a potential link between brassinosteroid-action and jasmonic-acid synthesis. *Journal of plant physiology* **157**(2), 143-152.

Nicolau L, Benkwitz F, Maggu M, Ellet N, Butler P, Tominaga T*, et al.* (2007). *New Zealand Sauvignon blanc: Revealing and protecting its unique aroma characteristics.* Paper presented at the Thirteenth Australian Wine Industry Technical Conference, Adelaide, Australia.

Noordermeer MA, Feussner I, Kolbe A, Veldink GA, Vliegenthart JFG. (2000a). Oxygenation of (3Z)-alkenals to 4-hydroxy-(2E)-alkenals in plant extracts: A nonenzymatic process. *Biochemical and Biophysical Research Communications,* **277**(1), 112-116.

Noordermeer MA, van Dijken AGH, Smeekens SCM, Veldink GA, Vliegenthart JF. (2000b). Characterization of three cloned and expressed 13-hydroperoxide lyase isoenzymes from alfalfa with unusual N-terminal sequences and different enzyme kinetics. *European Journal of Biochemistry,* **267**(9), 2473-2482.

Noordermeer MA, Veldink GA, Vliegenthart JFG. (2001a). Fatty acid hydroperoxide lyase: A plant cytochrome P450 enzyme involved in wound healing and pest resistance. *Chembiochem,* **2**(7-8), 494-504.

Noordermeer MA, Veldink GA, Vliegenthart JFG. (2001b). Spectroscopic studies on the active site of hydroperoxide lyase; the influence of detergents on its conformation. *FEBS Letters,* **489**(2-3), 229-232.

Ober D. (2005). Seeing double: gene duplication and diversification in plant secondary metabolism. *Trends in Plant Science,* **10**(9), 444-449.

Oliveira C, Barbosa A, Ferreira ACS, Guerra J, Pinho PGDE. (2006). Carotenoid profile in grapes related to aromatic compounds in wines from Douro region. *Journal of Food Science,* **71**(1), S1-S7.

Oliw EH. (2002). Plant and fungal lipoxygenases. *Prostaglandins and Other Lipid Mediators,* **68-69**, 313-323.

Padham AK, Hopkins MT, Wang T-W, McNamara LM, Lo M, Richardson LGL*, et al.* (2007). Characterization of a plastid triacylglycerol lipase from Arabidopsis. *Plant Physiol.,* **143**(3), 1372-1384.

Padilla MN, Hernández ML, Sanz C, Martínez-Rivas JM. (2009). Functional characterization of two 13-lipoxygenase genes from olive fruit in relation to the biosynthesis of volatile compounds of virgin olive oil. *Journal of Agricultural and Food Chemistry,* **57**(19), 9097-9107.

Parr WV, Frost A, White KG, Marfell J. (2004). Sensory evaluation of wine: deconstructing the concept of "Marlborough Sauvignon Blanc". *Annual technical issue*, 63-69.

Patron NJ, Waller RF. (2007). Transit peptide diversity and divergence: A global analysis of plastid targeting signals. *BioEssays,* **29**(10), 1048-1058.

Peña-Cortés H, Barrios P, Dorta F, Polanco V, Sánchez C, Sánchez E*, et al.* (2004). Involvement of jasmonic acid and derivatives in plant responses to pathogens and insects and in fruit ripening. *Journal of Plant Growth Regulation,* **23**(3), 246-260.

Perez Gilabert M, Carmona FG. (2002). Chromatographic analysis of lipoxygenase products. *Analytica Chimica Acta,* **465**(1-2), 319-335.

Petit A-N, Wojnarowiez G, Panon M-L, Baillieul F, Clément C, Fontaine F*, et al.* (2008). Botryticides affect grapevine leaf photosynthesis without inducing defense mechanisms. *Planta*.

Peyrot des Gachons C, Tominga T, Dubourdieu D. (2000). Measuring the aromatic potential of *Vitis vinifera* L. cv. Sauvignon blanc grapes by assaying s-cysteine

cojugates, precursors of the volatile thiols responsible for their varietal aroma. *Journal of Agricultural and Food Chemistry,* **48**, 3387-3391.

Peyrot des Gachons C, Tominga T, Dubourdieu D. (2002a). Localization of S-Cysteine Conjugates in the Berry: Effect of Skin Contact on Aromatic Potential of *Vitis vinifera* L. cv. Sauvignon blanc Must. *American Journal of Enology and Viticulture,* **53**(2), 144-146.

Peyrot des Gachons C, Tominga T, Dubourdieu D. (2002b). Sulfur aroma precursor present in S- glutathione conjugate form: Identification of S-3-(hexan-1-ol)-glutathione in must from *Vitis vinifera* L. cv. Sauvignon blanc. *Journal of Agricultural and Food Chemistry,* **50**, 4076-4079.

Phillips DR, Matthew JA, Reynolds J, Fenwick GR. (1979). Partial purification and properties of a cis-3: trans-2-enal isomerase from cucumber fruit. *Phytochemistry,* **18**(3), 401-404.

Ponginebbi L, Nawar W, Chinachoti P. (1999). Oxidation of linoleic acid in emulsions: Effect of substrate, emulsifier, and sugar concentration. *Journal of the American Oil Chemists' Society,* **76**(1), 131-138.

Porta H, Rocha-Sosa M. (2002). Plant lipoxygenases. Physiological and molecular features. *Plant Physiology,* **130**(1), 15-21.

Rabetafika H, Gigot C, Fauconnier M-L, Ongena M, Destain J, du Jardin P*, et al.* (2008). Sugar beet leaves as new source of hydroperoxide lyase in a bioprocess producing green-note aldehydes. *Biotechnology Letters,* **30**(6), 1115-1119.

Rachman G. (1999). The globe in a glass. *The Economist*.

Ramey D, Bertrand A, Ough CS, Singleton VL, Sanders E. (1986). Effects of skin contact temperature on Chardonnay must and wine composition. *American Journal of Enology and Viticulture,* **37**(2), 99-106.

Rand M, Clarke O, Riches L. (2007). *Oz Clarke's Grapes and Wines: The definitive guide to the world's great grapes and the wines they make*: Harcourt.

Reid K, Olsson N, Schlosser J, Peng F, Lund S. (2006). An optimized grapevine RNA isolation procedure and statistical determination of reference genes for real-time RT-PCR during berry development. *BMC Plant Biology,* **6**(1), 27.

Robinson DS, Wu Z, Domoney C, Casey R. (1995). Lipoxygenases and the quality of foods. *Food Chemistry,* **54**(1), 33-43.

Rogiers SY, Kumar GNM, Knowles NR. (1998). Maturation and ripening of fruit of *Amelanchier alnifolia* Nutt. are accompanied by increasing oxidative stress. *Ann Bot,* **81**(2), 203-211.

Roland A, Vialaret Jm, Razungles A, Rigou P, Schneider R. (2010). Evolution of S-cysteinylated and S-glutathionylated thiol precursors during oxidation of Melon B. and Sauvignon blanc musts. *Journal of Agricultural and Food Chemistry,* ( ).

Roufet M, Bayonove C, Cordonnier R. (1987). Etude de la composition lipidique du raisin, *Vitis vinifera* L.: evolution au cours de la maturation et localisation dans la baie (Lipid composition of grapevine berries, *Vitis vinifera* L.: changes during maturation and localization in the berry). *Vitis,* **26**, 85-97.

Royo J, Vancanneyt G, Pérez AG, Sanz C, Störmann K, Rosahl S*, et al.* (1996). Characterization of three potato lipoxygenases with distinct enzymatic activities and different organ-specific and wound-regulated expression patterns. *Journal of Biological Chemistry,* **271**(35), 21012-21019.

Rubio M, Alvarez-OrtiMΓ M, Alvarruiz A, FernaMΓndez E, Pardo JE. (2009). Characterization of oil obtained from grape seeds collected during berry development. *Journal of Agricultural and Food Chemistry,* **57**(7), 2812-2815.

Saitou N, Nei M. (1987). The neighbor-joining method: a new method for reconstructing phylogenetic trees. *Molecular Biology and Evolution,* **4**(4), 406-425.

Salas JJ, Garcia-Gonzalez DL, Aparicio R. (2006). Volatile compound biosynthesis by green leaves from an *Arabidopsis thaliana* hydroperoxide lyase knockout mutant. *Journal Of Agricultural And Food Chemistry,* **54**(21), 8199-8205.

Salas JJ, Sanchez C, Garcia-Gonzalez DL, Aparicio R. (2005). Impact of the suppression of lipoxygenase and hydroperoxide lyase on the quality of the green odor in green leaves. *Journal of Agricultural and Food Chemistry,* **53**(5), 1648-1655.

Salch YP, Grove MJ, Takamura H, Gardner HW. (1995). Characterization of a C-5,13-cleaving enzyme of 13(S)-hydroperoxide of linolenic acid by soybean seed. *Plant Physiology,* **108**(3), 1211-1218.

Salinas M, Zalacain A, Pardo F, Alonso GL. (2004). Stir bar sorptive extraction applied to volatile constituents evolution during *Vitis vinifera* ripening. *Journal of Agricultural and Food Chemistry,* **52**(15), 4821-4827.

Sambrook J, Russell DW (Eds.). (2001). *Molecular cloning: a laboratory manual* (3rd ed.). Cold Spring Harbor, N.Y Cold Spring Harbor Laboratory Press.

Sanchez J, Harwood JL. (2002). Biosynthesis of triacylglycerols and volatiles in olives. *European Journal of Lipid Science and Technology,* **104**(9-10), 564-573.

Schilstra MJ, Veldink GA, Verhagen J, Vliegenthart JFG. (1992). Effect of lipid hydroperoxide on lipoxygenase kinetics. *Biochemistry,* **31**(33), 7692-7699.

Schilstra MJ, Veldink GA, Vliegenthart JF. (1994). Effect of nonionic detergents on lipoxygenase catalysis. *Lipids,* **29**(4), 225-231.

Schneider C, Pratt DA, Porter NA, Brash AR. (2007). Control of oxygenation in lipoxygenase and cyclooxygenase catalysis. *Chemistry & Biology,* **14**(5), 473-488.

Schneider R, Charrier F, Razungles A, Baumes R. (2006). Evidence for an alternative biogenetic pathway leading to 3-mercaptohexanol and 4-mercapto-4-methylpentan-2-one in wines. *Analytica Chimica Acta,* **563**(1-2), 58-64.

Shah J. (2009). Plants under attack: Systemic signals in defence. *Current Opinion in Plant Biology,* **12**(4), 459-464.

Sheludko YV, Sindarovska YR, Gerasymenko IM, Bannikova MA, Kuchuk NV. (2007). Comparison of several *Nicotiana* species as hosts for high-scale *Agrobacterium*-mediated transient expression. *Biotechnology and Bioengineering,* **96**(3), 608-614.

Shewe T, Nigam S. (1997). Is lypoxygenation of pathogen-derived arachidonic acid involved in plant protection? In H. Sinzinger (Ed.), *Recent advantages in prostaglandin, thromboxane, and leukotriene research* (Vol. 433, pp. 221-227). New York, c1997: Plenum Press.

Shi X, Karkut T, Chahmanhkah M, Alting-Mees M, Hemmingsen SM, Hegedus D. (2002). 5'-RACEing across a bridging oligonucleotide. *BioTechniques,* **32**(3), 480-482.

Shibata D, Axelrod B. (1995). Plant lipoxygenases. *Journal of Lipid Mediators and Cell Signalling,* **12**(2-3), 213-228.

Shibata D, Slusarenko A, Casey R, Hildebrand D, Bell E. (1994). Lipoxygenases. *Plant Molecular Biology Reporter,* **12**, S41-42.

Shibata Y, Matsui K, Kajiwara T, Hatanaka A. (1995). Purification and properties of fatty acid hydroperoxide lyase from green bell pepper fruits. *Plant Cell Physiol.,* **36**(1), 147-156.

Shin JH, Van K, Kim DH, Kim KD, Jang YE, Choi B-S*, et al.* (2008). The lipoxygenase gene family: A genomic fossil of shared polyploidy between *Glycine max* and *Medicago truncatula*. *BMC Plant Biology,* **8**(1), 133.

Shiojiri K, Kishimoto K, Ozawa R, Kugimiya S, Urashimo S, Arimura G*, et al.* (2006). Changing green leaf volatile biosynthesis in plants: An approach for improving plant resistance against both herbivores and pathogens. *PNAS,* **103**(45), 16672-16676.

Siedow JN. (1991). Plant lipoxygenase: Structure and function. *Annual Review of Plant Physiology and Plant Molecular Biology,* **42**(1), 145-188.

Sloane DL, Leung R, Barnett J, Craik CS, Sigal E. (1995). Conversion of human 15-lipoxygenase to an efficient 12-lipoxygenase: the side-chain geometry of amino acids 417 and 418 determine positional specificity. *Protein Eng.,* **8**(3), 275-282.

Sloane DL, Leung R, Craik CS, Sigal E. (1991). A primary determinant for lipoxygenase positional specificity. *Nature,* **354**(6349), 149-152.

Srinivasulu S, Rao AGA. (1993). Kinetic and structural studies on the interaction of surfactants with lipoxygenase L1 from soybeans (*Glycine max*). *Journal of Agricultural and Food Chemistry,* **41**(3), 366-371.

Stumpe M, Feussner I. (2006). Formation of oxylipins by CYP74 enzymes. *Phytochemistry Reviews,* **5**(2), 347-357.

Subileau M, Schneider R, Salmon J-M, Degryse E. (2008). New insights on 3-mercaptohexanol (3MH) biogenesis in Sauvignon blanc wines: Cys-3MH and (E)-hexen-2-al are not the major precursors. *Journal of Agricultural and Food Chemistry,* **56**(19), 9230-9235.

Takamura H, Gardner HW. (1996). Oxygenation of (3Z)-alkenal to (2E)-4-hydroxy-2-alkenal in soybean seed (*Glycine max* L.). *Biochimica et Biophysica Acta - Lipids and Lipid Metabolism,* **1303**(2), 83-91.

Terp N, Gobel C, Brandt A, Feussner I. (2006). Lipoxygenases during *Brassica napus* seed germination. *Phytochemistry,* **67**(18), 2030-2040.

Thelander M, Narita JO, Gruissem W. (1986). Plastid differentiation and pigment biosynthesis during tomato fruit ripening. *Curr Top Plant Biochem Physiol,* (5), 128-141.

Thibon C, Shinkaruk S, Jourdes M, Bennetau B, Dubourdieu D, Tominaga T. (2010). Aromatic potential of botrytized white wine grapes: identification and

quantification of new cysteine-S-conjugate flavor precursors. *Analytica Chimica Acta,* **660**(1-2), 190-196.

Thompson JD, Higgins DG, Gibson TJ. (1994). CLUSTAL W: improving the sensitivity of progressive multiple sequence alignment through sequence weighting, position-specific gap penalties and weight matrix choice. *Nucleic Acids Research,* **22**(22), 4673-4680.

Tichopad A, Dilger M, Schwarz G, Pfaffl MW. (2003). Standardized determination of real-time PCR efficiency from a single reaction set-up. *Nucl. Acids Res.,* **31**(20), e122-.

Tominaga T, Darriet P, Dubourdieu D. (1996). Identification de l'acetate de 3-mercatptohexanol, compose a forte odeur de buis, intervenant dans l'arome des vins de Sauvignon. *Vitis,* **35**(4), 207-210.

Tominaga T, Furrer A, Henry R, Dubourdieu D. (1998a). Identification of new volatile thiols in the aroma of *Vitis vinifera* L. var. Sauvignon blanc wines. *Flavour and Fragrance Journal,* **13**, 159-162.

Tominaga T, Niclass Y, Frerot E, Dubourdieu D. (2006). Stereoisomeric distribution of 3-mercaptohexan-1-ol and 3-mercaptohexyl acetate in dry and sweet white wines made from *Vitis vinifera* (Var. Sauvignon blanc and Semillon). *Journal Of Agricultural And Food Chemistry,* **54**(19), 7251-7255.

Tominaga T, Peyrot Des Gachons C, Dubourdieu D. (1998b). A new type of flavour precursors in *Vitis vinifera* L. cv. Sauvignon blanc: *S*-cysteine conjugates. *Journal of Agricultural and Food Chemistry,* **46**, 5215-5219.

Toporkova YY, Gogolev YV, Mukhtarova LS, Grechkin AN. (2008). Determinants governing the CYP74 catalysis: Conversion of allene oxide synthase into hydroperoxide lyase by site-directed mutagenesis. *FEBS Letters,* **582**(23-24), 3423-3428.

Trought MCT. (1996). The New Zealand terroir: Sources of variation in fruit composition in New Zealand vineyards. In *Proceedings of the 4th International Symposium on Cool Climate Enology and Viticulture* (pp. 1:23-27).

Vancanneyt G, Sanz C, Farmaki T, Paneque M, Ortego F, Castanera P*, et al.* (2001). Hydroperoxide lyase depletion in transgenic potato plants leads to an increase in aphid performance. *Proceedings of the National Academy of Sciences of the United States of America,* **98**(14), 8139-8144.

Vandesompele J, De Preter K, Pattyn F, Poppe B, Van Roy N, De Paepe A*, et al.* (2002). Accurate normalization of real-time quantitative RT-PCR data by geometric averaging of multiple internal control genes. *Genome Biology,* **3**(7), research0034.0031 - research0034.0011.

Vellosillo T, Martinez M, Lopez MA, Vicente J, Cascon T, Dolan L*, et al.* (2007). Oxylipins produced by the 9-lipoxygenase pathway in Arabidopsis regulate lateral root development and defense responses through a specific signaling cascade. *Plant Cell*, tpc.106.046052.

Verhagen J, Vliegenthart JFG, Boldingh J. (1978). Micelle and acid-soap formation of linoleic acid and 13-L-hydroperoxylinoleic acid being substrates of lipoxygenase-1. *Chemistry and Physics of Lipids,* **22**(4), 255-259.

Vijayan P, Shockey J, Lévesque CA, Cook RJ, Browse J. (1998). A role for jasmonate in pathogen defense of Arabidopsis. *Proceedings of the National Academy of Sciences of the United States of America,* **95**(12), 7209-7214.

Viswanathan VK, Krcmarik K, Cianciotto NP. (1999). Template secondary structure promotes polymerase jumping during PCR amplification. *Biotechniques,* **27**(3), 508-511.

Wang WH, Takano T, Shibata D, Kitamura K, Takeda G. (1994). Molecular basis of a null mutation in soybean lipoxygenase 2: Substitution of glutamine for an iron-ligand histidine. *Proceedings of the National Academy of Sciences of the United States of America,* **91**(13), 5828-5832.

Wasternack C. (2007). Jasmonates: An update on biosynthesis, signal transduction and action in plant stress response, growth and development. *Annal of Botany,* **100**(4), 681-697.

Wasternack C, Stenzel I, Hause B, Hause G, Kutter C, Maucher H*, et al.* (2006). The wound response in tomato - Role of jasmonic acid. *Journal of Plant Physiology,* **163**(3), 297-306.

Weber H. (2002). Fatty acid-derived signals in plants. *Trends in Plant Science,* **7**(5), 217-224.

Wendl MC, Yang S-P. (2004). Gap statistics for whole genome shotgun DNA sequencing projects. *Bioinformatics,* **20**(10), 1527-1534.

Wolf AE, Dietz KJ, Schroder P. (1996). Degradation of glutathione S-conjugates by a carboxypeptidase in the plant vacuole. *FEBS Letters,* **384**, 31-34.

Ytterberg AJ, Peltier J-B, van Wijk KJ. (2006). Protein profiling of plastoglobules in chloroplasts and chromoplasts. A surprising site for differential accumulation of metabolic enzymes. *Plant Physiol.,* **140**(3), 984-997.

Zeng Y, Yang T. (2002). RNA isolation from highly viscous samples rich in polyphenols and polysaccharides. *Plant Molecular Biology Reporter,* **20**(4).

Zhang B, Chen K, Bowen J, Allan A, Espley R, Karunairetnam S*, et al.* (2006a). Differential expression within the LOX gene family in ripening kiwifruit. *J. Exp. Bot.,* **57**(14), 3825-3836.

Zhang FS, Wang XQ, Ma SJ, Cao SF, Li N, Wang XX*, et al.* (2006b). Effects of methyl jasmonate on postharvest decay in strawberry fruit and the possible mechanisms involved. *Acta Hort.,* **712**, 693-698.

Zimmerman DC, Coudron CA. (1979). Identification of traumatin, a wound hormone, as 12-oxo-trans-10-dodecenoic acid. *Plant Physiol.,* **63**(3), 536-541.

Zimmerman DC, Vick BA. (1970). Hydroperoxide isomerase: A new enzyme of lipid metabolism. *Plant Physiol.,* **46**(3), 445-453.

Zimmerman GL, Snyder HE. (1974). Role of calcium in activating soybeam lipoxygenase 2. *Journal of Agricultural and Food Chemistry,* **22**(5), 802-805.

Appendices

A.1 Appendices: Materials and methods

A.1.1 Different stages of fruiting cuttings development

The photographs illustrate different growth stages of fruiting cuttings prepared as described in section 3.3.2 (**A** – root propagation, **B** – flowering, **C** –plants with bunches bearing berries of late stages).

(A)

(B)

(C)

A.1.2 Berries of different developmental stages

The photos represent examples of bunches collected at different stages of berry development as describe in section 3.3.3 (stages 1-6 are shown here). The red arrows indicate examples of berries collected for molecular analysis.

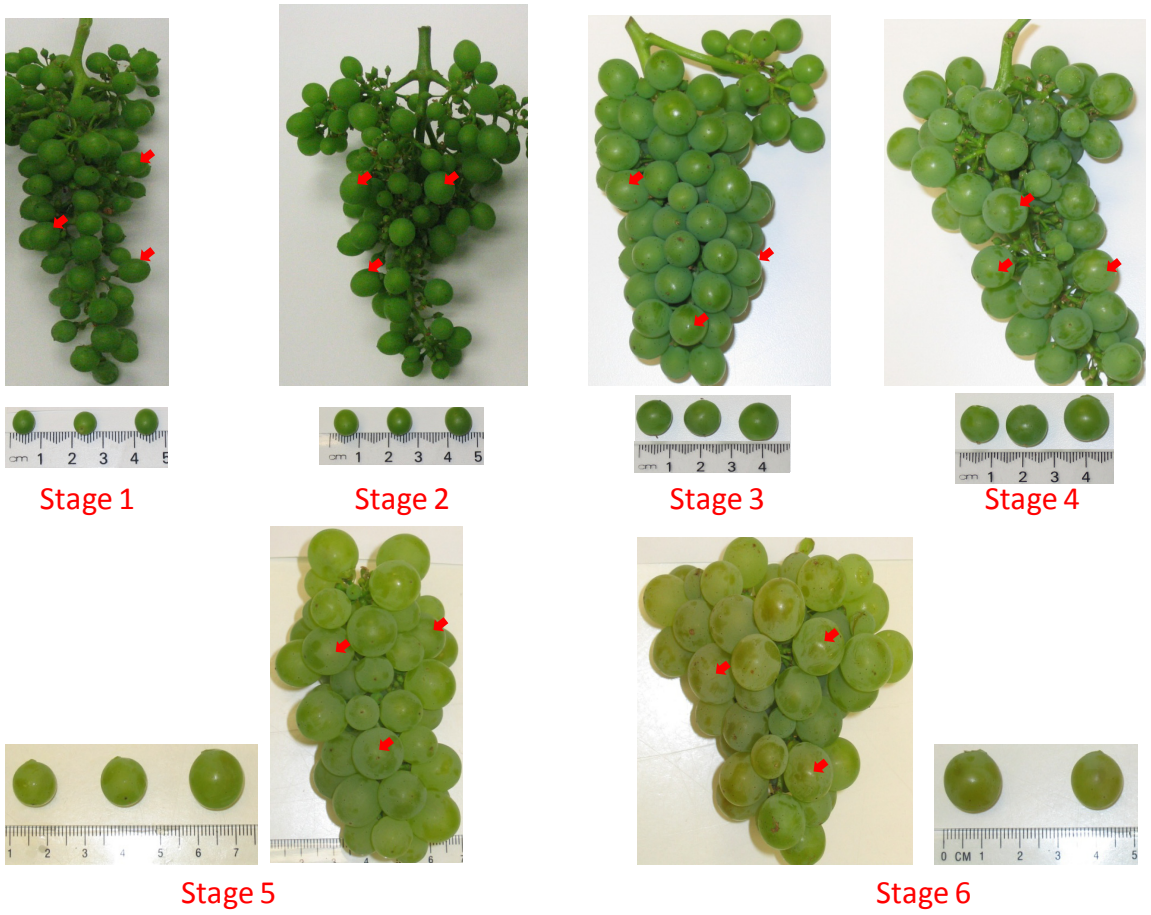

A.1.3 Wounding and Botrytis

A - berries were pierced with a syringe needle and collected as described in section 3.3.6. Yellow circles indicate the locations of wounding sites.

B - berries for studying effect of a pathogen on LOX and HPL gene expression were collected from bunches infected with *Botrytis cinerea* as described in section 3.3.7. Red arrows point to berries infected with the pathogen, and yellow arrows indicate visually uninfected berries, which were collected to study within-bunch systemic response

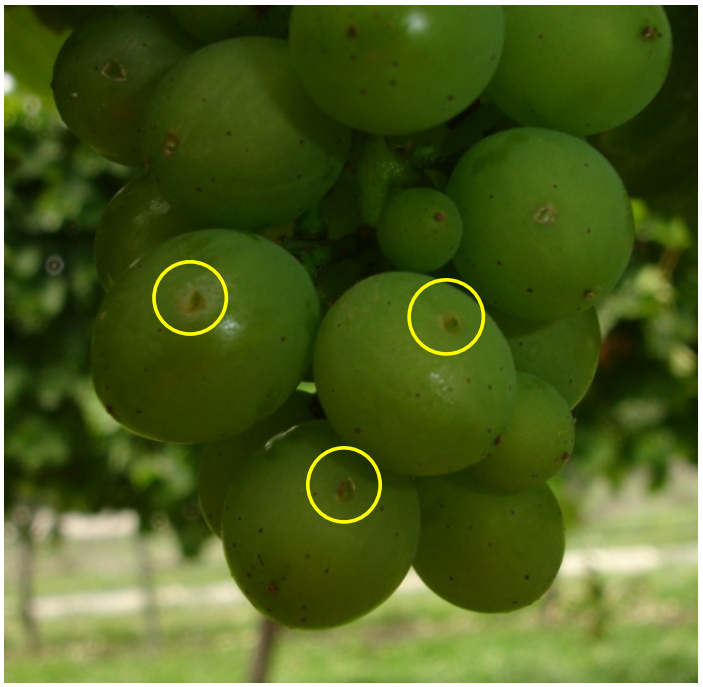

(A)

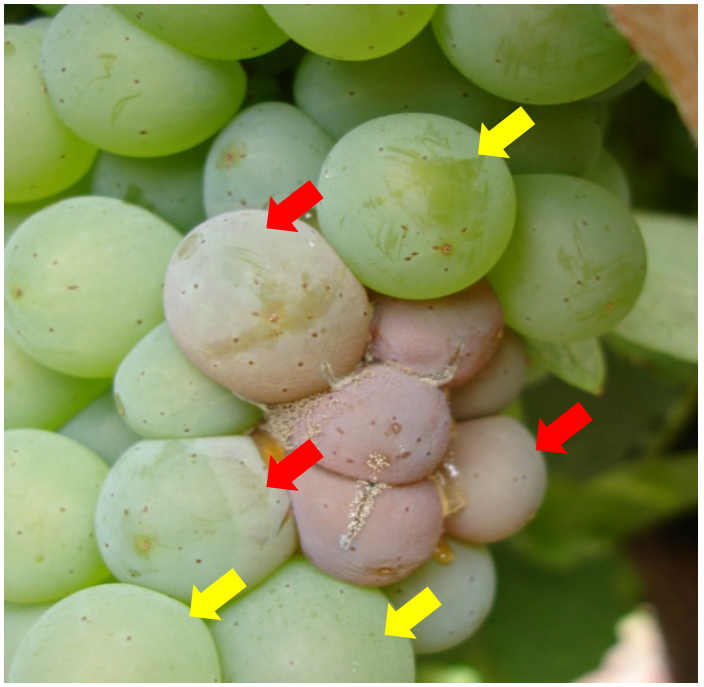

(B)

A.1.4 Flowchart outlining the 5´-RACE experiment performed in an attempt to obtain full-length CDS information for *VvLOXD*

5´ phosphorylated LOXDRT primer was used to synthesise first-strand (FS) cDNA using SuperScriptII (SSII) RT enzyme. Terminal transferase activity of SSII adds C residues to the 3´terminus of the FS cDNA complementary to 7-methylguanosine cap structures. The bridging oligo BOLOXD is then ligated to the phosphorylated 5´ terminus of the FS cDNA. The poly-C tail is then is then ligated to the poly-G tail, thereby forming a circular cDNA molecule. The circular cDNA is used in two rounds of PCR (primary and "nested") to obtain a PCR product containing the unknown 5´ terminus sequence information of VvLOXD.

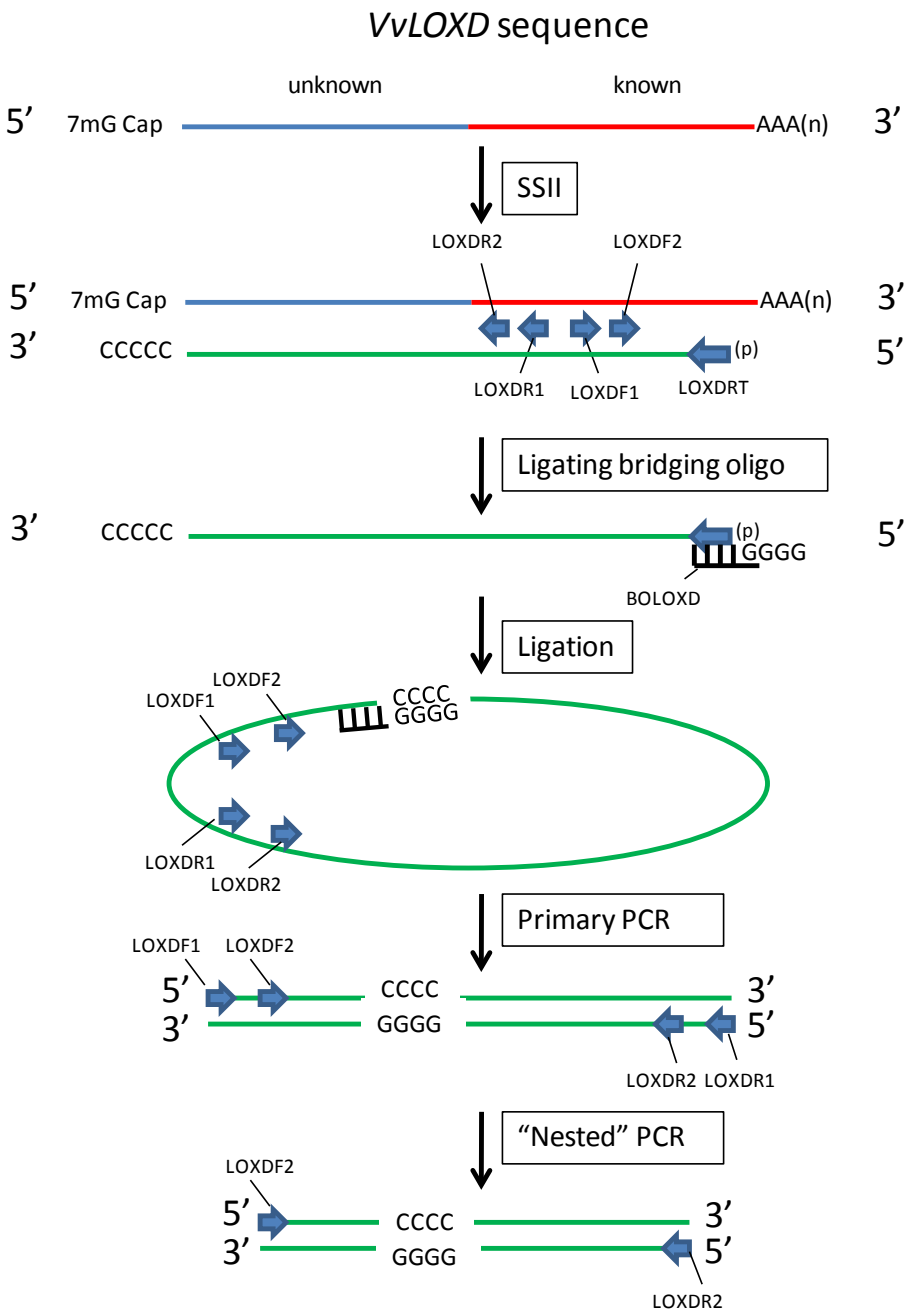

A.2 Appendices: Identification ofmembers of LOX and HPL gene families in the grape genome

A.2.1 LOX sequences identified in the grape genome, which do not have corresponding accessions in the GenBank

VvLOXD

```
CAAATCAAGGTATTCAGTTTAACTGCAAATCTTGGATATATCCATTTACAAAGACAAAAACCAATCGACTTTTCTTCTCAAACACTGTTTATCTGCCAAACGAAACGCCAGAAG
   N  Q  G  I  Q  F  N  C  K  S  W  I  Y  P  F  T  K  T  K  T  N  R  L  F  F  S  N  T  V  Y  L  P  N  E  T  P  E

CTTTGGATGAACTGAGAAAAGAAGAGCTTGAAAGCTTGAGAGGACATGGAACTGGGGAGCGGAAGGAGTGGGATCGGGTGTATGAATACGACTACTACAATGACCTTGGCAATC
A  L  D  E  L  R  K  E  E  L  E  S  L  R  G  H  G  T  G  E  R  K  E  W  D  R  V  Y  E  Y  D  Y  Y  N  D  L  G  N

CTGATAAAGGTCAAGAACATGTGAGACCCATTTTGGGTGGGTCAGATTCATACCCATATCCTCGCAGGGGAAGAACTGGCCGACCTCGTTGCAACCAAGATCCTCTAACTGAGA
P  D  K  G  Q  E  H  V  R  P  I  L  G  G  S  D  S  Y  P  Y  P  R  R  G  R  T  G  R  P  R  C  N  Q  D  P  L  T  E

GTCGGCCAACAAAATTCAACCTGGATATATATGTTCCTCCAGATGAGCGATTCAGTCCCAAGAAACTATCAGAGTTCATAGAGAATTCGGTCCAGGCTATTGTACATTTCCCTC
S  R  P  T  K  F  N  L  D  I  Y  V  P  P  D  E  R  F  S  P  K  K  L  S  E  F  I  E  N  S  V  Q  A  I  V  H  F  P

TCCCTGAGGCACAATCCATCGACGAGCAAGAATCCAATAGTTTTGAGTCATTGGAGGAGATAAAAGACATTTTCTCTAGACACAAAAGGCAAGGAGTAGAGGGATGGATTGCAG
L  P  E  A  Q  S  I  D  E  Q  E  S  N  S  F  E  S  L  E  E  I  K  D  I  F  S  R  H  K  R  Q  G  V  E  G  W  I  A

AGAAACTGAAGAGTTTAGTATCAGATGATCTTTTCAAAGAAATTAAGGAAGCAAGCAAAAAAGATCCCATCAAATTTCCATTACCAAAAATAATAGAAGAAAACGAACTGGCAT
E  K  L  K  S  L  V  S  D  D  L  F  K  E  I  K  E  A  S  K  K  D  P  I  K  F  P  L  P  K  I  I  E  E  N  E  L  A

GGAAGGATGACGAGGAGTTCGCACGCCAAATGCTGTCCGGAGTCAATCCAACAGTAATCAAAGGCTTGGAGGTGTTCCCCCCACAAAGCAGAAATGGAGTCTGGAGTTCAATAA
W  K  D  D  E  E  F  A  R  Q  M  L  S  G  V  N  P  T  V  I  K  G  L  E  V  F  P  P  Q  S  R  N  G  V  W  S  S  I

AGGCATCACACATACAGCACAATCTTGATGGTCTCACTATTGCAGAGGCAATGAACCAATGGAGGATCCTCATCCTGGATCACCATGACTATCTCTTGCCATTTTTAAACAGAA
K  A  S  H  I  Q  H  N  L  D  G  L  T  I  A  E  A  M  N  Q  W  R  I  L  I  L  D  H  H  D  Y  L  L  P  F  L  N  R

TAAACACAAAGGGCATTTGTGTTTATGCATCCCGGACTCTGTTGTTCCTAAGGGATGATCATACACTAAAACTATTGGCAATAGAACTAAGTTTGCCTGGCTCCTCTGCTGACA
I  N  T  K  G  I  C  V  Y  A  S  R  T  L  L  F  L  R  D  D  H  T  L  K  L  L  A  I  E  L  S  L  P  G  S  S  A  D

TGGAGATCAATAGGGTGTTTCTACCAACAACTCAGGGGACAGAAGCAGCACTTTGGCTTCTTGCTAAAGCTCATGTTGCAGTTAATGACTCTGCCTATCATCAATTAATCAGTC
M  E  I  N  R  V  F  L  P  T  T  Q  G  T  E  A  A  L  W  L  L  A  K  A  H  V  A  V  N  D  S  A  Y  H  Q  L  I  S

ATTGGTTAAACACTCATGCAGTAGTTGAACCATTCATTATCGCCACCAGAAGGCAGTTAAGTGTGATGCACCCAGTCCACCGGCTACTGGATCCTCATTTTAAAGACACCATGC
H  W  L  N  T  H  A  V  V  E  P  F  I  I  A  T  R  R  Q  L  S  V  M  H  P  V  H  R  L  L  D  P  H  F  K  D  T  M

ACATAAATGCATTGAGCCGGAGTATCATCATAAACTCTGGTGGGATCCTTGAGAAAATATTGTTTACTCAAGAAATCTCAATGGAGTTATCTTCAGCAATTTACAGAGACTGGA
H  I  N  A  L  S  R  S  I  I  I  N  S  G  G  I  L  E  K  I  L  F  T  Q  E  I  S  M  E  L  S  S  A  I  Y  R  D  W

GATTTGATGAACAAGGCCTTCCTGCTGACTTAATCAAAAGAGGCCTGGCTCTAAAAGATCCAGATAATCCCACCGGGGTTTATCCACTCTTAGAAGACTACCCTTATGGTGCAG
R  F  D  E  Q  G  L  P  A  D  L  I  K  R  G  L  A  L  K  D  P  D  N  P  T  G  V  Y  P  L  L  E  D  Y  P  Y  G  A

ATGGACTTGAGATATGGACTGCCATCAAGACATGGGTCACAGATTTTTGTTCACTCTTCTACACTGATGACGATTCTGTCAGGTCTGATGTGGAAATACAAGCATGGTGGTCAG
D  G  L  E  I  W  T  A  I  K  T  W  V  T  D  F  C  S  L  F  Y  T  D  D  D  S  V  R  S  D  V  E  I  Q  A  W  W  S

AGATTAAAAATGTGGGTCATGGTGATAAGTGCAATGAGAGATGGTGGTATCCACTGACAACTTTAATGGACCTAATAGAGGCTCTGACCACTCTGATATGGATTGCTTCAGCTC
E  I  K  N  V  G  H  G  D  K  C  N  E  R  W  W  Y  P  L  T  T  L  M  D  L  I  E  A  L  T  T  L  I  W  I  A  S  A

TTCACGCTTCAGTCAACTTTGGCCAATATGCATATGCTGGTTACCCACCAAATCGTCCCACACTATGTCGACAATTCATTCCAAATGAAGGAACACATGAATTTGCTGCTTTCC
L  H  A  S  V  N  F  G  Q  Y  A  Y  A  G  Y  P  P  N  R  P  T  L  C  R  Q  F  I  P  N  E  G  T  H  E  F  A  A  F

TTAAAGATCCAGACGGATACTATCTTAAAATGCTGCCTGCAAGATTTGAGATGACCATTGGTGTAGCATTGATAGAGGTACTCTCTCAGCACACATCAGACGAAGTGTATATAG
L  K  D  P  D  G  Y  Y  L  K  M  L  P  A  R  F  E  M  T  I  G  V  A  L  I  E  V  L  S  Q  H  T  S  D  E  V  Y  I

GTCAGAAGCCATCACCAGAGTGGACAGACAACGAAGAGGTCCGACAAAGATTTGAGAAGTTTCGTGAGAATCTTCAGAAGGTAGAGAGAAAAATTTTGGTAAGGAACAGGGATC
G  Q  K  P  S  P  E  W  T  D  N  E  E  V  R  Q  R  F  E  K  F  R  E  N  L  Q  K  V  E  R  K  I  L  V  R  N  R  D

CCAAGCTGAAGAACAGAAAAGGACCTGCCAAGATACCATACAAACTTTTGTACCCCGATACATCAAATATAGGAATTGGAAGAGGTATCACAGGAAAGGGGATTCCTAACAGCA
P  K  L  K  N  R  K  G  P  A  K  I  P  Y  K  L  L  Y  P  D  T  S  N  I  G  I  G  R  G  I  T  G  K  G  I  P  N  S

TATCCATCTAG
I  S  I  *
```

A.2.1 LOX sequences identified in the grape genome, which do not have corresponding accessions in the GenBank (continued)

VvLOXM

```
ATGTTCCTGGGTGTGGCAGAATTCACTTTCTTTGTAATTCCTGGCTTAGGCAAGGAGAATTGTCTGCTAAAGGAATGTACATATCTTCCAA
 M  F  L  G  V  A  E  F  T  F  F  V  I  P  G  L  G  K  E  N  C  L  L  K  E  C  T  Y  L  P

GTGAAACACCAGGGCCCCTACGCAAGTACAGAGAAGGTGAACTGGTGAATCTGAGGGGAGATGGAACCGGAGAGCTTAAGGAATGGGATCG
S  E  T  P  G  P  L  R  K  Y  R  E  G  E  L  V  N  L  R  G  D  G  T  G  E  L  K  E  W  D  R

AGTGTATGACTATGCTTACTATAATGATTTGGGGAATCCAGACAGGGATCTCAAATACACCCGCCCTGTGCTGGGAGGATCTGCGGAGTAT
  V  Y  D  Y  A  Y  Y  N  D  L  G  N  P  D  R  D  L  K  Y  T  R  P  V  L  G  G  S  A  E  Y

CCTTATCCCAGGAGGGGAAGAACTGGTAGACCACCATCTGAAAAAGATCCCAACACCGAGAGCATATTACCACTTCTGATGAGCTTAAACA
 P  Y  P  R  R  G  R  T  G  R  P  P  S  E  K  D  P  N  T  E  S  I  L  P  L  L  M  S  L  N

TATATGTTCCAAGAGATGAACGATTTGGTCACCTCAAGATGTTAGACTTCCTGGCTTATGCCCTGAAATCCATAGTTCAATTCCTTCTCCC
I  Y  V  P  R  D  E  R  F  G  H  L  K  M  L  D  F  L  A  Y  A  L  K  S  I  V  Q  F  L  L  P

TGAGTTTGAGGCTCTATGTGACAGCACCCCCAATGAGTTTGACAGCTTCCAAGATGTATTAGACCTCTACGAAGGAGGAATCAAGGTCCCA
  E  F  E  A  L  C  D  S  T  P  N  E  F  D  S  F  Q  D  V  L  D  L  Y  E  G  G  I  K  V  P

GAGGGCACTTTACTTGACAAAATTAAGGACAACATCCCTCTTGAGATGCTCAAGGAACTTGTTCGTACTGATGGGGAACATCTCTTCAAGT
 E  G  T  L  L  D  K  I  K  D  N  I  P  L  E  M  L  K  E  L  V  R  T  D  G  E  H  L  F  K

TCCCAATGCCCCAAGTCATCAAAGAGGATAAGTCTGCATGGAGGACTGATGAAGAATTTGCTAGAGAAATGCTGGCTGGACTCAACCCTGT
F  P  M  P  Q  V  I  K  E  D  K  S  A  W  R  T  D  E  E  F  A  R  E  M  L  A  G  L  N  P  V

TGTCATCCGTCTACTCCAAGAGTTTCCTCCAAAAAGCAAGCTGGATCTTGAAGTTTATGGCAACCAAAACAGTTCAATAACCAAAGAACAC
  V  I  R  L  L  Q  E  F  P  P  K  S  K  L  D  L  E  V  Y  G  N  Q  N  S  S  I  T  K  E  H

ATAGAGAATCACCTAGATGGCCTTACTATAAACAAGGCAATGAAGAAGAAGAGGCTATTCATATTAGATGACCATGATGTTTTCATGCCAT
 I  E  N  H  L  D  G  L  T  I  N  K  A  M  K  K  K  R  L  F  I  L  D  D  H  D  V  F  M  P

ACCGGAGGAGGATAAACACAACTTCCATGAAAACTTATGCCTCAAGGACTCTCCTCTTCCTGAAAGACGACAGAACTTTGAAGCCCCTAGC
Y  R  R  R  I  N  T  T  S  M  K  T  Y  A  S  R  T  L  L  F  L  K  D  D  R  T  L  K  P  L  A

GATTGAATTGAGCCTACCACATCCCAATGGCATGGTTCAAAGTCGCGGTATCGGTCACTGA
  I  E  L  S  L  P  H  P  N  G  M  V  Q  S  R  G  I  G  H  *
```

VvLOXN

```
ATGAAGAAGAATGTGTTGGATTTTAATGACTTCAATACATCGGCTCTGAACCTGGTTCATAAGCTCTTAGGACAGGGAGTCTCTCTGCAGCTC
 M  K  K  N  V  L  D  F  N  D  F  N  T  S  A  L  N  L  V  H  K  L  L  G  Q  G  V  S  L  Q  L

ATCAGTGAGAGCTATTCGAAGCTGGCAGACATTGAAGAAATGATCATAGAGAGAAATGGAGATGAGAGATTCAAGAACAGAGTTGGGCCTTTG
 I  S  E  S  Y  S  K  L  A  D  I  E  E  M  I  I  E  R  N  G  D  E  R  F  K  N  R  V  G  P  L

AAGATACCATACACACTGCTCTATCCCACAAGCGAAGGCGGGCTTACTGGCAAAGGGATTCCCAACAGTGTCTCCATCTAA
 K  I  P  Y  T  L  L  Y  P  T  S  E  G  G  L  T  G  K  G  I  P  N  S  V  S  I  *
```

A.2.2 Amino acid alignment of identified grape LOXs with characterised plant LOXs

DNA sequences of the predicted grape LOX members were *in silico* translated into amino acid sequences and the predicted amino acid sequences were then aligned with amino acid sequences of characterised LOXs from other plant species using the ClustalW algorithm (Thompson *et al.* 1994) as described in section 3.2.2. Amino acid residues involved in binding of catalytic iron are highlighted in yellow (positions 694, 699, 900, 904 and 1066 of alignment) . Amino acid residues involved in determining LOX regiospecificity and stereospecificity are highlighted in green (position 763) and purple (position 738) respectively.

A.2.2 Amino acid alignment of identified grape LOXs with characterised plant LOXs (continued)

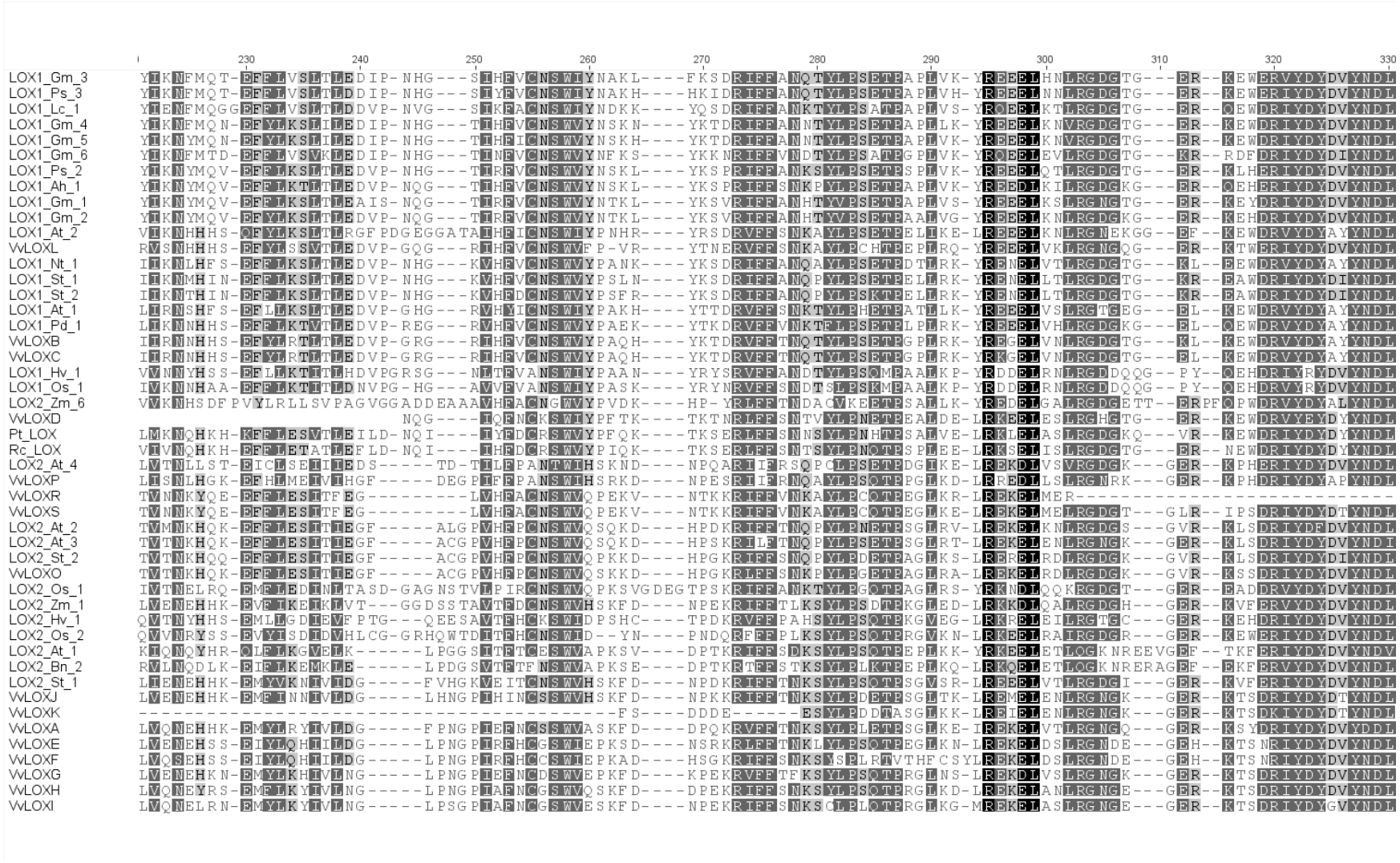

A.2.2 Amino acid alignment of identified grape LOXs with characterised plant LOXs (continued)

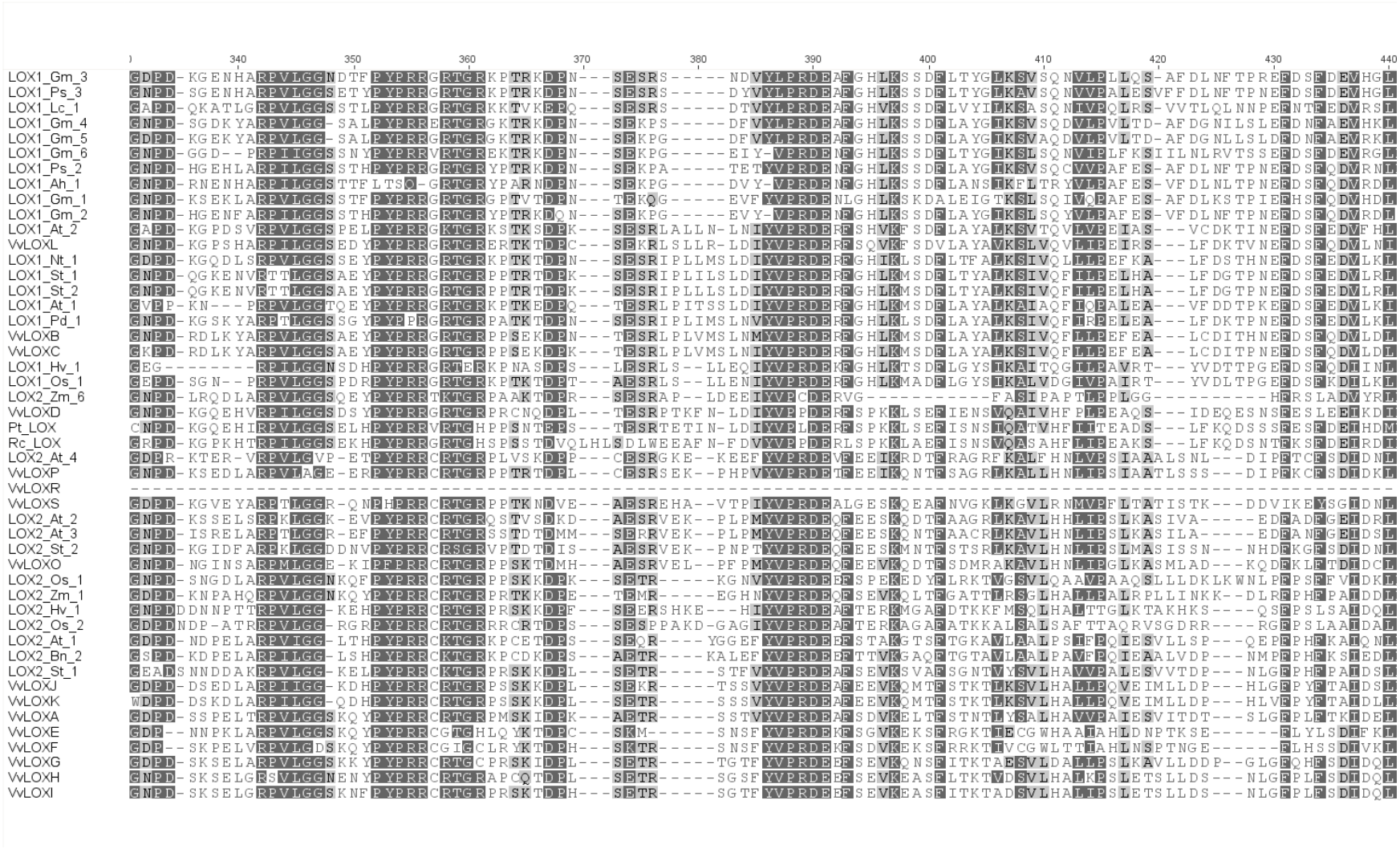

A.2.2 Amino acid alignment of identified grape LOXs with characterised plant LOXs (continued)

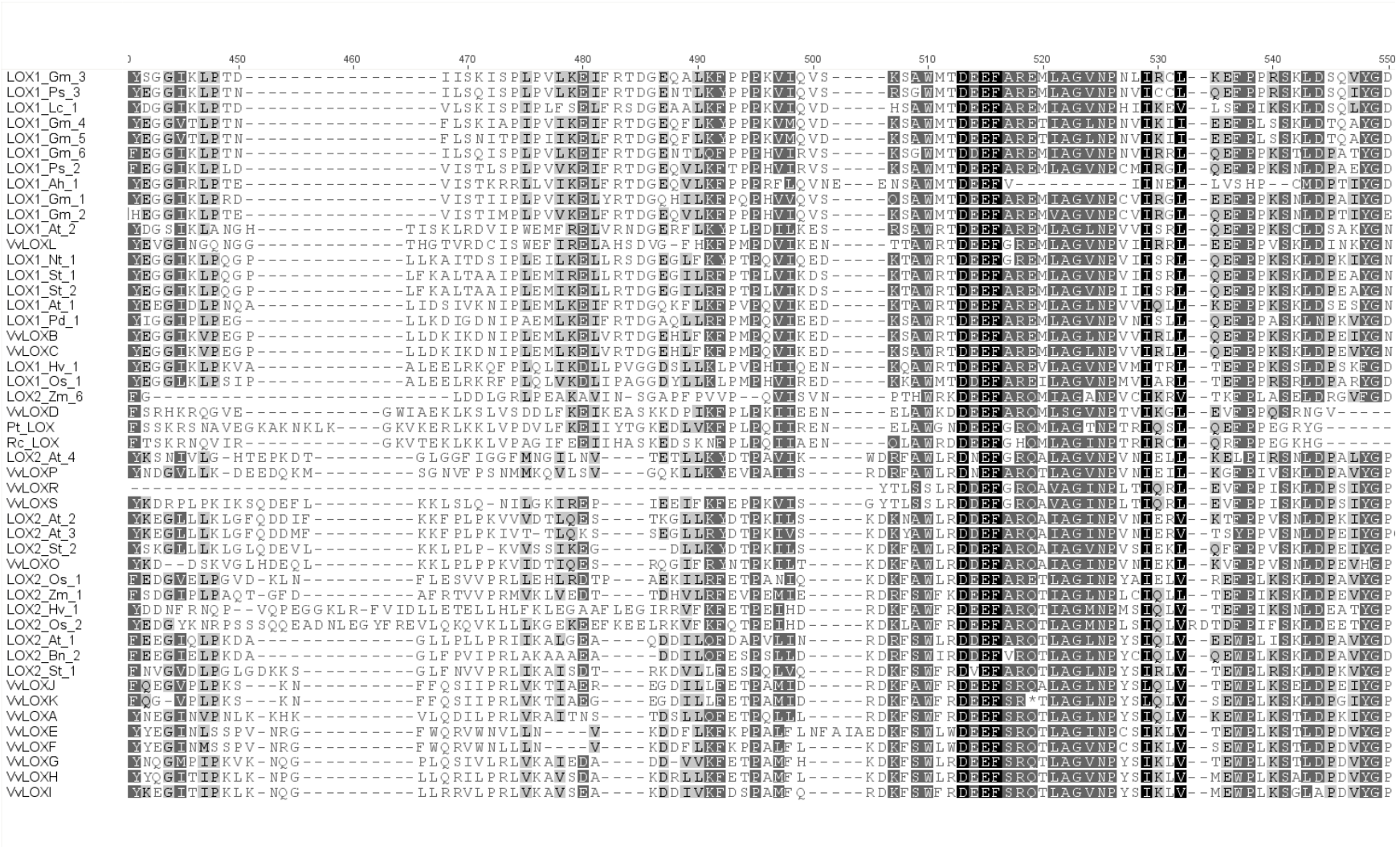

A.2.2 Amino acid alignment of identified grape LOXs with characterised plant LOXs (continued)

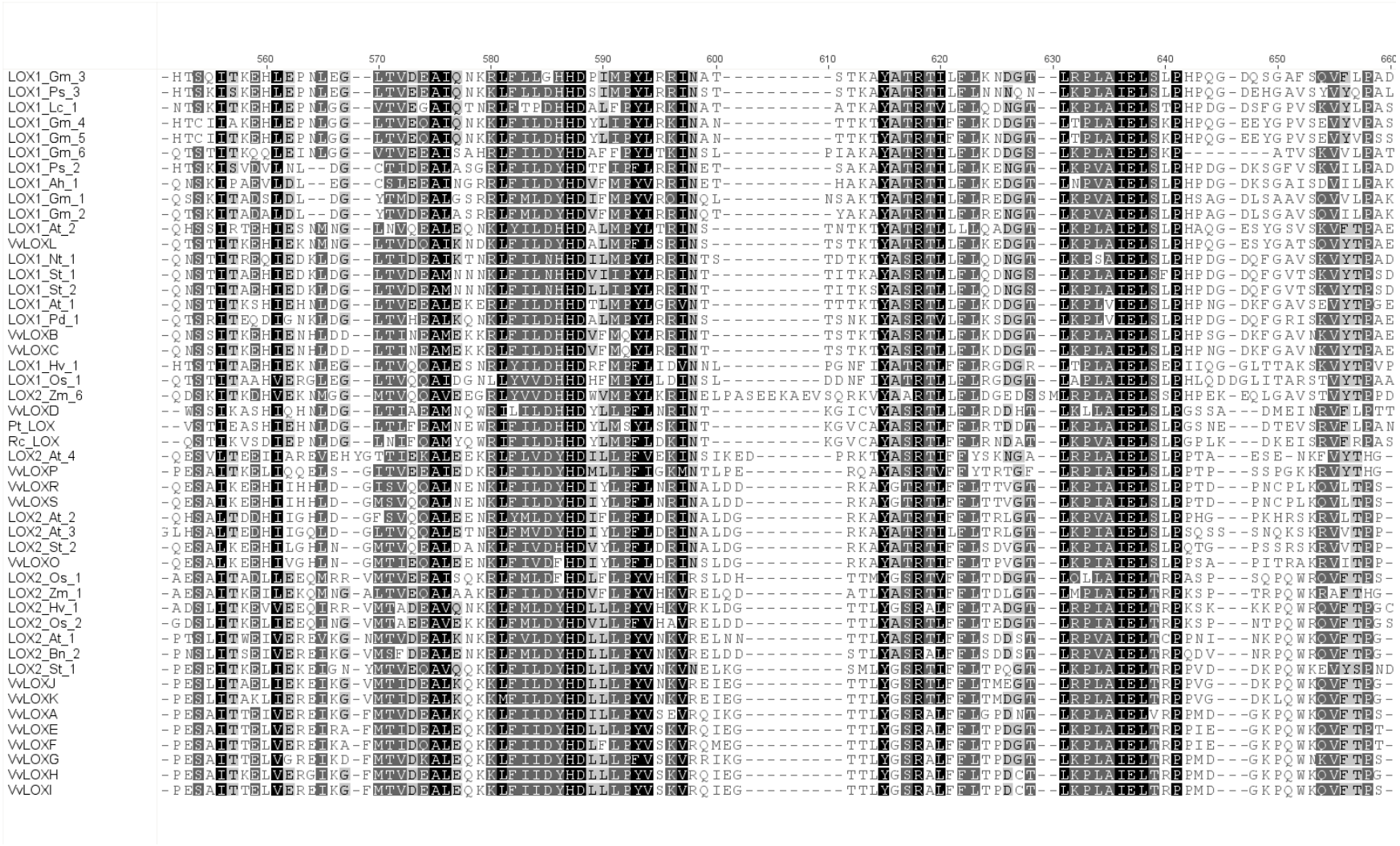

A.2.2 Amino acid alignment of identified grape LOXs with characterised plant LOXs (continued)

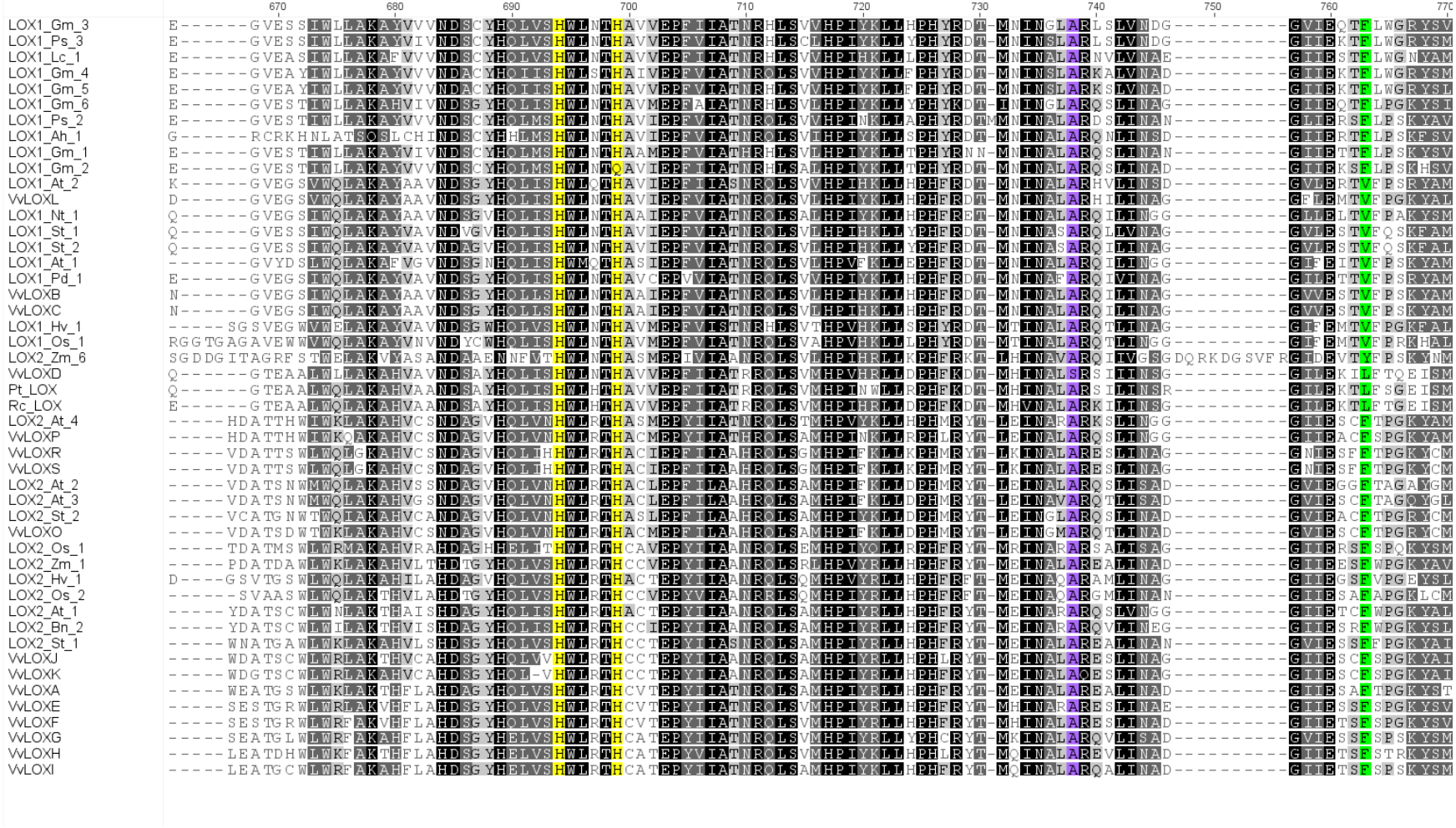

A.2.2 Amino acid alignment of identified grape LOXs with characterised plant LOXs (continued)

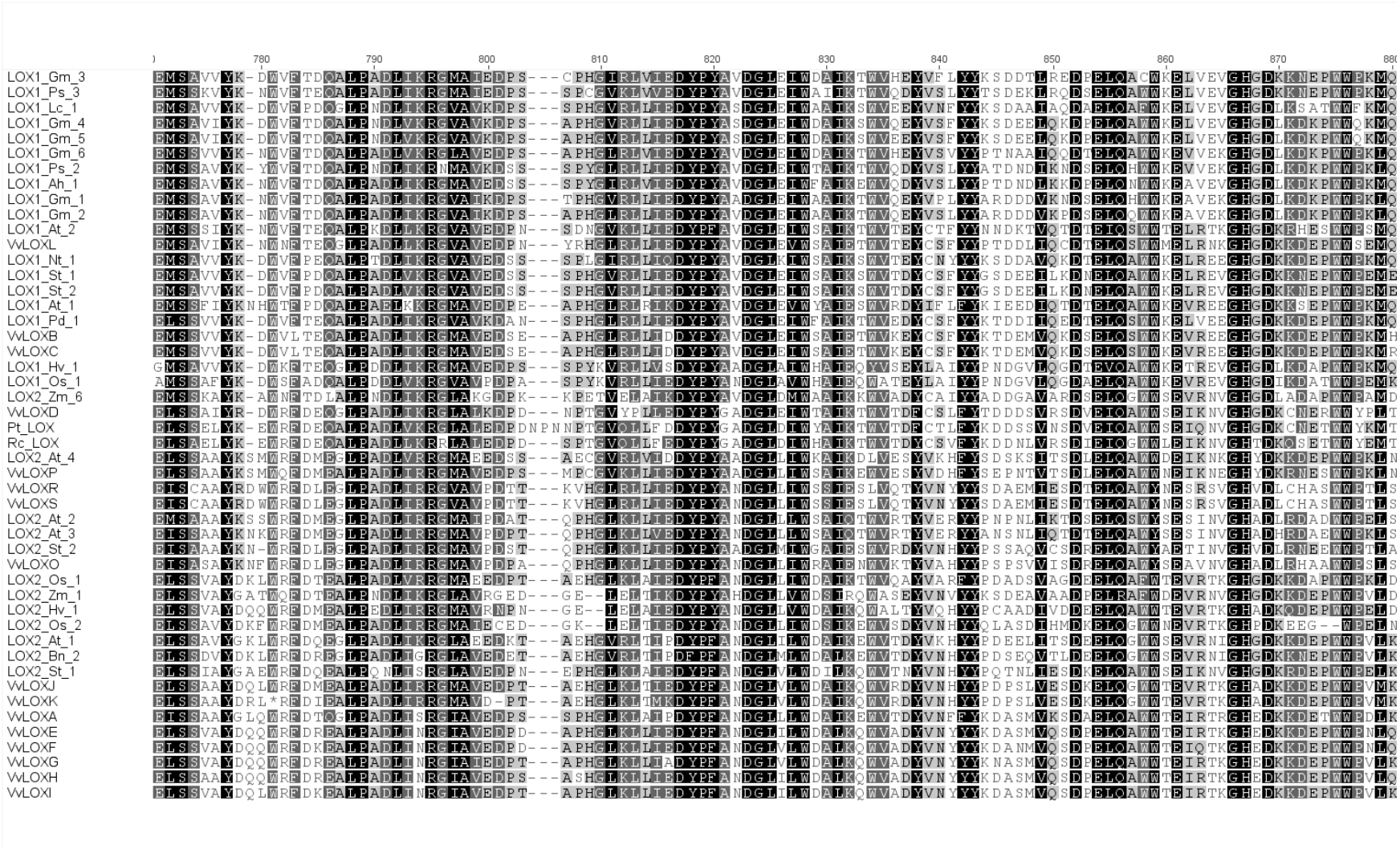

A.2.2 Amino acid alignment of identified grape LOXs with characterised plant LOXs (continued)

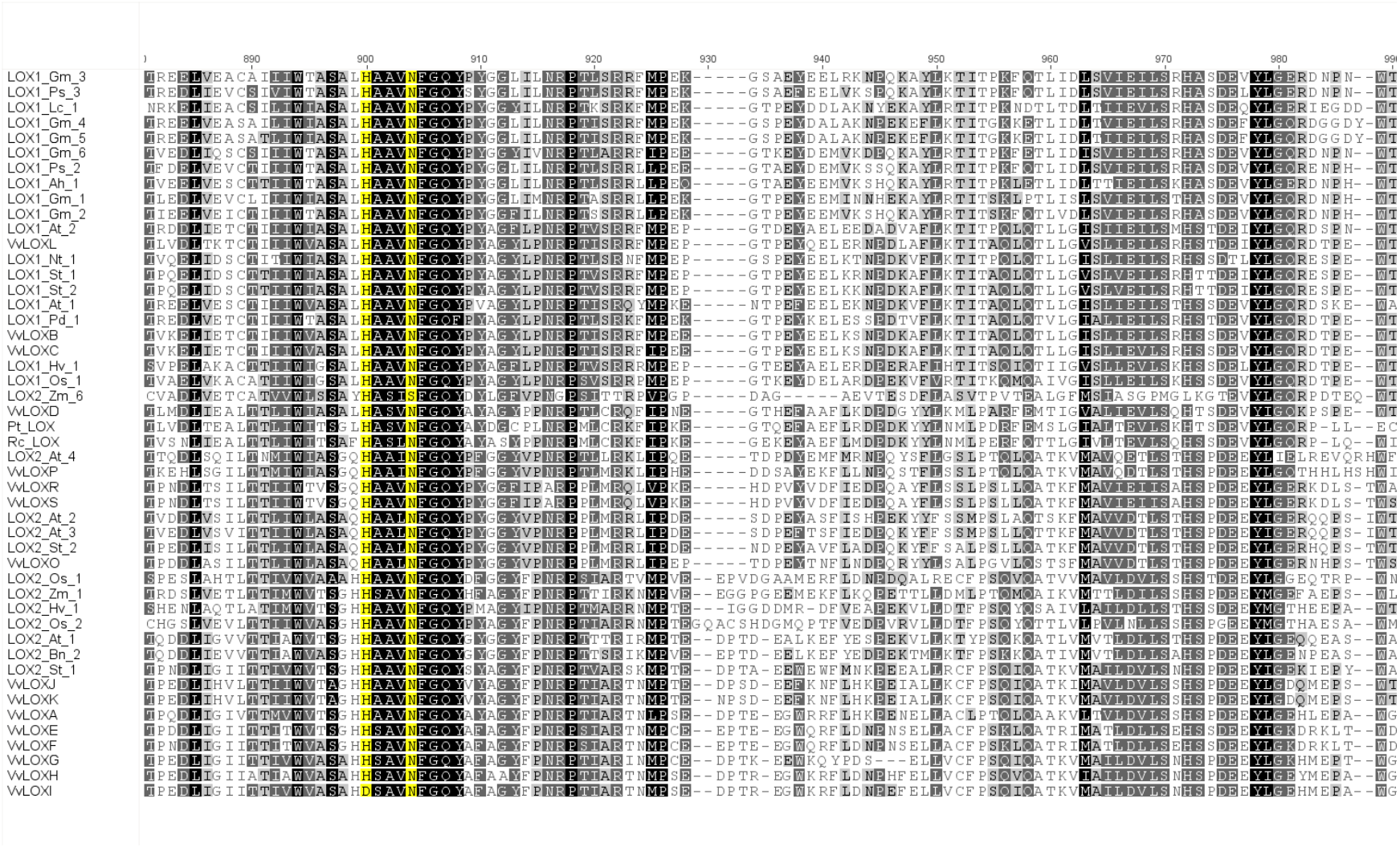

A.2.2 Amino acid alignment of identified grape LOXs with characterised plant LOXs (continued)

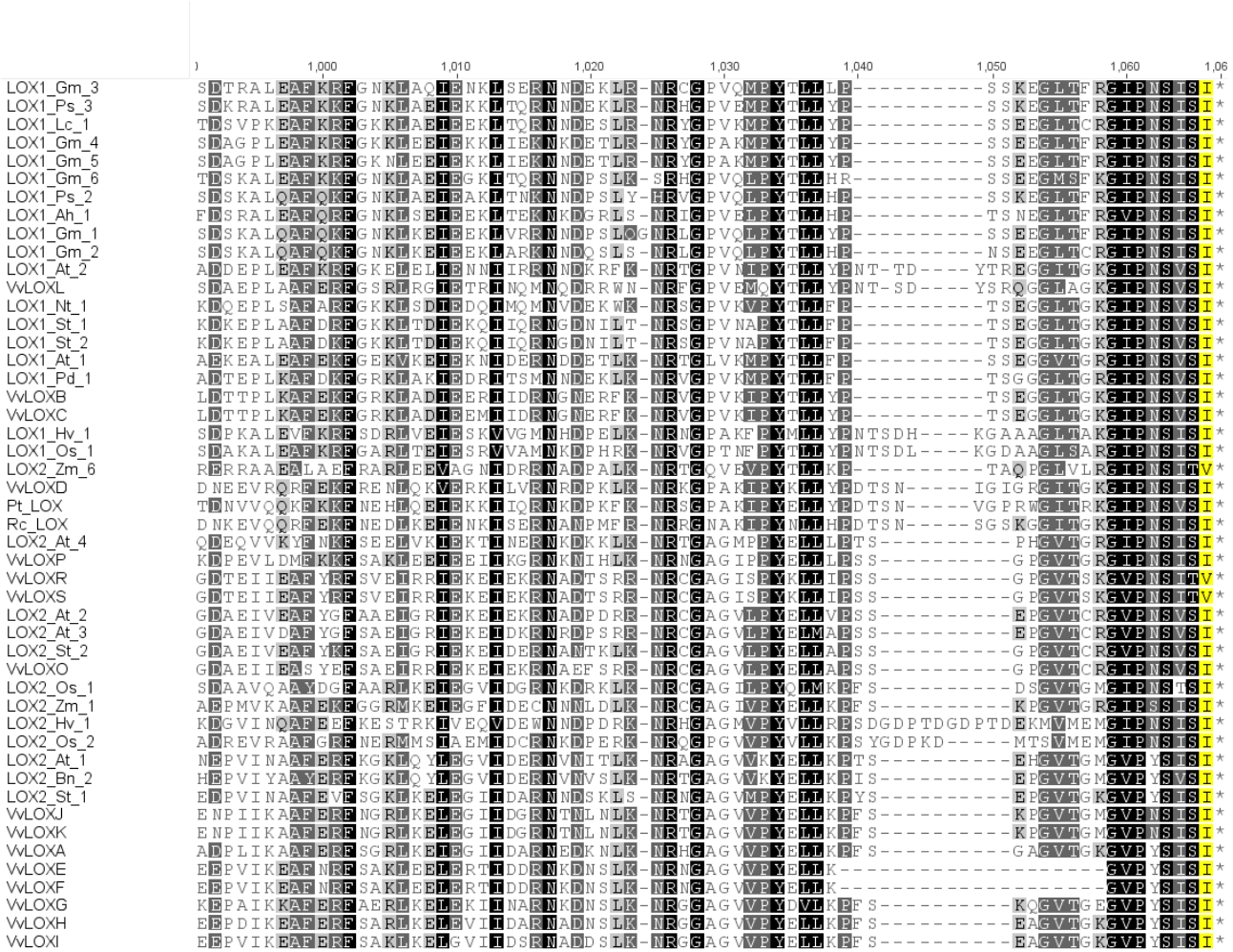

A.2.3 Phylogenetic tree constructed based on the alignment of conserved LOX regions of identified grape and characterised LOXs

To check if variation or missing sequence information in the N-terminal regions of the studied proteins affects their phylogenetic relationship, a part of the alignment (upstream of position 273, Appendix A.2.2) has been removed and a new unrooted phylogenetic tree was generated using the neighbour-joining method (Saitou and Nei 1987) applying 1000 bootstrap replicates as described in section 3.2.2.

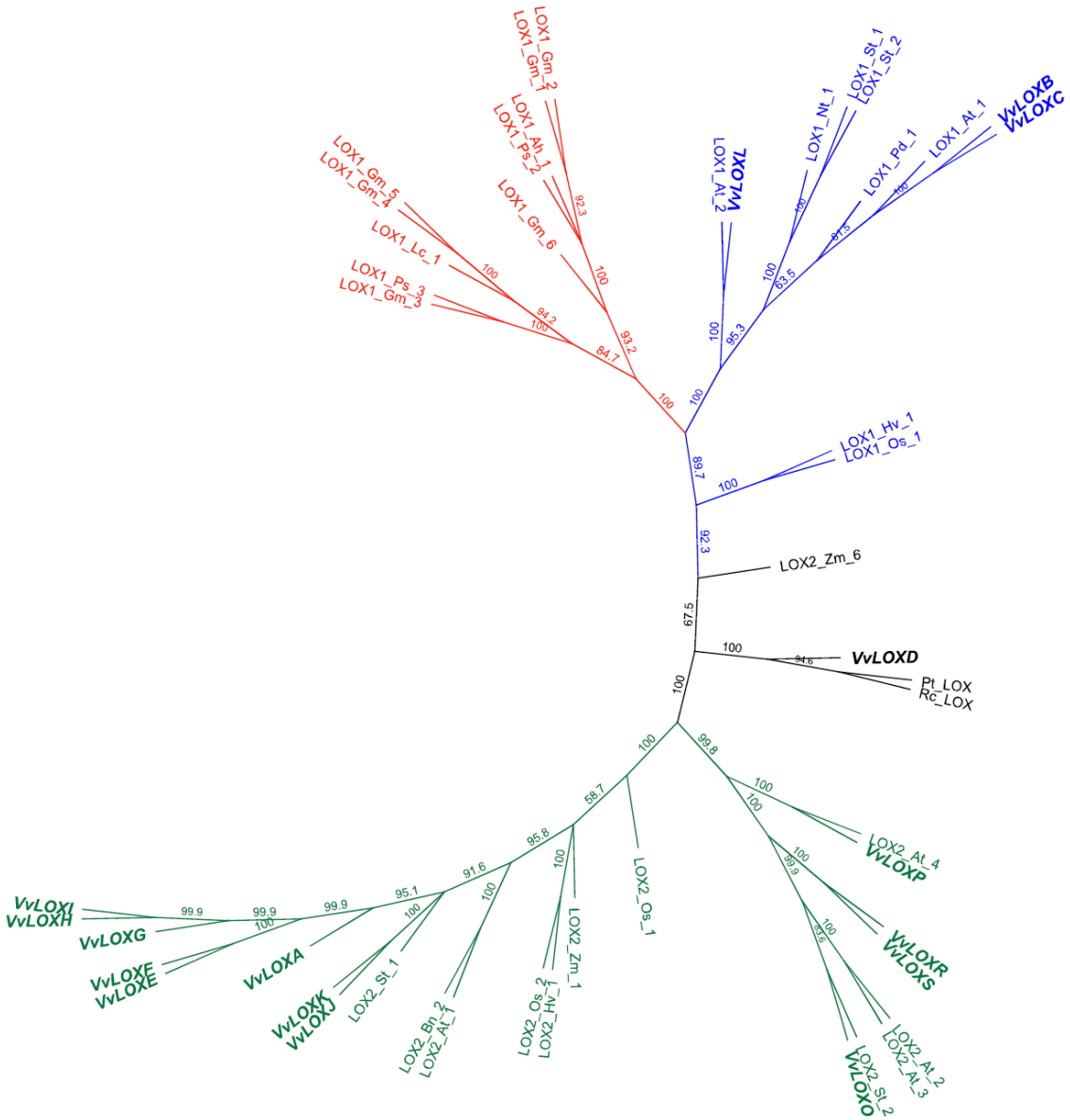

A.2.4 Amino acid alignment of identified grape CYP74 members with characterised CYP74s from other plant species

DNA sequences of the predicted grape CYP74 members were *in silico* translated into amino acid sequences and the predicted amino acid sequences were then aligned with amino acid sequences of characterised CYP74s from other plant species using the ClustalW algorithm (Thompson *et al.* 1994) as described in section 3.2.2. An 9 aa-insertion into the FxxGx$_3$CxG cytochrome P450 signature motif (residues 495-503) is highlighted in red. Amino acid residues involved in binding the catalytic molecule of haem are highlighted in blue (positions 157, 188, 192 and 505 of alignment). Amino acid residues serving as protein contributing ligands of Fe(III) molecule are highlighted in orange (position 507). The active site residues important for substrate binding and determining the mechanism of catalysis specific for different groups of CYP74 (see section 4.3.3) are highlighter in yellow (positions 161 and 179).

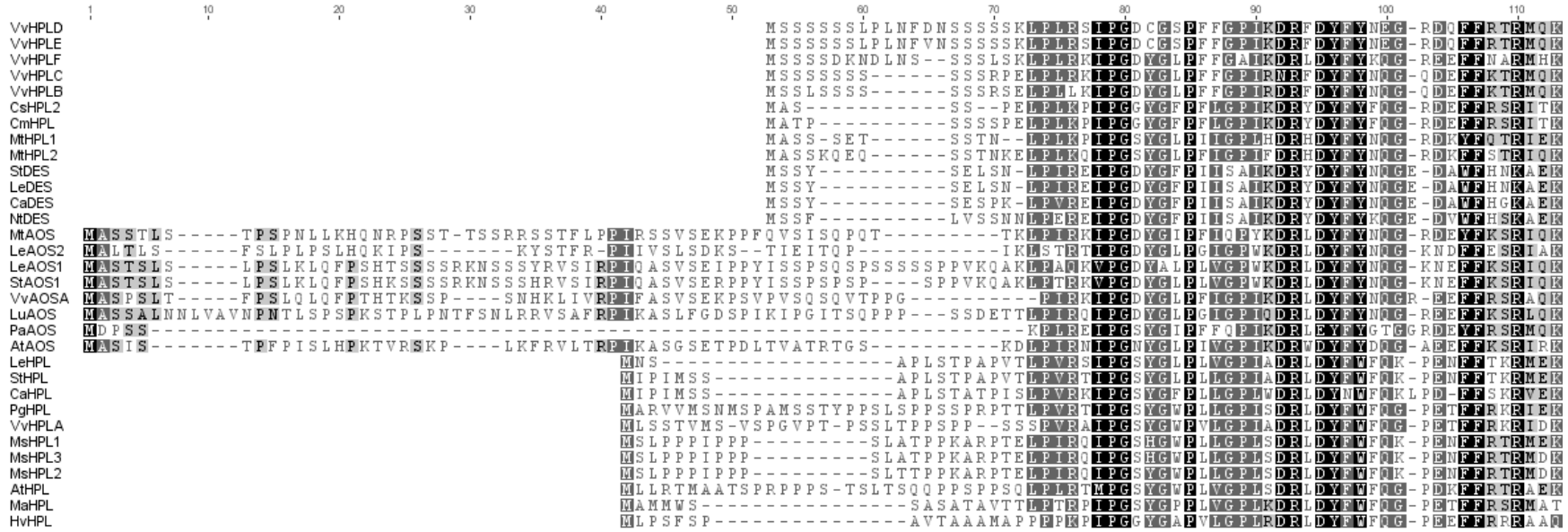

A. 2.4 Amino acid alignment of identified grape CYP74s with other plant CYP74s (continued)

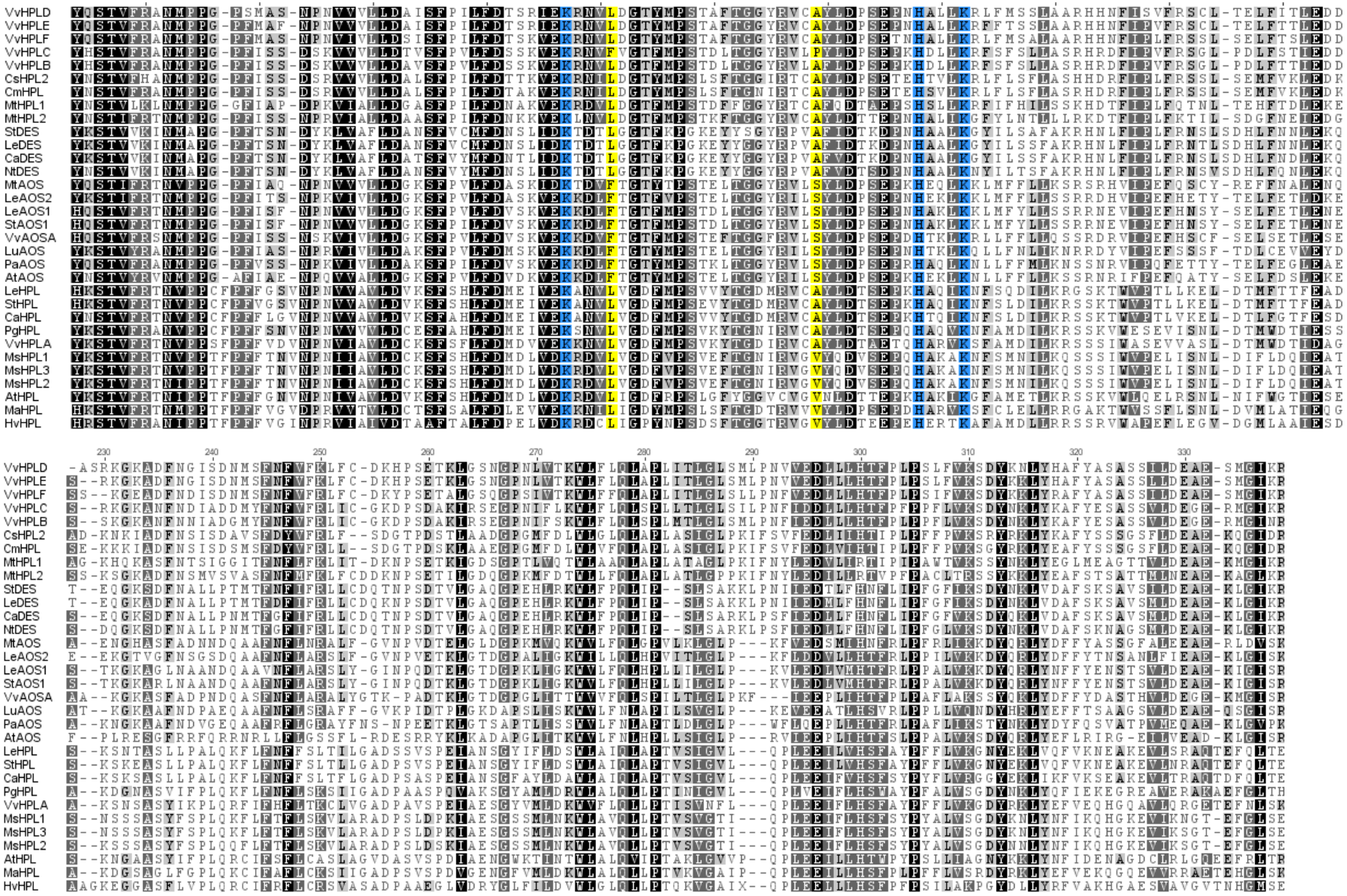

A. 2.4 Amino acid alignment of identified grape CYP74s with characterised plant CYP74s (continued)

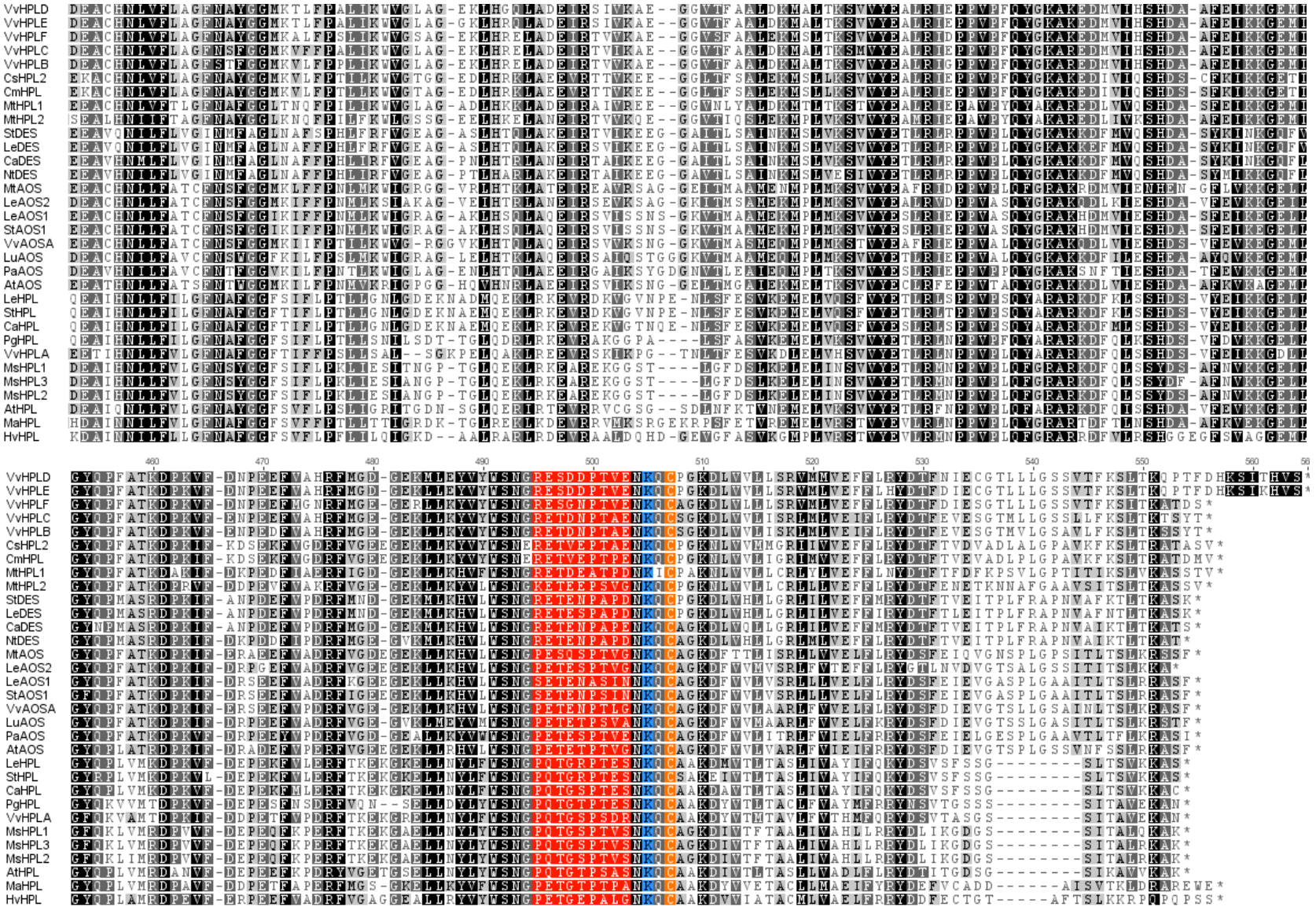

A.3 Appendices: Expression study of berry LOXs and HPLs

A.3.1 Nucleotide alignment of *VvLOXA* variants

Nucleotide coding sequences of 6 VvLOXA clones were aligned and analysed as described in section 5.3. Positions of sequence variation between clones are highlighted. A region selected for further analysis using Sauvignon blanc genomic DNA from different genotypes is outlined by dashed-line box (Appendix A.3.2).

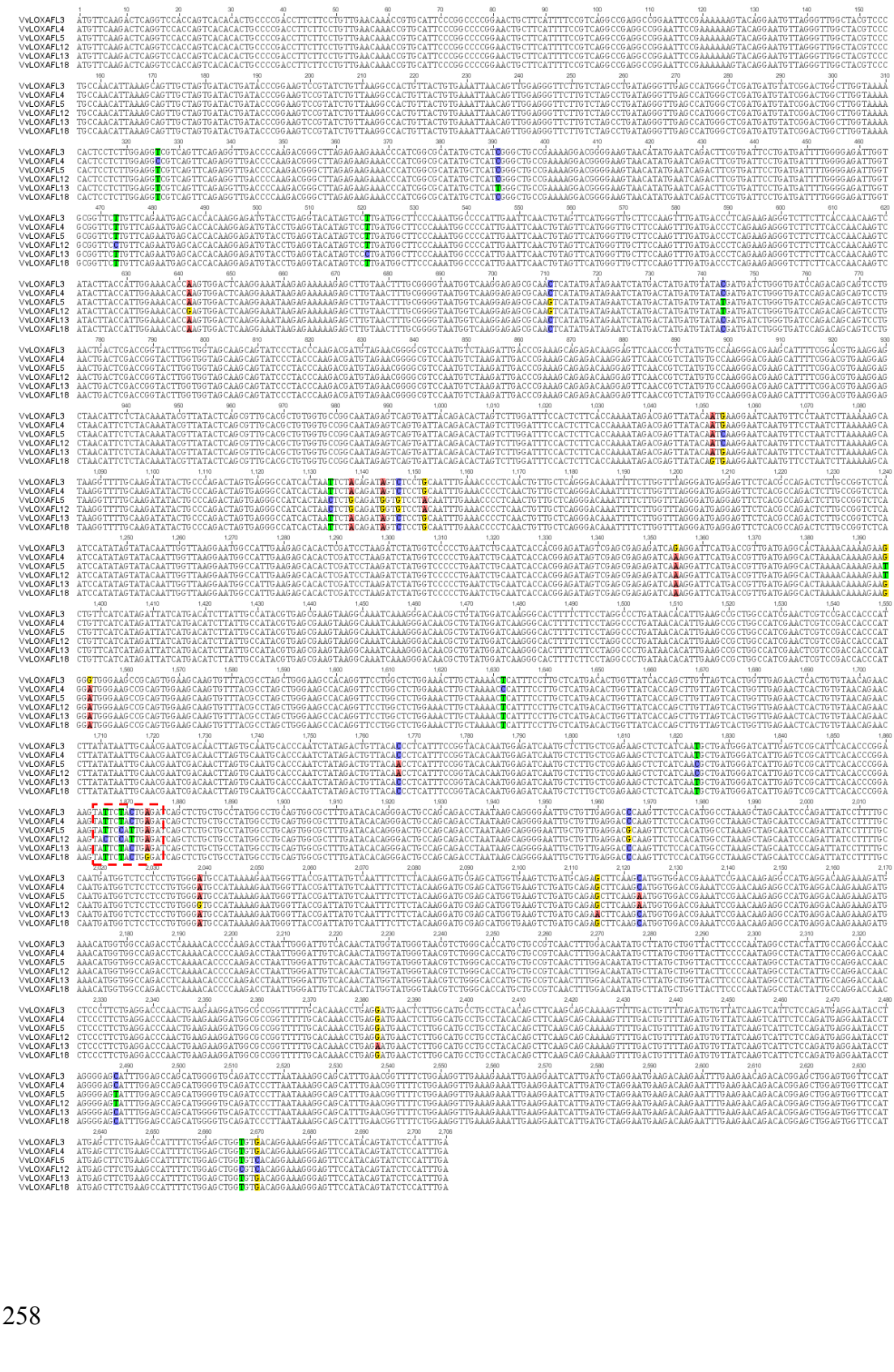

A.3.2 Traces alignment of VvLOXA variants

An 80 bp region of *VvLOXA* CDS containing 4 putative SNPs was PCR-amplified using gDNA from six different vines, and sequence chromatograms of obtained PCR products were compared to the corresponding regions of transcript *VvLOXA* variants (Appendix A.3.1) as described in section 5.3. Positions of the putative SNPs are highlighted and numbered 1 to 4. The top six chromatograms represent *VvLOXA* variants (labelled VvLOXA3, 4, 5, 12 13 and 18), while chromatograms corresponding to PCR products amplified from the genomic DNA of six different vines are positioned at the bottom of the alignment and labelled SB6, 12, 18, 20, 24 and 27.

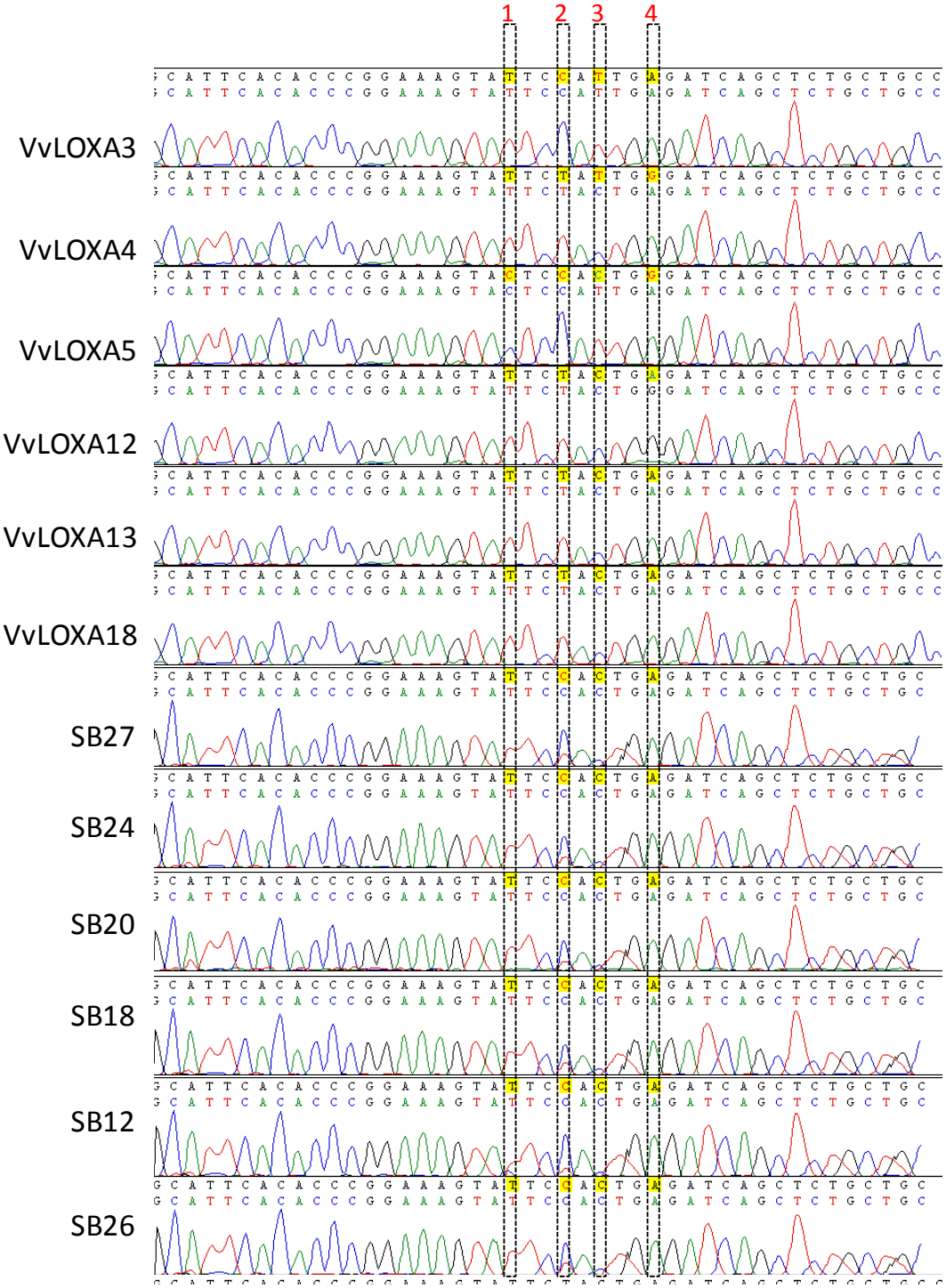

A.3.3 Superimposed 3D protein models of VvLOXA variants

Predicted amino acid sequences of six VvLOXA variants were used to predict the spatial configuration of the corresponding protein using Swiss-PDB viewer software with crystal structure of soybean LOX-1 as template as described in section 5.3. The predicted 3D models of six VvLOXA variants were then superimposed in order to deduce structural alignments and compare their active sites. Arrow indicates positions of iron-binding ligands.

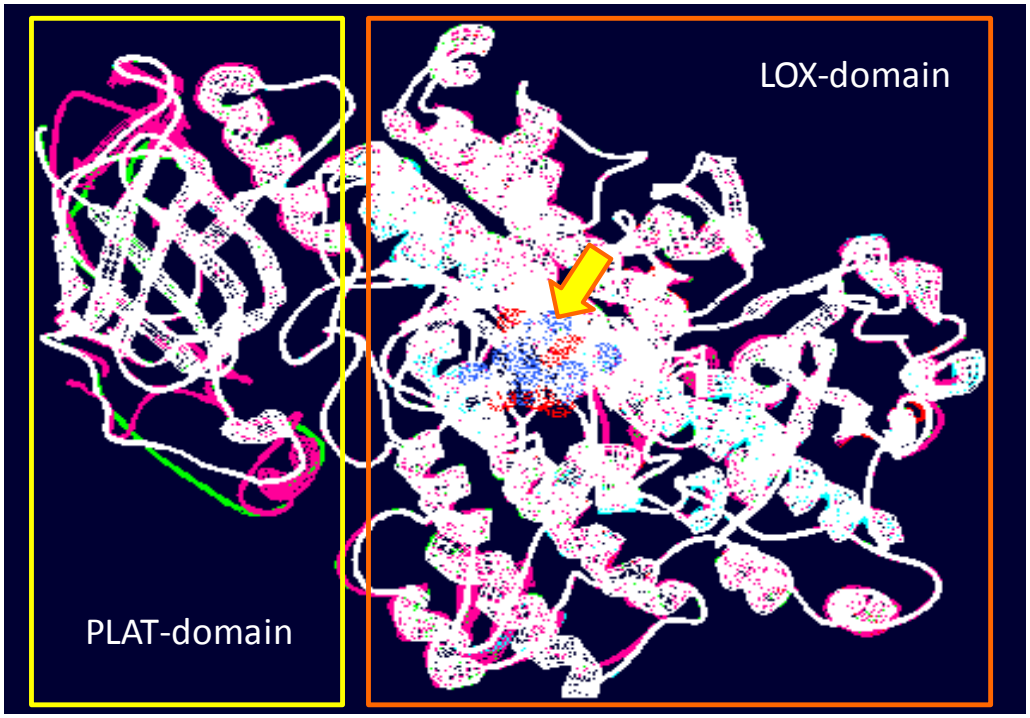

A.3.4 Nucleotide alignment of the deduced *VvLOXD* sequence with homologous sequences from other plants

Sequence of the largest *VvLOXD* fragment obtained by 5´RACE experiment was aligned with the two nearest matches identified in the GenBank, *Rc_LOX* (XM_002527220) from *Ricinus communis* and *Pt_LOX* (XM_002320535) from *Populus trichocarpa* as described in section 5.3. Predicted translation initiation sites for Rc_LOX and Pt_LOX highlighted in red.

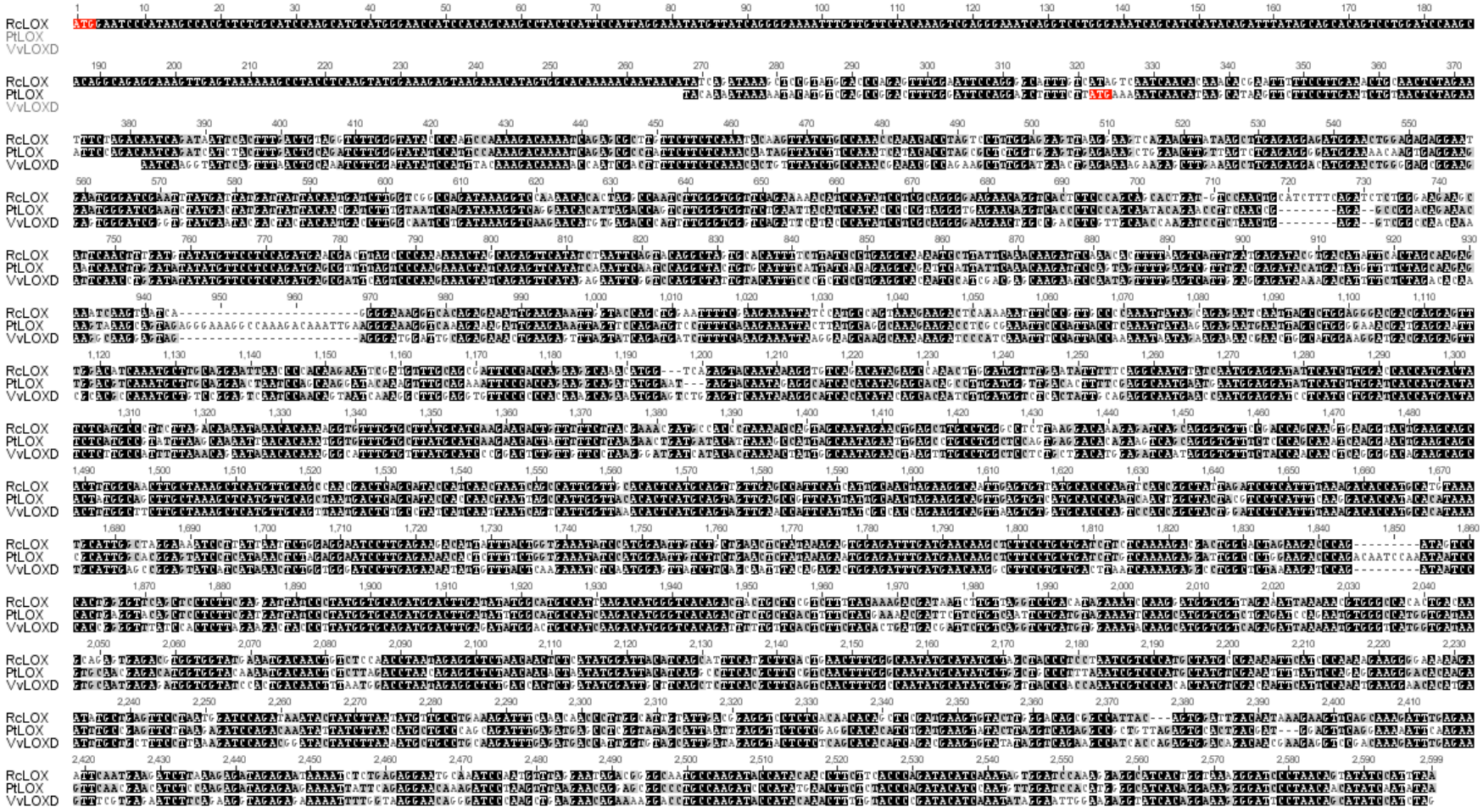

A.3.5 Expression stability test for four reference genes

The geNorm VBA applet for Microsoft Excel (Vandesompele *et al.* 2002) was used to evaluate expression stability of *Actin* (actin 1, XM_002282480), *GAPDH* (glyceraldehyde-3-phosphate dehydrogenase, XM_002263109), *SAND* (SAND family protein, XM_002285134), *EF1* (elongation factor-1 alpha, XM_002284888) genes in samples from different experiments as described in sections 3.8 and 5.4.1. The graphs represent the results of analysis conducted for four sets of samples: A – berry development, B – berry fractions, C – wounding experiment, D – pathogen infection experiment.

(A)

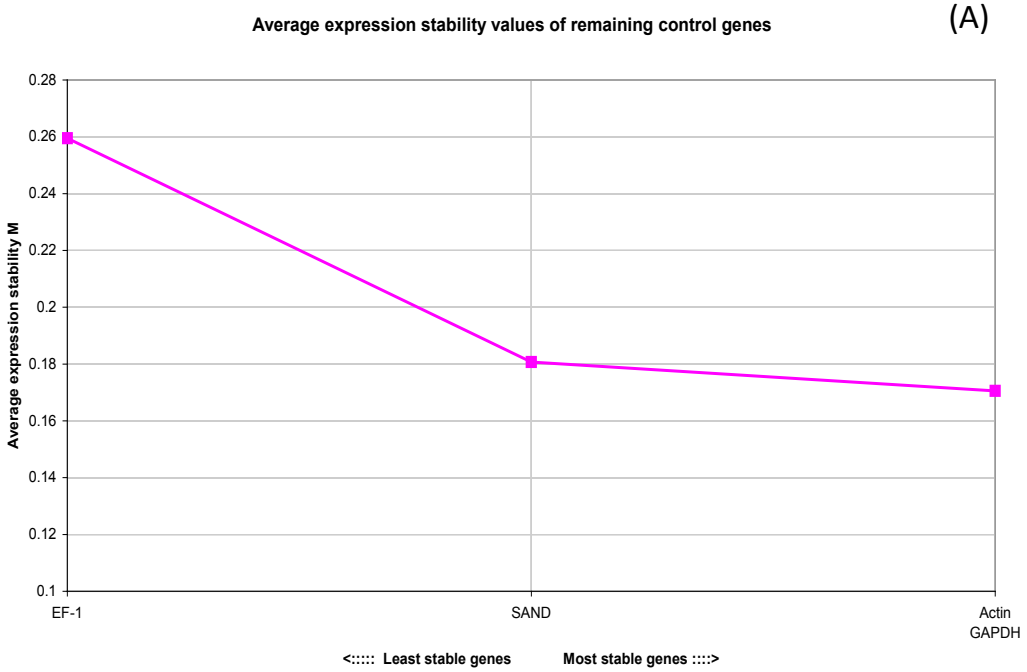

(B)

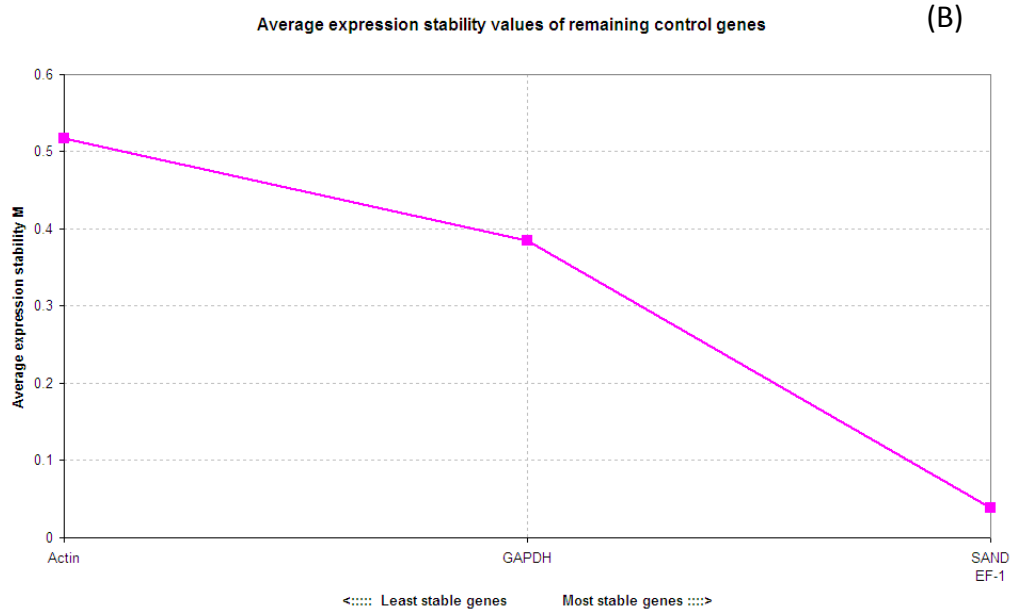

A. 3.5 Expression stability test for four reference genes (continued)

(C)

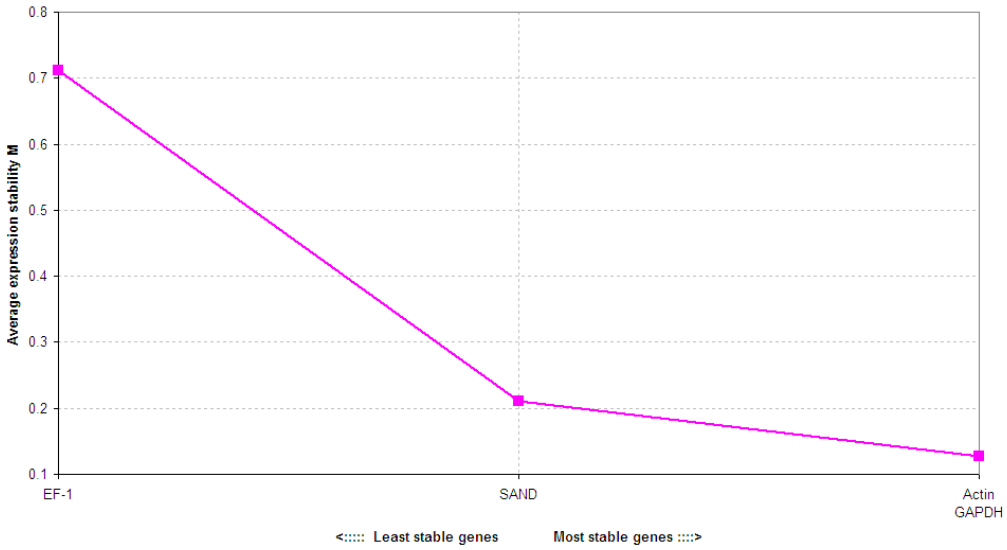

(D)

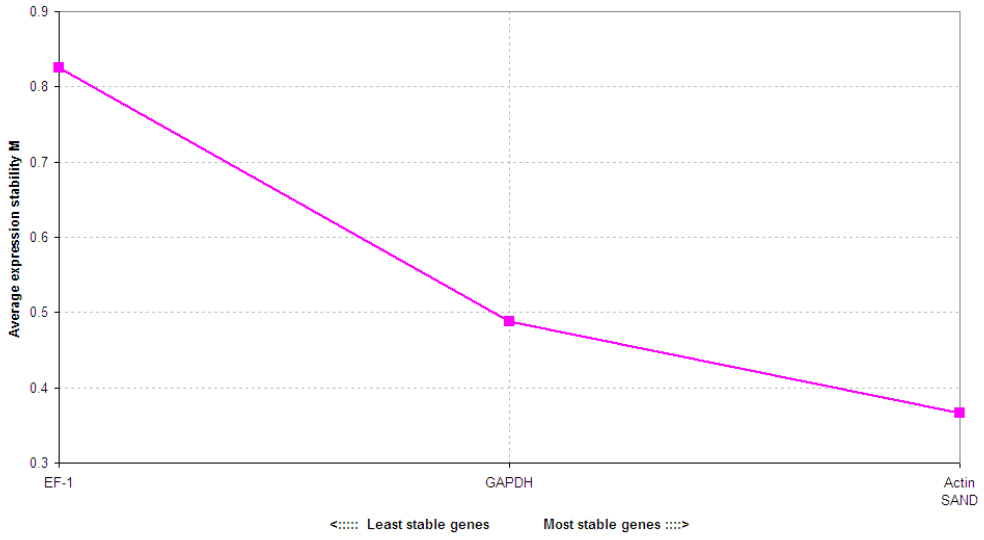

A.3.6 An example of qPCR standard curves

Standard curves were generated using a series 1:10 dilutions of standards, which were prepared as described in section 3.8. The screenshot below represent a typical example of the results obtained using Rotor-Gene™ 6000 real-time rotary analyser (Corbett, BioStrategy, Auckland, New Zealand) during qPCR experiments with serial dilutions of standards to generate standard curves and estimate amplification efficiency for each gene.

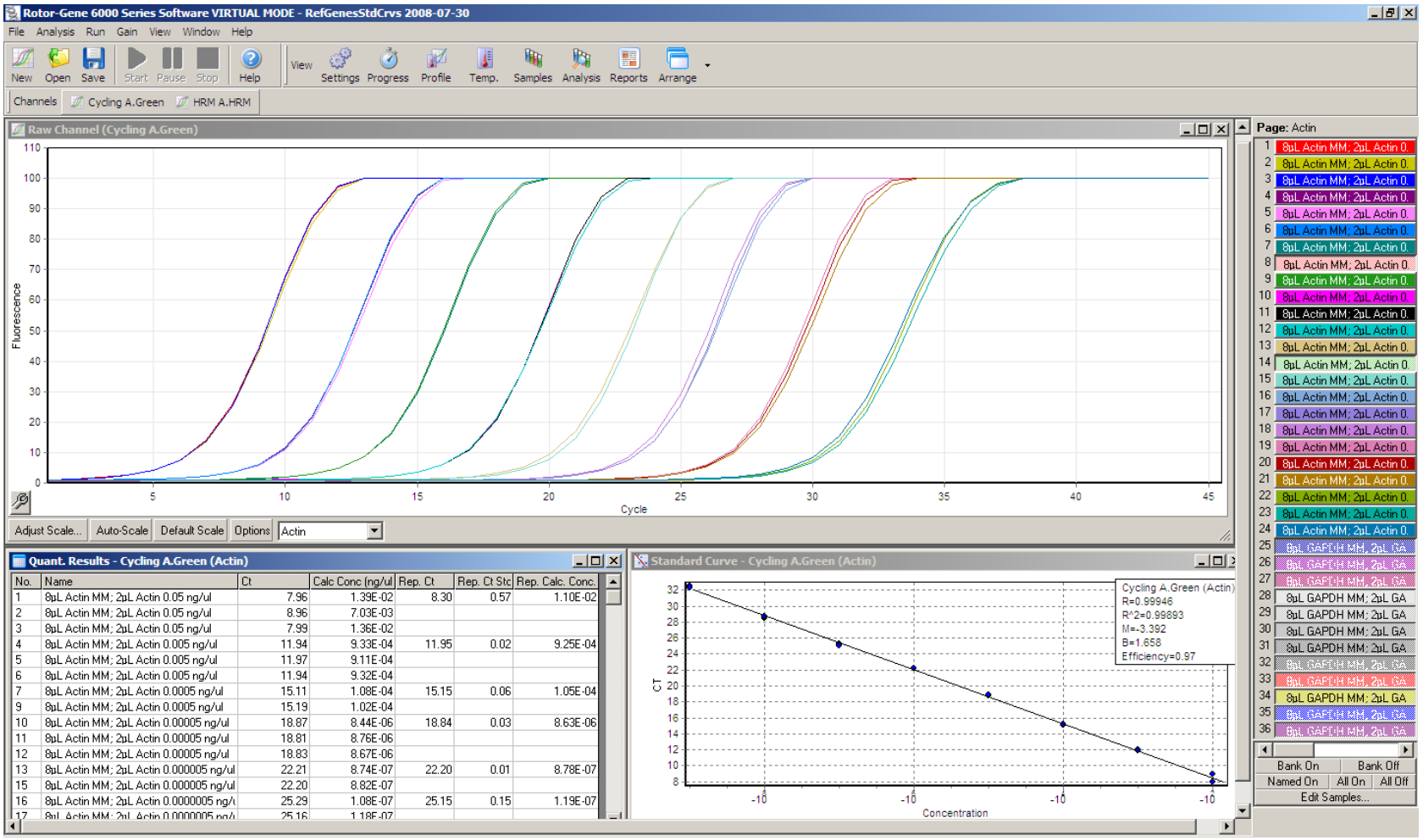

A.4 Appendices: Heterologous expression and biochemical characterisation of individual LOXs and HPL

A.4.1 General workflow for preparation of recombinant protein expression construct using Gateway® technology

Gene of interest (GOI) was PCR-amplified using forward primer containing 5'-CACC-overhand and blunt-end reverse primer (**A**). The resulted PCR product was cloned directionally into a pENTR™/TEV/D-TOPO® vector using Topoisomerase I-containing mix (**B**). The pENTR vector containing GOI was then propagated in non-expressing *E.coli* host cells and used in a subsequent LR-reaction for recombinant cloning of GOI into Gateway®pDEST17 expression vector (**C**).

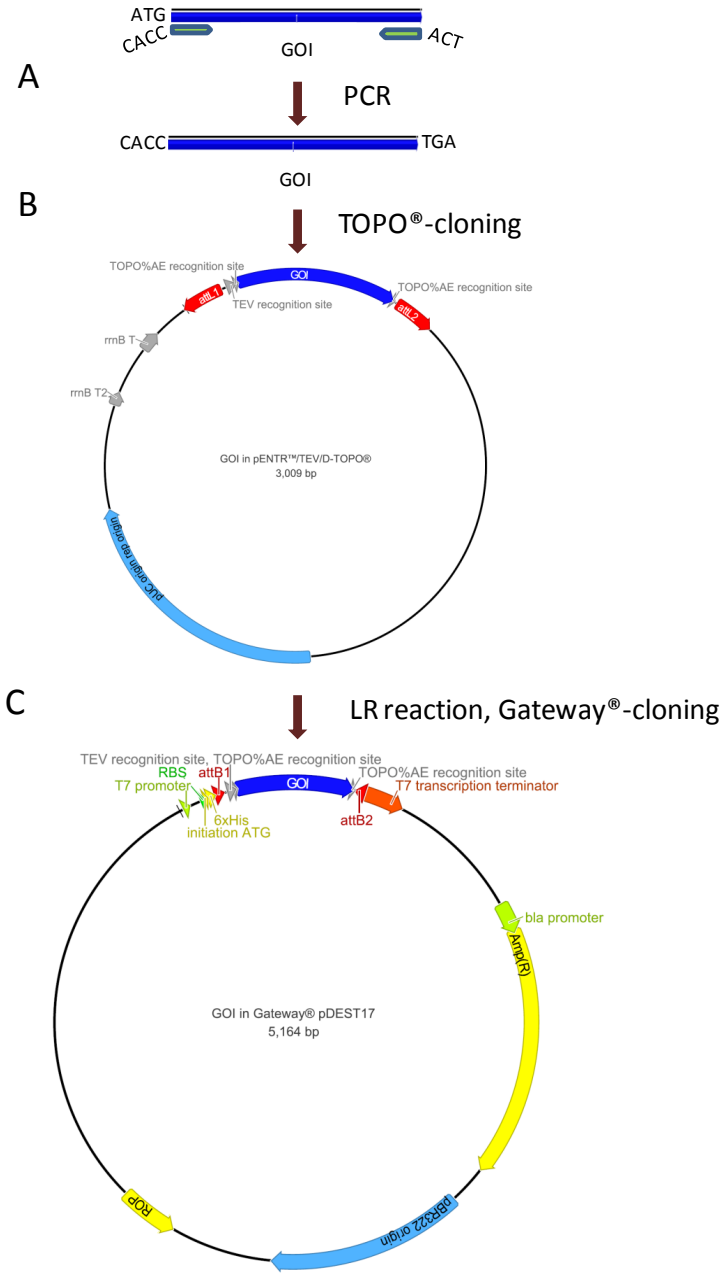

A.4.2 The regions of LOXAFL and LOXA-TP protein expression constructs

VvLOXA recombinant protein expression constructs were generated as described in section 3.9.1. Panel A schematically represents aligned regions of pDEST17-constructs containing LOXAFL and LOXA-TP coding sequences. Panel B shows a region of aligned amino acid sequences of the recombinant LOXAFL and LOXA-TP proteins.

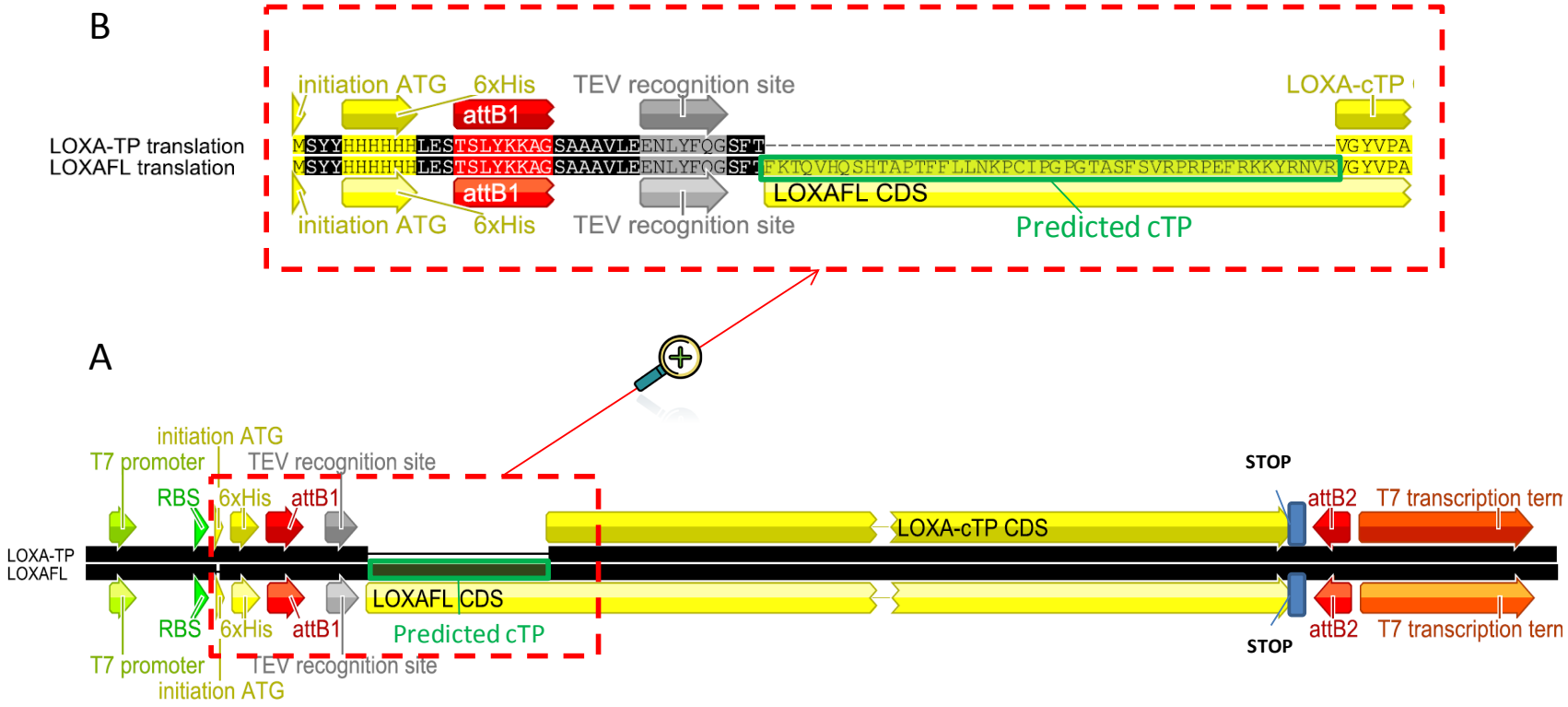

A.4.3 Activity check of LOXA-TP soluble fractions

10 µg of the soluble protein fractions of *E. coli* crude extracts expressing LOXA-TP constructs were incubated with LnA substrate (final concentration=60 µM) in 3 mL of sodium acetate buffer (pH 5.5), monitoring changes in absorbance at 234 nm. Grey, red and green curves indicate the activity of the extract before induction, post-induction after incubation at 14°C for 18 hours and heat-treated extract respectively.

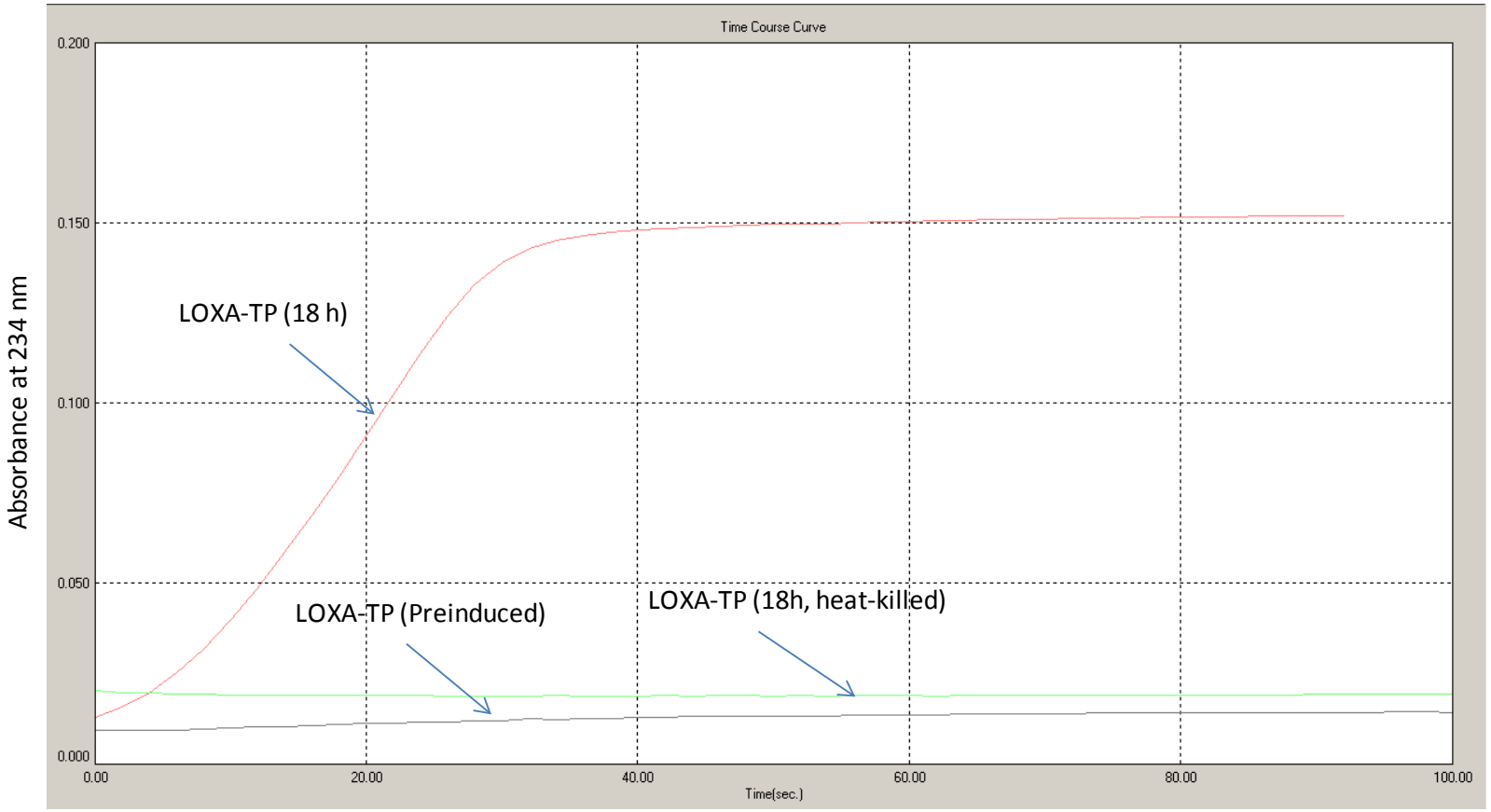

A.4.4 Purification of recombinant LOXA-TP with various concentration of imidazole in the wash buffer

Recombinant LOXA-TP protein was expressed as described in section 3.9.2 and extracted as described in section 3.9.3. The crude protein extract was then loaded onto 3×1mL pre-equilibrated HisTrap™ FF Columns (GE Healthcare Life Sciences, Global Science, Auckland, New Zealand) connected in series. The columns were subsequently washed with a number of washing steps, increasing concentration of imidazole at each subsequent step. Collected at each step during purification protein fractions were separated on NuPAGE® 4-12% Bis-Tris gel and stained with Fast Blue protein stain. The lanes are labelled as follows: **1** - total soluble fraction, **2** – HisTrap flowthrough fraction, **3** – column wash fraction (30 mM imidazole), **4** – column wash fraction (35 mM imidazole); **5** – column wash fraction (40 mM imidazole), **6** – column wash fraction (45 mM imidazole), **7** – column wash fraction (50 mM imidazole), **8** – first eluted fraction, **9** – second eluted fraction. Red arrow indicates expected band positions for the recombinant LOXA-TP protein. **PM** – Precision Plus Protein standard.

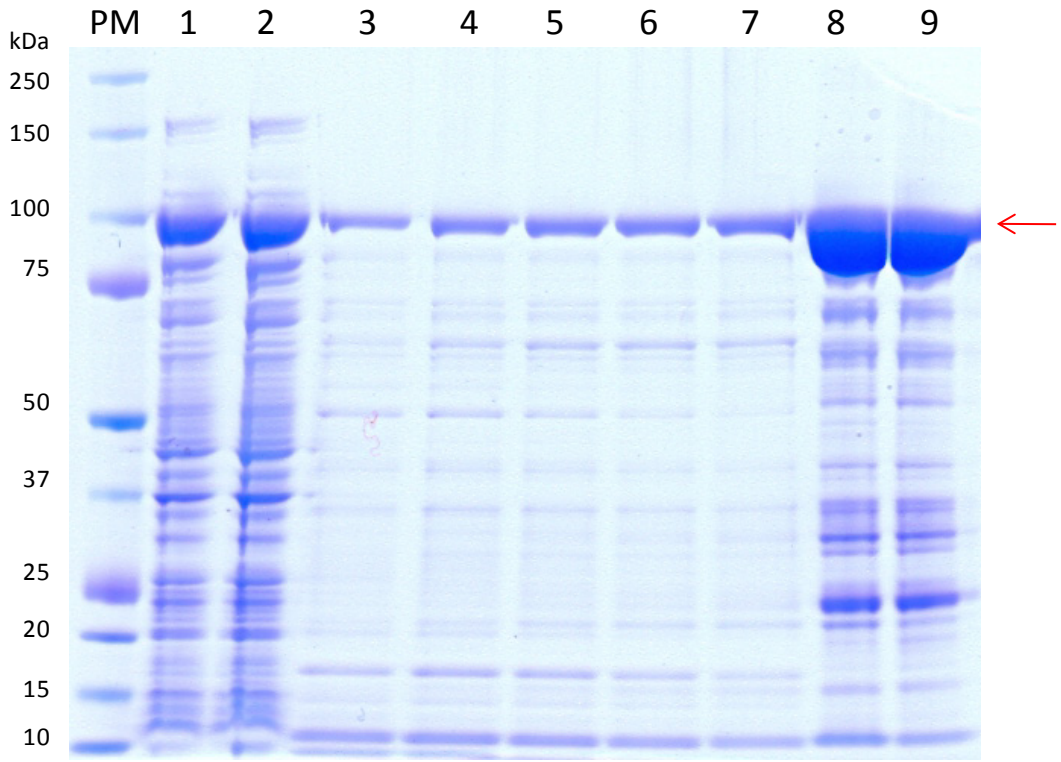

A.4.5 Activity check of LOXO-TP soluble fractions

10 µg of the soluble protein fractions of *E. coli* crude extracts expressing LOXO-TP constructs were incubated with LnA substrate (final concentration=300 µM) in 3 mL of sodium phosphate buffer (pH 7.5), monitoring changes in absorbance at 234 nm. Grey, red and blue curves indicate the activity of the extract from expressed at 14°C, 37°C and heat-treated extract respectively.

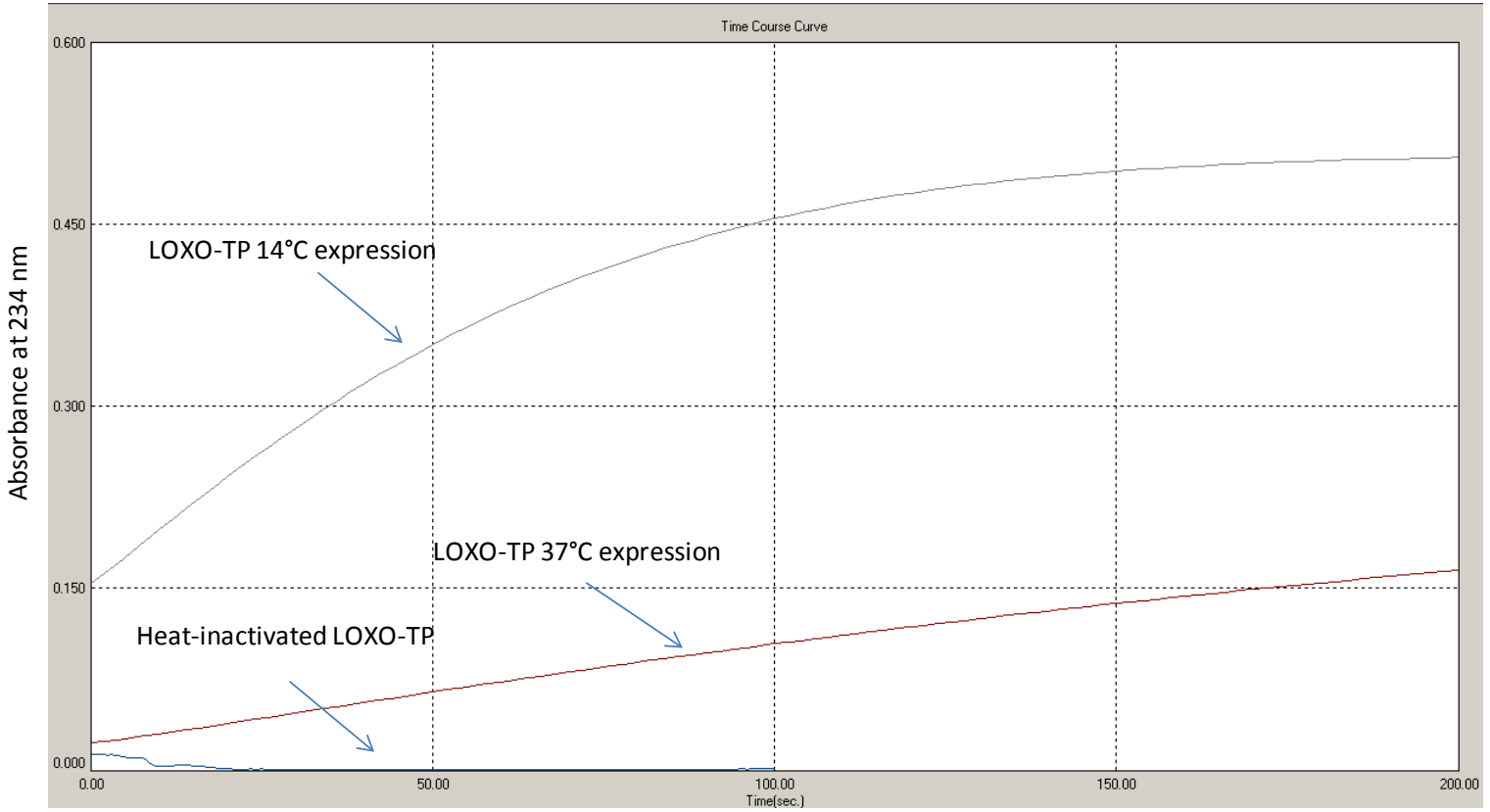

A.4.6 Stability of recombinant LOXO-TP protein

Stability of LOXO-TP IMAC-purified fraction was monitored over 90 minutes. Activity of freshly-thawed from stored at -80°C protein sample was measured as changes in absorbance at 234 nm and expressed as 100% activity. Subsequent measurements were taken at 15 minutes interval and plotted on the graph relative to the activity of the freshly-thawed protein. Error bars represent SD for two replicates.

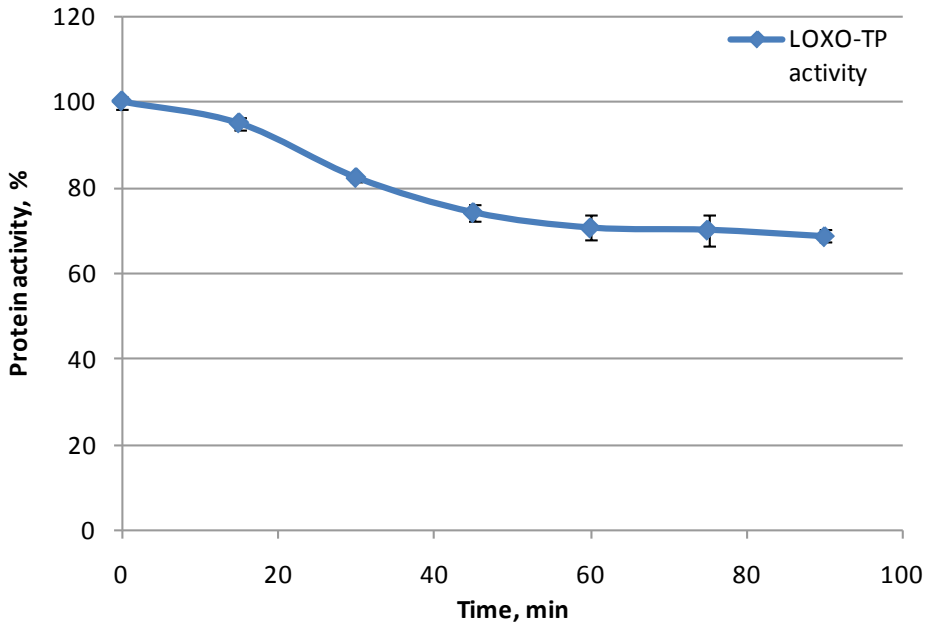

A.4.7 Preliminary HPL activity test of HPLAFL and HPLA-TP soluble and "membrane" fractions

Twenty microlitres of the soluble and "membrane" protein fractions of *E. coli* crude extracts expressing HPLAFL and HPLA-TP constructs were incubated with LnA-hydroperoxide substrate (final concentration=17 µM) in 3 mL of sodium acetate buffer (pH 5.0), monitoring changes in absorbance at 234 nm. Black and red lines correspond to results of incubation soluble fractions of HPLAFL and HPLA-TP and green and blue lines correspond to "membrane" fractions of HPLAFL and HPLA-TP respectively.

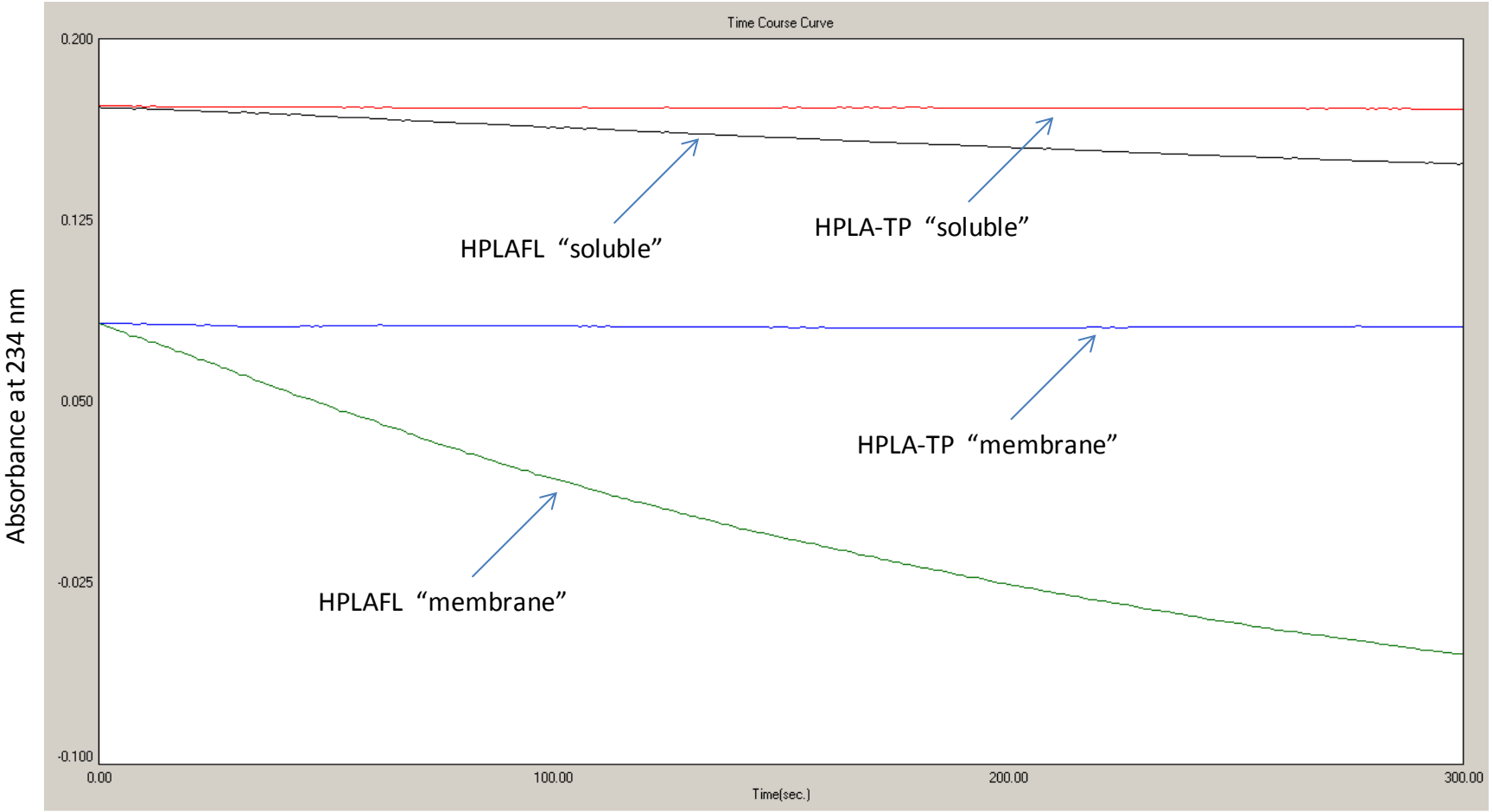

A.4.8 Effect of pH on self-oxidation rate of LnA

Fifty microlitres of 5 mM LnA stock was incubated in 3 mL of buffers at pH 4.0-9.5 at 20°C. Changes in absorbance at 234 nm were monitored over 100 seconds.

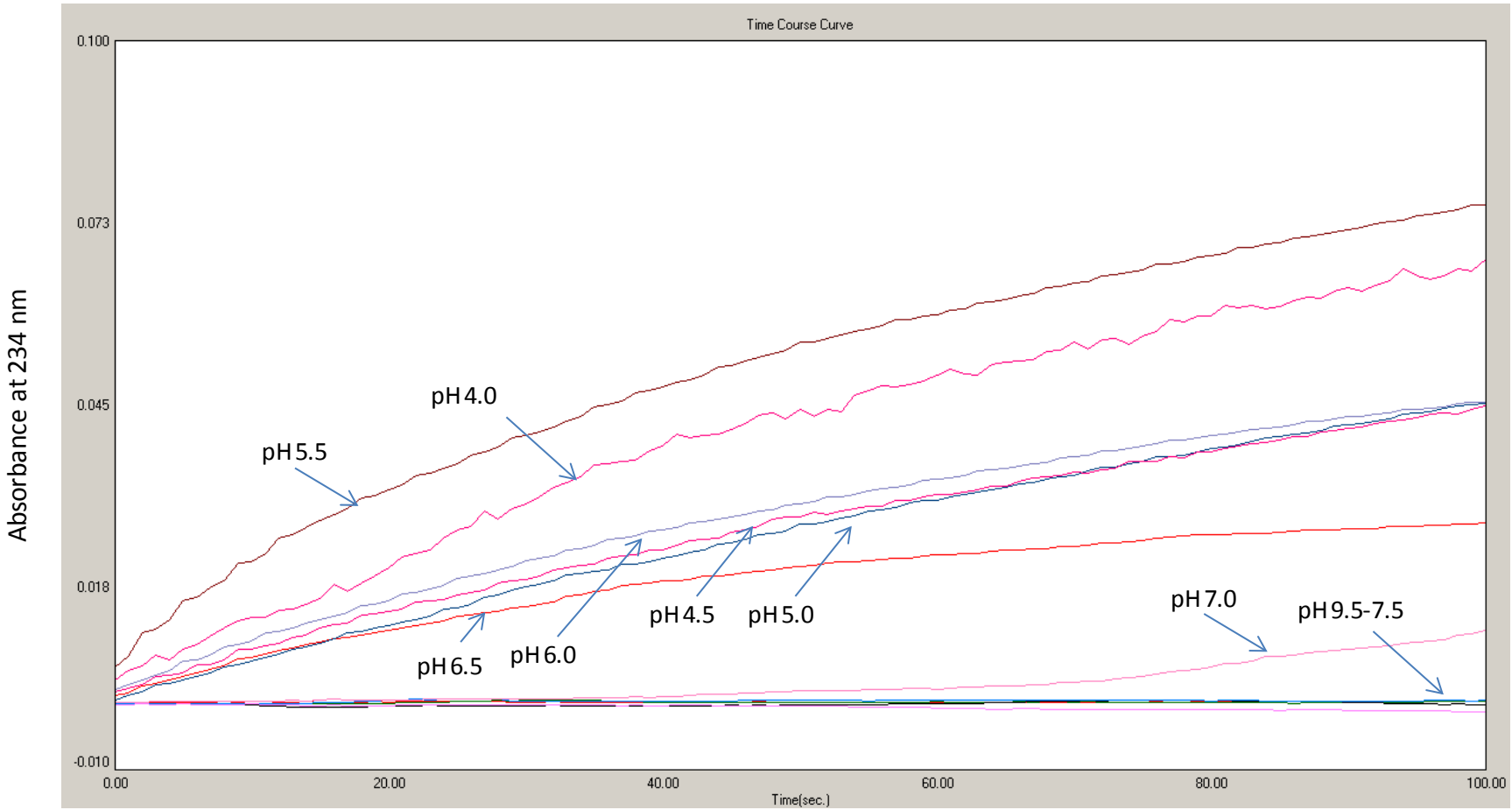

A.4.9 Effect of Tween 20 concentration on catalytic activity of LOXA-TP

A series of LOX assays was performed with recombinant LOXA-TP at the pH 5.5, 20°C and various LnA concentrations. At each substrate concentration a range of Tween 20 deterrent was added and changes in absorbance at 234 nm monitored. It was also taken into account that certain amounts of the detergent were brought into reactions with the substrate stock. For each substrate concentration, the conversion rates from reactions with different amounts of Tween 20 were then plotted as separate curves. Error bars represent a standard deviation of the mean obtained from duplicated experiments.

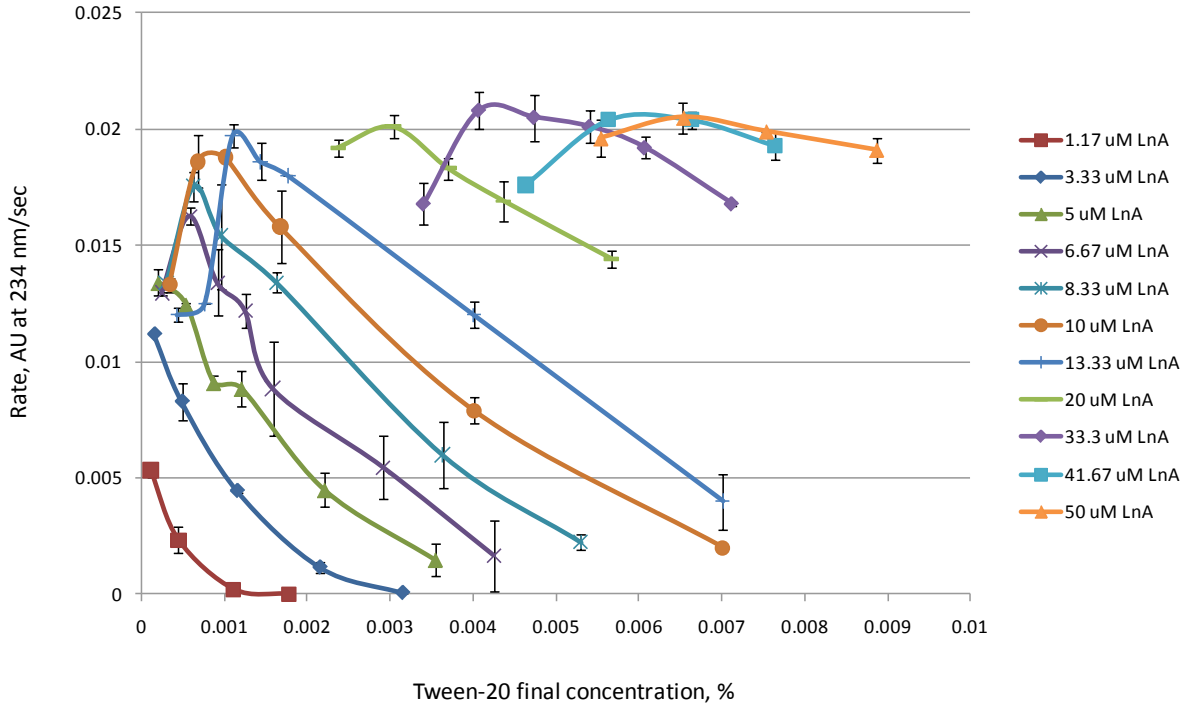

A.4.10 GC-MS analysis of volatile products of recombinant HPLAFL and HPLA-TP using 13(S)-HPOTrE as substrate

13(S)-HPOTrE was prepared and incubated with either E. coli " membrane" fractions containing HPLAFL or HPLA-TP recombinant protein, or heat-treated HPLAFL fraction, or with no enzyme added as described in section 3.9.9. Headspace volatile components from each reaction were collected and analysed using GC-MS as described in section 3.9.9. Panels A, B, C and D represent chromatograms obtained for HPLAFL, HPLA-TP, heat-killed HPLAFL and "no enzyme" experiments. The detected peaks were labelled 1-9 in order of their elution and identified compounds were identified by matching their mass spectra of reference compounds in the NIST EPA/NIH Mass Spectral Library (National Institute of Standards and Technology, NIST05). Based on their closest matches, the identified compounds were identified as follows: **1** – acetone; **3** – 2-methyl-4 pentanal; **4** – (*Z*)-3-hexenal; **5** – (*E*)-2-hexenal ; **6** – (*E*)-2-hexenal ; **7** – 2(E), 4(*E*)-hexadienal; **8** – 2(*E*), 4(*E*)-hexadienal and **9** – acetic acid. The corresponding spectra for the identified compounds are attached in Appendix A.4.13. Acetone (peak 1) and acetic acid (peak 9) in each sample were introduced from the reaction buffer and are not products of the reaction.

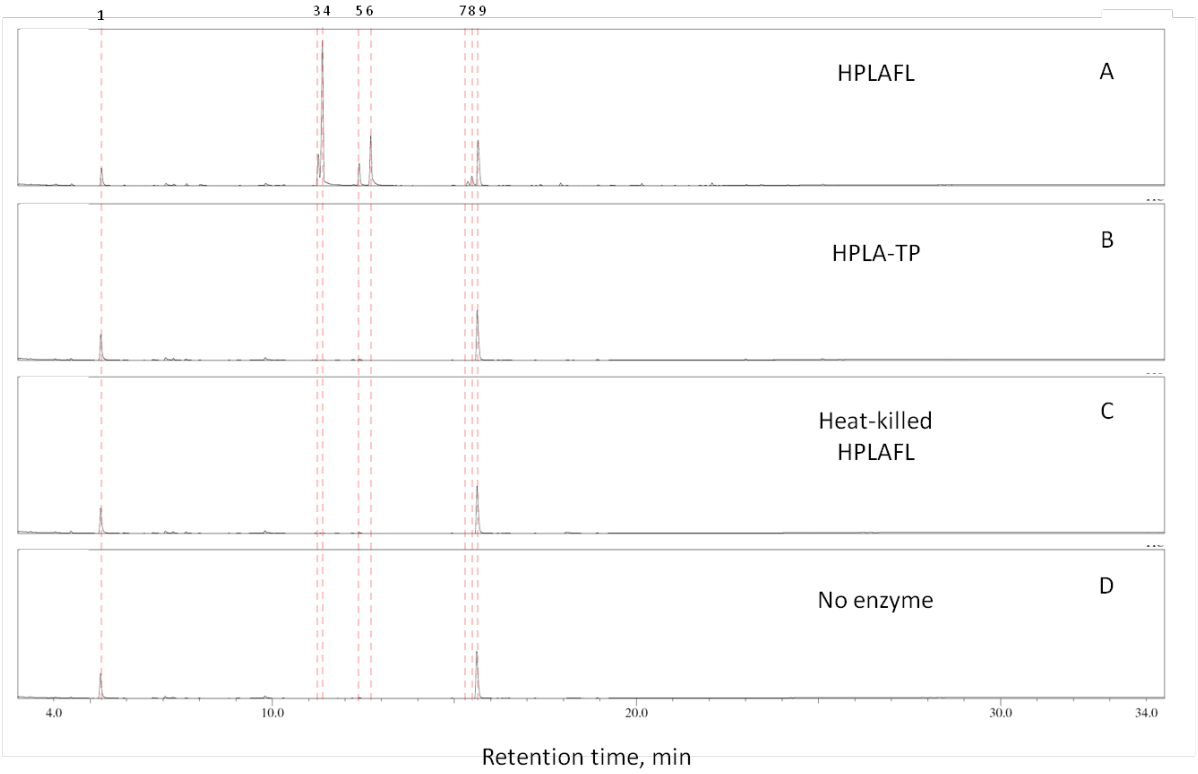

A.4.11 GC-MS analysis of volatile products of recombinant HPLAFL and HPLA-TP using 13(S)-HPODE as substrate

13(S)-HPODE was prepared and incubated with either E. coli " membrane" fractions containing HPLAFL or HPLA-TP recombinant protein, or heat-treated HPLAFL fraction, or with no enzyme added as described in section 3.9.9. Headspace volatile components from each reaction were collected and analysed using GC-MS as described in section 3.9.9. Panels A, B, C and D represent chromatograms obtained for HPLAFL, HPLA-TP, heat-killed HPLAFL and "no enzyme" experiments. The detected peaks were labelled 1-9 in order of their elution and identified compounds were identified by matching their mass spectra of reference compounds in the NIST EPA/NIH Mass Spectral Library (National Institute of Standards and Technology, NIST05). Based on their closest matches, the identified compounds were identified as follows: **1** – acetone; **2** – hexanal and **9** – acetic acid. The corresponding spectra for the identified compounds are attached in Appendix A.4.13. Acetone (peak 1) and acetic acid (peak 9) in each sample were introduced from the reaction buffer and are not products of the reaction.

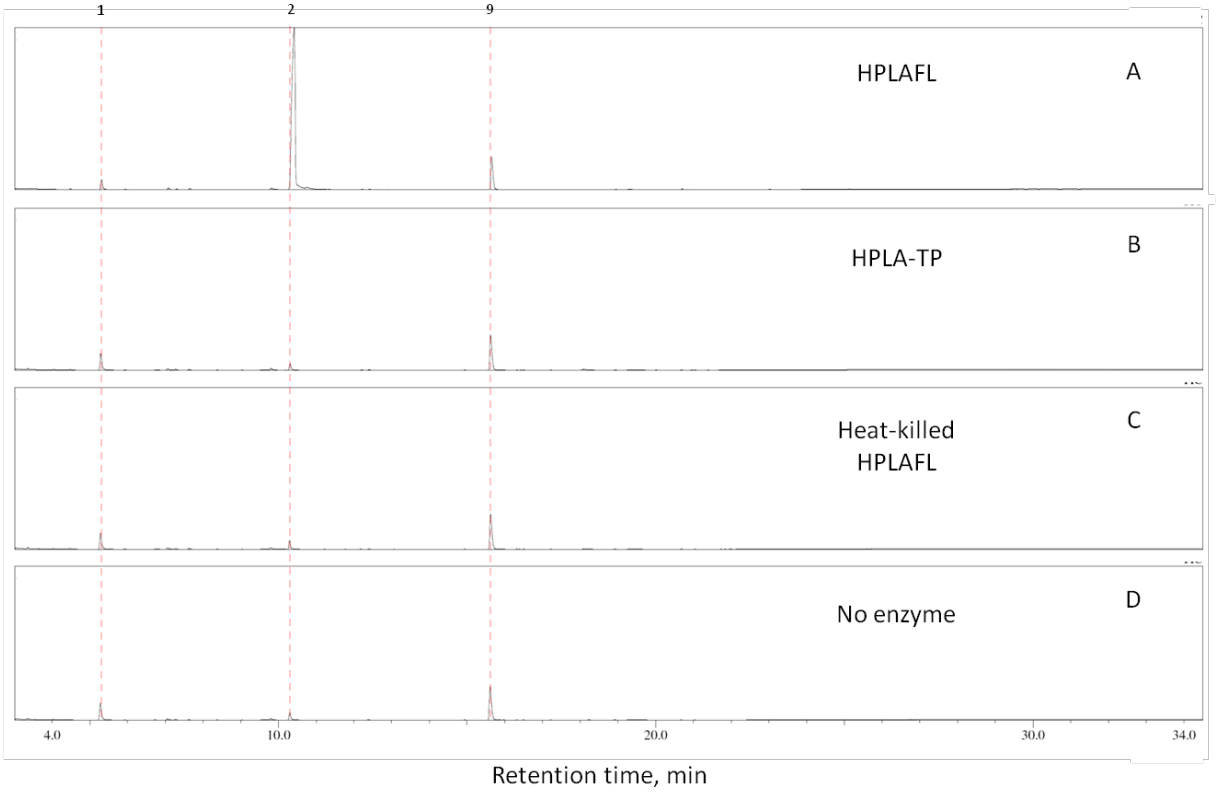

A.4.12 GC-MS analysis of volatile products of recombinant HPLAFL and HPLA-TP using 15(S)-HPETE as substrate

13(S)-HPOTrE was prepared and incubated with either E. coli " membrane" fractions containing HPLAFL or HPLA-TP recombinant protein, or heat-treated HPLAFL fraction, or with no enzyme added as described in section 3.9.9. Headspace volatile components from each reaction were collected and analysed using GC-MS as described in section 3.9.9. Panels A, B, C and D represent chromatograms obtained for HPLAFL, HPLA-TP, heat-killed HPLAFL and "no enzyme" experiments. The detected peaks were labelled 1-9 in order of their elution and identified compounds were identified by matching their mass spectra of reference compounds in the NIST EPA/NIH Mass Spectral Library (National Institute of Standards and Technology, NIST05). Based on their closest matches, the identified compounds were identified as follows: **1** – acetone; **2** – hexanal and **9** – acetic acid. The corresponding spectra for the identified compounds are attached in Appendix A.4.13. Acetone (peak 1) and acetic acid (peak 9) in each sample were introduced from the reaction buffer and are not products of the reaction.

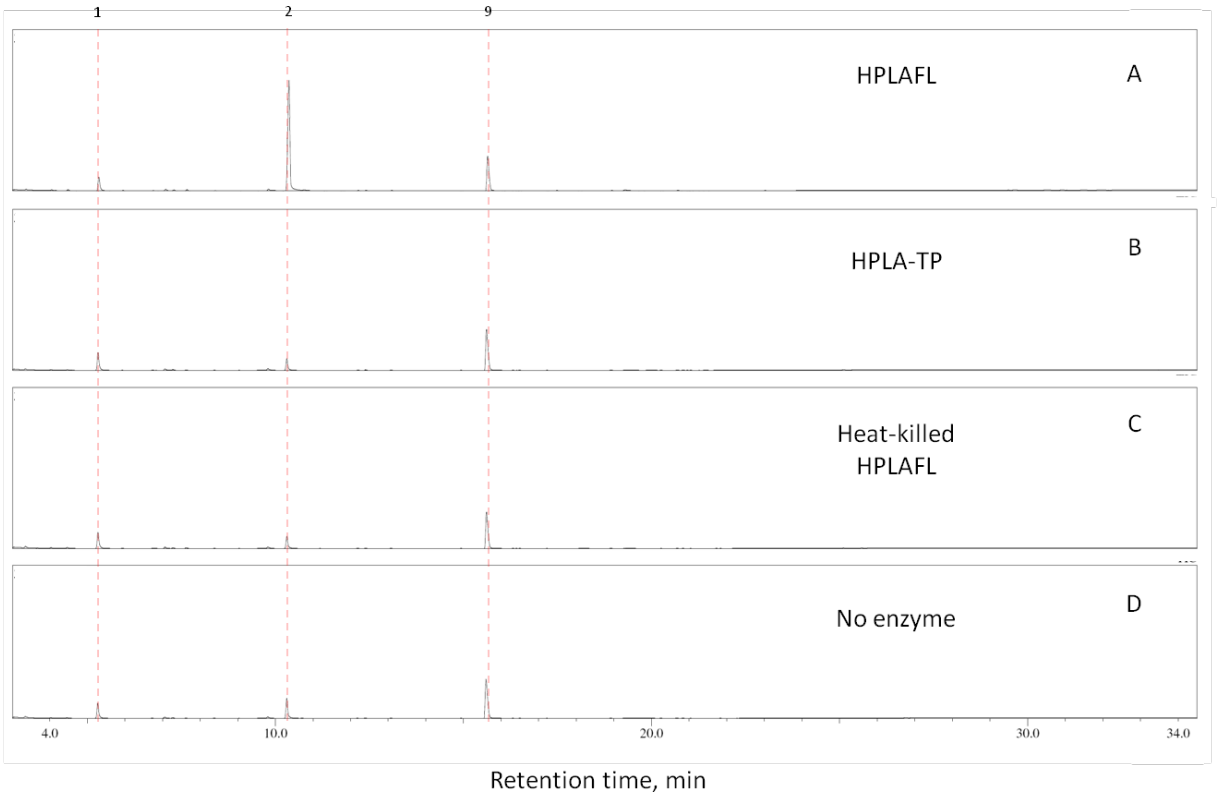

A.4.13 Spectra of identified by GC-MS head space volatile products

Spectra for each identified product were compared to the spectra of reference compounds in the NIST EPA/NIH Mass Spectral Library (National Institute of Standards and Technology, NIST05).l Numbers below each spectrum correspond to the designated numbers for each individual peak in order of their elution from the GC column (Appendices A.4.10-A.4.12). The matched compounds with the highest score are highlighted.

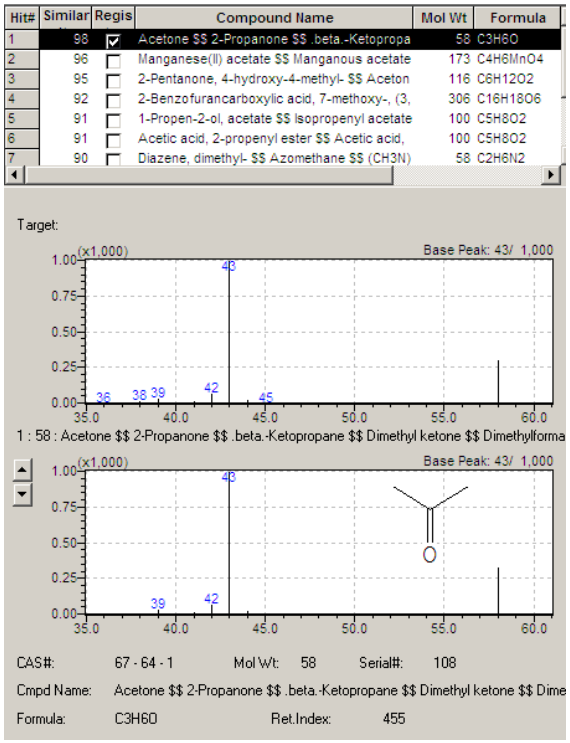

1)

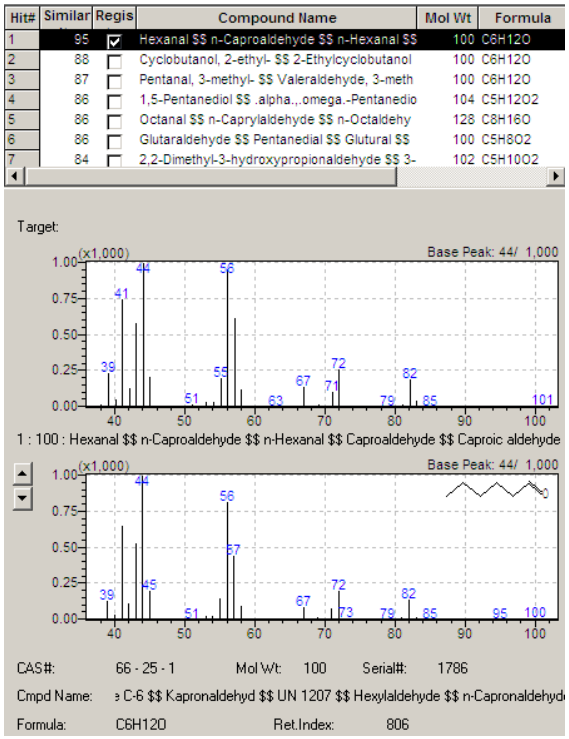

2)

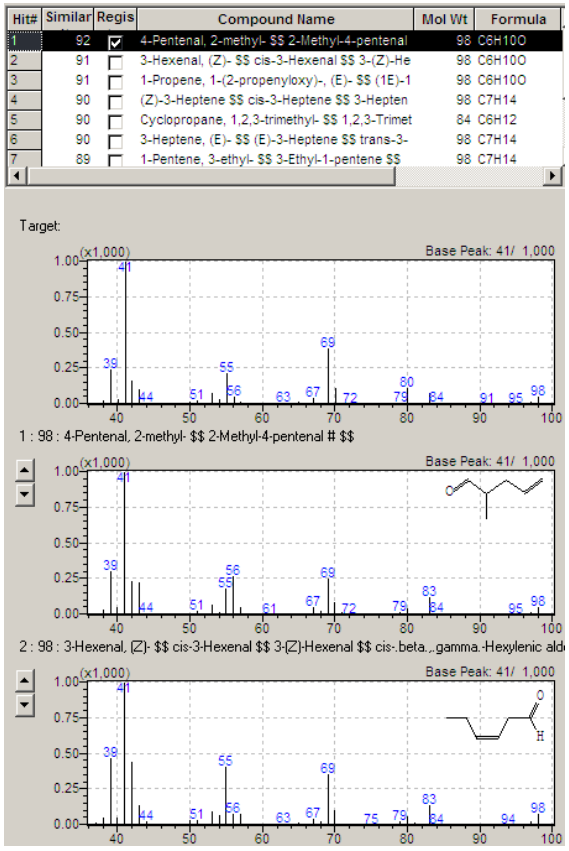

3)

A. 4.13. Spectra of identified by GC-MS head space volatile products (continued)

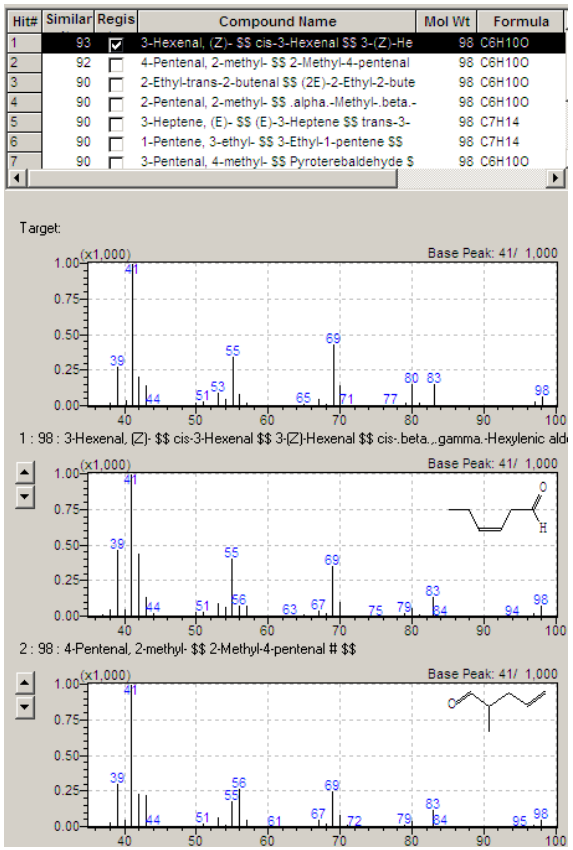

4)

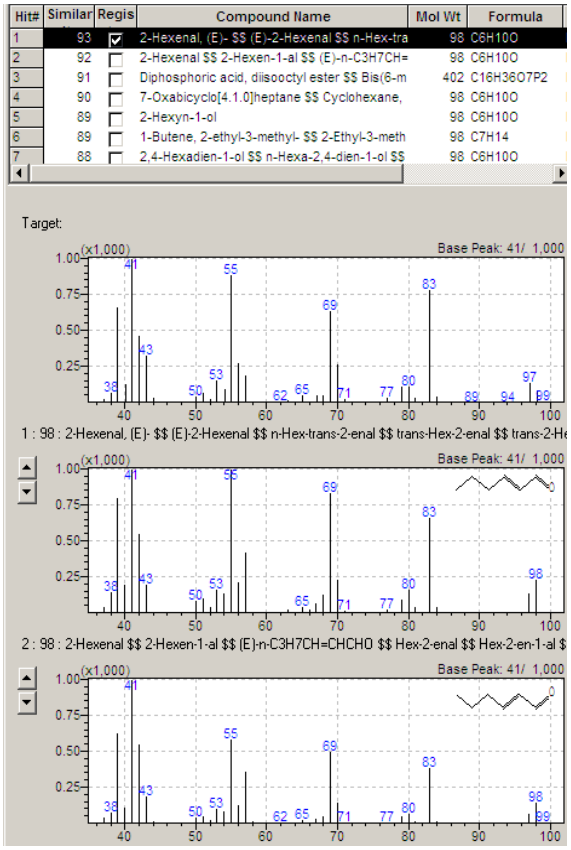

5)

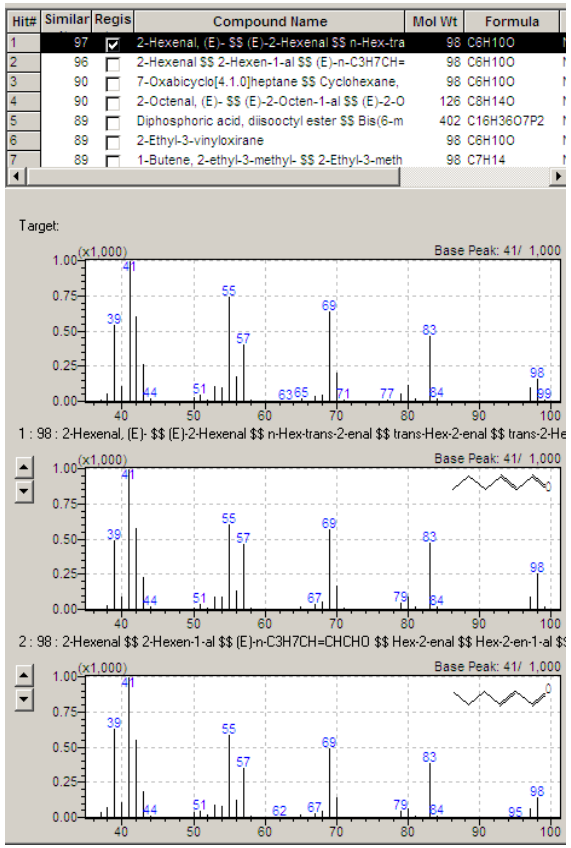

6)

4.13. Spectra of identified by GC-MS head space volatile products (continued)

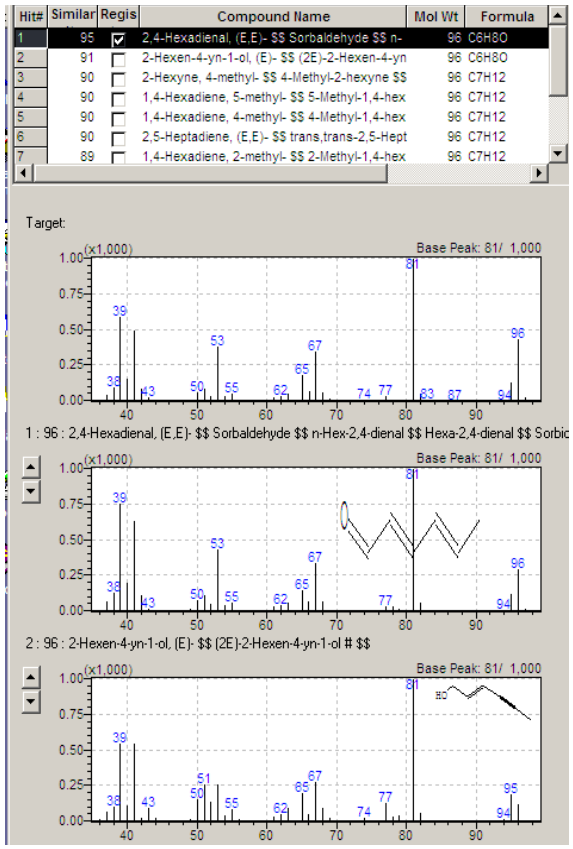

7)

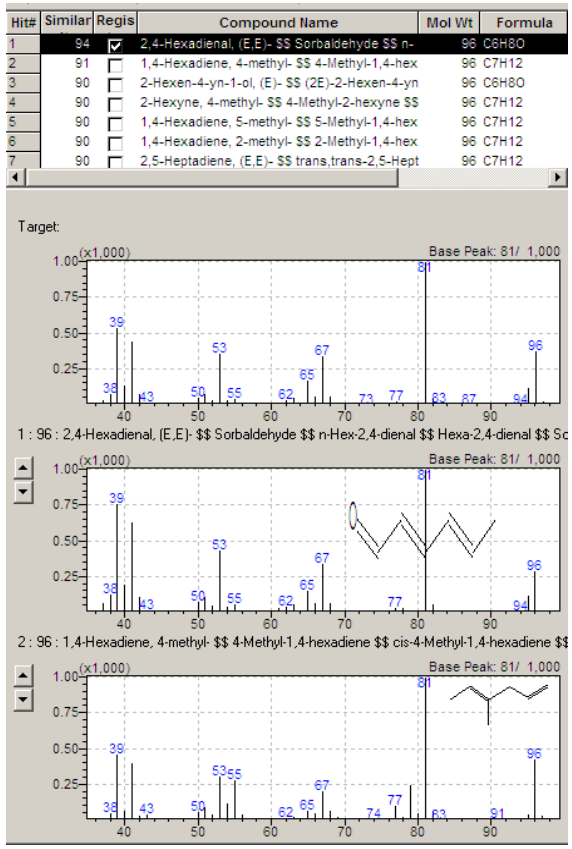

8)

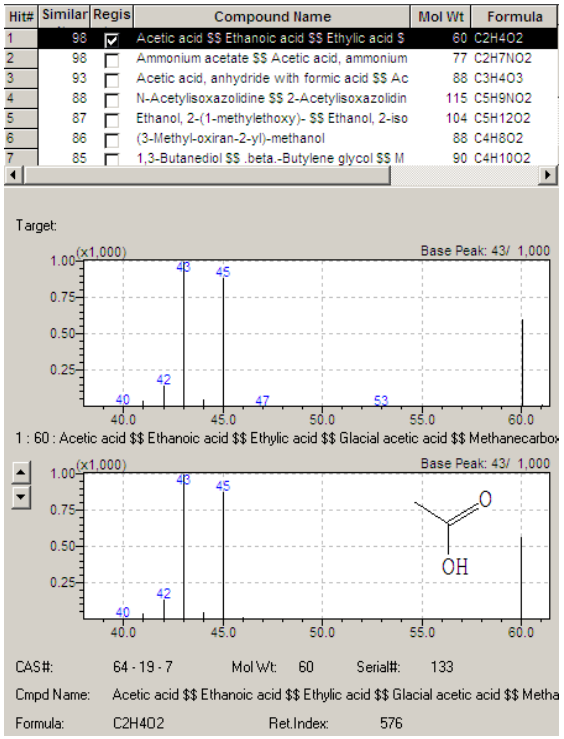

9)